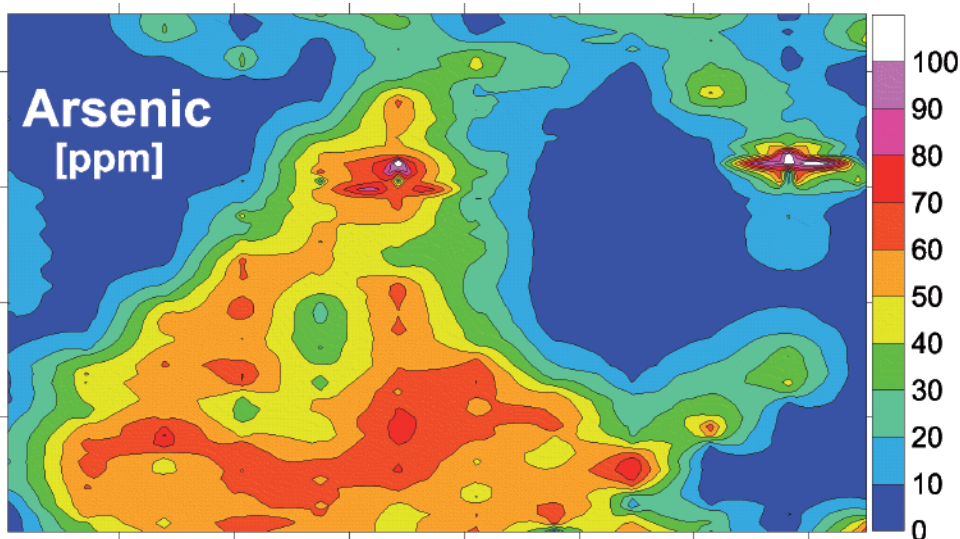


Elisabeth Eiche

Arsenic mobilization processes in the red river delta, Vietnam

Towards a better understanding
of the patchy distribution of
dissolved arsenic in alluvial deposits



Elisabeth Eiche

Arsenic mobilization processes in the red river delta, Vietnam

Towards a better understanding of the patchy distribution of dissolved arsenic in alluvial deposits

Karlsruher Mineralogische und Geochemische Hefte

Schriftenreihe des Instituts für Mineralogie und Geochemie,
Karlsruher Institut für Technologie

Band 37

Arsenic mobilization processes in the red river delta, Vietnam

Towards a better understanding
of the patchy distribution of
dissolved arsenic in alluvial deposits

by
Elisabeth Eiche

Dissertation, Universität Karlsruhe (TH),
Fakultät für Bauingenieur-, Geo- und Umweltwissenschaften, 2009
Referenten: Prof. Dr. Thomas Neumann, Prof. Dr. Walter Giger

Anschrift der Schriftleitung:

Karlsruher Institut für Technologie
Institut für Mineralogie und Geochemie
Karlsruher Mineralogische und Geochemische Hefte
D – 76128 Karlsruhe

Impressum

Karlsruher Institut für Technologie (KIT)
KIT Scientific Publishing
Straße am Forum 2
D-76131 Karlsruhe
www.uvka.de

KIT – Universität des Landes Baden-Württemberg und nationales
Forschungszentrum in der Helmholtz-Gemeinschaft



Diese Veröffentlichung ist im Internet unter folgender Creative Commons-Lizenz
publiziert: <http://creativecommons.org/licenses/by-nc-nd/3.0/de/>

KIT Scientific Publishing 2009
Print on Demand

ISSN: 1618-2677
ISBN: 978-3-86644-408-9

**ARSENIC MOBILIZATION PROCESSES IN THE RED RIVER
DELTA, VIETNAM – TOWARDS A BETTER UNDERSTANDING OF
THE PATCHY DISTRIBUTION OF DISSOLVED ARSENIC IN
ALLUVIAL DEPOSITS**

Zur Erlangung des akademischen Grades eines
DOKTORS DER NATURWISSENSCHAFTEN

von der Fakultät für

Bauingenieur-, Geo- und Umweltwissenschaften
der Universität Karlsruhe (TH)

genehmigte

DISSERTATION

von

Dipl. Geoökol. Elisabeth Eiche

aus Freiburg

Tag der mündlichen Prüfung: 20.05.2009

Referent: Prof. Dr. Thomas Neumann

Korreferent: Prof. Dr. Walter Giger

Karlsruhe 2009

**ICH SAH MANCHE WAHRHEIT SIEGEN, ABER
STETS DURCH DIE WOHLWOLLENDE
UNTERSTÜTZUNG VON HUNDERT IRRTÜMERN.**

Friedrich Nietzsche

ABSTRACT

The spatial variability of As concentrations in aquifers was studied in a small village in the vicinity of Ha Noi, Vietnam. In spite of intensive research over the last years, this phenomenon still raises a lot of questions. Two sites only 700 m apart, but substantially different with regard to dissolved As concentrations in groundwater (site L (low) $<10 \mu\text{g/L}$ vs. site H (high) $170 - 600 \mu\text{g/L}$) in the 20 - 50 m depth range, were characterized with respect to sediment geochemistry, mineralogy and hydrochemistry.

Concerning hydrochemistry, both sites are reducing in their redox character but to a different extent. Higher dissolved Fe, and SO_4^{2-} concentrations below detection limit (LOD) in groundwater at site H (Fe: $14.5 \pm 5.6 \text{ mg/L}$, SO_4^{2-} : $<\text{LOD}$) suggest more strongly reducing conditions as compared to site L (Fe: $1.8 \pm 0.6 \text{ mg/L}$, SO_4^{2-} : $5.6 \pm 2.8 \text{ mg/L}$). High concentrations of NH_4^+ ($10 \pm 7 \text{ mg/L}$), HCO_3^- ($490 \pm 70 \text{ mg/L}$), and dissolved P ($0.6 \pm 0.3 \text{ mg/L}$), in addition to elevated dissolved As concentrations at site H are consistent with As release coupled to microbially induced reductive dissolution of Fe oxyhydroxides. Other processes such as precipitation of siderite (saturation index (SI): 1.6 ± 0.2) and vivianite (SI: 2.0 ± 0.5), which are strongly supersaturated at site H, may also influence the partitioning of As between groundwater and aquifer sands.

However, no major differences were observed with respect to bulk geochemistry and mineralogy of the sediments. Arsenic concentrations in the aquifer were found to be in the range typical for unconsolidated sediments at both sites ($\sim 5 \text{ mg/kg}$). Different between both sites, though, was the extent of reduction of Fe oxyhydroxides in the aquifer as inferred from results of sequential extraction (site L: mainly crystalline Fe(III) oxyhydroxides, site H: high proportion of amorphous oxyhydroxides), from sediment colour (site L: brownish, site H: mainly greyish), from the diffuse spectral reflectance of the sediments (site L: $\Delta R > 0.7$, site H: $\Delta R < 0.3$), and, the way As is fixed in the solid phase. At site H, most of the As in the grey coloured sandy

sediments was found to be adsorbed to mixed valence Fe(II/III) minerals whereas at site L, As was mainly fixed in orange-brown Fe(III) oxyhydroxides as indicated by the sequential extraction.

Elemental mappings on a micrometer scale carried out by micro synchrotron (μ S) XRF analysis revealed elevated As concentrations in Fe bearing phyllosilicates (<60 ppm), As bearing sulphides (<140 ppm) and Fe oxyhydroxide coatings (<140 ppm) at both sites. The distribution of As within distinct mineral phases often showed very heterogeneous patterns. Samples which released high fractions of As during phosphate leaching showed distinct Fe oxyhydroxide coatings on the sediment particles as well as correlations between As and Fe. After dissolution of Fe oxyhydroxide coatings Fe-As correlation was preserved only in association with K, indicating the sole presence of both elements in silicate structures.

At both sites, the total content of organic carbon (OC) in the aquifer is similar and relatively low (<0.03 wt-%). Therefore, the capacity of the sediments to induce reducing conditions seems not to depend much on the amount of organic matter (OM) but more on its origin and the depositional environment, which determines its reactivity and availability, as well as on the groundwater flow patterns. Multiple sources of OM are suggested by the autochthonous and reworked marine or terrestrial character as indicated by the $\delta^{13}\text{C}$ and C/N signatures. Compared to site L, the aquifer at site H, which probably consists of sediment deposited in a Holocene paleochannel, as suggested by $\delta^{13}\text{C}$ values and sedimentological data, had a considerably higher contribution of marine derived OM (~45 vs. ~30%). OM from marine origin is more easily degradable by microorganisms and, consequently, can induce more strongly reducing conditions. Additionally, organic rich layers were only separated from the underlying aquifer by thin silt layers at site H. As a result, leaching of sufficient amounts of electron donors or dissolved As into the aquifer at this site is assumable which would, concurrently, further enhance the reducing conditions at site H and the release of As. At site L, an organic rich peat layer was embedded into the 23 m thick aquitard, which was deposited during Holocene in a paleointerfluvial position. The low hydraulic conductivity of this deposit seems to hinder migration of dissolved As and/or reactive OC and, therefore, protect the underlying aquifer.

The conceptual model developed based on the results of this study clearly indicates that the identification of paleochannel and paleointerfluvial structures in addition to the localization and characterization of layers rich in reactive OC would be very expedient to distinguish between high and low As areas. This knowledge is important in order to prevent the set-up of new wells in As burdened groundwaters and, consequently, provide the population with clean drinking water.

Key words: arsenic, groundwater, μ S-XRF, mobilization, organic matter, paleochannel, paleointerfluvial, patchy distribution, sequential extraction, Vietnam

KURZFASSUNG

Arsen belastete Grundwässer in Deltagebieten sind weltweit verbreitet und stellen eine große Gefahr für die Menschen dar, die dieses Wasser als Trink- oder Brauchwasser verwenden. Seit Jahren forschen zahlreiche Wissenschaftler über mögliche Ursachen für diese geogen hervorgerufene Belastung. Viele Unklarheiten konnten allerdings noch nicht zufrieden stellend geklärt werden, so zum Beispiel die sehr kleinräumig auftretenden Unterschiede hinsichtlich der gelösten As-Konzentrationen im Aquifer. An diesem Punkt setzt diese Arbeit an. Es soll versucht werden, basierend auf hydrologischen, geochemischen und mineralogischen Untersuchungen, Unterschiede zwischen zwei Standorten im Red River Delta, Vietnam, herauszuarbeiten, die stark unterschiedliche gelöste As-Konzentrationen aufweisen („site L (low)“: $<10 \mu\text{g/L}$ vs. „site H (high)“: $170 - 600 \mu\text{g/L}$) und sich nur 700 m voneinander entfernt befinden.

Hinsichtlich der Hauptmineralzusammensetzung, sowie der Gesamtelementkonzentrationen der Sedimente konnten keine signifikanten Unterschiede zwischen beiden Standorten festgestellt werden. Mit $\sim 5 \text{ mg As/kg}$ in den Aquifersedimenten an beiden Standorten liegen die Gesamtkonzentrationen an As in einem für Lockersedimente typischen Bereich. Jedoch haben Elementmessungen im Mikrometerbereich mittels $\mu\text{S-XRF}$ gezeigt, dass As punktuell sehr stark angereichert ist. Identifizierte Mineralphasen mit hohen As-Konzentrationen an beiden Standorten sind vor allem Fe Oxyhydroxide ($<140 \text{ ppm}$), die meist als Mineralüberzüge vorliegen, sowie Fe-haltige Silikate ($<60 \text{ ppm}$) und Sulphide ($<140 \text{ ppm}$). Innerhalb einzelner Mineralkörner sind die As-Konzentrationen kleinräumig oft sehr heterogen. Nach der Laugung der Sedimente mit einer Phosphat-Lösung, die zum Teil große Mengen an As freisetzte, sind die Fe-Überzüge immer noch deutlich erkennbar. Ebenso bleibt die Korrelation von Fe und As, die in den unbehandelten Mineralüberzügen meist auftritt, auch nach der Phosphat-Laugung erhalten. Die Auflösung der Fe-Überzüge in einem weiteren Laugungsschritt führt zu einer starken Freisetzung von As und Fe. Erhöhte As

und Fe Konzentrationen im Randbereich von Mineralen kommen größtenteils nur noch in Verbindung mit K vor, was darauf hindeutet, dass beide Elemente vor allem noch silikatisch vorkommen.

Unterschiede zwischen den Standorten treten bezüglich der herrschenden Redox-Bedingungen im Grundwasser, der Valenz der Eisenoxide sowie der Mobilisierbarkeit von Arsen auf. An „site H“ deuten die graue Farbe der Sedimente, die Ergebnisse der sequentiellen Extraktionen (hoher Anteil an amorphen Fe Oxy-hydroxiden) sowie die spektrale Reflektivität der Sedimente ($\Delta R < 0.3$), auf einen hohen Anteil an Fe(II)- oder Fe(II/III)-Mineralphasen hin, die wahrscheinlich durch den Einfluss der stark reduzierenden Bedingungen an diesem Standort gebildet wurden. Höhere Konzentrationen an gelöstem Fe^{2+} (14.5 ± 5.6 mg/L), sowie HCO_3^- (490 ± 70 mg/L), NH_4^+ (10 ± 7 mg/L) und P_{tot} (0.6 ± 0.3 mg/L) im Vergleich zu „site L“ deuten darauf hin, dass Arsen v.a. durch mikrobiell induzierte, reduktive Auflösung von Fe(III) Oxy-hydroxiden freigesetzt wird. Arsen liegt hier vorwiegend in adsorbierter Form vor, wie die Ergebnisse der sequentiellen Extraktion zeigen und ist somit als leicht mobilisierbar anzusehen. Des Weiteren scheinen Mineralneubildungen, wie z.B. von Siderit (Sättigungsindex (SI): 1.6 ± 0.2) oder Vivianit (SI: 2.0 ± 0.5), welche beide im Aquifer an „site H“ übersättigt sind, einen Einfluss auf die Konzentration an gelöstem As zu haben. Die Redox-Bedingungen an „site L“ scheinen weniger stark reduzierend zu sein, so dass die Konzentrationen an gelöstem Fe^{2+} (1.8 ± 0.6 mg/L) im Vergleich zu „site H“ deutlich geringer sind. Außerdem liegt SO_4^{2-} , im Gegensatz zu site H, in detektierbaren Konzentrationen vor (SO_4^{2-} : 5.6 ± 2.8 mg/L). Das gelbbraune Sediment im Aquifer an „site L“ wird von Fe(III) Oxy-hydroxiden dominiert (ΔR -Werten > 0.7). Die sequentiellen Extraktionen zeigen, dass ein Großteil des As in kristallinen Fe Oxy-hydroxiden gebunden vorliegt und deshalb nur durch eine Veränderung der Redox-Bedingungen verstärkt freigesetzt werden kann.

Der Gehalt an organischem Kohlenstoff (OC) ist an beiden Standorten gleich und relativ gering (< 0.03 Gew-%). Daher scheint die Verfügbarkeit und Reaktivität von organischem Material (OM), die stark von deren Zusammensetzung und den Ablagerungsbedingungen der Sedimente abhängt, einen großen Einfluss auf die Ausbildung von unterschiedlichen Redox-

Bedingungen, die Hydrogeologie und dadurch auch auf die Mobilisierung von As, auszuüben. Die Charakterisierung des OM mittels $\delta^{13}\text{C}$ - und C/N-Analysen zeigte, dass neben autochthonem oder umgelagertem OM mariner und terrestrischer Herkunft, auch OC aus Petroleum (Carbon preference index (CPI) ~ 1) eine Rolle als Elektronendonator im Sediment spielen könnte. Im Vergleich zu „site L“ weist das Sediment im Aquifer an „site H“ einen höheren Anteil (~ 45 vs. $\sim 30\%$) an marin abgelagertem OM auf. Marin gebildete Organik ist für Mikroorganismen leichter metabolisierbar und kann dadurch stärker reduzierende Bedingungen induzieren. Zusätzlich scheint an „site H“ gelöster organischer Kohlenstoff aus darüber liegenden, organikreichen Horizonten in den Aquifer einzusickern, was durch die höchsten Konzentrationen an HCO_3^- , NH_4^+ , PO_4^{3-} und DOC im obersten Aquiferbereich angedeutet wird. Organik-reiche Lagen, insbesondere so genannter „peat“, treten auch am gering belasteten Standort auf. Allerdings sind sie hier in einen 23 m mächtigen Aquitard, der den Aquifer überlagert, eingebettet, welcher zusätzlich durch eine Fe-Konkretion nach unten abgedichtet wird. Dies scheint den unterliegenden Aquifer vor einsickerndem gelöstem organischem Kohlenstoff und As zu bewahren.

Die Untersuchungen an beiden Standorten haben gezeigt, dass der Aufbau der Sedimente hinsichtlich Korngröße, Permeabilität sowie Anteil und Reaktivität an organischem Material kleinräumig sehr heterogen ist. Die Sedimente des As-belasteten Aquifers scheinen größtenteils während des Holozän in einem ehemaligen Flusslauf abgelagert worden zu sein, worauf sedimentologische Untersuchungen und die $\delta^{13}\text{C}$ -Signaturen hinweisen, wohingegen der unbelastete Aquifer pleistozänen Ursprungs ist, was die Unterschiede hinsichtlich der Reaktivität des OM erklären könnte. Der Aquitard am unbelasteten Standort ist ebenfalls holozänen Alters und lag während der eiszeitlichen Meeresspiegelschwankungen vermutlich erhöht, so dass nur sehr feines Material abgelagert wurde. Die unterschiedlichen Ablagerungsbedingungen an beiden Standorten scheinen daher einerseits die Zusammensetzung, andererseits die Zugänglichkeit des OM, die durch die hydraulischen Bedingungen bestimmt wird, stark beeinflusst zu haben. Diese Aspekte könnten von großem Interesse hinsichtlich der kleinräumigen Unterschiede in den gelösten As-Konzentrationen sein.

Übertragen auf andere As-belastete Regionen lässt sich schlussfolgern, dass die Lokalisierung und Charakterisierung organik-reicher Lagen innerhalb des Sedimentprofils zusammen mit der Identifizierung von ehemaligen Flussläufen und Hochflächen, einen wichtigen Beitrag dazu leisten könnten, gering belastete Gebiete auszuweisen. Der Bau zukünftiger Trinkwasserbrunnen nur in diesen Gebieten würde die Gefährdung der Menschen in den betroffenen Regionen, an chronischer Arsenvergiftung zu erkranken, stark herabsetzen.

ACKNOWLEDGEMENTS

Only oneself is responsible for a successful PhD thesis but no one can succeed without the support of many people. Therefore, I would like to thank...

... my supervisor Prof. Dr. Thomas Neumann for giving me the chance to do a PhD at the Institute. You always believed in me and supported me with regard to my work and also with respect to all the problems I encountered during my thesis. Thanks for the personal and constructive cooperation.

... Prof. Dr. Walter Giger for his friendly readiness for the takeover of the Koreferat of my thesis.

... Dr. Michael Berg who kindly offered to take part in his working group and on the field trips to Vietnam. He did not only provide me with samples and data if necessary but was also always willing to read through drafts. Thanks for the many scientific discussions, the suggestions and the Swiss chocolate.

... Dr. Zsolt Berner from whose broad knowledge and long experience in field work I could benefit so much in Van Phuc. You always had more than one open ear for my problems with regard to analytics and many other aspects. Thanks for the useful advices you had for me.

... the rest of the As working group at our Institute, especially PD Dr. Stefan Norra, for discussions, comments and helpful suggestions.

... Dr. Utz Kramar for all his support with regard to everything that has to do with X-ray analysis.

... Beth Weinman for analysing the grain size of my samples and also for the always friendly and open cooperation.

... Dr. Alexander van Geen for discussions, reflectance data and some corrections to my drafts.

... all technicians at the Institute who gave me a hand for all kinds of analytics I have carried out: Beate Oetzel (XRD), Gesine Preuss (IRMS, AAS, FIAS), Claudia Mössner (ICP-MS), Cornelia Haug (acid digestion), Kristian Nikoloski (sample preparation, thin section).

... Caroline Stengel for analysing water samples at the EAWAG.

... Bart van Dongen and Patrick Pionneau for the help with regard to organic matter characterization.

... Rolf Simon for his help at the Fluo-beamline at the ANKA.

... to Felix Frei, Zahid Aziz, Kathleen A. Radloff, and Hun-Bok Jung for the discussions and their participation in the field campaign.

... the colleagues at CETASD and HUMG, in particular Prof. Dr. Pham Hung Viet (director) and Dr. Pham Thi Kim Trang, Vi Mai Lan, Bui Hong Nhat and Pham Qui Nhan for their assistance during the field campaign and the villagers and authorities of Van Phuc for their hospitality.

... the International Bureau of the German Ministry of Education and Research (BMBF) and the LGK-BW for financial support.

... Jörg Göttlicher, Ralph Steiniger and Stefan Mangold of the ISS (FZK) who gave me the chance to work at their beamlines in order to earn the money I needed to finish my work. It was an interesting time for me and I have learned a lot. Thanks for your hospitality and numerous discussions.

... Dr. Gerhard Ott who always brought my computer back to life.

... the staff of the IMG because everyone contributed to the success of my work. So far I had a great time at the Institute.

... my antecessor in the field of As in the Institute, Frank Wagner, who tried to answer all the numerous questions I had in the beginning

... Steffi, Nina, Harald, Alexander, Dirk, Maren, Farooq, Apple, Aga and Antje for the many amusing things we have done and hopefully will do in future!

... all my friends, especially Mirjam, Michael, Simone, Astrid and Corina who offered me a shoulder to cry on, if necessary.

... my computer. I'm thankful that you hold up until the end.

... all I have forgotten to mention.

... the girls in my office. Steffi, for the special time we had as lone fighters on the PhD front of the Institute. Nina for enduring my blabber and my snide remarks. A special thanks to both for all the chocolate testing, their help and the fun we had despite the work we did. Felicitas and Oscar for always cheering me up.

... my parents Otto und Rita and my whole family to whom I want to dedicate this thesis. Thanks for the all the support and happiness you always gave me. You have made me to the person I am now.

TABLE OF CONTENT

ABSTRACT	I
KURZFASSUNG	V
ACKNOWLEDGEMENTS	IX
TABLE OF CONTENT	XI
1 INTRODUCTION AND OBJECTIVE OF THE STUDY	1
2 ARSENIC IN GROUNDWATER – AN OVERVIEW	5
2.1 GENERAL CHEMICAL PROPERTIES.....	5
2.1.1 ARSENIC IN NATURAL ENVIRONMENT.....	6
2.1.2 ARSENIC SPECIES AND TRANSFORMATION PROCESSES	10
2.2 ARSENIC BEARING PHASES IN AQUIFERS	13
2.3 PROCESSES INFLUENCING THE ARSENIC CONCENTRATION IN THE GROUNDWATER....	15
2.3.1 DISSOLUTION AND PRECIPITATION OF MINERAL PHASES.....	16
2.3.2 ADSORPTION AND DESORPTION PROCESSES.....	20
2.3.3 FURTHER INFLUENCING PARAMETERS OF ARSENIC CONCENTRATION IN THE WATER	23
2.4 CHARACTERISTICS OF HIGH ARSENIC REGIONS.....	24
2.5 IMPORTANCE OF ORGANIC MATERIAL.....	26
2.5.1 ROLE AND SOURCES OF ORGANIC MATTER.....	26
2.5.2 DEGRADATION OF ORGANIC MATTER.....	28
2.5.3 CHARACTERIZATION OF ORGANIC MATTER.....	30
2.6 ARSENIC TOXICITY AND EPIDEMIOLOGY	34
2.7 MITIGATION STRATEGIES AND ARSENIC FILTER SYSTEMS.....	36
3 RED RIVER DELTA, VIETNAM	41
3.1 CLIMATE AND HYDROLOGY	41
3.2 GEOLOGICAL SETTING	42
3.3 QUATERNARY GEOLOGY.....	43
3.4 HYDROGEOLOGY.....	44
3.5 STUDY SITE.....	46
4 THE DEVELOPMENT OF THE ARSENIC CALAMITY IN VIETNAM	49
4.1 ARSENIC CONTAMINATION IN THE RED RIVER DELTA	49
4.2 ORIGIN OF THE ARSENIC CONTAMINATION IN THE RED RIVER DELTA.....	51
4.3 MITIGATION MEASURES AND STRATEGIES IN VIETNAM.....	52
4.4 OPEN QUESTIONS	54
5 GEOCHEMICAL PROCESSES UNDERLYING THE SHARP CONTRAST IN DISSOLVED ARSENIC CONCENTRATIONS	57
5.1 INTRODUCTION	57

5.2	MATERIALS AND METHODS.....	58
5.2.1	WATER SAMPLING AND ANALYSIS.....	58
5.2.2	SEDIMENT SAMPLING AND ANALYSIS.....	59
5.2.3	GEOCHEMICAL MODELLING AND STATISTICAL ANALYSIS.....	63
5.3	RESULTS AND INTERPRETATION.....	64
5.3.1	LITHOLOGY AND REFLECTANCE.....	64
5.3.2	HYDROCHEMISTRY.....	67
5.3.3	MINERALOGICAL AND GEOCHEMICAL COMPOSITION.....	71
5.3.4	SEQUENTIAL EXTRACTIONS.....	72
5.4	DISCUSSION.....	74
5.4.1	ASSOCIATIONS OF ARSENIC IN THE SEDIMENT.....	74
5.4.2	FACTORS CONTRIBUTING TO ARSENIC RELEASE AND RETENTION.....	75
5.4.3	SOURCE OF ORGANIC MATTER RESULTING IN REDUCING CONDITIONS.....	76
6	ORIGIN AND REACTIVITY OF SEDIMENTARY ORGANIC MATTER IN THE SEDIMENTS OF VAN PHUC.....	79
6.1	INTRODUCTION.....	79
6.2	METHODS.....	80
6.2.1	EXTRACTION AND CHARACTERIZATION OF ORGANIC MATTER.....	80
6.2.2	ORGANIC CARBON AND NITROGEN ISOTOPIC ANALYSIS.....	81
6.3	RESULTS.....	83
6.3.1	CARBON AND NITROGEN ISOTOPIC SIGNATURES IN THE SEDIMENTS.....	83
6.3.2	DISTRIBUTION OF N-ALKANES IN THE SEDIMENT.....	85
6.4	DISCUSSION.....	87
6.4.1	DEPOSITIONAL ENVIRONMENT AND ORIGIN OF ORGANIC MATTER.....	87
6.4.2	REACTIVITY OF ORGANIC MATTER.....	93
6.4.3	ROLE OF ORGANIC MATTER FOR ARSENIC MOBILISATION IN VAN PHUC.....	94
7	DISTRIBUTIONS AND ASSOCIATIONS OF ARSENIC WITHIN SEDIMENT GRAINS.....	97
7.1	INTRODUCTION.....	97
7.2	METHODS.....	98
7.2.1	SEDIMENT MATERIAL AND PREPARATION.....	98
7.2.2	SCANNING ELECTRON MICROSCOPE (SEM).....	99
7.2.3	MICRO-SYNCHROTRON-XRF (μ S-XRF).....	100
7.2.4	STATISTICAL ANALYSIS.....	101
7.3	RESULTS.....	103
7.3.1	SURFACE STRUCTURES.....	103
7.3.2	ELEMENTAL DISTRIBUTIONS WITHIN GRAINS.....	104
7.3.3	STATISTICAL ANALYSIS.....	111
7.4	DISCUSSION.....	119
7.4.1	ARSENIC BEARING PHASES AND DIFFERENCES BETWEEN THE TWO SEDIMENT CORES 119	
7.4.2	EFFECTS OF SEQUENTIAL EXTRACTION ON THE SEDIMENT COMPOSITION.....	122
8	CONCEPTUAL MODEL FOR THE CURRENT DISSOLVED ARSENIC DISTRIBUTION IN VAN PHUC.....	125
9	CONCLUSIONS.....	133

ABBREVIATIONS	135
LIST OF FIGURES	137
LIST OF TABLES.....	141
REFERENCES.....	143
APPENDIX.....	167

1 INTRODUCTION AND OBJECTIVE OF THE STUDY

Arsenic has long been known as poisonous element and this feature was deliberately used by men for centuries. Nobody thought about the potential ability of As to become a natural mass poison as it is now the case in many countries throughout the world. Therefore, it was not included into routine water quality testing for many years which turned out to be a fatal mistake.

The whole As crisis started in Asia with the good intention of UNICEF and other NGOs (Non governmental organisations) to improve the drinking water quality in many developing countries by installing wells to provide the population with clean water in the mid 1970th. Surface water, until then the main drinking water source, suffered from increasing pollution and, consequently, water quality deteriorated dramatically eliciting water born diseases like cholera or diarrhoea (AHUJA, 2008). The program proved to be successful diminishing the number of illnesses and infant mortality, significantly. From today's point of view, however, the monitoring system was insufficient disregarding elements like As. The drilling of wells continues to this date in Asia, sometimes still in known As affected regions like in Cambodia (M. Simpson, personal communication), because the quality of surface water further deteriorated. Furthermore, the demand for water for drinking and agricultural purposes is still increasing as a result of an enormous population pressure.

Cases of arsenicosis have long ago been attributed to elevated arsenic levels in drinking water in countries such as Taiwan (TSENG ET AL., 1968), Chile (ZALDIVAR, 1974), Mexico (DEL RAZO ET AL., 1990) or Argentina (NICOLLI ET AL., 1989). However, the international scientific community was truly mobilized only after the discovery of numerous cases of melanoma and other As related illnesses like the Black Foot Disease known to arise from chronic As poisoning in the Bengal Delta in the mid 1990s (DAS ET AL., 1996, WORLD BANK, 2005). Other regions with elevated As levels in groundwater have since been identified, primarily in relatively young alluvial deposits,

such as the densely populated deltas of Mekong and Red River in Cambodia and Vietnam (BERG ET AL., 2001; POLYA ET AL., 2005; BUSCHMANN ET AL., 2007; BERG ET AL., 2007; BUSCHMANN ET AL., 2008). Estimated 60 million people are currently at risk in Asia to suffer from some kind of arsenicosis (WORLDBANK, 2005) which emphasises the urgent need for action.

Several water treatment technologies exist or were specially developed to successfully remove As to a satisfactory level (WORLDBANK, 2005). Especially rural areas, however, have often shortage in capital and infrastructure like central water supply systems which constrains an area-wide supply with clean water. Therefore, it is important to better understand the whole system which triggers the As release in order to be able to install wells in safe aquifers only, and, to prevent existing wells from deteriorating water quality. This is further important because an increasing amount of As burdened groundwater is used for irrigation probably leading to an enrichment of As in the food chain and, therefore, worsening the exposure.

In the meantime, much is known about the cause of the As calamity. There is common agreement among scientist that As results from a geogenic source and is released due to natural processes. In this regard, hydrological, geochemical, sedimentological as well as hydrochemical aspects seem to play an important role which will be discussed in detail in the following chapter. However, many questions still remain, especially how the different processes influence each other, the role of organic matter (OM) with regard to As release and especially the causes for the small scale spatial variability of As concentrations.

This thesis aims at approximating some of these open questions within a chosen study area in the Red River Delta, Vietnam, where As concentrations are known to be high and heterogeneously distributed (BERG ET AL., 2007). By means of geochemical, mineralogical and hydrochemical methods significant differences with regard to As release between two locations shall be determined. One focus was also on the small scale elemental distribution of As within sediment grains and occurring alterations due to sequential extractions. These extractions are widely used to get information about associations of As but not much is known about what actually happens within the sediment grains during leaching. In the end, a conceptual model shall be de-

veloped which tries to explain the current situation based on the collected data and might allow presumptions about the future development of As concentrations within the study area.

2 ARSENIC IN GROUNDWATER – AN OVERVIEW

2.1 GENERAL CHEMICAL PROPERTIES

Arsenic is in group 15 (third row, group five) of the periodic table of the elements together with nitrogen and phosphorus and is commonly described as a metalloid. Arsenic occurs in four different oxidation states: -III, 0, III and V (SMEDLEY & KINNIBURG, 2002; PLANT ET AL., 2005). ^{75}As is the only existing stable isotope. Three different allotropes of As are known: α -arsenic is grey, metallic and the most stable form; β - and γ -arsenic are rare, meta-stable and non-metallic (PLANT ET AL., 2005). In its metallic modification As was described by Albertus Magnus (1193 - 1280) for the first time (VAUGHAN, 2006).

Tab. 2.1: Physico-chemical properties of arsenic.

Atomic number	33
Atomic mass [g/mol]	74.9216
Melting point [°C]	817 (at 27,5 bar)
Boiling point [°C]	614 (sublimes)
Density [g/cm ³]	5.73
Electrical resistivity [$\mu\Omega$ /cm]	33.3
Atomic radius [pm]	124.5
Electron configura- tion	[Ar]3d104s24p3

The As bonding is essentially covalent (HIRNER ET AL., 2000). It bonds mainly to oxygen or sulphur as well as to a variety of ligands, which strongly influences its chemical behaviour and toxicity (O'DAY, 2006; Chapter 2.6). More physico-chemical characteristics are listed in Tab. 2.1.

Due to its toxic properties As is used in pesticides and wood preservatives. Furthermore, As is applied in semiconductor, colour or cosmetic industries, for example (HIRNER ET AL., 2000).

2.1.1 ARSENIC IN NATURAL ENVIRONMENT

Arsenic is an ubiquitous element found in the atmosphere, lithosphere, pedosphere, hydrosphere and biosphere. However, 99% of As worldwide is part of the lithosphere (MATSCHULLAT, 1999). Only for this thesis relevant compartments (lithosphere and hydrosphere) are briefly introduced in the following paragraphs. A more detailed overview is given in BGS & DPHE (2001) or SMEDLEY & KINNIBURG (2002).

LITHOSPHERE

In the lithosphere, As is commonly low in concentration. With an average crustal abundance of 1.5 mg/kg it is ranked 47th out of 88 natural occurring elements (BGS & DPHE, 2001; SMEDLEY & KINNIBURG, 2002; PLANT ET AL., 2005). It rarely occurs as native element, but is mainly found in association with sulphur, oxygen and iron (BREWSTER, 1994). The geochemical character of As can be considered as strongly chalcophile (SMEDLEY & KINNIBURG, 2002; PLANT ET AL., 2005). As major constituent, As is part of more than 200 minerals (Tab. 2.2), but most of these minerals are very rare (SMEDLEY & KINNIBURG, 2002). Most common are arsenates (60%) like scorodite, followed by sulphides, like realgar or orpiment (20%). The missing 20% is represented mainly by arsenides, arsenites and oxides. Several of these minerals are of secondary origin formed by weathering processes (BGS & DPHE, 2001).

Tab. 2.2: Selected As minerals and their occurrence in nature (BGS & DPHE, 2001).

Mineral	Composition	Major Occurrence
Realgar	AsS	vein deposits
Orpiment	As ₂ S ₃	hydrothermal veins
Arsenopyrite	FeAsS	mineral veins
Niccolite	NiAs	vein deposit
Arsenolite	As ₂ O ₃	secondary mineral
Scorodite	FeAsO ₄ × 2H ₂ O	secondary mineral

Arsenic can either be incorporated into the crystal lattice and substitutes for S in sulphides or for Si⁴⁺, Al³⁺, Fe³⁺ or Ti⁴⁺ in silicates, or it can be ad-

sorbed, mainly to oxy-hydroxide surfaces (Fe, Mn, Al). Arsenopyrite is the most abundant As bearing mineral, globally (SMEDLEY & KINNIBURG, 2002). More details about As bearing phases are given in Chapter 2.2.

Tab. 2.3: Typical As concentrations of selected rocks, sediments and soils (BGS & DPHE, 2001, and references therein).

Rock/sediment type	As concentration [mg/kg]	
	average	range
Basic rock (basalt)	2	0.18 - 113
Marine shale/mudstone	3 - 15	3 - 490
Sandstone	4.1	0.6 - 120
Bituminous shale	no data	100 - 900
Unconsolidated sediment	3	0.6 - 50
Soil	7.2	0.1 - 55

The concentration of As in different rocks and sediments depends strongly on the mineralogical composition (Tab. 2.3). Igneous and metamorphic rocks mainly have concentrations below 5 mg/kg. In sedimentary rocks the As concentrations are more variable, mostly depending on the abundance of clay minerals, Fe oxy-hydroxides, sulphides and OM which are commonly enriched in As. The mean value found in different sedimentary rocks can be in the range of 20 to 200 mg As/kg. Lower concentrations (~4 mg/kg) are found in sandstones which are mainly composed of quartz and feldspars. Highest concentrations can be found in mudstones, shales, slates, coals (up to 35,000 mg/kg) or in ore deposits (BGS & DPHE, 2001; VAUGHAN, 2006). In aquifers, built up of unconsolidated sediments, the values are basically within a range of 3 - 10 mg/kg, depending on texture and mineralogy (SMEDLEY & KINNIBURG, 2002).

HYDROSPHERE

The concentration of As in the hydrosphere can vary by more than four orders of magnitude under natural conditions (Tab. 2.4). It is dependent on the source of As and influenced by several processes like adsorption-desorption, precipitation-dissolution, oxidation-reduction, and, biological and anthropogenic activities (ROBERTSON, 1989; SMEDLEY & KINNIBURG, 2002). Lowest concentrations commonly occur in rain water (<0.03 µg/L) unless it is affected by smelters, coal burning industries or volcanoes (16 µg/L near copper smelter) (CRECELIUS, 1975; SMEDLEY & KINNIBURG, 2002). In general, rain cannot be considered as an important source for As in groundwater.

Tab. 2.4: Typical As concentrations in different water bodies (SMEDLEY & KINNIBURG, 2002, and references therein).

Water Body	As concentration [µg/L]	Water Body	As concentration [µg/L]
Rain water	0.013 - 0.46	Groundwater	<0.5 - 10
River water	0.13 - 2.1	As-rich provinces	10 - 5,000
Lake water	0.06 - 1.9	Mining related groundwater	50 - 850,000
Seawater	1.0 - 1.8	Geothermal affected groundwater	<10 - 50,000

Concentrations in surface waters are also normally relatively low (typically 0.1 - 2 µg/L, Tab. 2.4). Due to oxic conditions, As is mainly adsorbed to particulate matter which lowers the concentration considerably. Influencing parameters are bedrock lithology, surface recharge as well as hydrothermal (<264 µg/L) or mining affected infiltration (<7,900 µg/L) (BENSON & SPENCER, 1983; SMEDLEY ET AL., 1996; SMEDLEY & KINNIBURG, 2002).

The highest range, resulting from natural processes, can be found in groundwater (<0.5 - 50,000 µg/L, Tab. 2.4). On average, however, the As concentrations are below 10 µg/L (ELLIS & MAHON, 1977; WELCH ET AL., 2000). The distribution of As in groundwater is primarily controlled by the local

geology, hydrology, geochemical conditions, microbiology as well as geothermal and anthropogenic input, but only to a minor degree by high As contents in the source rocks (SMEDLEY & KINNIBURG, 2002).

High As regions are widely distributed around the world (Fig. 2.1). However, they are by no means typical for groundwater environments and only develop under special circumstances. Groundwater As problems result from natural sources (young aquifers, geothermal input) as well as from anthropogenic activities (mostly mining activities) and can occur under both oxidizing and reducing conditions in humid, temperate and arid areas.

Reducing environments: In young, unconsolidated aquifers, high As concentrations in groundwater are mainly due to reducing conditions under which Fe and other oxy-hydroxide minerals are dissolved and adsorbed or incorporated As is released to the groundwater. Typical examples occur in Bangladesh (<2,500 µg/L), West Bengal (<3,200 µg/L), Inner Mongolia (<2,400 µg/L), Vietnam (<3,050 µg/L) etc. (DAS ET AL., 1996; LUO ET AL., 1997; BERG ET AL., 2001; BGS & DPHE, 2001). Arsenic release in reducing environments will be discussed in more detail in Chapter 2.3.

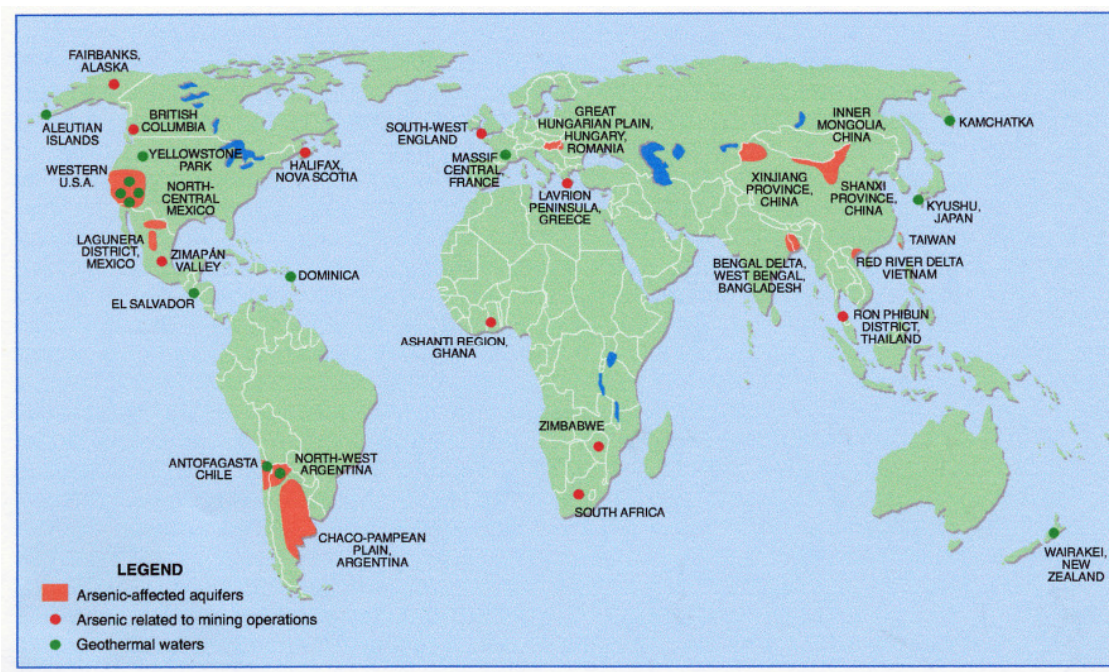


Fig. 2.1: Global distribution of known As affected regions in 2001, divided into As affected aquifers, geothermal groundwaters and some major mining related As problems (BGS & DPHE, 2001). In the meantime more areas suffering from natural As problems have been detected (see text).

Oxidizing environments: In arid and semiarid areas evaporation can result in groundwater pH values >8. Arsenic(V), which is mainly present in oxic conditions, can get easily desorbed under such conditions (Chapter 2.1.2). Examples can be found in Mexico (<620 µg/L) or Argentina (5,300 µg/L) (NICOLLI ET AL., 1989; DEL RAZO ET AL., 1990).

Geothermal sources: Geothermal waters are usually highly mineralized because they can leach elements out of rocks on their way to the surface. High As concentrations are found, for example, in Chile (>50,000 µg/L), Kamchatka (5,900 µg/L) or New Zealand (<3,800 µg/L) (WHITE ET AL., 1963; ELLIS & MAHON, 1977; ROBINSON ET AL., 1995).

Mining related environments: Arsenic bearing sulphides, which are typical for hydrothermally affected areas and ore deposits, get oxidized during different mining activities and, consequently, As can be released into the groundwater. Examples can be found in Canada (<10,000 µg/L), USA (<2,000 µg/L) and many other countries (WELCH ET AL., 1988; AZCUE ET AL., 1995; BGS & DPHE, 2001).

2.1.2 ARSENIC SPECIES AND TRANSFORMATION PROCESSES

Several organic and inorganic As species exist in the environment. Their occurrence is controlled by redox and methylation processes. Each species has different properties with regard to mobilization, bioavailability and toxicity (Chapter 2.3.2; 2.6) (HERING & KNEEBONE, 2002). The inorganic forms are dominant in natural waters as oxyanions of trivalent arsenite (As(III)) and pentavalent arsenate (As(V)). The speciation is mainly controlled by the redox environment (Eh) and the pH (Fig. 2.2). Under oxidizing conditions As(V) is dominant in form of H_2AsO_4^- at pH 2 - 6.9 and HAsO_4^{2-} at higher pH values. Reducing conditions lead to a prevalence of As(III) as uncharged species H_3AsO_3 at pH <9.2 (SMEDLEY & KINNIBURG, 2002). Presence of high sulphur concentrations in strongly reducing, mainly acidic environments can lead to the formation of arsenite-sulphide species (thioarsenites: $\text{As}_3\text{S}_4(\text{SH})_2^-$ or $\text{AsO}(\text{SH})_2^-$). Recent studies have indicated that thioarsenates ($\text{HAsO}_3\text{S}^{2-}$, $\text{HAsO}_2\text{S}_3^{2-}$, AsOS_3^{3-} , AsS_4^{3-}) might be dominating in natural waters which contain sulphur. Due to the high affinity between As(III) and sulphur, thioarsenate and some elemental As is formed instead of thioarsenite due to

a disproportionation reaction (STAUDER ET AL., 2005). Acidic conditions also favour the precipitation of orpiment (As_2S_3) and realgar (AsS) (Fig. 2.2; CULLEN & REIMER, 1989; SCHWEDT & RIECKHOFF, 1996; ROCHETTE ET AL., 2000). In anoxic groundwaters, high bicarbonate concentrations can support the dissolution of As sulphides, leading to the formation of As carbonate species, as proposed by KIM ET AL. (2000).

Fig. 2.2 gives an overview about the stability of the different species of the As-O-S system. However, this Eh-pH-diagram is only a simplification of a complex natural system. Iron, for example, also strongly influences the speciation of As.

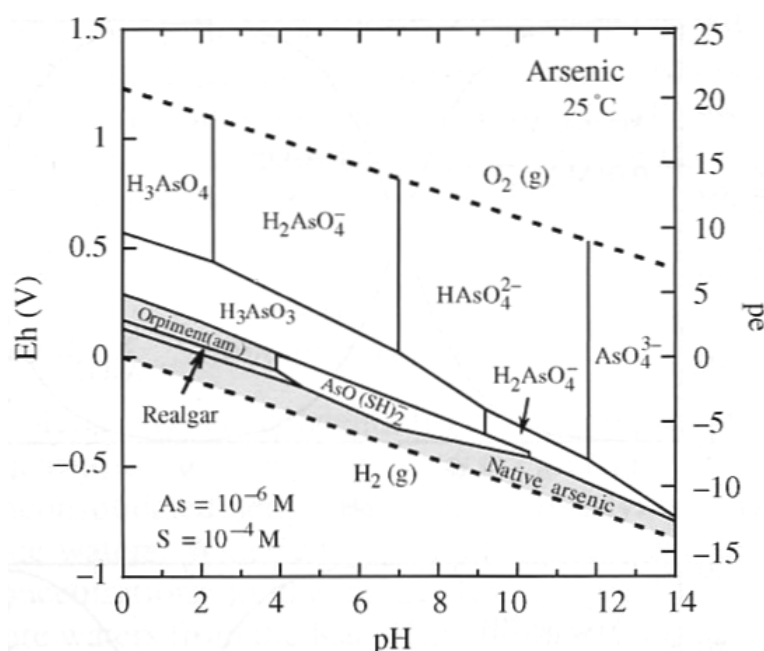


Fig. 2.2: Eh-pH stability diagram of As species in the presence of sulphur at 25°C, 1bar. The grey area represents solid phases (PLANT ET AL., 2005).

Inorganic As species can be transformed due to redox processes as well as microbial activity. Thermodynamic calculations predict that As(V) should be dominant in all but strongly reducing groundwaters. However, in reality the ratio of As(V) to As(III) can vary considerably, depending on the abundance of redox active solids, organic carbon (OC), activity of microorganisms as well as on the extent of convection and diffusion of dissolved oxygen (KORTE & FERNANDO, 1991; SMEDLEY & KINNIBURG, 2002). In Bangladesh, for example, the As(III)/As(total) ratio can vary from 0.1 to 0.9 (BGS & DPHE, 2001).

Kinetic considerations also play a role with regard to the speciation of As. In principle, As(III) should not be present under aerobic conditions. The oxidation of As(III) by dissolved oxygen, however, is very slow. EARY AND SCHRAMKE (1990) determined a half life of 1 - 3 years for As(III) in water equilibrated with oxygen. In presence of Mn oxides the reaction rate increases dramatically (OSCARSON ET AL., 1981). Oxidation by Fe oxyhydroxides is slower compared to Mn oxides. REDMAN ET AL. (2002) highlighted the influence of natural organic matter (NOM) on As speciation, due to its ability to catalyse both oxidation and reduction reactions.

Less is known about As transformation in solid state. MASSCHELEYN ET AL. (1991) detected As(V) reduction already under moderately reducing conditions. Microorganisms, however, highly influence transformation processes in both solid and aqueous phase, accelerating the reactions by orders of magnitude (SMEDLEY & KINNIBURG, 2002). Some microbes are able to use As as energy source. Chemoautotrophic arsenite oxidizing bacteria (CAO's) can oxidize As(III) by using oxygen or nitrate as electron acceptor and CO₂ as sole carbon source. Oxidation by heterotrophic organisms (HAO's) is mainly seen as a detoxification mechanism, taking place on the cell's outer membrane, using OC as energy source. Furthermore, As(V) can be reduced by organisms, called dissimilatory As(V)-reducing prokaryotes (DARP), through oxidizing H₂ or OM compounds (e.g. lactate, acetate, formate) (AHMANN ET AL., 1994; OREMLAND ET AL., 2000; OREMLAND & STOLZ, 2003). No obligate DARP's were isolated so far; all of them can also use other electron acceptors. These biotic processes seem to play an essential role in the mobilization of As into groundwater (HARVEY ET AL., 2002; OREMLAND & STOLZ, 2003).

Some organisms reduce As(V) for detoxification purposes and not in order to gain energy (MACUR ET AL., 2001). Biomethylation of inorganic As through bacteria (e.g. *Escherichia coli*) and fungi, for example, is historically seen as such a process (FERGUSON, 1990; YAMAUCHI & FOWLER, 1994). In the course of reaction, As(V) is firstly reduced to As(III) followed by a stepwise methylation (substitution of -O by -CH₃) into mono-, di-, and tri-methylated products (CHALLENGER, 1945). These are mainly mono-methyl arsonic acid (MMA), di-methyl arsenic acid (DMA) and tri-methyl arsine oxide (TMA).

MMA and DMA are also built through human or animal metabolism and excreted via urine into the environment (CULLEN & REIMER, 1989). Under anaerobic conditions these organo-arsenicals will be reduced to volatile methylarsines (MANDAL & SUZUKI, 2002; MUKHOPADHYAY ET AL., 2002). Further organo-arsenicals like arsenobetain and arsenosugars mostly play a role in the marine environment as they are enriched in algae (arsenosugars) and marine organisms like fish and invertebrates (arsenobetain) (MUKHOPADHYAY ET AL., 2002). Their role in the groundwater is normally negligible (SMEDLEY & KINNIBURG, 2002).

2.2 ARSENIC BEARING PHASES IN AQUIFERS

More than 200 As minerals are known, but they are rare or absent in aquifer environments. Instead, As is partitioned into different primary rock forming minerals or weathering formed secondary minerals (e.g. siderite, Fe oxyhydroxide coatings) (SENGUPTA ET AL., 2004). There, As is either incorporated into the mineral structure or is adsorbed on its surface. The concentrations are generally low (Tab. 2.5), but vary according to the source of the minerals and the geochemical processes that have occurred during the deposition of the aquifer material (SMEDLEY & KINNIBURG, 2002).

Most of the silicates are not considered as major As carrier, with concentrations of ~ 1 mg As/kg which is probably true for quartz or feldspars (BAUER & ONISHI, 1969). Frequently, however, they are coated with Fe oxyhydroxides (e.g. hematite, goethite or ferrihydrite) which enhances the average concentrations of the grains to 30 mg As/kg or more (e.g. PAL ET AL., 2002; HORNEMAN ET AL., 2004; SENGUPTA ET AL., 2004). The coatings itself are seen as one of the primary As hosts in oxic sedimentary environments (NICKSON ET AL., 2000; SWARTZ ET AL., 2004). The close association of As and Fe in sediments is reflected by a sometimes strong correlation (PLANT ET AL., 2005). Arsenic can be highly enriched in Fe bearing phases (coatings or clastic minerals), especially when they are formed from pyrite oxidation. Additionally, Fe minerals (notably Fe oxyhydroxides) have a high As adsorption capacity, forming inner-sphere surface complexes (BRANNON & PATRICK, 1987; WAYCHUNAS ET AL., 1993; MANNING ET AL., 1998). Concentrations of ≤ 160 mg As/kg were measured in hematite (BAUER & ONISHI, 1969) and $\leq 2,000$

mg/kg in undifferentiated Fe oxy-hydroxides (BOYLE & JONASSON, 1973). Ilmenite and magnetite show much lower As contents of 8 - 40 mg/kg (SENGUPTA ET AL., 2004). Siderite, mainly formed as a secondary phase in aquifers, is also known to host As (5 - 20 mg/kg) (BHATTACHARYA ET AL., 2003; GUO ET AL., 2007). SENGUPTA ET AL. (2004) assumed that siderite, grown on clastic minerals, is responsible for the relatively high As concentrations at their study site in Bengal Delta sediments. Oxides of Mn, Al and Ti are also known to adsorb As and can, therefore, be considered as possible As carriers (DRIEHAUS ET AL., 1995; LENOBLE ET AL., 2004; BALAJI ET AL., 2000; SINGH & PLANT, 2004; BANG ET AL., 2005).

Tab. 2.5: As concentrations in different rock forming minerals.

Mineral	As concentration [mg/kg]	Mineral	As concentration [mg/kg]
Hematite	<160 ^[1]	Biotite	<50 ^[4]
Ilmenite/Magnetite	8 - 40 ^[2]	Chlorite	5 - 50 ^[2]
Pyrite	100 - 77,000 ^[1]	Illite	10 - 41 ^[3]
Quartz/Feldspar	<0.1 - 2.1 ^[1]	Siderite	5 - 20 ^[5]
Iron oxide coated quartz	30 ^[3]	Calcite	9 - 40 ^[3]

[1]SMEDLEY & KINNIBURG, 2002; [2]SENGUPTA ET AL., 2004; [3]PAL ET AL., 2002; [4]SEDDIQUE ET AL., 2008; [5]GUO ET AL., 2007

Several authors also highlighted the importance of some Fe bearing silicate phases (biotite, chlorite, amphibole etc.) for the As pool of the aquifers (e.g. ANAWAR ET AL., 2002; DOWLING ET AL., 2002; NATH ET AL., 2005; WAGNER ET AL., 2005; CHARLET ET AL., 2007). In their study in Bangladesh, SEDDIQUE ET AL. (2008) identified biotite as main As carrier (26.5 - 49.6 mg/kg). PAL ET AL. (2002) and SENGUPTA ET AL. (2004) measured a considerable As content in different silicate minerals like illite (10 - 40 mg/kg), chlorite (5 - 50 mg/kg) or biotite (9 mg/kg). These minerals mainly belong to the pelitic fraction where As can also adsorb on the edges of the structure because of the oxide-like

character of the phyllosilicates (GOLDBERG & GLAUBIG, 1988; SMEDLEY & KINNIBURG, 2002).

Despite the high affinity of As for sulphur, authigenic pyrite is the only sulphide mineral in aquifers with a considerable enrichment of As (Tab. 2.5; O'DAY, 2006). Arsenic rich pyrite can contain up to 10% As (PLANT ET AL., 2005). Several authors assign pyrite a major role in the As partitioning in sediments (e.g. ANAWAR ET AL., 2002; LOWERS ET AL., 2007). Biogenic pyrite formation, for example, can remove large amounts of As together with other elements like Pb, Ag, Au, Co and Ni from solution (SCHOLZ & NEUMANN, 2007) depending on the sulphur content of the aquifer (SAUNDERS ET AL., 1997; SMEDLEY & KINNIBURG, 2002). While SEDDIQUE ET AL. (2008) could not prove any importance of pyrite at their study site, DAS ET AL. (1996) hold oxidation of pyrite responsible for high As concentrations in groundwater (Chapter 2.3.1).

Further noteworthy As bearing phases in sediments are calcite (e.g. HARVEY ET AL., 2002; SWARTZ ET AL., 2004) and OM (MEHARG ET AL., 2006; SEDDIQUE ET AL., 2008). PAL ET AL. (2002) found 9 - 40 mg As/kg in peat layers in West Bengal. Diagenetic processes can remobilize As and, therefore, constantly change the association and concentration of As in aquifer material.

Several analytical techniques are available in order to get information about where, how and to what extent As is fixed in different mineral phases. Sequential extractions are frequently applied because they are easy to perform; however, the results are arguable and definitely give only a hint about the actual circumstances. More detailed, small scale information can be gained through more modern, synchrotron (μ S) based methods like μ S-XRF, μ S-XRD or μ S-XAS. However, these analyses are more complex and not easily available.

2.3 PROCESSES INFLUENCING THE ARSENIC CONCENTRATION IN THE GROUNDWATER

The release of As into groundwater in the affected regions worldwide is generally seen as a natural phenomenon and does not call for truly exceptional conditions. Over the years, various hypotheses have been postulated

in order to explain high As concentrations in groundwater, but it is difficult to evaluate, which process is driving the mobilization. Most probable a variety of mechanisms in combination with special hydrogeological conditions are responsible (BGS & DPHE, 2001).

Arsenic concentrations are very sensitive to any shifts in sediment and water chemistry (BGS & DPHE, 2001), therefore, total concentrations of As in the sediment do not give any information about its potential mobility. More important is the proportion of easily mobilizable As (HUDSON-EDWARDS ET AL., 2004; ZHENG ET AL., 2005). A small change in the partitioning of As between sediment and water can give rise to a significant increase in the As concentrations of the groundwater (RADU ET AL., 2005; MEHARG ET AL., 2006). A loss of only 0.1 μg As/g from the solid can increase the As concentration in the solution by 200 $\mu\text{g}/\text{L}$ (VAN GEEN ET AL., 2003).

In order to evaluate the type of interaction between dissolved As and sediment as well as to assess main release mechanisms it is, therefore, important to estimate the response of As concentrations to changes in the environment.

2.3.1 DISSOLUTION AND PRECIPITATION OF MINERAL PHASES

REDUCTIVE DISSOLUTION OF FE-OXIDES/HYDROXIDES

Iron oxy-hydroxides are well known As bearing phases (Tab. 2.5; Chapter 2.2) which are thermodynamically stable only under oxidizing conditions. The reductive dissolution of different Fe oxy-hydroxides, which are common in sedimentary environments, is widely accepted as a key process for the release of As into groundwater (NICKSON ET AL., 2000; BGS & DPHE, 2001; DOWLING ET AL., 2002; HARVEY ET AL., 2002; STÜBEN ET AL., 2003; CHARLET & POLYA, 2006). Which Fe oxy-hydroxide phase dissolves first mostly depends on its stability which is related to the crystallinity of mineral phases (BGS & DPHE, 2001).

Occasionally, low dissolved Fe concentrations in high dissolved As regions, however, indicate that processes involved are more complicated than sole congruent dissolution of Fe oxy-hydroxides with subsequent release of

incorporated or adsorbed As. Processes like re-adsorption of As or Fe(II) to surfaces as well as re-precipitation and transformation of Fe phases (see page 19) may conceal the assumable correlation between As and Fe in the groundwater (HORNEMAN ET AL., 2004; KOCAR ET AL., 2006; PEDERSEN ET AL., 2006). Furthermore, the place of Fe reduction and the occurrence of high As concentrations can be decoupled. POLIZZOTTO ET AL. (2006) proposed that As is released from Fe oxy-hydroxides through redox cycling in surface soils and subsequently transported downwards into the aquifer.

Manganese oxides are also known to adsorb or incorporate As in high amounts. -Consequently, their reductive dissolution, which already occurs at higher redox conditions, will also release As to the groundwater (SMEDLEY & KINNIBURG, 2002; STÜBEN ET AL., 2003).

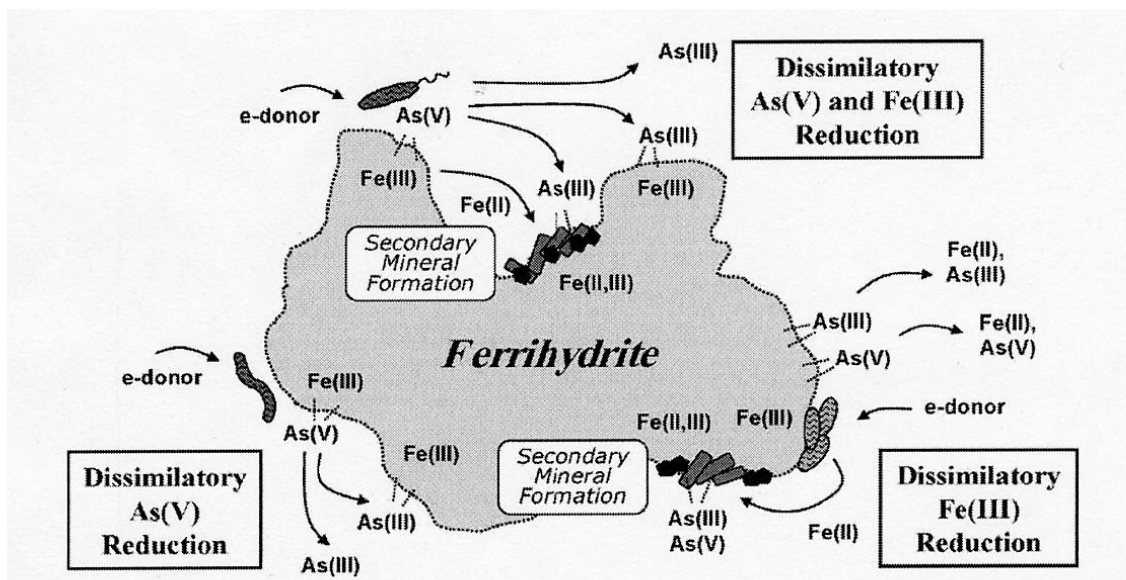


Fig. 2.3: Effects of biotic and abiotic processes on the release of As. Fe(III) and As(V) can be microbially reduced using OC as electron donor, releasing Fe(II) and As(III) into the solution. Re-adsorption, competition and precipitation of secondary mineral phases can influence the As mobility (HERBEL & FENDORF, 2006).

What is clear is that the microbially driven decomposition of OM plays an important role for the onset and the maintenance of reducing conditions in aquifers (LOVLEY, 1992; LOVLEY & CHAPELLE, 1995; ROWLAND ET AL., 2006; ROWLAND ET AL., 2007). Consequently, the supply of reductants as well as microbial activity is a prerequisite for the reductive dissolution of Fe oxy-hydroxides (BGS & DPHE, 2001). The rapid burial of relatively young sedi-

ments high in OC seems to promote reducing conditions (NICKSON ET AL., 2000). Further possible sources of OC are currently under discussion, like leaching of OC from peat layers or confining sediments (STÜBEN ET AL., 2003; ZHENG ET AL., 2004), groundwater recharge from surface water rich in dissolved OC (DOC) (HARVEY ET AL., 2002) or anthropogenic sources (BUKAU ET AL., 2000; MCARTHUR ET AL., 2001). For more details see Chapter 2.5.

Direct reduction of Fe oxy-hydroxides by dissimilatory Fe reducing bacteria (DIRB) using OM as electron donor is also known to occur and could, therefore, have an influence on the As mobilization (Fig. 2.3; ISLAM ET AL., 2004). *Shewanella alga* (strain BrY), for example, can reduce Fe(III) to Fe(II) in scorodite ($\text{FeAsO}_4 \cdot 2\text{H}_2\text{O}$), leading to the release of As(V) (CUMMINGS ET AL., 1999). Furthermore, microorganisms have been isolated (e.g. *Sulfospirillum barnesii* (strain SES-3); *Shewanella putrefaciens* (strain Cn-32)) which are able to reduce both Fe(III) and As(V) and, consequently, could promote As mobilization by simultaneously reducing the capacity for As adsorption (LAVERMAN ET AL., 1995). However, KOCAR ET AL. (2006) have shown that Fe(III) reduction induced by *Sulfospirillum barnesii* or *Shewanella putrefaciens* can also lead to mineral transformations accompanied by retention of As due to its incorporation into the freshly build mineral structure.

DISSOLUTION AND PRECIPITATION OF PYRITE

Pyrite is able to incorporate As in considerable amounts (Tab. 2.5; Chapter 2.2). However, it is thermodynamically only stable under reducing conditions, therefore, it was proposed, that oxidation of pyrite in aquifers could explain the As enrichment in groundwater. Oxidizing conditions could develop near the surface or due to heavy groundwater withdrawal leading to a drawdown of the water table and exposing the before reducing sediments to oxygen (DAS ET AL., 1996; CHOWDHURY ET AL., 1999). Consequently, high As and sulphate concentrations would be expectable in more oxidized zones which is not the case in most of the affected aquifers in Bangladesh where conditions are mainly reducing. Furthermore, it is assumed that ~90% of the released As would have to be readsorbed by precipitating Fe oxy-hydroxides turning pyrite oxidation into an inefficient mechanism (BGS & DPHE, 2001; STÜBEN ET AL., 2003). NICKSON ET AL. (2000) and HARVEY ET AL.

(2002) concluded from their study, that the influence of pyrite oxidation on the As concentration is negligible. High As concentrations in groundwater due to pyrite oxidation seems only to be important in close vicinity of mines (PLANT ET AL., 2005).

More important is the role of pyrite as a sink for As (MCARTHUR ET AL., 2001; ANAWAR ET AL., 2002; STÜBEN ET AL., 2003, SCHOLZ & NEUMANN, 2007). In presence of sufficient dissolved Fe(II) and S^{2-} under strongly reducing conditions pyrite will precipitate and incorporate As. According to LOWERS ET AL. (2007) high dissolved As/S ratios favour the incorporation of greater amounts of As. Furthermore, the formation of thioarsenate is assumable (Chapter 2.1.2) which can adsorb onto different mineral phases (STAUDER ET AL., 2005).

PRECIPITATION AND TRANSFORMATION OF MINERAL PHASES

Transformation of mineral phases in aquifers can either enhance or lower their ability to retain As. Secondary Fe oxy-hydroxides, for example, go through aging processes which generally increases their crystallinity but reduces the specific surface area (SSA). The SSA, however, significantly controls the sorption of As. Consequently, loss of SSA results in release of As to the groundwater (DIXIT & HERING, 2003). Which mineral develops during transformation depends on the dissolved Fe(II) concentration, pH, temperature, redox of the system and foreign ions (PEDERSEN ET AL., 2006). Transformation into more stable minerals like goethite (α -FeOOH) or magnetite (Fe_3O_4), however, does not always lead to a release of As, because it can also get incorporated into the newly evolving mineral structure (PEDERSEN ET AL., 2006).

There are indications that solid state transformation of Fe(III) oxy-hydroxides under reducing conditions can lead to the formation of mixed-valence minerals, like green rust (Fe(II)-Fe(III) hydroxide) or magnetite which is visible in the change of sediment colour from brownish to greyish. The change in oxidation state will probably also alter the surface structure and charge (e.g. point of zero charge), leading to a modification of the adsorption capacity (BGS & DPHE, 2001; SMEDLEY & KINNIBURG, 2002).

Precipitation of new mineral phases also influences the As distribution in the aquifer, probably mainly in terms of As removal. Under more oxidizing conditions, precipitation of Fe bearing minerals can significantly reduce the As concentration in the solution (REYNOLDS ET AL., 1999). Under reducing conditions, typical in As affected aquifers, these Fe phases will be dissolved releasing As(III) and Fe(II). DIXIT AND HERING (2006) and HERBAL AND FENDORF (2006) proposed that re-adsorption of As(III) and Fe(II) to oxide surfaces can lead to the formation of As(III)-Fe(II) bearing surface precipitates which diminishes the As release. Additionally, the concentrations of HCO_3^- and PO_4^{3-} are usually high in reducing aquifers (Chapter 2.4), resulting in the precipitation of minerals like siderite (FeCO_3), vivianite ($\text{Fe}_3(\text{PO}_4)_2 \times 8\text{H}_2\text{O}$) or green rust. The formation of these minerals can also be microbially mediated (FREDRICKSON ET AL., 1998). Siderite is known to effectively remove As from solutions due to adsorption or incorporation (BHATTACHARYA ET AL., 2003; GUO ET AL., 2007). Much less is known about the role of vivianite. In a study of ISLAM ET AL. (2007), As(III) was considerably retained by vivianite.

2.3.2 ADSORPTION AND DESORPTION PROCESSES

Several sediment constituents are known to be able to highly adsorb As (Chapter 2.2) and, therefore, considerably regulate the As mobility in aquifers. Consequently, every process that influences the adsorption capacity, can lead to release or fixation of As. The amount of As adsorbed is mainly controlled by the As concentration in the solution and the available surface sites. Further important influencing factors are the speciation of As, pH of solution, charge and specific area of sorbent surface, concentration of possible competitors as well as microbial activity (BGS & DPHE, 2001; DIXIT & HERING, 2003; GUO ET AL., 2007; STOLLENWERK ET AL., 2007). Reducing the SSA by dissolution or transformation of mineral phases (see paragraphs above) or by blocking the active surface with competitors might be one cause for high As concentrations in aquifers systems worldwide (DIXIT & HERING, 2003).

As mentioned in chapter 2.1.2 the charge of inorganic As species strongly depends on the pH (Fig. 2.4). In the range common in groundwater (pH 6-7.5), As(V) occurs as negatively charged species, whereas As(III) is

mainly neutral. The sorption itself depends on the surface charge which is mainly positive for most of the sediment particles between pH 3 - 7 (STOLLENWERK, 2003). Consequently, As(V) is thought to generally adsorb more strongly and to a higher extent on mineral phases compared to As(III) in natural groundwaters with $\text{pH} \leq 7$. This is considered to be the main cause for the higher mobility of As(III) (KORTE & FERNANDO, 1991; BGS & DPHE, 2001; SMEDLEY & KINNIBURG, 2002). However, the pH at which both species are sorbed equally is further influenced by the type and crystallinity of mineral phases, the solid/solution ratio as well as by the presence of further ions (DIXIT & HERING, 2003; KOCAR ET AL., 2006). DIXIT AND HERING (2003), for example, showed that As(III) can sorb to a similar or even greater extent on goethite in a pH range of 6 - 9.

As illustrated in Fig. 2.4, a shift of pH or the reduction of As(V) can alter the adsorption behaviour in sediments. In As affected aquifers the pH is mainly neutral so the first option is less likely to be the major cause for As release in most groundwater environments. Reduction and oxidation of As, however, is known to occur frequently in aquifers due to changes in the redox state of the groundwater (MENG ET AL., 2001; SMEDLEY & KINNIBURG, 2002). Furthermore, several microorganisms exist which are able to reduce As(V) (DARP) or oxidize As(III) (CAO's, HAO's) both in solid phase and in solution (Chapter 2.1.2). Mn oxides like birnessite (MnO_2) or Ti oxides (TiO_2) are also able to oxidize As(III) to As(V) (PLANT ET AL., 2005) and, therefore, have an influence on the adsorption of As. Desorption from different minerals (Fe-, Mn-, Al-oxides or clay) due to reduction of As(V) to As(III) is regarded as a considerable mobilization mechanism (BGS & DPHE, 2001; SMEDLEY & KINNIBURG, 2002). ZOBRIET ET AL. (2000), for example, showed that microbial reduction (*Sulphospirillum barnesii*) of As(V) sorbed to amorphous Al oxides can result in high dissolved As(III) concentrations in the solution.

The influence of competing ions on the sorption of As is widely discussed. In reducing aquifers PO_4^{3-} , HCO_3^- and DOC are considered as possible competitors depending on the pH and the minerals present (PLANT ET AL., 2005). SWARTZ ET AL. (2004) proposed that competition with these compounds is able to sustain elevated As levels in Bangladesh. Cations like Ca^{2+} ,

Mg^{2+} or Fe^{2+} , however, are known to counteract to some extent by increasing As adsorption to the surface (BGS & DPHE, 2001; DIXIT & HERING, 2003).

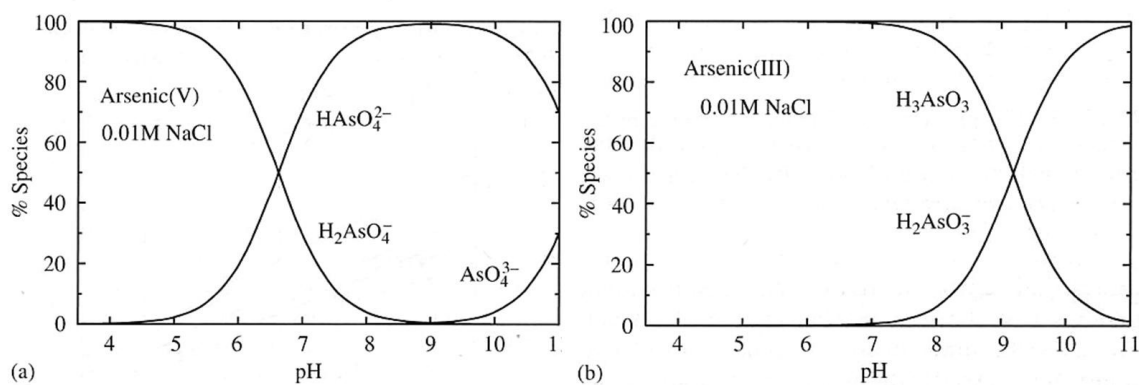


Fig. 2.4: Speciation of As(V) and As(III) as a function of pH in a 0.01M NaCl medium at 25°C (SMEDLEY & KINNIBURG, 2002, modified).

Due to similar chemical properties, PO_4^{3-} is able to greatly reduce sorption of As. In this regard, As(V) is much more affected as compared to As(III) (JAIN & LOEPPERT, 2000; BGS & DPHE, 2001; SU & PULSE, 2001). The presence of silicate ions in solution also influences the As adsorption onto ferric oxides (MENG ET AL., 2000). Arsenic(III) and silicate form both weak acids and, therefore, competition with As(III) is much more pronounced. The effect of carbonate species is more controversial. APELLO ET AL. (2002) and ANAWAR ET AL. (2004) concluded from their experiments that high concentrations of HCO_3^- result in considerable desorption of As. However, MENG ET AL. (2000) and RADU ET AL. (2005) could not confirm these results in their studies.

Dissolved organic matter (DOM) can influence the adsorption of As in various ways. Firstly, it can bind to several minerals typical for sedimentary environments (Fe, Al oxides, and kaolinite) and reduce the available sorption sites or displace already sorbed As (XU ET AL., 1988; GRAFE ET AL., 2001). Secondly, DOM can enhance As leaching by forming aqueous As complexes (REDMAN ET AL., 2002). Thirdly, DOM is known to catalyze both oxidation and reduction reactions and, therefore, promoting transformation of As species and reductive desorption (BAUER & BLODAU, 2006).

So far a lot of laboratory experiments have been performed with different model oxide compounds, but still not enough is known about the sorp-

tion behaviour of As with natural materials, notably as a function of the great variety of possible influencing parameters in aquifers.

2.3.3 FURTHER INFLUENCING PARAMETERS OF ARSENIC CONCENTRATION IN THE WATER

In addition to the above discussed processes (chapters 2.3.1, 2.3.2) a series of other factors are considered to directly or indirectly influence the As distribution in aquifers, like e.g., the age of water and sediment (e.g. BGS & DPHE, 2001; RADLOFF ET AL., 2007), the flushing history of the aquifer (e.g. DOWLING ET AL., 2002; VAN GEEN ET AL., 2008A), geology (e.g. PAL ET AL., 2002), geomorphology (e.g. BUSCHMANN ET AL., 2007), hydrology/hydrogeology (e.g. SMEDLEY & KINNIBURG, 2002; HARVEY ET AL., 2006; STUTE ET AL., 2007) as well as anthropogenic factors (e.g. DAS ET AL., 1996; BGS & DPHE, 2001).

Groundwaters high in dissolved As mainly occur in Holocene sediments with relatively young groundwater (<30 a) whereas deep wells, penetrating into Pleistocene deposits are frequently low in As. STUTE ET AL (2007), for example, found a linear relationship between groundwater age and As levels on a time scale of 30 years. RADLOFF ET AL. (2007) assumed a constant As release with time ($19 \pm 2 \mu\text{g As /L/yr}$) and, therefore, concluded that groundwater age in combination with flow patterns are determinative.

Shallow water is mainly low in As due to oxic conditions, dilution with infiltrating water and short contact time with sediment. In deep aquifers, on the other hand, the groundwater is relatively old (<50 a) and the sediment is mainly deposited during Pleistocene epoch. It could be speculated that the OM content in the older sediments was low from the very beginning and, therefore, conditions never have been favourable for As mobilization. Furthermore, enhanced flushing of the aquifer during Pleistocene could be an explanation for low concentrations by constantly exchanging high As groundwater with water low in As. At that time the hydraulic gradient was much higher compared to today due to a much lower sea level (BGS & DPHE, 2001). At present, the groundwater movement is very slow because the delta morphology is nearly flat. VAN GEEN ET AL. (2008) proposed that the distribution of As in the Bengal Basin might reflect the variable flushing history of the sediments.

There is a general consensus about the importance of hydrology and hydrogeology on the distribution of As concentrations because both have a considerable influence on infiltration of surface water, groundwater movement as well as transport of As (DOWLING ET AL., 2002; STUTE ET AL., 2007; POLIZZOTTO ET AL., 2008). HARVEY ET AL. (2006), for example, related the distribution of As concentrations to the flow pattern of the groundwater. Fast flowing can enhance the flushing of As from the aquifer, e.g., due to excessive pumping for irrigation (HARVEY ET AL., 2002; STUTE ET AL., 2007).

Furthermore, As can be released elsewhere than where the high concentrations occur (e.g., near-surface sediments), and where release conditions are more favourable being subsequently transported through groundwater flow into the aquifer (HARVEY ET AL., 2006; POLIZZOTTO ET AL., 2008). In this case, As concentrations will depend on the rate of release and the groundwater flow velocity. Areas of enhanced recharge can additionally introduce compounds like OM or PO_3^{3-} from fertilizers that might have an influence on the As partitioning (BGS & DPHE, 2001; HARVEY ET AL., 2006). However, fertilizers have only been used excessively for a relatively short time; therefore, PO_3^{3-} from fertilizers is only considerable competitor in very young, shallow groundwater (HARVEY ET AL., 2002).

Hydraulic conductivity depends on the grain size and, therefore, also on the lithology of the aquifer. PAL ET AL. (2002), for example, proposed to define safe groundwater zones with regard to the lithology. Low As regions are mainly protected by thick clay toppings preventing the introduction of labile OM. ZHENG ET AL. (2005) concluded from their study, that deep water is low in As partly because of its protection by a separating clay layer. By contrast, VAN GEEN ET AL. (2006B) assumed that high recharge through permeable surface soils might dilute groundwater and, therefore, prevent As accumulation. The transport of solutes into the underground and within the aquifer is highly complex; consequently, hydrogeological modelling is an important tool to better understand the As distribution in aquifers (HARVEY ET AL., 2006).

2.4 CHARACTERISTICS OF HIGH ARSENIC REGIONS

A lot of knowledge about the As problem has been gathered over the years. For prediction and detection of further affected areas it is important to

summarize the characteristics of high As regions. Generally, comparable situations are found in deltaic areas with low hydraulic gradients (SMEDLEY & KINNIBURG, 2002). The As content of the alluvial sediment is within a normal range (<2 - 20 mg/kg), but there seems to be some kind of association between As and Fe in the solid phase (HARVEY ET AL., 2002). Characteristic are high amounts of easily mobilizable As in the sediment, i.e. of As adsorbed to mineral surfaces (STUTE ET AL., 2007). The sediments are relatively young, mainly of Holocene age, and are often rich in OM. The material was buried rapidly after sedimentation; consequently, reducing conditions ($E_h < 100$) are widespread in this environment (BGS & DPHE, 2001; SMEDLEY & KINNIBURG, 2002).

Along with As, Fe and Mn are typically high in concentration in the groundwater because their oxide phases will get dissolved in reducing environments. Additionally, levels of HCO_3^- , NH_4^+ and PO_4^{3-} are elevated being products of OM degradation or mineral dissolution. Reducing conditions can only develop when electron acceptors like O_2 , NO_3^- or SO_4^{2-} are gradually consumed. The pH is commonly around 7 (BGS & DPHE, 2001; DOWLING ET AL., 2002; SMEDLEY & KINNIBURG, 2002).

A patchy distribution of high and low concentrated areas occurring in close vicinity is typical for As affected deltas. Pronounced differences in As levels can be found within distances of 100 m (BGS & DPHE, 2001; VAN GEEN ET AL., 2003; MCARTHUR ET AL., 2004). Recent studies in some areas of the Red River Delta (RRD) have revealed significant differences even within short distances of 10 - 20 m (BERG ET AL., 2008). Several explanations have been proposed for the heterogeneous spatial distribution of As, including differences in the subsurface lithology, mineralogy (difference in adsorption capacity), geochemistry, local hydrology, and the abundance of organic material (PAL ET AL., 2002; VAN GEEN ET AL., 2006A; STUTE ET AL., 2007). Areas of recharge (ponds, river channels) and discharge (irrigation), for example, are often situated apart from each other leading to chemical heterogeneity in the subsurface (HARVEY ET AL., 2006). Furthermore, some areas are protected from infiltration of DOC rich surface water by thick clay layers (PAL ET AL., 2002). LARSEN ET AL. (2008), for example, concluded from their results that the patchy As distribution is controlled by the hydraulic properties of the over-

lying clay layer, which controls the recharge rate as well as the chemical composition of the percolating water. What is clear is that hydrology is important in controlling the distribution of As (STUTE ET AL., 2007). Considerable uncertainty remains, however, and too little is known to predict with confidence how As concentrations will evolve in space and time and to what extent aquifers currently providing potable water can be relied on in the future (ZHENG ET AL., 2005).

2.5 IMPORTANCE OF ORGANIC MATERIAL

Over the years, the importance of OM in the As problem has come into the focus of investigations. Despite its conjectural importance, still not enough is known about the role, nature and the origin of this OM (Rowland et al., 2006). In the following paragraphs, some relevant observations concerning the role, degradation and characteristics of OM will be considered in more detail.

2.5.1 ROLE AND SOURCES OF ORGANIC MATTER

A lot of processes related to the mobilization of As are directly or indirectly linked to microbial activity (Chapters 2.1.2, 2.3.1, 2.3.2). These microbial processes require some kind of degradable OM as electron donor (CHARLET & POLYA, 2006). Several experiments have shown that excess of labile OM can significantly increase the As release due to stimulation of microbial activity (HARVEY ET AL., 2002; GAULT ET AL., 2005; ROWLAND ET AL., 2007). In this context, the rate controlling factors are the concentration, availability and reactivity of the OM (HARTOG ET AL., 2004; GAULT ET AL., 2005; POSTMA ET AL., 2007). But not everywhere As concentrations seem to be depending on microbial processes (POLIZZOTTO ET AL., 2006). RADLOFF ET AL. (2007) showed in their experiments that addition of acetate only had a limited impact on the As mobilization. However, where As release is microbially mediated the nature and content of OM in sediments could be an important issue (ROWLAND ET AL., 2007).

It is also a matter of discussion if OM degradation may contribute or not, directly to high As levels in groundwater because it is known that organic compounds are able to fix As to a certain extent (BGS & DPHE, 2001; ANAWAR

ET AL., 2002). Concentrations of As in OM, however, are often much too low to represent a sizeable source of As (DOWLING ET AL., 2002).

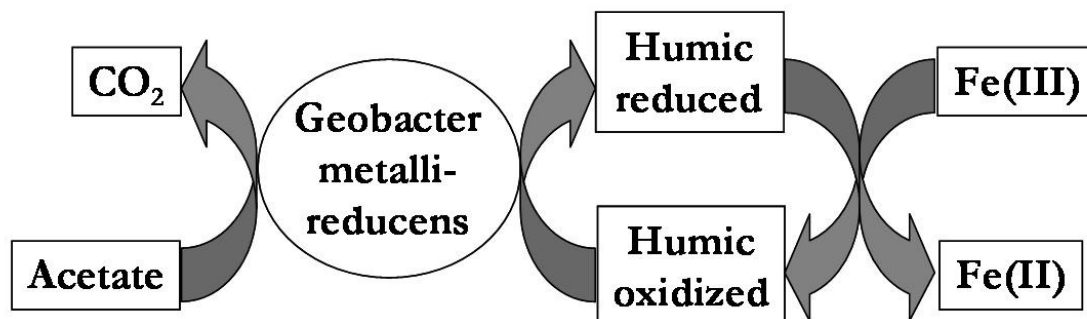


Fig. 2.5: Model for the reduction of Fe(III) through electron shuttling by humic substances (LOVLEY, 1996, modified). Fe reducing bacteria can use OC in order to transform already oxidized humic substances back into a reduced state. Each humic molecule can be re-oxidized several times.

Furthermore, degradation products like humic substances could compete for sorption sites and, consequently, lead to an increase of the As concentrations (GRAFE ET AL., 2001; Chapter 2.3.2). Humic substances are also capable of shuttling electrons between the electron donor (OC) and Fe(III) bearing solids and can so influence the As mobilization (Fig. 2.5, LOVLEY, 1996). Each humic molecule can be reduced and oxidized several times; thus, considerable reduction can take place even in aquifers low in OC (LOVLEY, 2001; ROWLAND ET AL., 2007).

As mentioned above, OC is the main electron donor for microbial activity in sediments and may play an important role in As release. Aquifers, however, often are depleted in electron donors, as indicated by the frequently low TOC content (mainly far below 1%) (LOVLEY & CHAPELLE, 1995; BGS & DPHE, 2001; MCMAHON, 2001; MCARTHUR ET AL., 2004). Over the years, different internal and external sources for OC supply have been considered.

Peat layers are common in delta environments, resulting from the development of mangrove flats, during the last sea level high stand (MATHERS ET AL., 1996). Several authors highlighted the possible role of OC leaching from peat layers in the release of As from sediments (e.g., MCARTHUR ET AL., 2001; STÜBEN ET AL., 2003). Furthermore, organic rich units could fuel aquifers with OC. Confining clay layers, for example, are often enriched in OM, be-

cause small pore sizes generally slow down microbial activity and OM degradation, concurrently. Sufficient soluble OM degradation products like organic acids or humic substances could migrate into the aquifer, anyway, supporting microbial activity (Fig. 2.6, MCMAHON, 2001; MCARTHUR ET AL., 2004; BERG ET AL., 2008). ROWLAND ET AL. (2006) further proposed petroleum derived hydrocarbons, seeping into shallow aquifers as possible carbon source.

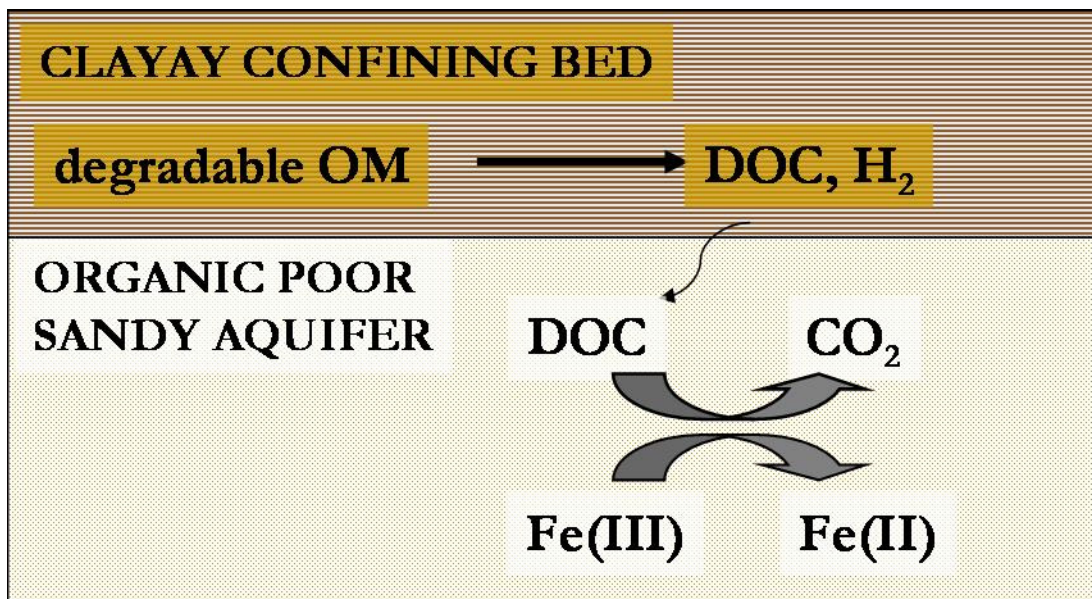


Fig. 2.6: Products of OM degradation in confining clay layers, rich in OC, can leach or diffuse into the aquifer fuelling redox reactions, here illustrated by the example of Fe(III) reduction (LOVLEY & CHAPELLE, 1995, modified).

Natural as well as anthropogenic (e.g. from latrines) derived OM might infiltrate into the aquifer by recharge from surface runoff, river beds, ponds or from soil solutions, commonly known to be rich in organic compounds. Infiltration could further be enhanced by extensive irrigation that draws down the groundwater table and enhances recharge (MCARTHUR ET AL., 2001; HARVEY ET AL., 2002; HARVEY ET AL., 2006).

2.5.2 DEGRADATION OF ORGANIC MATTER

Organic matter in sediments is highly heterogeneous often containing both recently introduced and old components (COWIE & HEDGES, 1994). Natural organic matter (NOM) consists of a complex mixture of polymeric organic

molecules whose exact composition depends on the source and degradation state of the original material.

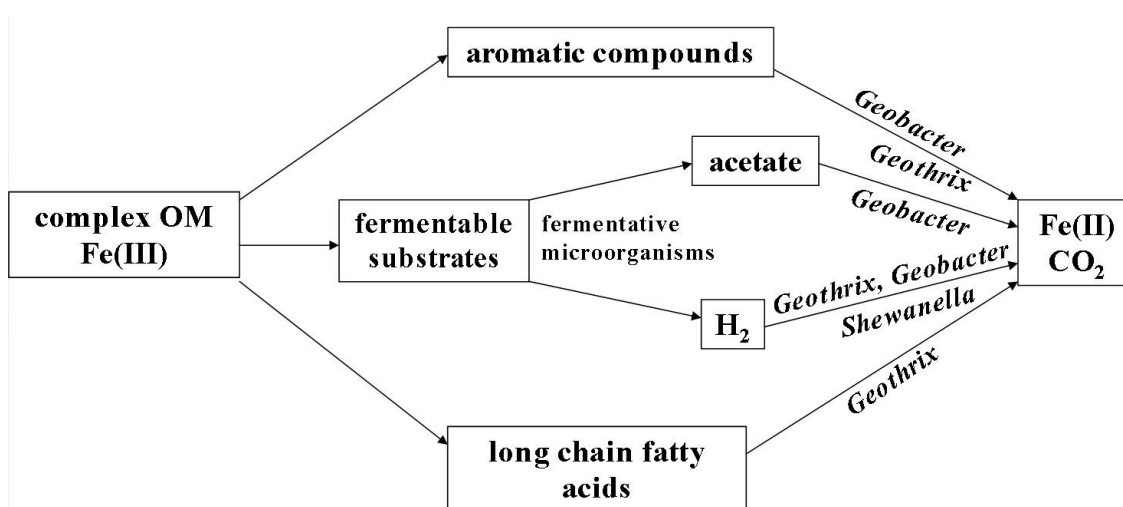


Fig. 2.7: Model for OM degradation pathways and possible products in sedimentary environments in which Fe(III) reduction is predominating (LOVLEY, 2001, modified).

During decomposition the more easily degradable constituents will be used first by microorganisms and broken down to monomeric components like carbohydrates, amino acids, and monoaromatics which are further transformed under ideal conditions to the end products CO_2 , CH_4 , H_2 , H_2O and biomass (Fig. 2.7; COWIE ET AL., 1992; CANFIELD, 1994; LOVLEY & CHAPPELLE, 1995; ROUTH ET AL., 1999). Consequently, more recalcitrant compounds like complex hydrocarbons (long chain alkanes, steranes, hopanes), which are less available for microbes, will accumulate over time if no input of fresh OM occurs, leading to a diminished microbial activity (VOLKMAN ET AL., 1992; PETERS ET AL., 2005; ROWLAND ET AL., 2006).

Aerobic degradation is thought to be orders of magnitude faster than anaerobic degradation; therefore, exposure to oxygen seems to diminish the reactivity of OM in the sediment. Also refractory substrates will be degraded to a much higher amount under oxidizing compared to reducing conditions. Under anaerobic conditions microorganisms can only completely oxidize a very limited number of organic compounds and consequently, some characteristic organic molecules will be enriched (LOVLEY & CHAPPELLE, 1995). Saturated hydrocarbons, for example, are quite resistant under reducing conditions and are prone to accumulate (CANFIELD, 1994).

2.5.3 CHARACTERIZATION OF ORGANIC MATTER

The analysed TOC content implies OM in various degradation states and, therefore, does not give enough information to estimate the reactivity of OM. Characterization of OM could help to assess the natural reductive capacity of sediments which highly influences the redox status of groundwater systems and, therefore, also the As mobilization (HARTOG ET AL., 2004; ROWLAND ET AL., 2007). Apart from chemical composition the reactivity of OM does further depend on environmental conditions (pH, T, oxidant concentration), physical protection (sorption to mineral surfaces) and microbial community (MAYER, 1994; COLLINS ET AL., 1995; VAN BERGEN ET AL., 1998).

Some elemental and molecular compounds of the sediment can be used as indicators (biomarkers) in order to characterize the origin and quality of OM. Quality describes the reactivity of OM with respect to diagenetic alteration and can also be used to assess the bioavailability of OC. Several parameters are commonly used as indicators, but one should always take into account the specificity and stability of each compound, which can get lost as the maturity of OM increases (PHILIP, 1985). Often the combination of different parameters is advisable (ARNOSTI & HOLMER, 2003). Some of such indicators will be discussed in the following paragraphs. An overview of different source related parameters is given in Tab. 2.6.

C/N-RATIO

It is assumed that nitrogen containing compounds are preferentially degraded during early diagenesis. An increase in the C/N ratio would, therefore, indicate a higher degradation status. C/N ratios can further provide source related information. Terrestrial OM is dominated by nitrogen poor macromolecules like cellulose or lignin (C/N >20) whereas marine OM is more enriched in nitrogen rich proteins (C/N = 5 - 7 for fresh material, 12 for degraded material) (HEDGES ET AL., 1986). A C/N ratio of 15 was suggested as cutting point between allochthonous vegetation and autochthonous organisms by COWIE AND HEDGES (1994). However, input of fresh OM could superimpose the original signal of the C/N ratio (ARNOSTI & HOLMER, 2003). Furthermore, the C/N ratio in sediments can be influenced by the deposition rate (ZHOU ET AL., 2006; QUICKSALL ET AL., 2008).

Tab. 2.6: Overview of different source indicators which allow differentiating between marine and terrestrial origin.

Property	Marine	Terrigenous	
C/N ratio ^[1]	5 to 12	>20	
$\delta^{13}\text{C}$ ^[2]	-22 to -19‰	-26 to -28‰ (C ₃)	-12 to -16‰ (C ₄)
$\delta^{15}\text{N}$ ^[3]	3 to 12‰	-5 to 18‰	
CPI ^[4]	close to 1	5 to 10	
ACL ^[5]	low	high	
n-alkane maxima ^[4]	C ₁₇	C ₂₇ , C ₂₉ , C ₃₁	

[1]HEDGES ET AL., 1986; [2]FRY & SHERR, 1984, MEYERS, 1994; [3]MÜLLER & VOSS, 1999; MAKSYMOWSKA ET AL., 2000; [4]RIELEY, ET AL., 1991; [5]PHILIP, 1985;

CARBON ISOTOPIC COMPOSITION

Carbon isotope measurements can give hints about the source of OM (Tab. 2.6). Photosynthetic plants using C₃ pathway produce a shift of -20‰ in their C isotopic composition compared to inorganic sources, whereas C₄ plants only lead to a shift of -7‰. As a consequence, terrestrial plants using CO₂ ($\delta^{13}\text{C} = -7\text{‰}$) as carbon source show isotopic signatures of around -27‰ (C₃) and -14‰ (C₄), respectively. Marine organisms, using HCO₃⁻ (~ 0‰) have $\delta^{13}\text{C}$ signatures of -22 to -19‰ (FRY & SHERR, 1984; HAYES, 1993; MEYERS, 1994). The $\delta^{13}\text{C}$ composition remains relatively unchanged during decomposition in contrast to C/N ratios (HEDGES ET AL., 1986; KENNEDY ET AL., 2004). A mixture of C₃ and C₄ plants, however, can result in similar signatures compared to marine OM. Thus, a combination of C/N ratio and isotopic composition is advisable.

NITROGEN ISOTOPIC COMPOSITION

Only a few processes, are responsible for the fractionation of nitrogen. These are mainly kinetic fractionations during microbial reactions like assimilation of inorganic nitrogen, nitrification, denitrification or ammonification (OSTROM ET AL., 1998; VOSS ET AL., 2001). The isotopic effect during nitrogen

fixation is $\sim 0\%$, whereas denitrification leads to a shift of up to 30% (HOEFS, 1987). Terrestrial vascular plants have $\delta^{15}\text{N}$ signatures of -5 to 18% (average: $\sim 3\%$) and marine phytoplankton of 3 to 12% (average: $\sim 6\%$) (MÜLLER & VOSS, 1999; MAKSYMOWSKA ET AL., 2000). WASER ET AL. (1998) constrain the ratios for terrestrial material to $0.5 - 2.3\%$ and for marine phytoplankton to $2.8 - 5.1\%$. $\delta^{15}\text{N}$ signatures vary in a much wider range and even overlap compared to $\delta^{13}\text{C}$; therefore, source related predictions are difficult. $\delta^{15}\text{N}$ signatures are more suitable to reflect the extent of biogenic alterations (THORNTON & MCMANUS, 1994).

MOLECULAR COMPOSITION

Hydrocarbons in sediments can result from deposited land plants, animals, bacteria, macro- and micro-algae etc. (EGLINTON & HAMILTON, 1963; VOLKMAN ET AL., 1992). Complex hydrocarbons are difficult to use for microorganisms as they first have to be activated or because their transport across the cell membranes is hampered (PETERS ET AL., 2005). Within the hydrocarbon group short chain n-alkanes ($<C_{24}$) and simple aromatics are degraded most rapidly (PHILIP, 1985). Long chain n-alkanes are much more stable while cyclic molecules like steranes and hopanes are rarely affected by microbial degradation (VOLKMAN ET AL., 1992; PETERS ET AL., 2005). Consequently, ratios of more labile to more recalcitrant compounds will give information about the degradation state and the bioavailability of the remaining OM, respectively. Furthermore, the occurrence of some specific hydrocarbons can also give source related information.

(A) CARBON PREFERENCE INDEX (CPI)

The CPI describes the ratio between odd- and even- numbered C-atoms of high molecular weight (HMW) n-alkanes ($>C_{20}$) (Eq. ()); BRAY & EVANS, 1961).

$$CPI = 0.5 \times \frac{(C_{25} + C_{27} + C_{29} + C_{31} + C_{33})}{(C_{24} + C_{26} + C_{28} + C_{30} + C_{32})} + \frac{(C_{25} + C_{27} + C_{29} + C_{31} + C_{33})}{(C_{26} + C_{28} + C_{30} + C_{32} + C_{34})} \quad (2.1)$$

Originally the CPI was used to characterize the degradation state of petroleum but it is also useful in organic geochemistry. Bacteria, for example,

have a preference for even chained n-alkanes which will be degraded first. Therefore, immature OM is relatively enriched in odd-numbered carbon. On the other hand, a CPI of ~1 is typical for diagenetically and thermally mature OM (EGLINTON & HAMILTON, 1963, CRANWELL, 1982). For relatively fresh OM, information about the source of OM can also be gained from the CPI (PHILIP, 1985). Land plants, for example, show a predominance of odd-numbered carbon (CPI: 5-10) whereas marine organisms do not have a distinct preference (CPI: close to 1) (KENNICUTT ET AL., 1987; RIELEY, ET AL., 1991).

(B) AVERAGE CHAIN LENGTH (ACL)

The ACL characterizes the number of C-atoms in a molecule based on the abundance of odd-carbon numbered HMW n-alkanes (Eq. (2.2)).

$$ACL = \frac{iC_i + \dots + nC_n}{C_i + \dots + C_n} \quad (2.2)$$

Some information about source and degradation state of OM can be gained from the ACL. Terrestrial derived n-alkanes are longer chained, compared to ones of marine origin, leading to a high ACL (PHILIP, 1985). Maxima for OM from terrestrial environment are typically found at C₂₇, C₂₉ and C₃₁ whereas phytoplankton derived alkanes show predominance at C₁₇ (BROOKS & SMITH, 1967; PHILIP, 1985). During decomposition, the n-alkane maximum tends to shift towards lower carbon numbers (PHILIP, 1985). Lowest ACL values are expected for highly mature petrogenic hydrocarbons (POYNTER ET AL., 1990). The ACL, however, might be influenced by vegetation type as well as latitude, making it difficult to draw clear conclusions (POYNTER ET AL., 1990).

(C) UNRESOLVED COMPLEX MIXTURE (UCM)

The presence of an UCM is indicated by an increase in the baseline of the total ion chromatogram measured with GC/MS (Fig. 2.8). An UCM consists of a mixture of bioresistant compounds including highly branched and cyclic saturated, aromatic and polar molecules which cannot be further resolved by GC/MS analysis (GOUGH & ROWLAND, 1990). UCM is used as indicator for the presence of biodegradable petroleum which is further sup-

ported by the presence of thermally mature hopanes and steranes (VOLKMAN ET AL., 1992; PETERS ET AL., 2005).

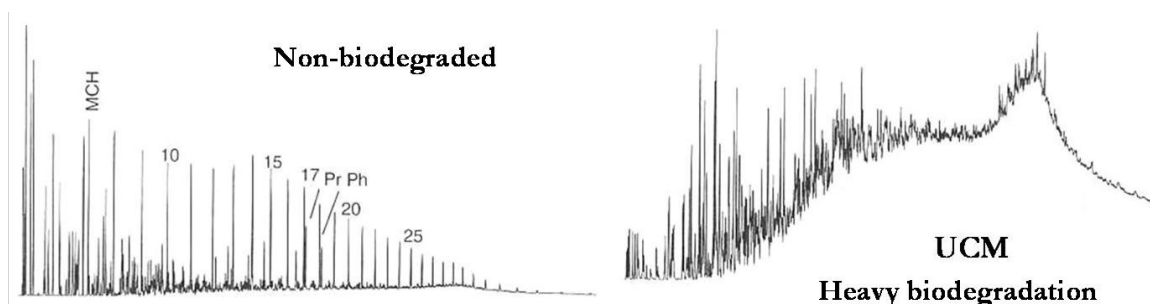


Fig. 2.8: Gas chromatograms of crude oil. Visible are the changes from non-biodegraded to heavy biodegraded oil which is indicated by the presence of UCM (PETERS ET AL., 2005, modified).

2.6 ARSENIC TOXICITY AND EPIDEMIOLOGY

Arsenic is famous for its deleterious health effects. Ingestion of As can be lethal. First symptoms are similar to diarrhoea; therefore, its use as murder weapon had been very popular for centuries (MEAD, 2005).

Apart from duration and amount of exposure, the toxicity of As mainly depends on the bioavailability of As which is influenced by its form (e.g. oxidation state, organic or inorganic) and the matrix of ingestion (e.g. water, food, soil) (JAIN & ALI, 2000, MANDAL & SUZUKI, 2002). Generally, inorganic compounds, which have a longer residence time in the organism, are considered to be more toxic (~100 times) compared to organic ones (KORTE & FERNANDO, 1991). Among the inorganic forms, arsine is most poisonous (it induces haemolysis) followed by As(III), which is about 60 times more toxic than As(V) (FERGUSON & GAVIS, 1972; PENROSE, 1974; PUTTEMANS & MASSART, 1982; NAGY & KOROM, 1983). In the human body, As(V) can be reduced to As(III). Methylation of inorganic species is considered as a detoxification process because it reduces the affinity of As to human tissue (VAHTER & MARAFANTE, 1988; MANDAL & SUZUKI, 2002). However, recent studies showed that trivalent intermediates of biomethylation (e.g. methylarsonous, dimethylarsinous acid) could exceed arsenite in its cytotoxicity and genotoxicity (PETRICK ET AL., 2000; STYBLO ET AL., 2000).

Due to its chemical similarity with PO_4^{3-} , As(V) negatively influences catabolic reactions by inhibiting the ATP synthesis (MANDAL & SUZUKI, 2002). The toxicity of As(III) results from its high reactivity towards -SH (sulfhydryl) groups, which are abundant in enzymes and proteins. By blocking these molecules, important enzymatic controlled processes like DNA repair will be inhibited (MANDAL & SUZUKI, 2002; MEAD, 2005). The high affinity of As(III) to -SH groups leads to its accumulation in keratin-rich tissues, like hair and nail, which therefore are commonly used as biomarkers for As exposure (GOLDSMITH ET AL., 1972; MANDAL & SUZUKI, 2002).

Apart from particular circumstances at work places, humans are mainly exposed to As through drinking water and food, whereof ingestion of contaminated drinking water is more harmful because it contains As mostly in its inorganic form (MEAD, 2005; KAPAJ ET AL., 2006). Ingestion of high concentrations of As produces acute toxic effects whereas long-term uptake of lower concentrations (ingestion > excretion) leads to As accumulation in the body. This chronic exposure gives rise to several adverse health symptoms summarized as arsenicosis. Among others, typical effects are mutations of skin (hyper- and hypo-pigmentation, hyperkeratosis), liver, nervous and cardiovascular system, respiratory tract (cough, bronchitis), as well as mutagenic and carcinogenic effects (e.g. MANDAL & SUZUKI, 2002; KAPAJ ET AL., 2006). Arsenic is considered as one of the most significant environmental causes of cancer worldwide (SMITH ET AL, 1992) and is classified by the EU as a highly dangerous carcinogen substance (EU-class 1, EPA-class A) (UMWELTBUNDESAMT, 1999).

Arsenicosis is difficult to diagnose as it has a long latent stage between the start of exposure and occurrence of first signs, which are normally skin lesions or the so called “black foot disease” (MANDAL & SUZUKI, 2002; MEAD, 2005; KAPAJ ET AL., 2006). The longer the time of exposure and the higher the As concentration, the more severe are the symptoms (dose-response relationship). First signs normally occur after 5 - 10 years of constant intake of groundwater high in As (SMITH ET AL., 2000; BERG ET AL., 2001; KAPAJ ET AL., 2006); however, in Cambodia detectable effects appeared already within 2 - 3 years (Mickey Simpson, personal communication). Synergetic effects with other elements or other factors like age, gender, nutrition, lifestyle (e.g.,

smoking) can influence the course of arsenicosis (MEAD, 2005; KAPAJ ET AL., 2006).

In order to protect people against As related illnesses the WHO advised in 1993 to lower the drinking water quality guideline from 50 to 10 µg/L (WHO, 2003). In the meantime, most industrial countries met this advice (Germany in 1991). In many developing countries, like Bangladesh, however, the limit of 50 µg/L is still valid, mainly because they do not have appropriate treatment technologies to reach lower values. A lowering to 10 µg/L could considerably reduce mortalities due to bladder, skin and lung cancer (USEPA, 2002). Vietnam has changed the limit to 10 µg/L in 2002. But even this limit is under discussion globally, as it is based on a 6×10^{-4} excess skin cancer risk, which is 60 times the factor normally used. In future, values <3 µg/L are targeted, because several adverse health effects are known to occur even at this low concentrations (KAPAJ ET AL., 2006).

2.7 MITIGATION STRATEGIES AND ARSENIC FILTER SYSTEMS

The countries most affected by the As calamity are mainly developing countries which do not have money and infrastructure to offer central water supply or pay for expensive treatment technologies to reduce As to an acceptable level. So far, a lot of misbeliefs and misconceptions circulate among the population about arsenicosis and different mitigation measures. Therefore, holistic mitigation strategies have to be developed which should include education of the population, management of arsenicosis patients and provision of safe water supply (AHMED ET AL., 2007; JAKARIYA & BHATTACHARYA, 2007). In all cases risks, needs, balances and acceptability of different options have to be considered, thoroughly (MILTON ET AL., 2007). The overall aims of mitigation strategies should be (1) to reduce the cumulative As intake (food and drinking water) in order to prevent further harm on the population and (2) to identify and help already affected people in the individual countries (BGS & DPHE, 2001; AHMED, 2005; JAKARIYA & BHATTACHARYA, 2007).

In principal, there are two ways to supply people with As free drinking water, which is the main cause for arsenicosis. Firstly, to implement easy and low cost filter technologies in order to reduce As concentrations, or sec-

ondly, to provide As free water from other sources than contaminated tube wells (SMITH ET AL., 2000; MILTON ET AL., 2007). Regardless of the chosen measure, social acceptance of the method and the willingness of the people to change current habits are of uttermost importance for a sustainable success (BGS & DPHE, 2001; AHMED ET AL., 2007; JAKARIYA & BHATTACHARYA, 2007; MILTON ET AL., 2007).

Most of the globally developed filter systems are based on coagulation, flocculation, ion exchange treatment, membrane separation, lime softening, adsorption and precipitation, sometimes in combination with uptake by plants or additional input of oxidants (JECKEL, 1994; KARTINEN & MARTIN, 1995; DRIEHAUS, 2005; AHMED, 2005; CHOONG ET AL., 2007; PETRUSEVSKI ET AL., 2008). Several filter technologies were tested under laboratory as well as field conditions, but many of them are not applicable in developing countries, because they are too expensive, too complex to use and maintain, ineffective under the circumstances prevailing locally or not reliable enough. Therefore, such techniques would never be socially accepted (DRIEHAUS, 2005; CHOONG ET AL., 2007; MILTON ET AL., 2007).

Mainly simple sand filter devices have been established over the years. Some of them use Fe oxy-hydroxide coated sand to remove As (PETRUSEVSKI ET AL., 2008). If the dissolved Fe concentration in the groundwater is high enough, percolation over sand or just letting the water untouched over night leads to precipitation of Fe oxy-hydroxides and, consequently, As concentrations can be reduced considerably (BGS & DPHE, 2001; WAGNER ET AL., 2005; BERG ET AL., 2006). In some villages, community based filter units are of great success, as shown in a 5 year study done by SARKAR ET AL. (2008). The community was included into the decision process and is now responsible for the operation and maintenance of the filter which has proven to be beneficial for the long-term success. Household level filter systems are commonly seen only as a short- to medium-term solution (MILTON ET AL., 2007).

Two options are feasible if water, initially low in As, shall be provided. On the one hand, to further use the existing sources, but to switch to as “save” marked tube wells. On the other hand, alternative water sources like surface water, rain water harvesting, very shallow groundwater (dug wells) or exploiting deep aquifers could be a solution (SMITH ET AL., 2000; BGS &

DPHE, 2001; AHMED, 2005; KABIR & HOWARD, 2007). Not all options are available or possible everywhere. For choosing and planning the appropriate measure, people responsible locally, have to be integrated in the process (SMITH ET AL., 2000; JAKARIYA & BHATTACHARYA, 2007). At the moment, drilling of deep wells is the most popular alternative, especially if community is involved (KABIR & HOWARD, 2007). These waters are mainly low in As, without odour, colour or microbial contaminants, as regularly observed in surface water (AHMED, 2005; ZHENG ET AL., 2005). However, deep aquifers are not present everywhere (BGS & DPHE, 2001). Furthermore, some studies raise concern, that pollution of these deep wells might occur over time due to over-exploitation or improperly installed wells which leads to leakage of more shallow, contaminated water (SHIBASAKI ET AL., 2007; VAN GEEN ET AL., 2007). Therefore, the water quality has to be tested regularly, even in so called "save areas" (AHMED, 2005; VAN GEEN ET AL., 2006B).

The use of new technologies could support access to save drinking water. Results of previous As mappings in addition to geological and geomorphological information combined in GIS could help to find suitable locations for the drilling of new wells (HASSAN, 2005; JAKARIYA & BHATTACHARYA, 2007). This data should be made accessible to the public by mobile phones as proposed by VAN GEEN ET AL. (2006) as they are common even among the rural population.

Very shallow groundwater, collected from dug wells, is normally also low in As because of oxic conditions. If people are educated to use and maintain these wells properly, they can provide save and clean drinking water (SMITH ET AL., 2003; MILTON ET AL., 2007). However, they cannot be developed in all geological and hydrological settings (AHMED, 2005). Dug wells are often socially not accepted, because the water can taste, smell, have turbidity or microbial contamination (CHENG ET AL., 2004). Furthermore, it is seen as old-fashioned (MILTON ET AL., 2007). Rain water harvesting is practised locally, but not well accepted by most communities. Problems arise from the unequal distribution in the course of the year (only sufficient in rainy season) and the long-time storage, which leads to quality deterioration (AHMED, 2005).

For the long-term success of mitigation measures, more research is necessary in many different aspects. Furthermore, a sustainable management has to be implemented, which includes a real concept of safe drinking water supply, legal aspects, monitoring networks, research and training, giving access to information and improving public awareness (AHMED, 2005).

3 RED RIVER DELTA, VIETNAM

The Red River Delta (RRD, also Song Hong Delta) lies in the northern part of Vietnam and borders the countries of China in the North and East, Laos in the West. Apart from the region around Ho-Chi-Minh-City, the RRD is the social and economic centre of Vietnam (DAN & HA, 2006). About 11 - 15 million people are currently living in the delta, leading to one of the highest population densities in Vietnam (MATHERS ET AL., 1996; BERG ET AL., 2001). Due to frequent flooding the area is very fertile and, therefore, mainly agriculturally used (above all rice but also jute, wheat, corn, beans or vegetables). To contain the RR and to irrigate the rice-fields a network of dykes and canals was constructed, some of them already 1 kyr ago (LARSEN ET AL., 2008). Several centres of heavy industries are located in the delta (MATHERS ET AL., 1996) and, as a result of the fast growing economy, many new factories are currently build mainly around Ha Noi and Hai Phong, leading to an increasing anthropogenic influence on the environment. This fast growth of population and industries in the delta enforces the need for safe and uncontaminated drinking water sources, e.g. groundwater which is considered as safe especially with regard to microbiological contamination.

3.1 CLIMATE AND HYDROLOGY

The climate in the RRD is tropical-subtropical (TANABE ET AL., 2003A; LI ET AL., 2006) with an average annual temperature of 23.4 °C (Ha Noi) and an average rainfall of 1,800 mm/yr (BERG ET AL., 2001). It is highly affected by the Southeast Asian monsoon regime with rainy season from May to September and dry season from October to April. During the rainy season the daily rainfall is typically around 10 - 50 mm/day but can go up to 100 - 200 mm/day (LARSEN ET AL., 2008).

The drainage area of the Red River is ~168,000 km² (FUNABIKI ET AL., 2007). The discharge is highly variable (700 - 23,000 m³/s) depending on the season (TANABE ET AL., 2003A, 2006), which leads to water table fluctuations of

up to nine meters throughout the year (BERG ET AL., 2008). The river got its name from the characteristic colour which originates from huge quantities of silt transported in the water ($\leq 12 \text{ kg/m}^3$ and $130 \times 10^6 \text{ t/yr}$, respectively), which are rich in Fe oxy-hydroxides. 80 - 90% of the annual sediment discharge occurs throughout the rainy period (MATHERS ET AL., 1996; MATHERS & ZALASIEWICZ, 1999). As a consequence of the high sediment discharge (mean: 1.08 kg/m^3), the delta is still actively growing with progradation rates of 30 - 40 m/yr during the past 100 years (TANABE ET AL., 2006; FUNABIKI ET AL., 2007).

3.2 GEOLOGICAL SETTING

The RRD is the fourth largest delta in Southeast Asia (TANABE ET AL., 2006) and comprises an area of $\sim 10,000 \text{ km}^2$ (FUNABIKI ET AL., 2007). The whole RR basin stretches from $20^{\circ}00'$ to $25^{\circ}30'$ N and from $100^{\circ}00'$ to $107^{\circ}10'$ E (BERG ET AL., 2001).

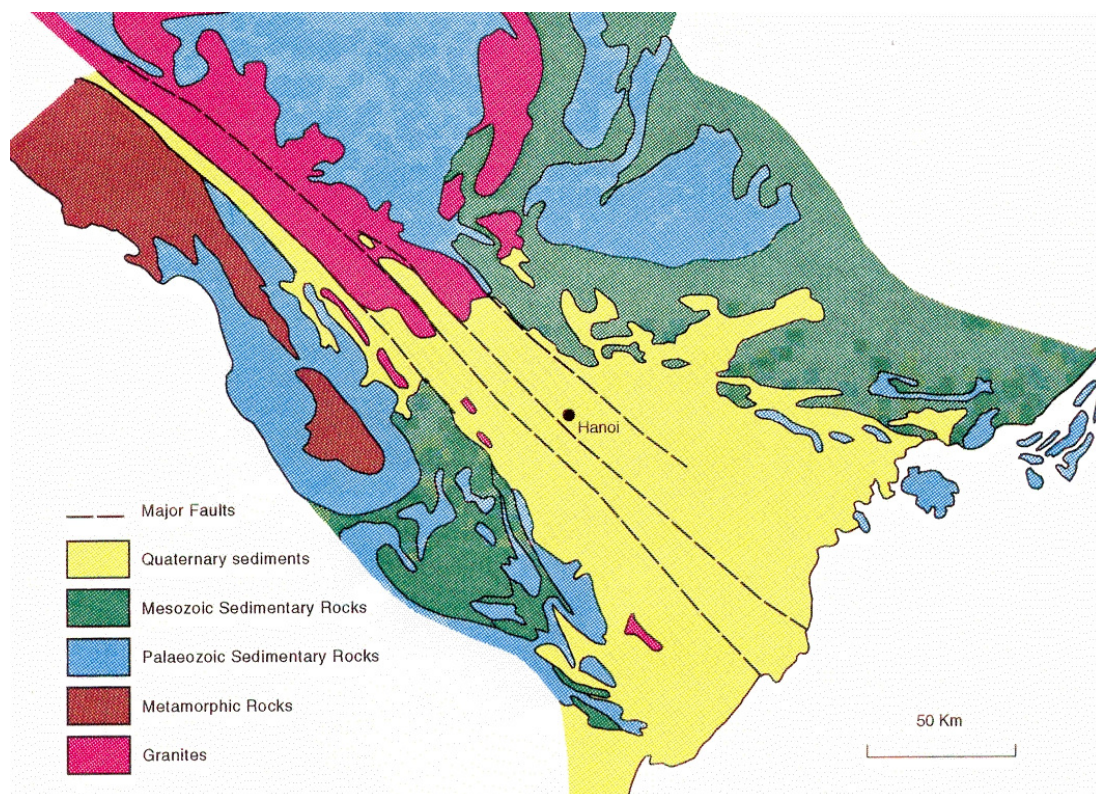


Fig. 3.1: Generalized geological map of the Red River delta and the surrounding monotonous area (MATHERS ET AL., 1996).

The development of the delta basin is heavily influenced by the NW-SE-aligned Red River Fault system which can be followed from Tibet to the South China Sea for more than 1,000 km (RANGIN ET AL., 1995). It results from the collision of the Indian and Asian tectonic plates in the Eocene. The whole basin is filled with more than 3 km of Neogene and Quaternary deposits and subsides with 0.04 - 0.12 mm/yr (MATHERS & ZALASIEWICZ, 1999; TANABE ET AL., 2003A).

The river itself originates in the mountainous part of the neighbouring Yunnan Province, China, and flows in a northwest-southeast direction for ~1,200 km in a more or less straight narrow valley, before it drains into the Gulf of Tonkin (Bac Bo). This valley follows a graben structure formed by the Red River Fault zone (MATHERS & ZALASIEWICZ, 1999; TANABE ET AL., 2003A; 2006). In the upper reaches of the RR, Precambrian crystalline (Granites, Metamorphic rocks) as well as Palaeozoic sedimentary rocks are present, whereas the mainly flat delta plain (5 - 8 m above mean sea level) is surrounded by Mesozoic and Palaeozoic sedimentary rocks (MATHERS ET AL., 1996; BERG ET AL., 2001). All these rocks act as source for the sediment deposited in the RRD (Fig. 3.1).

3.3 QUATERNARY GEOLOGY

Present and past morphology as well as the Quaternary geology of the delta plain are stamped by the highly variable discharge of the RR over the past millennia mainly in response to eustatic sea level changes leading to erosion and accumulation of alluvial material due to frequent riverbed movement. These processes were superimposed by a succession of transgression and regression periods since the last glacial maximum bringing in also material from marine origin.

Quaternary sediments in the RR basin, which unconformably overlay Neogene deposits, consist of Pleistocene and Holocene sequences of gravel, sand and clay, ranging from a few meters in the Northwest to 100 - 200 m in coastal areas (MATHERS & ZALASIEWICZ, 1999; TANABE ET AL., 2003A, 2006). The boundary between fluvial and marine dominated depositional environments has shifted since the last cold phase in response to eustatic sea level changes (TANABE ET AL., 2003B). The marine influence during the Quaternary period,

however, has never progressed further inland as Ha Noi (TANABE ET AL., 2003A). Within the Holocene clay deposits organic rich layers (mainly referred to as peat) are common (MATHERS ET AL., 1996) which result from the development of large mangrove flats between 9 - 4 cal. kyr BP as a result of the overall sea-level rise, sometimes even above the current level (TANABE ET AL., 2003A). Due to the multitude of processes occurring, the lithology of the RRD is highly complex and varies considerable within short distances. Some layers can be missing totally in some parts.

3.4 HYDROGEOLOGY

Around Ha Noi the Quaternary sequence has a thickness of 50 - 100 m (MATHERS ET AL., 1996; MATHERS & ZALASIEWICZ, 1999). It contains several aquifer units which are of great importance as drinking water source. Simplified, the sequence can be divided into a lower (LAS) and an upper aquifer system (UAS) (Fig. 3.2). The two main aquifers are not always separated by clay layers as a result of frequent riverbed migrations. The UAS comprises sand, silt and clay (mainly 20 - 40 m) and encloses peat layers in several regions (TRAFFORD ET AL., 1996). In some parts, the UAS can be further separated into two minor aquifers, one from Holocene and the other from Pleistocene age. Leaching of groundwater into the underlying LAS occurs to some extent. This aquifer is mainly exploited in rural areas by shallow dug wells (TRAFFORD ET AL., 1996).

The lower part (LAS) is dominated by sand and gravel with subordinate lenses of clay and silt derived mainly from Pleistocene sea-level low stand. It can reach a thickness of up to 50 m around Ha Noi and is underlain by sands of Neogene age. The LAS is highly permeable and, therefore, used as main source for Ha Noi's water supply (TRAFFORD ET AL., 1996). In 2005, ten major well fields exploited ~650,000 m³/day (BERG ET AL., 2007) leading to depression cones of up to 30 m (NHEGD, 2002). The heavy pumping might, therefore, influence the natural groundwater flow as well as the groundwater quality. Ammonium concentrations, for example, have significantly increased over the past 15 years in response to the extensive pumping (NHEGD, 2002).

The RR incises deeply into the sediment. As a consequence, the LAS is sometimes directly connected to it and, therefore, mainly recharged by river water in a 5 km wide zone along the RR. In the rest of the delta leakage from the UAS is the main water source for LAS. The large withdrawal of groundwater, supplying the city of Ha Noi further facilitates recharge of river water into both Pleistocene and Holocene aquifers close to the RR as well as leakage from UAS to LAS (TRAFFORD ET AL., 1996; BERG ET AL., 2007; 2008).

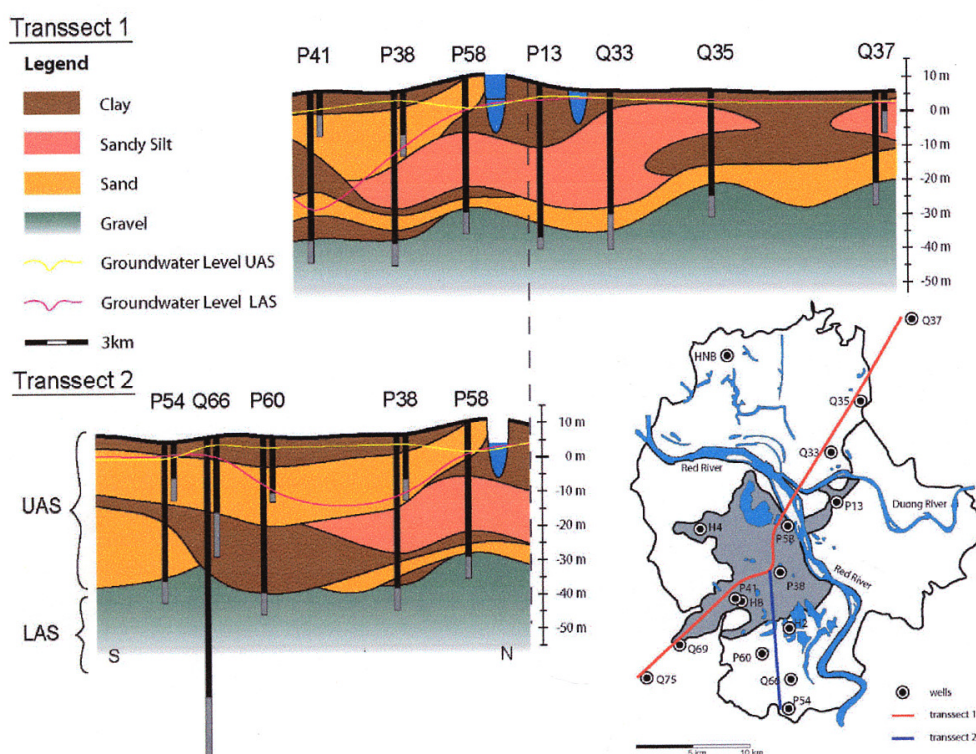


Fig. 3.2: Distribution of lower (LAS) and upper (UAS) aquifer system in two transects through the city of Ha Noi. Included are the different hydraulic heads of the water table of each aquifer (AUTENRIETH, 2005, modified).

Recharge of the Holocene aquifer can also take place via infiltration of surface water, which, however, depends on the presence and thickness of a confining layer as well as on the presence of fractures or other preferential flow paths (LARSEN ET AL., 2008). High fluctuations in the groundwater table are indicative for infiltration of river water during rainy season when the river stage is high. With increasing distance to the river, recharge from rain water is dominant leading to much lower fluctuations. As a result of seasonal changes of the ground- and riverwater table as well as the highly in-

homogeneous sediment lithology (Chapt. 3.3), the groundwater flow pattern is highly dynamic and difficult to predict.

3.5 STUDY SITE

Van Phuc village is located ~10 km southeast of Ha Noi between a RR bend and a dyke that protects the south-western parts of Ha Noi from annual flooding (Fig. 3.3). As a consequence, the village itself is occasionally flooded for a few days during the rainy season and can, therefore, be considered as a mainly natural and undisturbed system compared to the areas protected by the dykes. The water table varies widely in both the aquifer ($\bullet 4$ m) and in the Red River (7 - 9 m) between the seasons.

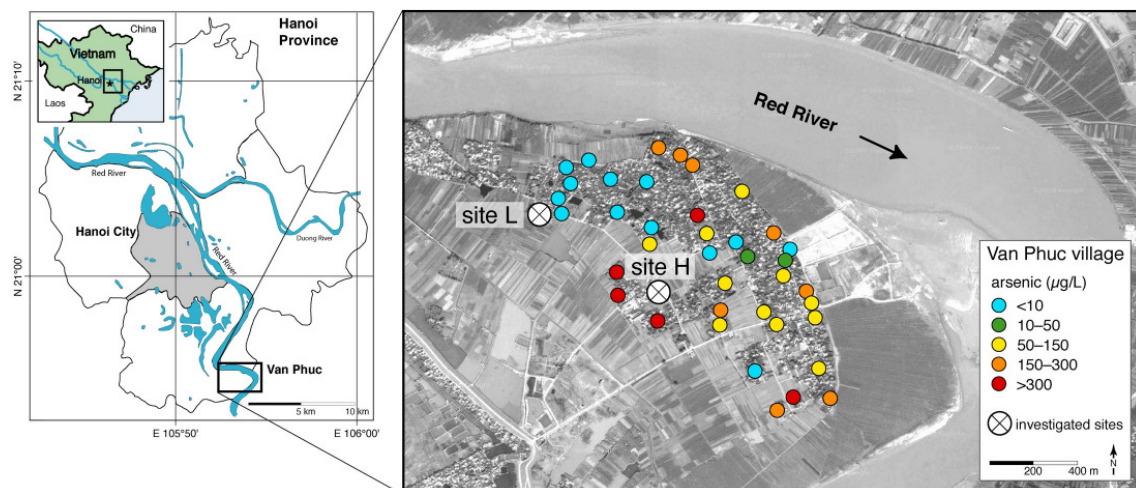


Fig. 3.3: Map depicting the study sites in Van Phuc village situated some 10 km south of the centre of Ha Noi city (modified map from BERG ET AL., 2007). Arsenic in groundwater shows a patchy distribution in this village. Site L (low) has particularly low levels of dissolved arsenic (3 ± 2 $\mu\text{g/L}$), whereas site H (high) features very high arsenic concentrations (400 ± 135 $\mu\text{g/L}$). The two sites are 700 m apart from each other. The satellite image was taken from google-earth (earth.google.com).

The aquifer consists of a loose bedding of Holocene and Pleistocene sediments up to a depth of more than 40 m. It is overlain by a clay layer with variable thickness, depending on the distance to the river bed. There are indications for groundwater recharge either by river water or through surface water infiltration (BERG ET AL., 2007). High groundwater ages of more than 15 years (FREL, 2006), however, point towards low recharge rates and slow

groundwater dynamics despite the high water table fluctuations. An influence of the groundwater drawdown induced by extensive pumping of the Ha Noi well-fields is small or nonexistent (BERG ET AL., 2007).

The land is mainly used for agriculture (corn, medicinal plants, cabbage). Most of the fields are irrigated during the dry season either by water from ponds or, to a lesser amount, by groundwater from dug wells. However, no paddy rice is cultivated in the region of Van Phuc. Groundwater is the main source of drinking water in Van Phuc but households commonly treat raw groundwater through sand filters which lower As concentrations on average by 80% due to co-precipitation with Fe oxy-hydroxides (BERG ET AL., 2006).

Van Phuc was chosen as a study site because of the known high As concentrations discovered by BERG ET AL. (2001) south of Ha Noi. Furthermore, a more detailed study in 2001 revealed a great heterogeneity of As concentrations ranging from <1 - 540 µg/L in different private tubewells in Van Phuc (BERG ET AL., 2007). With the aim to further elucidate reasons for the highly patchy distribution worldwide, Van Phuc turned out to be ideal.

4 THE DEVELOPMENT OF THE ARSENIC CALAMITY IN VIETNAM

4.1 ARSENIC CONTAMINATION IN THE RED RIVER DELTA

Comparable to Bangladesh and India, the promotion of digging shallow wells by UNICEF in order to gain microbially clean drinking water and to reduce related diseases like diarrhoea can be taken as beginning of the As crisis in Vietnam. Before, the city of Ha Noi already exploited groundwater from the UAS for around 90 years (Chapt. 3.4; BERG ET AL., 2001, 2008). Due to high dissolved Fe concentrations aeration and sand filtration of the groundwater, which are typical procedures during drinking water treatment, as well as adsorption processes along the pipe system lowered the As concentrations significantly (average: 31 µg/L), so that no signs of arsenic related illnesses were noticeable over the past centuries (BERG ET AL., 2007). Since 1993, more than 1 million tube wells have been installed in Vietnam (SON & HOA, 2006) which was accompanied by a shift to use groundwater as drinking water supply by most of the rural population (BERG ET AL., 2001). Only a small number still uses surface or rain water as main source (LUZI ET AL., 2004), some households additionally collect rain water during rainy season (AGUSA ET AL., 2006, BUSCHMANN ET AL., 2008).

Due to geological similarities with the Ganges Delta, first studies were carried out at the end of the 1990s in order to evaluate a possible groundwater As contamination. Concentrations of 1 - 3,050 µg As/L were found in the larger Ha Noi region (~1,000 km²), however, with considerable spatial variations. The highest values were measured south of the city on the southern margin of the Red River (BERG ET AL., 2001). Elevated As levels were found both in the LAS as well as UAS (Chapt. 3.4), with maximum values in the shallow groundwater of private tube wells (SMEDLEY, 2005). TONG (2002) detected high As levels also in the West and East of the city, confirming the highly patchy distribution. Lowest concentrations were generally observed

north of the RR. Since that time several studies in the larger Ha Noi area have further clarified the picture of the As contamination (e.g. POSTMA ET AL., 2007; BERG ET AL., 2008, NORRMAN ET AL., 2008). In a first study in other provinces of the RRD, carried out by UNICEF and Vietnam Geological Survey in 1999, 12.5% of the sampled wells were above the Vietnamese limit of 50 $\mu\text{g As/L}$ valid at that time (SMEDLEY, 2005). A risk map based on geological, climatic and land use information published by WINKEL ET AL. (2008) show, that large parts of the delta, especially along the river itself, have a medium to high risk for As concentrations $>10 \mu\text{g/L}$ in the groundwater. Large scale random testing revealed that several provinces along the RR have much higher levels than 10 $\mu\text{g/L}$ (new national limit since 2002), 77% in Ha Nam province, for example (SON & HOA, 2006). So far, however, not enough reliable data is available to assess the magnitude of As contamination in the whole RRD, especially because the high spatial variability (Chapt. 4.2) requires even more information (LUZI ET AL., 2004). Estimated 11 million people are currently using As contaminated water in Vietnam, including the also affected areas in the Mekong Delta, South Vietnam (BERG ET AL., 2007), and are therefore at risk to contract arsenicosis (BERG ET AL., 2001). BERG ET AL. (2001) concluded from their study that at least the Ha Noi area, if not the whole delta, is as strongly affected as Bangladesh and West Bengal. In the meantime, the focus stretches also on the southern part of Vietnam, where elevated As concentrations were detected in the Mekong Delta (TRANG ET AL., 2005; BERG ET AL., 2006; BUSCHMANN ET AL., 2008). Significantly higher As concentrations in hair of affected villages compared to control villages indicate that people are chronically exposed (TRANG ET AL., 2005).

So far only few cases of arsenic related illnesses have emerged (NGOC ET AL., 2006; SON & HOA, 2006; BERG ET AL., 2006; BERG ET AL., 2007). This might be due to the only short-time use of groundwater and the much better nutrition in Vietnam compared to Bangladesh (BERG ET AL., 2007). Chronic As poisoning strongly depends on concentration and exposure time. Therefore, first symptoms of arsenicosis are normally only expected after 5 - 15 years of consumption of water with more than 50 $\mu\text{g As/L}$ (SMITH ET AL., 2000; BERG ET AL., 2001; BERG ET AL., 2007). Furthermore, first signs are difficult to diagnose and depend largely on the qualification of the local doctors (SAHA ET AL., 1999). Arsenic concentration in hair, which is a widely used biomarker for

exposure to heavy metals (AGUSA ET AL., 2006), was measured in several studies. The results showed a significant enrichment of As close to or above the threshold value for elevated risk to develop skin problems (1 µg/g), if groundwater high in As was consumed, regularly (AGUSA ET AL., 2006; NGOC ET AL., 2006; TRANG ET AL., 2006, BERG ET AL., 2007). Consequently, As related health problems are probably only beginning to be identified (SMEDLEY, 2005). Manganese concentration above the WHO advised limit of 0.5 mg/L are also frequently observed in the groundwater and might pose an additional threat for the well-being of the population as it can cause teratogenicity and neurotoxic effects (AGUSA ET AL., 2006; BERG ET AL., 2006, BUSCHMANN ET AL., 2008).

4.2 ORIGIN OF THE ARSENIC CONTAMINATION IN THE RED RIVER DELTA

Similar to Bangladesh and India high concentrations of As in aquifers of the RRD probably originate mainly from geogenic sources (BERG ET AL., 2001). In a widely accepted theory all started with rock erosion in the catchments of young river deltas, which released the rock forming minerals and exposed them to weathering processes subsequently releasing both As and Fe to the hydrosphere (BGS & DPHE, 2001; AHMED ET AL., 2004; MCARTHUR ET AL., 2004). Under oxidizing conditions Fe oxy-hydroxide coatings or particles were formed which are able to adsorb high amounts of As onto its surface (e.g. BOYLE & JONASSON, 1973; BGS & DPHE, 2001; SMEDLEY & KINNIBURG, 2002). The suspended particles got transported downstream, in this case by the RR, and deposited in the delta basin (WELCH ET AL., 1988; POSTMA ET AL., 2007). Over the centuries sediment has accumulated in the RRD up to its present state (Chapt. 3.3) burying the As sorbing particles. As long as the system stays oxic, As will remain associated to the solid phase.

For releasing As to the aquifers, microbially induced reductive dissolution of Fe oxy-hydroxides is widely accepted as a key process which also seems valid for the RRD (e.g. NICKSON ET AL., 2000; BGS & DPHE, 2001; DOWLING ET AL., 2002; SMEDLEY & KINNIBURG, 2002; BERG ET AL., 2007; POSTMA ET AL., 2007; NORRMAN ET AL., 2008). As explained in Chapter 3.3, high OM contents are common in the delta sediment and its microbial degradation can,

therefore, trigger reducing conditions (BERG ET AL., 2001). POSTMA ET AL. (2007) assumed that in Dan Phuong (~30 km upstream of Ha Noi) the rate of As release is controlled by the degradation rate of sedimentary OM. DOC-burdened water, for example, resulting from organic rich clay layers near the surface could percolate vertically leading to the onset of reducing conditions and subsequent As release in the Ha Noi area as concluded by BERG ET AL. (2008). If the confining clay layer is thinner than 2 - 3 m, infiltration of surface water rich in DOC and electron acceptors could also play a role as shown in Dan Phuong (LARSEN ET AL., 2008). The excessive groundwater abstraction from deep wells for the Ha Noi water supply could further intensify this vertical movement leading to a downward shift of the redox-front and, concurrently, enhance the As mobilization (BERG ET AL., 2008; NORRMAN ET AL., 2008). Some of the in Chapter 2.3 listed further possible mobilization mechanisms, like adsorption-desorption processes (NHAN ET AL., 2006; NORRMAN ET AL., 2008) or precipitation of new phases (POSTMA ET AL., 2007; BERG ET AL., 2008), are also of importance at least to a certain extent in the RRD as discussed later in Chapter 5.

Like in other affected areas (BGS & DPHE, 2001; VAN GEEN ET AL., 2003; MCARTHUR ET AL., 2004), a highly heterogeneous distribution of As in the groundwater within distances of less than 100 m has been observed in the RRD. BERG ET AL. (2007) found pronounced differences in the RRD within 10 - 20 m, especially in Van Phuc, the study site of this thesis (Fig. 3.3). Several explanations have been proposed for the complex spatial distribution of As, including differences in the subsurface lithology, mineralogy, geochemistry, local hydrology, and the abundance of OM (PAL ET AL., 2002; VAN GEEN ET AL., 2006A; STUTE ET AL., 2007) but still many open questions remain.

4.3 MITIGATION MEASURES AND STRATEGIES IN VIETNAM

In order to prevent similar health problems to Bangladesh and West Bengal, reasonable mitigation measures are of great importance for Vietnam. Government implemented a National Action Plan which shall address the problem on various levels (LUZI ET AL., 2004). Some important topics are briefly addressed below.

FILTER TECHNOLOGIES

In order to be implemented on a big scale, filter technologies have to be socially accepted, efficient, easy to use and maintain, operated without chemicals, locally available and cheap (LUZI ET AL., 2004). Simple sand filters have proven to satisfy these requirements and reduce As significantly in groundwater in Vietnam. BERG ET AL. (2006) tested sand filters in three villages in the RRD, including Van Phuc (study site). On average, 80% of As was removed from the groundwater by simply letting it percolate through the sand. However, the groundwater has to be relatively Fe rich ($\text{Fe/As} > 50$) in order to reach As concentrations $> 50 \mu\text{g/L}$. The efficiency of the filter is clearly hampered by high P concentrations ($< 2.5 \text{ mg/L}$). Meanwhile, further systems were tested in the RRD, like filtration with Mn oxides or combined sand filtration with plant cultivation (CAT ET AL., 2006). Especially the success of the latter does not seem to be influenced by high P concentrations.

EDUCATION

Firstly, the population itself has to be better informed about the As calamity, potential health effects and possible safety measures. The construction and use of sand filters has to be explained through training courses or by distributing manuals, leaflets etc. In regions where the common sand filters do not work properly (low Fe/high As, high P; see above) alternative sources of drinking water like rain water or switching to “save” wells have to be promoted or access to communal water supply has to be provided.

Secondly, government officials have to be further made aware of the seriousness of the situation (BUSCHMANN ET AL., 2008) and regularly informed and educated about new developments e.g. with regard to filter techniques as well as new scientific knowledge in order to promote necessary new measures (see below). Furthermore, training of health staff is necessary in order to recognize and medicate As related illnesses as soon as possible (LUZI ET AL., 2004).

IMPROVEMENT OF EXISTING WATER SUPPLY

Several communal and urban water plants are in operation, some of them pumping As contaminated water (BERG ET AL., 2001). As some of the plants

cannot decrease As below 10 µg/L, constant improvement of treatment technologies as well as testing of the water quality is necessary (CHIEU ET AL., 2006). Furthermore, staff has to be trained regularly, how to maintain the filter systems in order to prevent water quality deterioration (LUZI ET AL., 2004).

KNOWLEDGE EXTENSION AND COMMUNICATION

In order to be able to improve the measures permanently, more has to be known about the extent of the As distribution in Vietnam. Large areas have to be monitored with regard to dissolved As, Fe and P (for filter efficiency) and data has to be made accessible. On basis of the mapping recommendations can be circulated about the applicability of the filter systems and alternative possibilities. Furthermore, the basic knowledge about As mobilization as well as the processes occurring in filter systems has to be improved and discussed on a worldwide basis (LUZI ET AL., 2004).

4.4 OPEN QUESTIONS

The present situation in the RRD and worldwide highlights the need for intensive scientific studies. Therefore, many open questions can be posed concerning the As problem in general as well as specified on the situation in Van Phuc. The main question on which most of the other questions and also a lot of research is based on is about As mobilization in general. This question is still not answered satisfactorily. Not all of the below listed questions can be answered within the framework of this thesis.

GENERAL QUESTIONS:

- How does As mobilization work? This question is still not answered, satisfactorily.
- How and where is As fixed within the mineral structure? How stable is this association?
- Which minerals play a role in regulating the partitioning of As between the dissolved and solid phase?
- What causes the highly heterogeneous As distribution?

- How will As concentrations evolve over time, especially in case of increasing anthropogenic influence (waste water, industries etc.)?
- Does the excessive pumping have an influence on the As mobilization and distribution?
- What is the influence of hydrology and hydrogeology on As mobilization and distribution in time and space?
- How important is the composition and reactivity of OM with regard to the As mobilization?
- What is the role of microorganisms in the whole process?
- How do other elements counteract with As especially with regard to the uptake of several elements which surpass the WHO advised limit in groundwater?
- How does As behave in the nutrition chain?

QUESTIONS ARISING IN VAN PHUC:

- Where is As fixed in the mineral structure and are there noticeable differences between the two sites?
- Do the currently proposed release mechanisms apply in Van Phuc? Which of them are reasonable?
- What exactly is the redox driver?
- Is there a sharp boundary between redox zones?
- Does OM composition play a role?
- Are there different possible sources for OM?
- What is the reason for the patchy distribution of As in Van Phuc itself?
- Is the As rich zone expanding towards the low As zone?
- Does the “save” part of Van Phuc run a risk of As contamination in future and what could be the triggers for that?
- Are there old river channels within Van Phuc, being responsible for high As concentrations or the patchy distribution as proposed by some authors for other affected regions?

- What is the hydrogeological situation in Van Phuc? What is the contribution of infiltration of river and surface water to the groundwater chemistry as well as the As release?
- Will a rising water demand in the Ha Noi area also have an influence on the groundwater flow in Van Phuc, which does not seem to be the case at the moment?

5 GEOCHEMICAL PROCESSES UNDERLYING THE SHARP CONTRAST IN DISSOLVED ARSENIC CONCENTRATIONS

5.1 INTRODUCTION

The contamination of natural waters with As from geogenic sources poses a severe health problem throughout the world. Over the years, various processes have been postulated in order to explain high As concentrations in groundwater (Chapt. 2.3). The reductive dissolution of different Fe oxyhydroxides, which are common in sedimentary environments, is widely accepted as a key process for the release of As into groundwater (e.g. NICKSON ET AL., 2000; DOWLING ET AL., 2002; HARVEY ET AL., 2002; STÜBEN ET AL., 2003; CHARLET & POLYA, 2006). However, the reduction of Fe oxyhydroxides alone cannot explain the wide range of groundwater As concentrations encountered in similarly reducing aquifers (POLIZZOTTO ET AL., 2006; STUTE ET AL., 2007; VAN GEEN ET AL., 2008A). What is clear is that the microbially driven decomposition of OM plays an important role for the onset and the maintenance of reducing conditions in aquifers (LOVLEY 1992; LOVLEY & CHAPPELLE, 1995; ROWLAND ET AL., 2006; ROWLAND ET AL., 2007). Further processes under discussion which could influence the As concentration in groundwater are competition with other dissolved ions like PO_4^{3-} (SU & PULSE, 2001) or HCO_3^- (HARVEY ET AL., 2002; APELLO ET AL., 2002), oxidation of pyrite (CHOWDHURY ET AL., 1999) or precipitation and dissolution of secondary mineral phases (e.g. siderite, magnetite, amorphous phases incorporating arsenic) (SENGUPTA, 2004; SWARTZ ET AL., 2004; HERBEL & FENDORF, 2006).

There is still much disagreement about causes underlying the patchy As distribution commonly observed in affected areas. Several explanations have been proposed for the complex spatial distribution of As, including differences in the subsurface lithology, mineralogy, geochemistry, local hydrology, and the abundance of OM (PAL ET AL., 2002; VAN GEEN ET AL., 2006B; STUTE ET AL., 2007). In this chapter, geochemical results from sediment cores recov-

ered from the two contrasting sites in Van Phuc, as well as profiles of groundwater properties obtained from nests of wells installed at the same two locations are presented and discussed. The aim of this chapter is (1) to describe the lithology of the two sites, and, (2) to reveal considerable differences with regard to (organic) geochemistry, mineralogy and hydrology between the two sites in order to better understand processes responsible for the patchy distribution of As.

5.2 MATERIALS AND METHODS

In April 2006, two ~55 m-long sediment cores were recovered by rotary drilling at site L, located in the low-arsenic area, and at site H in the high-arsenic area (Fig. 3.3). The distance between the two sites is only 700 m. Nine monitoring wells ranging from 17 to 55 m in depth and consisting of PVC casings with a 1-m long sand trap at the bottom were installed at each site. To avoid infiltration of surface water, concrete pads surrounding the upper steel casing were installed and each well was capped with a steel screw cap (Fig. 5.1).

5.2.1 WATER SAMPLING AND ANALYSIS

Water samples were taken from the nine monitoring wells at each site (Fig. 5.1, Fig. 5.2). Prior to sampling, groundwater was pumped for about 10 min with an electrical pump to avoid any contamination by stale water. A portable system YSI 556 and a WTW Multi 340i (John Morris Scientific Pty Ltd.) was used to measure Eh, pH, temperature, conductivity and oxygen. Disposable cartridges that selectively adsorb As(V) were used in the field to determine the speciation of As (MENG ET AL., 2001) by difference relative to total dissolved As concentrations. For analysis of metals, NH_4^+ and total phosphorus (P_{tot}) samples were filtered on-site (cellulose nitrate filter, 0.45 μm) and acidified by HNO_3 (65%, Fluka, Switzerland) to a pH <2. For anions, alkalinity ($\sim\text{HCO}_3^-$) and DOC, the samples were left unfiltered and non-acidified. These samples were filled in pre-rinsed polypropylene bottles, sealed tightly and stored in the dark at 4 °C until analysis. For alkalinity the samples were filtered in the lab before analysis. In order to check the quality of the alkalinity analysis in the lab, control-measurements were done in the field with a test kit (Merck, Germany). The results of lab and field measurements were

within 10% and, therefore, a significant alteration of the alkalinity during storage and transport can be excluded.

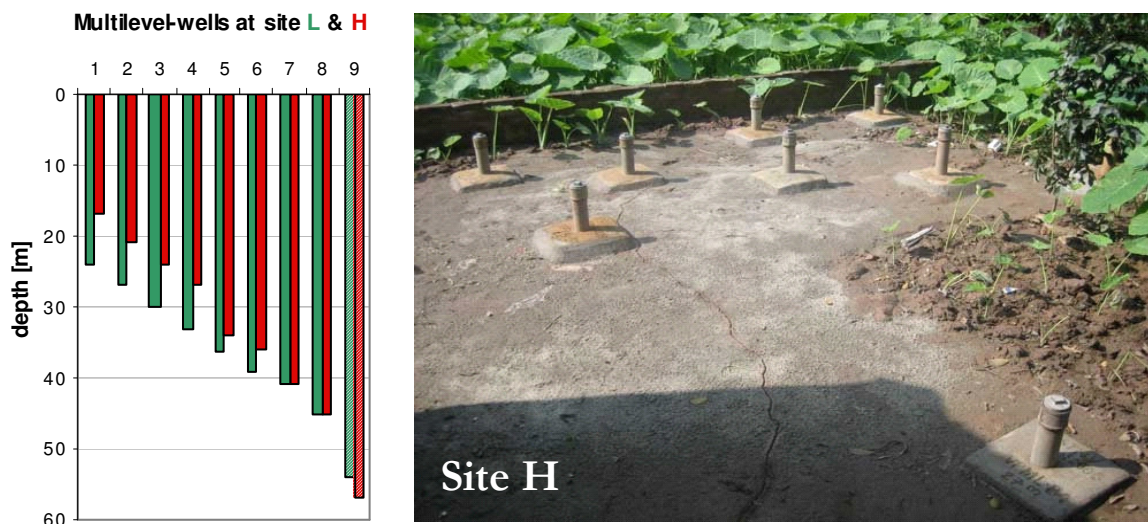


Fig. 5.1: Depth distribution (left) of the nine multi-level wells at site L (green) and H (red). To protect the wells from infiltration of surface water, they were sealed with a concrete pad and a metal cap (right) (picture: M. Berg).

Dissolved As, P_{tot} and S concentrations were measured by high-resolution ICP-MS (Element 2, Thermo Fisher, Bremen, Germany). The analysis of Fe, Mn, Ca, Mg and Ba was conducted by ICP-OES (Spectro Ciros CCD, Kleve, Germany). NH_4^+ was analysed by photometry; NO_3^- and Cl⁻ by ion chromatography (Dionex, Switzerland), alkalinity by titration and DOC by means of a TOC 5000 Analyser (Shimadzu, Switzerland). All groundwater analyses were carried out at Swiss Federal Institute of Aquatic Science and Technology (EAWAG). The quality of the results can be taken as reasonably good as the ion balance varies within less than 10%.

5.2.2 SEDIMENT SAMPLING AND ANALYSIS

Samples were taken from the sediment cores in intervals of 1-m and more frequently in cases of significant changes in colour, grain size or texture. About 100 g of fresh sediment material was filled in polypropylene bags and later flushed with nitrogen to minimize oxidation processes in the time between sampling and analysis. Before transport the samples were packed into Mylar bags and flushed again with nitrogen to avoid oxidation and altera-

tion of the sediment. The samples were sent to Germany where they were frozen until further analysis. Prior to analysis, subsamples of the sediment were dried at 40 °C and ground to powder or fresh, unfrozen sediment was used.

The labelling of the samples consists of the site where they were taken (L or H), the consecutive number of the run during drilling (first two numbers) and the depths where the sample was taken within the corresponding run in centimetre. In all tables the respective depth in metre within the whole sediment profile is given.

ENERGY DISPERSIVE X-RAY FLUORESCENCE (EDX)

The bulk elemental composition of the sediments was determined by energy dispersive X-ray fluorescence analysis (Spectra 5000, Atomica). A rhodium X-ray tube was used as radiation source whereas a Si(Li)-detector was used for detection and quantification. In order to optimize the fluorescence measurements each sample was analysed by consecutively applying an Al-, Cu- and Pd-filter. Precision (better than 5%) was calculated from repeated measurements of a standard material, whereas accuracy (better than 10%) was checked by including different reference materials, e.g. GXR 2 (Park City, Utah, USA).

CARBON AND SULPHUR ANALYSIS

Total sulphur (TS) and carbon contents were quantified by a Carbon-Sulphur-Analyser (CSA 5003, Leybold Heraeus, Germany), and inorganic carbon (TIC) was determined by a Carbon-Water-Analysis (CWA 5003, Leybold Heraeus, Germany). The organic carbon content (TOC) was calculated by subtracting inorganic carbon from total carbon.

X-RAY DIFFRACTION ANALYSIS (XRD)

The bulk mineral composition of the sediment samples was analysed by means of X-ray diffraction (XRD) analysis (Kristalloflex D500, Siemens, Germany) at 40 kV and 25 mA. CuK α 1-radiation was used at angles between 3° and 63°. The semi-quantitative evaluation of the spectra was based on

calibration curves obtained from different samples with known mineral composition (SNYDER & BISH, 1989).

GRAIN SIZE DISTRIBUTION

The grain size distribution of the sediment was measured at Vanderbilt University using a laser-granulometer (Mastersizer 2000, Malvern). The grain sizes were grouped as follows: clay: < 2 μm , silt: 2 - 63 μm , sand: > 63 μm .

REFLECTANCE MEASUREMENTS

A CM2005d spectrophotometer (Minolta Corp., USA) was used in order to measure the diffuse reflectance spectrum of freshly collected sediment in the field relative to a white standard plate consisting of barium sulphate (B. Weinman, Vanderbilt University). Exposure to air considerably alters the reflectance over time, therefore, the measurements, which were repeated three times, had to be done immediately.

The difference in reflectance between 530 and 520 nm was calculated from the measurements in order to obtain a value (ΔR in % reflectance) that previous work has shown is inversely related to the Fe(II)/Fe ratio in the acid-leachable fraction of aquifer particles in Bangladesh and, therefore, indicates the predominance of Fe(II) or Fe(III) bearing mineral phases. Grey sediments, which mainly contain Fe(II) bearing minerals have ΔR values from 0.1 to 0.6, whereas it can go up to 1 in orange sediments, where Fe(III) minerals predominate. In peat the ΔR -value is close to zero (HORNEMAN ET AL., 2004).

SEQUENTIAL EXTRACTION

Sequential extractions are often used in order to get information about the solid-phase partitioning of As in order to estimate its potential mobility within aquifers (Keon et al., 2001). Over the past years several different extraction methods were developed whereupon the most common are described in KEON ET AL. (2001), WENZEL ET AL. (2001) and VAN HERREWEGHE ET AL. (2003).

In general, solutions with increasing strength are added subsequently, either leading to ion exchange reactions (e.g. phosphate exchanges for arse-

nate) or mineral dissolutions. However, each fraction is only operationally defined. Further disadvantages arise from possible alterations, re-adsorption processes, a sometimes poor reproducibility and a lack of selectivity of solutions for some phases (HUDSON-EDWARDS ET AL., 2004). Nevertheless, sequential extractions are widely used in scientific studies (e.g. SWARTZ ET AL., 2004; POSTMA ET AL., 2007; BERG ET AL., 2008) and are an easy way to get a hint about the dominant association of As with different phases without the need for very specialized and cost intensive instruments (μ S-XAS, Infrared-spectroscopy etc.) (KEON ET AL., 2001).

In this study, the procedure of KEON ET AL. (2001), which was specially developed for sediments, was used in a slightly modified version (Tab. 5.1). In order to avoid interferences with ICP-MS measurements, 0.05 M $(\text{NH}_4)_2\text{SO}_4$ (WENZEL ET AL., 2001) was used instead of MgCl_2 in the first step. In the presence of chloride, argon-chlorine complexes develop, which are difficult to separate from As in the ICP-MS. Furthermore, in step 5 the application of the potentially explosive Ti-citrate-EDTA was exchanged by a dithionite-citrate-bicarbonate (DCB) solution described in Van Herreweghe et al. (2003). Finally, steps 7 and 8 of the original procedure were combined into one step. Specific conditions and the phases targeted by each step are listed in Tab. 5.1.

For sequential extractions of sediment from seven intervals at site L and nine at site H (Fig. 5.2), that were chosen based on their As concentration, 0.5 g of fresh sediment was weighed into centrifuge tubes and the appropriate amount of leaching solution was added (Tab. 5.1). After each step the solutions were centrifuged at 4500 rpm for 15 min and then decanted. The solutions were kept in a refrigerator until further measurements by (HR-) ICP-MS (Axiom, VG Elemental). The precision for As, calculated from three repeated measurements was $\pm 2\%$. The detection limit for As was $0.09 \mu\text{g/L}$, calculated as $3\sigma_{\text{blank}}$ (WILLIAMS, 2001). Accuracy ($< \pm 5\%$ for As, $< \pm 10\%$ for all elements) was checked by including the multi-element standard HPS CRM-TMDW into the analysis. In order to check the reproducibility of the sequential extraction, one subsample was first homogenized and afterwards separated into three aliquots. In five out of seven of the fractions the results for

Fe and As concentrations did not differ more than 10 %, which constitutes a reasonable level of reproducibility.

Tab. 5.1: Sequential extraction scheme used for the sediment leaching.

Step	Target phase	Extractant	Conditions	Ref.
F1	Ionically bound	0.05 M (NH ₄) ₂ SO ₄	25 mL, 4 h, 25 °C one repetition, one water wash	[1]
F2	Strongly adsorbed	0.5 M NaH ₂ PO ₄	40 mL, 16 h & 24 h, 25 °C, pH 5 one repetition of each time duration, one water wash	[2]
F3	Coprecipitated with acid volatile sulphides, carbonates, Mn-oxides, very amorphous Fe oxy-hydroxides	1 M HCl	40 mL, 1 h, 25 °C one repetition, one water wash	[2]
F4	Coprecipitated with amorphous iron Fe oxy-hydroxides	0.2 M NH ₄ ⁺ -Oxalate/oxalic acid	40 mL, 2 h, 25 °C, pH 3 kept dark (wrapped in Al-foil), one repetition, one water wash	[2]
F5	Coprecipitated crystalline Fe hydroxides	with DCB: 0.5 M Na-Citrate + 1 M NaHCO ₃ ; 0.5 g Na ₂ S ₂ O ₄ ·xH ₂ O	35 mL Na-Citrate + 2.5 mL NaHCO ₃ (heating to 85 °C), addition of 0.5 g Na ₂ S ₂ O ₄ ·xH ₂ O, 15 min at 85 °C, one repetition, one water wash	[3]
F6	Coprecipitated silicate	with 10 M HF 5 g boric acid	40 mL, 1 & 24 h, 25 °C one repetition of each time step, after 16 h addition of boric acid, one hot wash	[2]
F7	As-sulphides, coprecipitated with sulphides, organic matter	16 M HNO ₃ 30 % H ₂ O ₂	Method according to EPA 3050B	

[1] WENZEL ET AL. (2001); [2] KEON ET AL. (2001); [3] VAN HERREWEGHE ET AL. (2003)

5.2.3 GEOCHEMICAL MODELLING AND STATISTICAL ANALYSIS

The saturation indices (SI) of different minerals like calcite, dolomite, siderite etc. were calculated on basis of the hydrochemical results with the PHREEQC-program (PARKHURST & APPELO, 1999).

For the interpretation of sediment and water data it is helpful to reveal possible relations between different elements in order to draw conclusions about release mechanisms, associations of elements etc. Therefore, correlation coefficients according to Pearson, referred to as *r*-values, were calculated after the removal of outliers. Spearman's rank correlation coefficient, referred to as *r_s*-values, which are less sensitive for outliers, were calculated for sediments. By definition, the *r*-value can vary between 1 and -1, whereupon values close to |1| indicate good and a value of zero no correlation. Statistical analysis of water as well as sediment data was done using the STATISTICA program package (StatSoft, USA, Version 6). The *p*-value, indicating the confidence for the given correlations, is always < 0.01.

5.3 RESULTS AND INTERPRETATION

5.3.1 LITHOLOGY AND REFLECTANCE

Based on grain-size, the core at site L can be separated into three distinct layers: a silty (75 ± 12 %) layer extending from the top to a depth of 23 m, a sandy (65 ± 16 %) intermediate layer with varying amounts of silt to a depth of 48 m, and a coarse gravel layer extending to a depth of 54 m where drilling stopped (Fig. 5.2).

Noteworthy, are two distinct black, organic rich intervals at depths of ~12 and ~19 m, respectively, within the upper silty layer. This layer can be considered as aquitard, based on the low hydraulic conductivity (*K*: $\sim 7 \times 10^{-8}$ m/s, for more details see Tab. A-6) estimated from the grain size distribution (BEYER, 1964). The transition to the underlying aquifer at a depth of 23 m is marked by an Fe concretion consisting of goethite and quartz. The aquifer is separated into an upper sand (*K*: $\sim 2 \times 10^{-6}$ m/s) and a lower gravel deposit (Fig. 5.3a). The upper part is ~25 m thick and mainly composed of fine to medium sands interspersed with silty layers, mostly brown to yellowish-brown in colour.

The lithology of core H differs significantly from core L and is more heterogeneous (Fig. 5.3b). The upper silt (68 ± 20 %) layer is only ~10 m thick and the colour changes from reddish-brown to greyish at ~7 m. The esti-

mated permeability in this layer is comparable to the aquitard at site L ($K: \sim 7 \times 10^{-8}$ m/s, Tab. A-7). Below this layer, alternating clayey silt, silty fine sands, and fine sands were observed to a depth of ~ 21 m. Within this layer the hydraulic conductivity increases to ($K: \sim 4 \times 10^{-6}$ m/s) until deeper in the aquifer when hydraulic conductivity increases further ($K: \sim 7.6 \times 10^{-6}$ m/s) due to the prevalence of sand ($61 \pm 20\%$) with varying amounts of silt. Noteworthy, is a change in colour from greyish to brownish at ~ 44 m. At a depth of 55 m, a much coarser gravel layer like at site L appears.

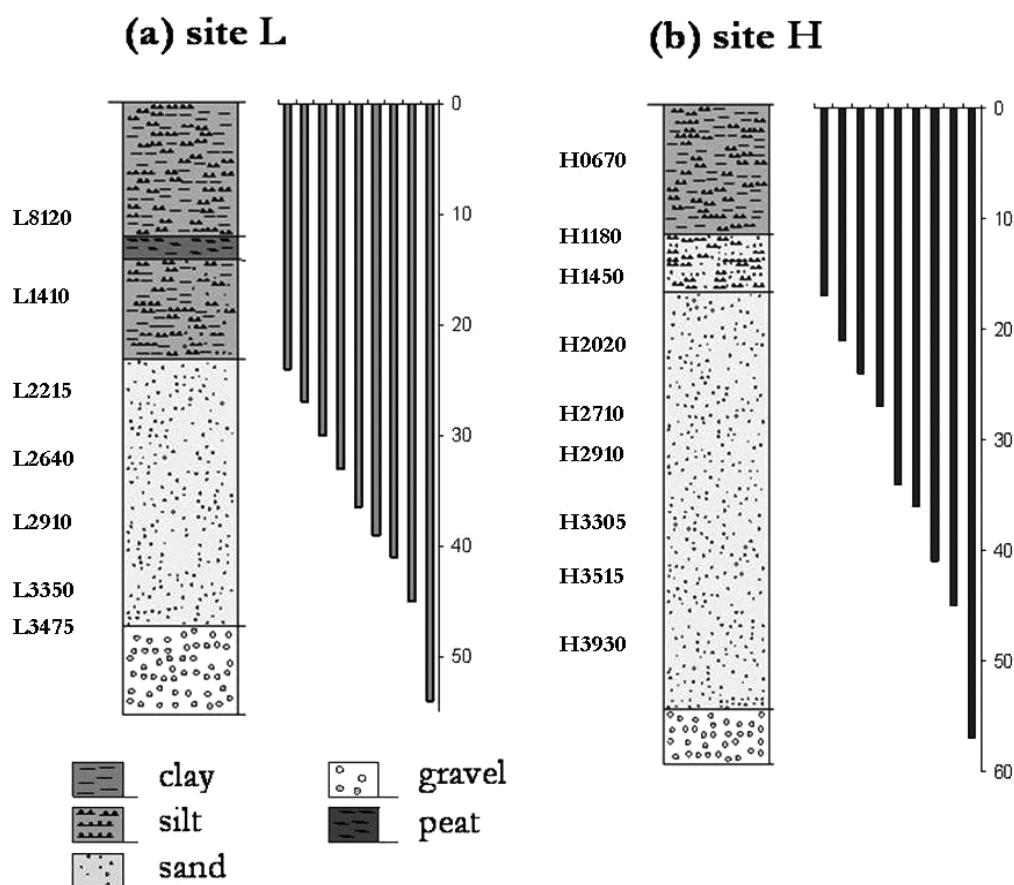


Fig. 5.2: Lithological logs of the boreholes drilled in April 2006 at (a) site L and (b) site H. Each site was equipped with a nest of nine monitoring wells. The labelling on the left side of each log marks the samples taken for sequential extraction procedure.

The spectral reflectance data are consistent with changes in the colour of the sediment and can be related more quantitatively to changes in the redox state of acid-leachable Fe oxy-hydroxides (HORNEMAN ET AL., 2004). At site L, the peat layer corresponds to an interval of particularly low ΔR (< 0.1)

whereas values >0.7 (Fig. 5.3a) in the underlying aquifer are typical for oxidized orange sediments. Values of $\Delta R < 0.25$ in the grey sands at site H (Fig. 5.3b) are consistent with more reducing conditions throughout the 7 to 44 m depth range (VAN GEEN ET AL., 2006A). An increase in $\bullet R$ towards the bottom of the core at site H parallels the observed change in colour and indicates a transition towards less reducing conditions.

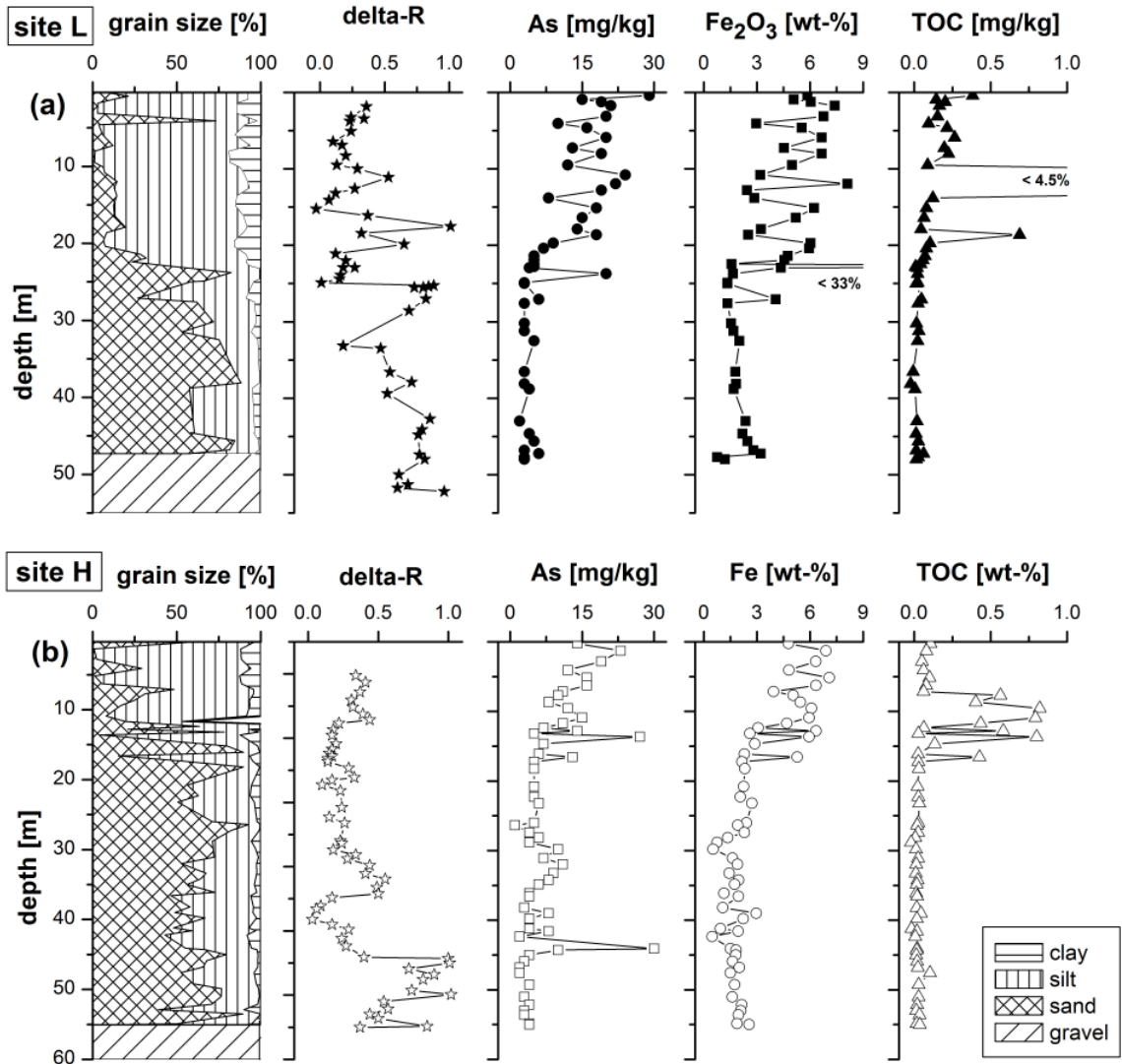


Fig. 5.3: Depth profiles of grain size distribution in cumulative percentage of clay (<2 μm), silt (<63 μm), sand (>63 μm) and gravel (>2 mm), reflectance ($\bullet R$ at 520 nm) and concentration of arsenic, iron and total organic carbon (TOC) in the sediment at site L (3a) and site H (3b).

5.3.2 HYDROCHEMISTRY

SITE L

The hydrochemistry is distinctly different at the two sites. As indicated by the Piper diagram in Fig. 5.4, the water at site L can be classified as Ca-(Na)-Mg-HCO₃ type, whereas the water at site H belongs to a Ca-HCO₃ type. Low Cl concentration in combination with Ca²⁺ over Mg²⁺ predominance is typical for deltaic groundwater (WHITE ET AL., 1963; STÜBEN ET AL., 2003) and the RR (BERG ET AL., 2008). A detailed overview of the hydrochemical data is given in Appendix 1.

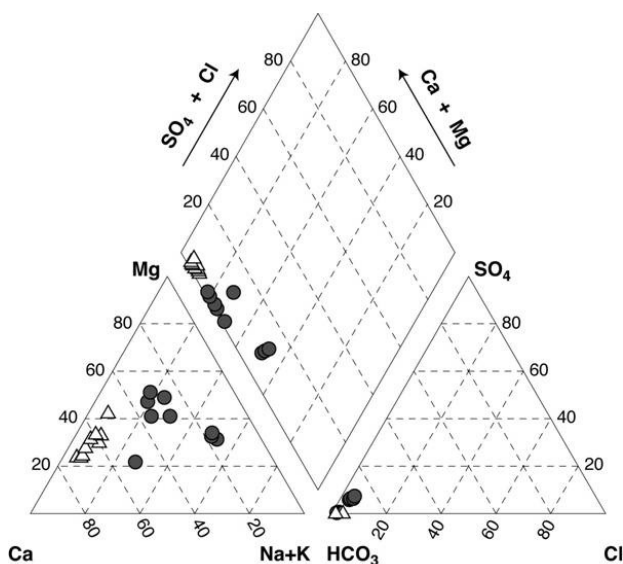


Fig. 5.4: Piper diagram based on the hydrochemical data at site L (•) and H (Δ). The groundwater can be classified as Ca-(Na)-Mg-HCO₃ type at site L, and as Ca-HCO₃ type at site H.

Concentrations of dissolved As in groundwater at site L range from 0.9 to 7.8 µg/L and are below the WHO-limit of 10 µg/L. Concentrations remain very low throughout the sandy aquifer, with 7.8 µg/L reached only in the gravel layer (Fig. 5.5). 50 to 90% of As in groundwater is present as As(III) at site L. The pH (6.7 ± 0.2) is also rather constant throughout the depth profile. The absence of NO₃⁻ and high dissolved Mn concentrations (1.1 ± 1.1 mg/L) (Fig. 5.5) suggest that the groundwater at site L can be considered as Mn-reducing with regard to the classical redox sequence, at least in the upper part of the profile. However, the presence of dissolved Fe (1.8 ± 0.6 mg/L) throughout the depth range and the decrease in dissolved S (which is probably mainly present as sulphate) to <0.4 mg/L below 30 m

depth (Fig. 5.5) suggest some overlap with reactions typically associated with more strongly reducing conditions (sulphide and methane were not measured, but the freshly pumped groundwater did not smell of H_2S).

The mean molar Fe/As ratio in the water at site L is very high (>1000), although both Fe and As concentrations are very low. The conductivity ($230 \pm 64 \mu\text{S}/\text{cm}$) points towards relatively low mineralization in the aquifer at site L, which is consistent with low concentrations of Ca^{2+} ($25 \pm 13 \text{ mg}/\text{L}$), Mg^{2+} ($21 \pm 10 \text{ mg}/\text{L}$) and Ba^{2+} ($67 \pm 32 \mu\text{g}/\text{L}$) compared to site H. Typical indicators of biodegradation such as NH_4^+ ($0.2 \pm 0.1 \text{ mg}/\text{L}$), DOC ($1.3 \pm 0.6 \text{ mg}/\text{L}$), HCO_3^- ($250 \pm 80 \text{ mg}/\text{L}$) as well as P_{tot} ($70 \pm 40 \mu\text{g}/\text{L}$) are generally low in concentration (Fig. 5.5), suggesting limited organic turnover in the aquifer at site L.

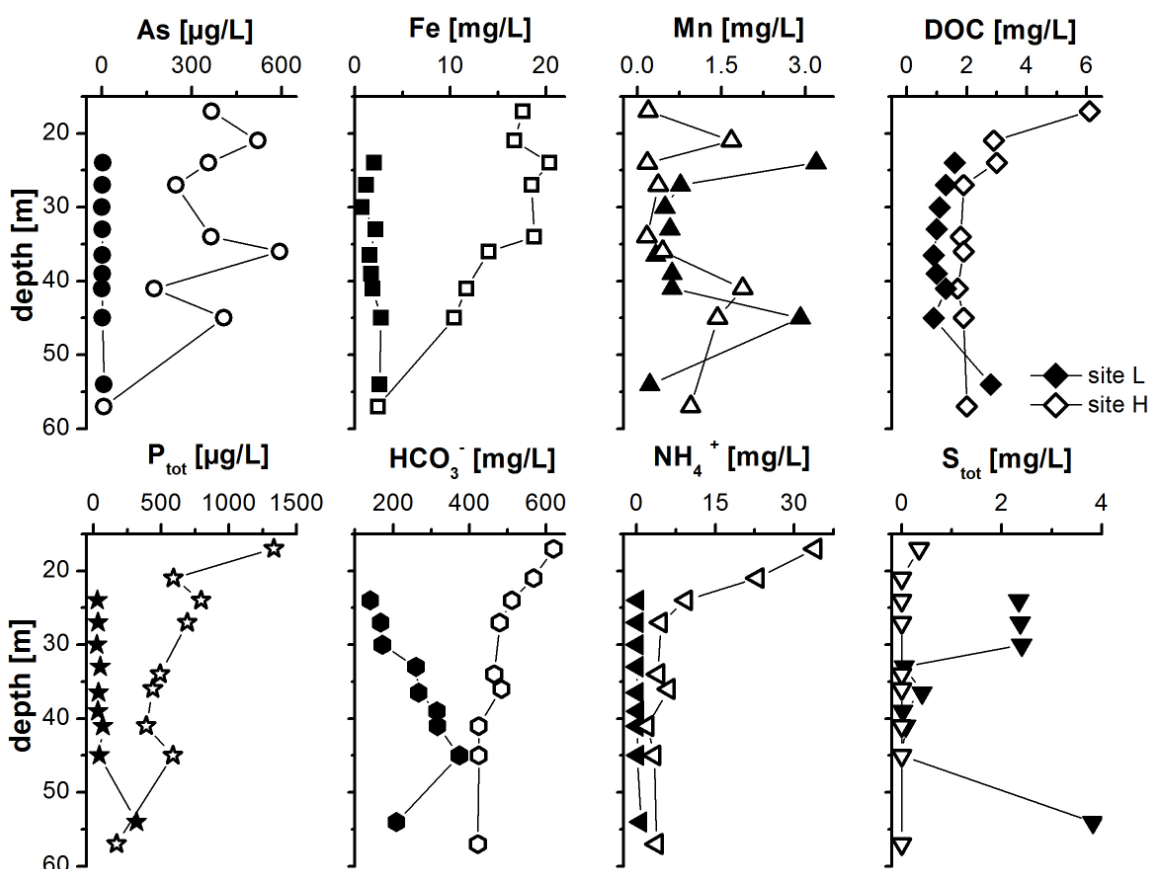


Fig. 5.5: Depth profile of dissolved arsenic, iron, manganese, dissolved organic carbon (DOC), total phosphorous, hydrogen carbonate, ammonium and total sulphur (zero values: below detection limit of $5 \text{ mg}/\text{L}$) analysed in the groundwater from site L (closed symbols) and site H (open symbols).

The significant correlation between the sum of Ca^{2+} and Mg^{2+} with HCO_3^- ($r = 0.99$, $n = 9$) suggests that these three ions mainly originate from the dissolution of calcite and dolomite. Calcite ($\text{SI}_{\text{calcite}} = -1 \pm 0.6$) and dolomite ($\text{SI}_{\text{dolomite}} = -1.7 \pm 1$) are subsaturated, especially in the upper part of the aquifer at site L (Fig. 5.6a). The corresponding molar ratio of $[\text{HCO}_3^-]/[\text{Mg}^{2+} + \text{Ca}^{2+}] \sim 3$ indicates, however, that sources other than carbonate dissolution contribute to the bicarbonate in the groundwater.

SITE H

In contrast to site L, As concentrations at site H are generally well above 10 $\mu\text{g/L}$ and range from 170 to 600 $\mu\text{g/L}$ in the sandy aquifer. More than 90% of As in groundwater occurs in the reduced As(III) form. The concentration of As declines sharply to 7 $\mu\text{g/L}$ (Fig. 5.5) in groundwater pumped from the coarse gravel layer at the bottom of the section. The pH (7.1 ± 0.1) at site H is slightly higher than at site L. The groundwater is characterized by high concentrations of dissolved Fe (14.5 ± 5.6 mg/L) although dissolved Mn (0.8 ± 0.7 mg/L) levels are comparable to site L. Concentrations of NO_3^- and dissolved S are not detectable throughout at site H (Fig. 5.5). There is a significant correlation between dissolved Fe and Eh ($r = 0.89$, $n = 9$), suggesting reductive dissolution of Fe minerals in the aquifer at site H.

The molar Fe/As-ratio of ~ 100 in groundwater is comparable to Fe/As ratios reported by BERG ET AL. (2008) in Van Phuc and Thuong Cat for aquifers that are elevated in As. Concentrations of NH_4^+ (10 ± 7 mg/L), P_{tot} (0.6 ± 0.3 mg/L), HCO_3^- (490 ± 70 mg/L) as well as DOC (2.59 ± 1.4 mg/L) all suggest microbial degradation of organic material that is most pronounced in the upper part of the profile at site H and decreases in intensity with depth (Fig. 5.5). Higher conductivities (490 ± 40 $\mu\text{S/cm}$) measured at site H compared to site L points towards enhanced mineralization, especially in the upper part of the profile (Fig. 5.5). Elevated concentrations of dissolved Ca^{2+} (110 ± 15 mg/L) and Ba^{2+} (590 ± 230 $\mu\text{g/L}$) suggest dissolution of minerals such as gypsum or barite, which are both undersaturated over the entire profile at site H (data not shown). However, the groundwater is supersaturated with respect to calcite as well as dolomite at this site (Fig. 5.6b). Since there is no correlation between HCO_3^- and the sum of Ca^{2+} and Mg^{2+} concen-

trations, elevated levels of HCO_3^- in shallow aquifers at site H are probably not the result of calcite or dolomite dissolution but, instead, the product of mineralization of OM. This interpretation is consistent with a significant correlation between HCO_3^- and NH_4^+ ($r = 0.95$, $n = 9$) as well as DOC ($r = 0.86$, $n = 9$).

The composition of groundwater suggests the formation of new Fe minerals at site H. There is a correlation between HCO_3^- concentrations and the SI for siderite ($r = 0.71$, $n = 8$) as well as dissolved Fe and $\text{SI}_{\text{siderite}}$ ($r = 0.95$, $n = 9$). Siderite was detected in the XRD-measurements, and geochemical modeling shows that it is strongly supersaturated throughout the profile ($\text{SI}_{\text{siderite}} = 1.5 \pm 0.3$) (Fig. 5.6b). This suggests siderite precipitation, despite reported slow kinetics at low temperatures (POSTMA, 1982). Dissolved Fe concentrations also correlate well with P concentrations ($r = 0.84$, $n = 8$), suggesting that phosphate originally adsorbed onto Fe oxy-hydroxide minerals may be released during the dissolution of these phases at site H. The result is that groundwater at site H is also supersaturated with respect to vivianite ($\text{SI}_{\text{vivianite}} = 1.95 \pm 0.5$) (Fig. 5.6b). Vivianite was detected in the sediment by XRD, especially in the upper part of the profile.

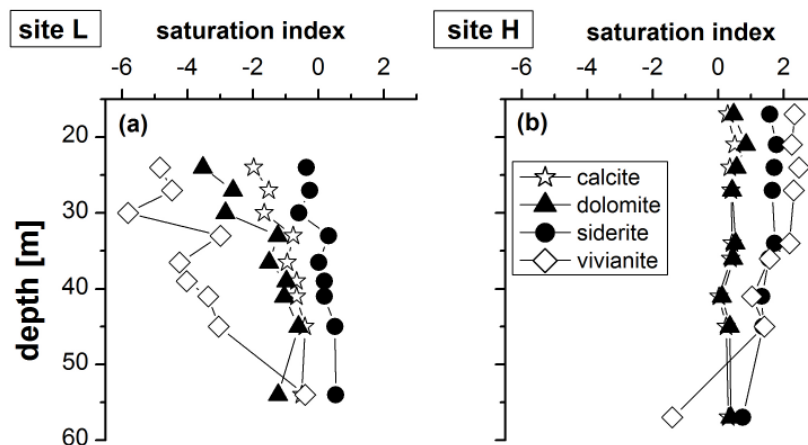


Fig. 5.6: Depth profiles of saturation indices of calcite, dolomite, siderite and vivianite at site L (a) and site H (b).

The hydrochemistry of groundwater at the depth of the gravel layer is broadly similar at both sites (Fig. 5.5). This holds for dissolved As ($\sim 7 \mu\text{g/L}$) as well as dissolved Fe (2 mg/L) and P_{tot} ($0.3 - 0.6 \text{ mg/L}$). The deepest groundwater at both sites is supersaturated with respect to calcite and dolomite, as in the shallower sandy aquifer at site L. The concentration of

dissolved S, present as sulphate, is significantly higher in the gravel layer at site L compared to site H, however. The overall patterns suggest that the composition of groundwater at depth in Van Phuc may rather be controlled by region-wide flow through the Pleistocene gravel layer than by differing local conditions.

5.3.3 MINERALOGICAL AND GEOCHEMICAL COMPOSITION

The bulk mineralogical composition of the sediment at site L and H is very similar (for details see Appendix 4). The dominant minerals are quartz (L: 56 ± 19 , H: 59 ± 15 wt-%), mica (19 ± 5 , 17 ± 8 wt-%), feldspars (10 ± 6 , 14 ± 6 wt-%) and kaolinite (7 ± 2 , 5 ± 3 wt-%). Variations in their relative proportions with depth depend primarily on grain size. In clayey silt, quartz (44 ± 12 , 40 ± 7 wt-%) and feldspars (5 ± 1 , 5 ± 1 wt-%) are less abundant, whereas in sand their contribution is significantly higher (quartz: 74 ± 11 , 65 ± 11 wt-%; feldspars: 14 ± 4 , 15 ± 4 wt-%). The increase is mainly at the expense of phyllosilicates like mica, chlorite, and kaolinite, which are much less abundant in the sandy layers. The presence of calcite and dolomite was low or absent throughout the profiles and could be quantified only in clayey silt (~ 1 wt-%). Fe minerals such as hematite, goethite, and hornblende are present throughout at site L and in most intervals at site H but their amounts could not be quantified. Minerals such as siderite, ilmenite, vivianite, gibbsite, and boehmite were detectable in some but not all intervals at both sites. In the aquifer of site L, pyrite was detected in some samples.

The concentration of As in the solid phase at both sites is within the typical range reported for unconsolidated sediments (SMEDLEY & KINNIBURGH, 2002). Concentrations of 1 - 30 mg/kg As (Fig. 5.3) are also comparable to previous observations in alluvial systems in Bangladesh or West Bengal where groundwater As levels are elevated (e.g. NICKSON ET AL., 2000; SWARTZ ET AL., 2004; POLIZZOTTO ET AL., 2006). The concentration of solid As in the sandy deposits is low at both sites with ~ 5 mg/kg, on average, compared to higher values in the upper silty layers of 14.5 ± 7 mg/kg (Fig. 5.3).

Concentrations of Fe in the solid phase (~ 5 wt-%) are higher in the upper part of the profile at both sites compared to the underlying sandy aquifer.

fer (2 wt-%, Fig. 5.3). Throughout the entire core of site L, there is also a clear relationship between As and Fe concentrations in the solid phase ($r_s = 0.74$, $n = 42$). The relationship is weaker at site H ($r_s = 0.62$, $n = 55$). The molar solid Fe/As ratio is slightly higher in the aquifer at site L (4000 ± 1500) compared to site H (3200 ± 2000). The ratio is within the range of 4200 - 4600 previously reported by BERG ET AL. (2008) for sediments in contact with groundwater high in As in the region. The elemental concentration of further elements is listed in appendix 4.

At both sites organic rich layers were found in the upper part of the profile (Fig. 5.3). The TOC content is up to 4.5 wt-% in the aquitard at site L but only up to 0.8 wt-% at site H. On average, the concentration of TOC in the sandy deposits is below 0.03 wt-% at both sites. These values are in the same range as previous TOC measurements for aquifers in the Ha Noi region of 0.04 - 0.74 wt-% and 0.02 - 2.5 wt-% by POSTMA ET AL. (2007) and BERG ET AL. (2008), respectively.

5.3.4 SEQUENTIAL EXTRACTIONS

SITE L

Arsenic appears to be associated in the sediment with different phases in the silty aquitard and in aquifer sands at site L. In the aquitard (L8120, L1410, Fig. 5.2), more than 40% of As was released by PO_4^{3-} extraction (F2, Tab. 5.2, Appendix 2), a fraction associated with strong adsorption. The HCl extractable fraction is another important pool in this interval (F3, 10 - 20%) and may represent other host phases such as Mn-oxides, very amorphous Fe oxyhydroxides, siderite, vivianite and amorphous Al oxides. A molar Fe:Al ratio of 9:1 and the low quantities of Mn released in the HCl-treatment compared to Fe and Al suggest that only Fe minerals contribute, significantly. Additionally, the extractions indicate that sulphides and organic matter (F7) may also contain significant levels of As (20 - 30 %), which would be consistent with elevated TS (0.2 - 0.6 wt-%) and TOC (0.7 - 4 wt-%) concentrations in the upper layer. Compared to fractions F2, F3, and F7, other extractions did not release significant quantities of As from the aquitard at site L (Tab. 5.2). Iron was mainly released in the HCl-, HF- and $\text{HNO}_3/\text{H}_2\text{O}_2$ extraction steps

(F3-F6-F7). Possible Fe phases released by these extractions include very amorphous Fe oxy-hydroxides (i.e., ferrihydrite), siderite, phyllosilicates (i.e., chlorite and biotite), amphiboles, and Fe sulphides (e.g. pyrite). Extraction F3 may also include adsorbed Fe(II) (DIXIT & HERING, 2006).

In aquifer sands from site L, instead, little As was released by the PO_4^{3-} extraction whereas more than 90% of As was released by HCl (F3: 35 - 54 %) and DCB (F5: 25 - 65 %, Tab. 5.2). The lack of correlation between Fe and As released in F3 and F5 suggests non-Fe containing minerals may be significant hosts of As in aquifer sands at site L. These may include amorphous Al oxides, as suggested by similar Fe and Al concentrations in F3 (3:2). All the other extraction released minor or undetectable levels of As (Tab. 5.2). Most of the Fe presented in aquifer sands at site L was released by DCB (13 - 48 %) or HF (26 - 54 %), suggesting the dominance of crystalline Fe oxy-hydroxides like hematite or goethite, as well as Fe containing silicates (Tab. 5.2).

Tab. 5.2: Average partitioning of iron and arsenic in each fraction of the sequential extraction for all samples of site L and H.

	Core L				Core H	
	Silt		sand		As [%]	Fe [%]
	As [%]	Fe [%]	As [%]	Fe [%]		
F1 (SO_4 -step)	4	2	4	<1	5	<1
F2 (PO_4 -step)	44	8	<1	3	56	8
F3 (HCl-step)	17	20	46	14	16	16
F4 (Ox-step)	2	4	<1	5	6	8
F5 (DCB-step)	7	6	38	35	6	32
F6 (HF-step)	1	38	9	41	9	37
F7 ($\text{HNO}_3/\text{H}_2\text{O}_2$ -step)	25	22	2	<1	2	<1
	As [mg/kg]	Fe [g/kg]	As [mg/kg]	Fe [g/kg]	As [mg/kg]	Fe [g/kg]
Total amount in sediments (average)	41	23	2	19	8	23

SITE H

In contrast to site L, strongly adsorbed As liberated by the PO_4^{3-} extraction was by far the dominant pool (F2: >50 %) throughout the sandy aquifer at site H (Tab. 5.2). Additional quantities of As were also extracted by HCl (F3: 10 - 20 %) and HF (F6: ~ 9 %) solutions. The average molar Fe:Al ratio of 5:2 in the solid phase suggests that amorphous Al oxides are probably less important at site H than at site L. Contributions of As from other extractions were minor.

At site H, concentrations of Fe in the sediment extractable with DCB and HF are roughly balanced (32 - 37 %) and larger than in the HCl extractable pool (16 %, Tab. 5.2). These observations indicate that Fe is mainly bound in crystalline phases like oxy-hydroxides and silicates (hematite, biotite, hornblende, etc.) as well as amorphous phases. Some Fe is also released by the PO_4^{3-} extraction (~ 8 %), indicating that Fe(II) might also be adsorbed to mineral surfaces, and by the oxalate extraction (~ 8 %).

5.4 DISCUSSION

5.4.1 ASSOCIATIONS OF ARSENIC IN THE SEDIMENT

The main difference in sediment geochemistry between the two sites is the extent of reduction of Fe oxy-hydroxides which, as inferred from colour and reflectance, is much more pronounced in all but the deepest sandy interval at site H compared to site L. In Bangladesh, ΔR values ranging from <0.1 to ~1 correspond to leachable Fe(II)/Fe ratios ranging from >0.9 to ~0.1, respectively (HORNEMAN ET AL., 2004). There are no other significant mineralogical differences between the two sites, as previously reported elsewhere for aquifers associated with contrasting levels of As in groundwater (PAL ET AL., 2002; VAN GEEN ET AL., 2008A). The presence of crystalline Fe(III) oxy-hydroxides like hematite inferred from the sequential extractions is consistent with the brown colour and reflectance of aquifer sands at site L ($\Delta R > 0.7$) (Fig. 5.3a). The sequential extractions indicate that most of the As in the sediment is associated with these crystalline Fe(III) oxy-hydroxides at site L (Tab. 5.2) and, based on the dissolved As profiles, relatively insoluble. Similar associations

have previously been reported for deeper Pleistocene aquifers of Bangladesh (BGS & DPHE, 2001; HARVEY ET AL., 2002; SWARTZ ET AL., 2004; ZHENG ET AL., 2005; STOLLENWERK ET AL., 2007).

In contrast, amorphous Fe phases of mixed Fe(II/III) valence are indicated by the grey colour and low ΔR values (<0.25) of aquifer sands at site H (Fig. 5.3b). The sequential extraction data indicate that As is primarily adsorbed to these phases (Tab. 5.2) and, arguably for that reason, also elevated in groundwater (ZHENG ET AL., 2005; VAN GEEN ET AL., 2006A; 2008A). Elevated Fe(II)/Fe ratios and high concentrations of PO_4^{3-} extractable As in grey aquifer sands measured at several nearby locations (VAN GEEN ET AL., 2008B) indicate that conditions at site H are representative of the larger area within Van Phuc where groundwater As concentrations are elevated. The high proportion of adsorbed As in reducing sands is consistent with previous observations by BERG ET AL. (2008) in this and other areas of Vietnam based on a simplified version of the extraction scheme of KEON ET AL. (2001). POSTMA ET AL. (2007) concluded from their analysis of aquifer sediment from a shallow grey aquifer near the RR associated with elevated dissolved As that, rather than being adsorbed, As in the solid phase is primarily bound within the lattice of Fe oxy-hydroxides. The step in their extraction scheme used to identify adsorbed As relies on a 10-fold lower PO_4^{3-} concentration (WENZEL ET AL., 2001), which may explain the different attribution.

5.4.2 FACTORS CONTRIBUTING TO ARSENIC RELEASE AND RETENTION

Whereas contrasting redox conditions between sandy aquifers at the two sites are likely to play a role, there is no simple correlation at site H between As and other constituents of groundwater indicative of microbially induced Fe oxy-hydroxide reduction such as dissolved Fe, NH_4^+ or HCO_3^- . One potential confounding factor is competitive adsorption of As with PO_4^{3-} (SU & PULSE, 2001; DIXIT & HERING, 2003; RADU ET AL., 2005) and HCO_3^- . Dissolved PO_4^{3-} concentrations are at least an order of magnitude higher at site H compared to site L, and HCO_3^- levels up to 3-fold higher (Fig. 5.5). The sequential extraction data show that very little As is adsorbed at site L, however, suggesting that other factors control the release of As to groundwater at this location. There is no clear correlation between dissolved As and PO_4^{3-} levels

even within the profile at site H either. Whereas HCO_3^- levels are also generally higher at site H than at site L, the influence of HCO_3^- on the adsorption of As remains controversial. APELLO ET AL. (2002) and ANAWAR ET AL. (2004) concluded from their experiments that high concentrations of HCO_3^- result in considerable desorption of As. MENG ET AL. (2000) as well as RADU ET AL. (2005) could not confirm these results in their studies, however.

The precipitation of secondary mineral phases may be another reason why processes that are likely to influence the partitioning of As between groundwater and aquifer particles are difficult to separate. Several studies have pointed out that siderite can adsorb As or co-precipitate with As (ANAWAR ET AL., 2004; SENGUPTA ET AL., 2004; GUO ET AL., 2007). Siderite as well as vivianite are both supersaturated at site H and therefore likely to precipitate (Fig. 5.6). The reflectance data suggest the formation of amorphous Fe(II)-As(III)-precipitates at site H and these may have a relatively low affinity for As (SWARTZ ET AL., 2004; HORNEMAN ET AL., 2004; VAN GEEN ET AL., 2004; HERBAL & FENDORF, 2006; PEDERSEN ET AL., 2006; DIXIT AND HERING, 2006; COKER ET AL., 2006). DIXIT AND HERING (2006) provided evidence, that sorption of As(III) on Fe minerals is enhanced at higher dissolved Fe concentrations which is the case between 20 and 35 m at site H (Fig. 5.5) leading to surface-precipitation of Fe(II)-As(III)-bearing phases. The existence of Fe-As bearing solids at site H is supported by the results of the sequential extraction which indicate that very amorphous Fe oxy-hydroxides have their highest abundance where dissolved As concentrations are lowest (20 - 30 m). Correspondingly, lower As concentrations can be expected where the dissolved molar Fe/As ratio is highest (BERG ET AL., 2008). The formation of sulphide phases known to be able to incorporate large amounts of As (LOWERS ET AL., 2007) does not seem to have a considerable influence on the As concentrations at site H because of the very low amount of As and Fe released by the sulphide targeting extraction step.

5.4.3 SOURCE OF ORGANIC MATTER RESULTING IN REDUCING CONDITIONS

The geochemistry of the sediment and groundwater at sites H and L show that both aquifers are reducing, although to a different extent. This raises the

question of the origin of this contrast in redox conditions. The concentration of NH_4^+ , a good indicator of the intensity of OM degradation (POSTMA ET AL., 2007), is much higher at site H (< 34 mg/L) compared to site L (< 1 mg/L). The depth profiles, therefore, suggest a higher OM accessibility at site H compared to site L that is consistent with a more advanced state of reduction. The TOC content of sandy intervals at both sites is comparable and fairly low (L: 0.03 wt-%; H: 0.02 wt-%), which means that the OM would have to be of a different nature to account for the observed contrast. Therefore, the composition of OM was also analysed within this thesis and the results will be discussed in Chapter 6 in detail.

An alternative explanation is that the reactive OM reaching sandy aquifers originates primarily from intercalated confining layers which are typically enriched in OM (CHAPELLE & BRADLEY, 1996; MCMAHON, 2001). The contrast in redox conditions between sites H and L could, therefore, be related to differences in the downward transport of reactive OM from the top organic rich silt layers which is indicated by differences in the concentration and depth distribution of dissolved Fe and ions indicative for OM degradation (NH_4^+ , HCO_3^- , P_{tot} and DOC) (Fig. 5.5). This possible explanation will be discussed in detail in Chapter 6.4.3.

6 ORIGIN AND REACTIVITY OF SEDIMENTARY ORGANIC MATTER IN THE SEDIMENTS OF VAN PHUC

6.1 INTRODUCTION

It is generally acknowledged that microbes play a key role in the mobilization of As in aquifers, either by directly reducing Fe oxy-hydroxides or by inducing redox changes through OM degradation (e.g. ZOBRIET ET AL., 2000; NICKSON ET AL., 2000; MCARTHUR ET AL., 2001; DOWLING ET AL., 2002; STÜBEN ET AL., 2003). Whichever microbial process is more important, it requires some kind of degradable OM (CHARLET & POLYA, 2006). Different internal and external OM sources are discussed in literature (Chapt. 2.5.1), like peat layers in sediments (NICKSON ET AL., 2000; MCARTHUR ET AL., 2001; DOWLING ET AL., 2002) or surface-derived material of natural or anthropogenic origin, percolating into the aquifer (HARVEY ET AL., 2002). ROWLAND ET AL. (2006, 2007) found indications for petroleum, seeping into the aquifer from deeper zones, as additional source in West-Bengal, hints they could reconfirm in samples from Cambodia (VAN DONGEN ET AL., 2008).

The content of TOC which is generally low in aquifers (HARTOG ET AL., 2004), however, does not give any information about its reactivity. Several authors proposed that the type of OM as well as its availability might control the activity of the microbial communities and, consequently, also geochemical processes in the aquifer (HARTOG ET AL., 2004; ISLAM ET AL., 2004; POSTMA ET AL., 2007; ROWLAND ET AL., 2007). There are still many open questions about the reactivity of OM in aquifers. For that reason, more knowledge about the sources and the composition of OM would help to better understand the microbial processes in the sediment, especially with regard to As mobilization (HU ET AL., 2006). Furthermore, the characterization could provide information about the depositional environment as well as possible diagenetic transformations (QUICKSALL ET AL., 2008). Bulk parameters like $\delta^{13}\text{C}$ signatures or C/N ratios are often used for characterizing OM as they are

source specific, at least to a certain degree (KENNEDY ET AL., 2004). Interspecies differences and environmental conditions, however, can have an influence on the $\delta^{13}\text{C}$ signature or C/N ratios (FORQUREAN ET AL., 1997). Furthermore, post-depositional changes as well as deposition of fresh material might alter the original signal, complicating the interpretation of these parameters (PRAHL ET AL., 1980; ARNOSTI & HOLMER, 2003). Better information about the source as well as the reactivity of OM could be obtained from specific organic molecules called biomarkers (VOLKMAN ET AL., 1998). From the compositional characteristics of sedimentary hydrocarbons, for example, some conclusions about the origin and transport can be gained (GIGER ET AL., 1980). The CPI, indicating the proportion of odd and even n-alkanes, could help to distinguish between different biogenic as well as anthropogenic n-alkane sources according to PIETROGRANDE ET AL. (2009). However, unique biomarkers are often not known for each possible source of OM (VOLKMAN ET AL., 1998).

Based on the results of the previous chapter (Chapt. 5), it could be assumed that differences in OM reactivity are responsible for the different dissolved As concentrations between both sites. Furthermore, it is possible that differences in the depositional history of the sediment may influence the hydrology and, consequently, the availability of OM at both sites. In addition, by analysing the distribution of n-alkanes, steranes and hopanes it was aimed at testing if signs for petroleum derived hydrocarbons, which are thought to possibly be an additional external OC source (ROWLAND ET AL., 2006; ROWLAND ET AL., 2007; VAN DONGEN ET AL., 2008), might play a role in Van Phuc. In order to test these hypotheses, the OM was characterized by means of bulk parameters as well as through the distribution of alkanes.

6.2 METHODS

6.2.1 EXTRACTION AND CHARACTERIZATION OF ORGANIC MATTER

In order to extract OM from the sediment, five sediment samples from the whole sediment profile of site L (L10110, L1410, L17045, L2640, L3475) and site H (H08140, H1450, H2020, H3030, H37100) were chosen in order to get information about differences in the distribution n-alkane, hopanes and ster-

anes within each core. At first, the samples were freeze-dried and grinded to powder. Depending on the TOC content which was determined previously (Chapt. 5.3.3), 3 - 10 g of the material was weighed into glass tubes. For the extraction of the total lipid fraction (TLF) the following solvents were used consecutively: (1) dichlormethane (DCM), (2) DCM/MeOH (1:1, v/v) and (2) MeOH. After centrifugation, the solutions were decanted and androstane was added as internal standard. The neutral lipid fraction (NLF) was separated from the TLF by means of solid phase extraction (column chromatography: Strata NH₂, 50 μm, 70Å) applying a DCM/isopropanol solution (2:1, v/v, 12 mL) as eluent. Subsequently, the NLF was further divided into a polar and apolar fraction by elution with hexane/DCM (9:1, v/v, 3mL; apolar fraction) and DCM/MeOH (1:2, v/v, 3 mL; polar fraction) using a column filled with activated alumina. The apolar fraction could be measured directly by gas chromatography coupled to a mass spectrometer (GC-MS), whereas the polar fraction had to be derivated first. In the polar fraction no compounds could be identified, that's why this fraction is not further addressed.

An Agilent 6890/5873 was used for GC-MS analysis, equipped with an on-column injector. Chromatographic separation was carried out with a Varian CP 7842 (CPSIL5CB) capillary column using helium as carrier gas. The starting temperature during injection of the sample was 40°C. Afterwards the oven was first heated to 140°C at 20°C/min and then to 300°C at 4°C/min. The final temperature was held for 22 min. The electron ionisation of the MS was 70 eV, scanning from m/z 50 - 700 with a cycling time of 1.7 scans/s. For identification and quantification of n-alkanes a standard solution (C₂₁-C₄₀, Fluka 04071) was included into the measuring procedure. The extraction scheme and analytical parameters are based on ROWLAND ET AL. (2006) with minor adjustments.

6.2.2 ORGANIC CARBON AND NITROGEN ISOTOPIC ANALYSIS

Due to the low TOC content, known from the CSA/CWA-measurements (Chapt. 5.3.3), only a limited number of samples from site L (L0135, L0580, L0990, L10110, L1245, L1410, L2215, L3475) and site H (H0115, H08140, H1125, H1345, H1450, H3305, H37120) could be analysed for their isotopic composition, expressed as δ ¹³C and δ ¹⁵N, and their total nitrogen content

(TN)(L0135, L0580, L0990, L1410 H08140, H1125, H1450, (Tab. 6.1). Additionally, material taken from a slip-of slope of the RR was analyzed. The measurements were carried out with an elemental analyzer (EuroEA3000, EuroVector, Italy) in continuous flow mode which was connected by an open split to a gas ion mass spectrometer (GI-MS: IsoPrime, Fa. GV Instruments, UK). In order to exclusively determine the isotopic signature of OC, the inorganic part was volatilized by HCl (2%) before the sediment was filtered with Mili-Q water in order to remove excess chloride ions. Depending on the bulk TOC concentration different amounts of sediment were weighed into Sn-cups (C: 3-150 mg; N: 8-100 mg). The cups were inserted into a reactor tube (1030 °C) and combusted in a temporarily oxygen enriched atmosphere. Cup and sample were melted in an exothermal reaction at 1800 °C producing gaseous products which were transported in a He stream through the two reaction columns. The oxidation of carbon and nitrogen was catalyzed by Cr₂O₃ in the first column. Furthermore, sulphur and halogens were bound to silver coated cobalt oxide. In the second column (650 °C), copper fixed the remaining oxygen and reduced nitrogen oxides to N₂. Subsequently, water vapour that may have been built was trapped with Mg-perchlorate before the gases were separated with a chromatographic column and analyzed for elemental concentrations with a thermal conductivity detector. Afterwards the separated gases were transferred to a mass spectrometer (MS) via open split interface.

The precision calculated from three repeated sample measurements was better than ±0.19‰ (for carbon) and ±0.36‰ (for nitrogen), respectively. The accuracy was checked with the certified reference materials USGS24 and NBS21 for carbon (±0.04‰), and, USGS25 and IAEA-N1 for nitrogen (±0.04‰). The delta values were calculated according to equation 6.1:

$$\delta E[\text{‰}] = \left(\frac{R_{\text{sample}}}{R_{\text{standard}}} - 1 \right) \times 10^3 \quad (6.1)$$

E = ¹³C, ¹⁵N

R_{sample} = isotope ratio in the sample (¹³C/¹²C, ¹⁵N/¹⁴N)

R_{standard} = isotope ratio in the standard ((¹³C/¹²C)_{VPDB}, (¹⁵N/¹⁴N)_{air})

6.3 RESULTS

6.3.1 CARBON AND NITROGEN ISOTOPIC SIGNATURES IN THE SEDIMENTS

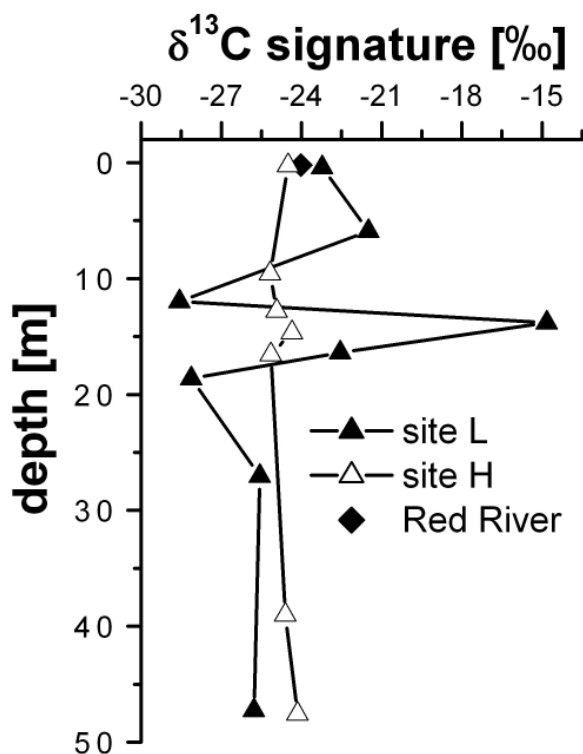


Fig. 6.1: Depth distribution of $\delta^{13}\text{C}$ ratios at both sites. Also included is the ratio of fresh sediment material from the Red River (RR).

At site H, the $\delta^{13}\text{C}$ values vary only to a minor degree ($\delta^{13}\text{C} = -24.7 \pm 0.4\text{‰}$) and do not show a trend towards depth (Fig. 6.1).

With regard to $\delta^{15}\text{N}$ signatures, only the peat sample at 12 m depth ($\delta^{15}\text{N} = 2.1$) shows considerably different results at site L ($\delta^{15}\text{N} = 3.9 \pm 1.9\text{‰}$), whereas at site H the signature only varies in a small range ($\delta^{15}\text{N} = 3.7 \pm 0.3\text{‰}$). No preferential trend is detectable, perhaps caused by the limited data set (Fig. 6.2). The TN content at both sites is very low (site L: 0.15 ± 0.13 ; site H: 0.1 ± 0.03 wt-%), with exception of the peat sample at 12 m depth (0.35 wt-%) at site L, but with a slight decreasing content at site H. There is a clear correlation of TOC and TN at site H ($r = 0.99$, $n = 3$) with an intercept of 0.02 thought to result from contribution of NH_4^+ to the TN pool (CALVERT, 2004).

The $\delta^{13}\text{C}$ signatures of the aquitard of site L (0 - 23 m) are highly heterogeneous ($\delta^{13}\text{C} = -24.8 \pm 3.3\text{‰}$). Especially the two samples taken from the black, organic rich peat layers (depth: 12 and 19 m, respectively) have relatively low $\delta^{13}\text{C}$ signatures ($< -28\text{‰}$) compared to all other samples (Fig. 6.1). On the contrary, a whitish layer at 14 m depth is characterized by a high $\delta^{13}\text{C}$ value of -14.8‰ . In the sandy aquifer at site L (> 23 m), the signatures seem to be more evenly distributed with $\delta^{13}\text{C}$ value of $\sim -25.6\text{‰}$.

Tab. 6.1: Overview of the results of total organic carbon (TOC), total nitrogen (TN), $\delta^{13}\text{C}$ and $\delta^{15}\text{N}$ - isotopic signatures as well as calculated molar C/N ratios from selected samples at both sites and the Red River (n.d. = not determined).

Sample	depth [m]	TOC [%]	$\delta^{13}\text{C}$ [‰]	TN [%]	$\delta^{15}\text{N}$ [‰]	C/N-ratio
L0135	0.5	0.38	-23.2	0.09	5.0	4.8
L0580	6	0.27	-21.5	0.10	4.0	3.1
L0990	12	4.55	-28.6	0.35	2.1	15.4
L10110	14	0.12	-14.8	n.d.	n.d.	n.d.
L1245	16	0.07	-22.6	n.d.	n.d.	n.d.
L1410	19	0.69	-28.1	0.06	4.3	12.6
L2215	27	0.05	-25.6	n.d.	n.d.	n.d.
L3475	47	0.07	-25.8	n.d.	n.d.	n.d.
H0115	0.5	0.10	-24.5	n.d.	n.d.	n.d.
H08140	10	0.82	-25.2	0.12	3.8	7.7
H1125	13	0.58	-24.5	0.10	3.8	7.1
H1345	15	0.13	-24.7	n.d.	n.d.	n.d.
H1450	17	0.43	-25.2	0.07	3.4	6.7
H3305	39	0.04	-24.6	n.d.	n.d.	n.d.
H37120	48	0.10	-24.2	n.d.	n.d.	n.d.
Red River	0	0.08	-24.0	n.d.	n.d.	n.d.

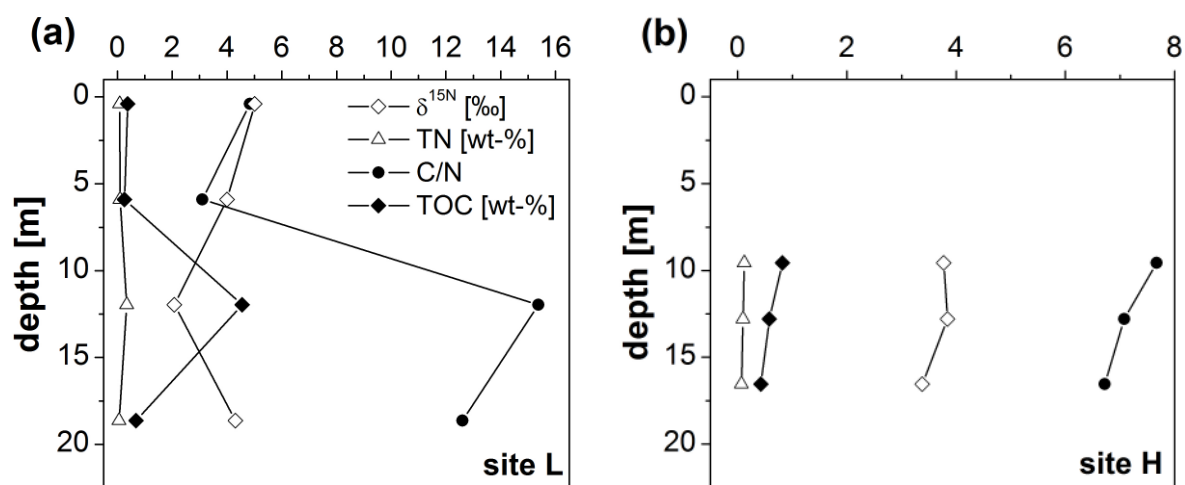


Fig. 6.2: Depth distribution of $\delta^{15}\text{N}$ values and C/N ratios as well as total organic carbon (TOC) and total nitrogen (TN) concentration at site L (a) and site H (b).

Comparable to the $\delta^{13}\text{C}$ signatures the calculated molar C/N ratios vary considerably at site L (C/N: 9.0 ± 5.9), with much higher values in the peat layers (12 and 19 m, respectively) (Tab. 6.1). At site H, the ratios seem to be more homogenous (C/N: 7.2 ± 0.5) and decreasing with depth (Fig. 6.2). There is a good correlation ($r = 0.97$) between C/N ratios and $\delta^{13}\text{C}$ signatures. In general, large C/N ratios correspond to small $\delta^{13}\text{C}$ values.

6.3.2 DISTRIBUTION OF N-ALKANES IN THE SEDIMENT

High molecular weight (HMW) n-alkanes (C_{21} to C_{36}) could be detected at both sites with varying amounts of specific n-alkanes as well as the sum of all n-alkanes (Tab. 6.2, Appendix 6). At site L, three samples (depth: 14 (L10110), 33 (L2640) and 47 m (L3475), respectively) are characterized by relatively high amounts of total HMW n-alkanes (205 - 691 $\mu\text{g/g}$), a smooth distribution in the range of C_{25} to C_{36} and an average chain length (ACL, for more details see Chapt. 2.5.3) close to 30. In the other two samples from site L at a depth of 19 (L1410) and 24 m (L17045) the concentration of n-alkanes is about ten fold lower (25 - 65 $\mu\text{g/g}$) compared to the above described ones with an ACL of just below 30. All samples of site L have a comparable carbon preference index (CPI, for more details see Chapt. 2.5.3) of 0.9 to 1.1 indicating a balanced odd-to-even distribution. An unresolved complex mixture (UCM, for more details see Chapt. 2.5.3) as well as hopanes and steranes could not be detected.

At site H, only the uppermost sample (depth: 10 m, H08140) can be characterized by a high n-alkane abundance of 255 $\mu\text{g/g}$ (Tab. 6.2). The lower four samples, have a much lower n-alkane abundance (37.5 ± 7.4 $\mu\text{g/g}$) (Tab. 6.2). The concentration of the single n-alkanes does not show a smooth distribution but indicates preferential degradation or enrichment of some components (Fig. 6.3d). In the sample taken from 34 m depth (H3030), the abundance of the n-alkanes is similar in the range C_{21} to C_{31} . In all four samples, C_{34} is the main n-alkane, whereas C_{35} is always missing (Fig. 6.3b). The ACL is close to 30 with exception of the lowest sample at 48 m depth (H37100, Tab. 6.2). The CPI is 1 in the uppermost sample decreasing with increasing depth (Tab. 6.2). An odd-over-even-predominance is only detect-

able in the range of C_{28} to C_{32} in the sample at a depth of 17 m (H1450) (Fig. 6.3d). Comparable to site L, hopanes and steranes as well as an UCM could not be detected.

Tab. 6.2: Total concentration of organic carbon (TOC), higher molecular weight (HMW) n-alkanes and indicative ratios calculated from the n-alkane distribution.

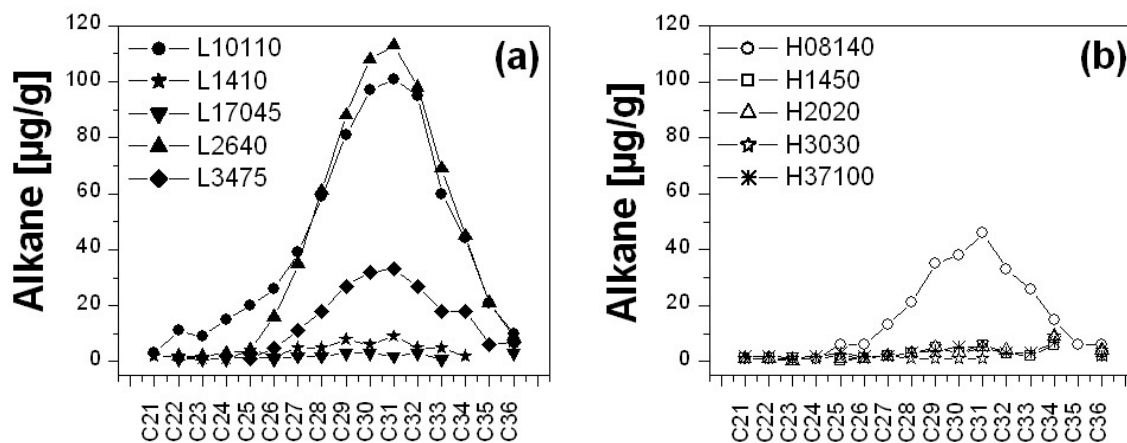
Sample	depth [m]	TOC [wt-%]	n-alkanes ^[1] [µg/g]	C_{max} ^[2]	CPI ^[3]	ACL ^[4]
L10110	14	0.122	691	31	0.9	30.0
L1410	19	0.690	65	31	1.1	29.7
L17045	24	0.022	25	30	0.9	29.2
L2640	33	0.023	673	31	0.9	30.6
L3475	47	0.061	205	31	0.9	30.8
H08140	10	0.821	255	31	1.1	30.4
H1450	17	0.427	38	34	0.8	30.2
H2020	23	0.033	38	34	0.5	30.6
H3030	34	0.023	28	34	0.4	30.2
H37100	48	0.104	46	34	0.6	22.8

[1] Sum of the concentration of n-alkanes $\sum (C_{21} \text{ to } C_{36})$.

[2] Chain length of alkane with highest concentration.

[3] CPI = carbon preference index over the range of C_{22} to C_{36} .

[4] ACL = average chain length over range of C_{21} to C_{36} .



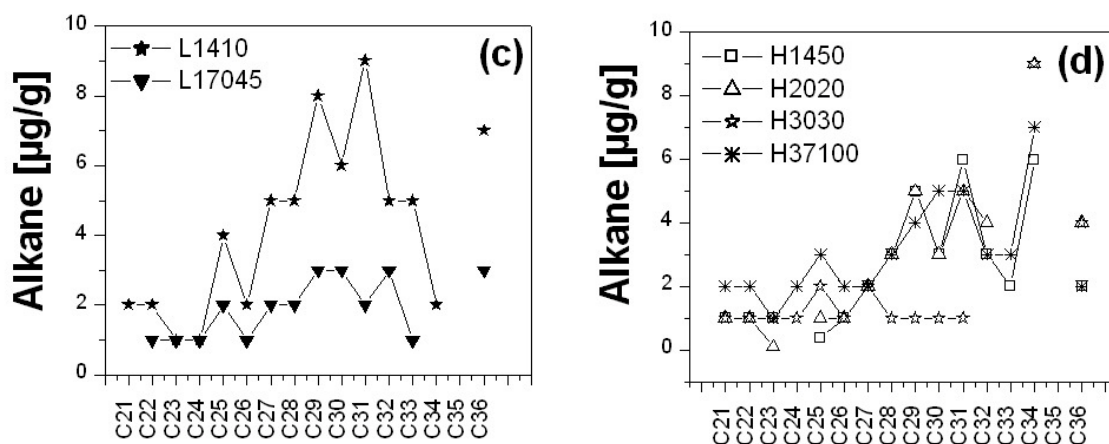


Fig. 6.3: Abundance of C₂₁ to C₃₆ n alkanes in dried sediments of site L (a)/(c) and site H (b)/(d).

6.4 DISCUSSION

6.4.1 DEPOSITIONAL ENVIRONMENT AND ORIGIN OF ORGANIC MATTER

Molar C/N ratios, $\delta^{13}\text{C}$ and $\delta^{15}\text{N}$ signatures are frequently used to delineate depositional environments as well as sources of OM (e.g. ANDREWS ET AL., 1998; JAFFÉ ET AL., 2001; HU ET AL., 2006; PERDUE & KOPRIVNJAK, 2007; HARMELIN-VIVIEN ET AL., 2008; QUICKSALL ET AL., 2008). In the aquitard of site L the $\delta^{13}\text{C}$ signatures show great variations with depth (Fig. 6.1), which probably reflects a change in the OM supply and its reactivity with time because OM degradation typically only leads to small alterations of $\delta^{13}\text{C}$ signatures (HEDGES ET AL., 1986; ANDREWS ET AL., 1998; KENNEDY ET AL., 2004). Eustatic sea level changes occurring during the Holocene, the time span when the aquitard was deposited (Prof. Tran Nghi, personal communication), have probably strongly influenced the origin of sediment supply in Van Phuc and, concurrently, the origin of OM. The boundary between fluvial and marine dominated depositional environments in the RRD is thought to have progressed as far inland as Ha Noi during Holocene (TANABE ET AL., 2003A, B).

High abundance of OC and low $\delta^{13}\text{C}$ values ($< -26\%$, FRY & SHERR, 1984) are usually indicative of terrestrial input from C₃ plants (MISEROCCHI ET AL., 2007) like in the two samples of the peat layers at site L at 12 and 19 m depth, respectively (Tab. 6.1). Carbon/N ratios are relatively low (15.4 and 12.6, respectively, Fig. 6.2) for terrestrial derived material in this two samples but

might be indicative of mangrove derived OM due to a $\delta^{13}\text{C}$ signature lower than -28‰ and C/N ratios close to 14 (Tab. 6.1, JAFFÉ ET AL., 2001). Peat is thought to be deposited during sea-level high-stand when large mangrove flats developed in the area around Ha Noi. $\delta^{15}\text{N}$ signatures are more difficult to interpret, as they are not as source specific as $\delta^{13}\text{C}$ signatures and might be altered during decomposition (THORNTON & MCMANUS, 1994). However, in combination with $\delta^{13}\text{C}$ signatures and the occurrence of leaf and wood remains, they also point towards predominant terrestrial input of OM in the peat layers (Fig. 6.4, Fig. 6.5). The relatively high $\delta^{13}\text{C}$ value of -14.8‰ (Tab. 2.6, Chapt. 2.5.3) at ~ 14 m depth at site L indicate terrestrial origin of OM, but in contrast to the peat, mainly resulting from C_4 plants (FRY & SHERR, 1984; MEYERS, 1994).

With $\delta^{13}\text{C}$ signatures of -23.2 to -21.5‰ (Tab. 6.1) the other layers of the aquitard of site L suggest preferential deposition of marine phytoplankton (Tab. 2.6; Chapt. 2.5.3; FRY & SHERR, 1984). This assumption is supported by the identification of marine bivalves collected at a depth of ~ 6 m (Fig. 6.4, B. Weinman, personal communication). Additionally, low C/N ratios (<5) and relatively high $\delta^{15}\text{N}$ values ($>4\text{‰}$; Fig. 6.5) are indicative of comparatively fresh, marine material as major OM compound in the corresponding sediment layers (HEDGES ET AL., 1986; WASER ET AL., 1998).

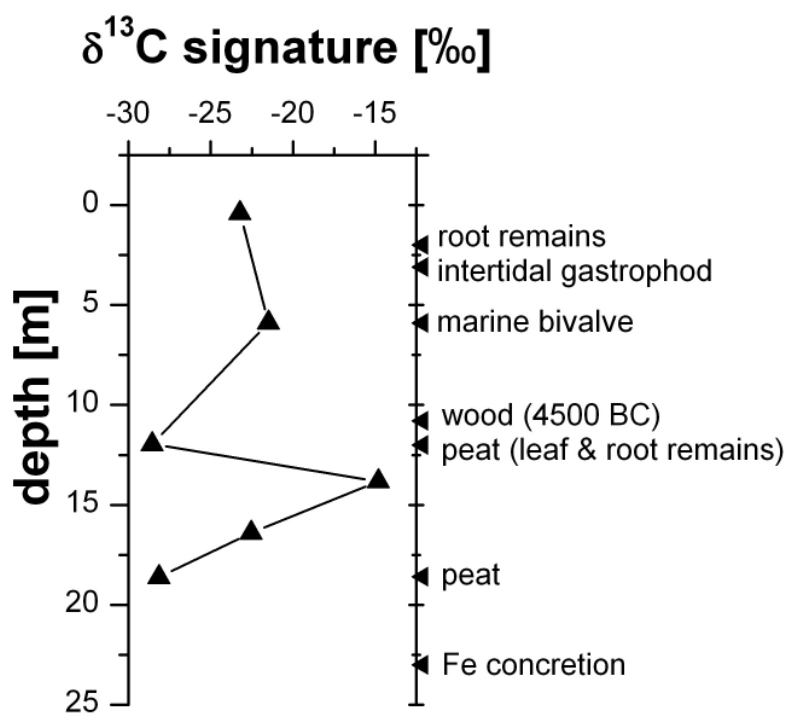


Fig. 6.4: Depth distribution of $\delta^{13}\text{C}$ ratios and macroscopic indicators for the depositional environment in the silty part of site L acquired from visual sediment description.

In the uppermost part of the sediment profile at site L, however, a strong terrestrial impact is assumable due to root remains that were found at a depth of ~2 m (Fig. 6.4) and annual floodings by the RR. Consequently, recent as well as older, eroded and transported OM is deposited by the RR leading to a mixed marine and terrestrial signal. Current RR sediment material, for example, taken from a slip-off slope of the RR near Van Phuc, shows a mixed marine/terrestrial $\delta^{13}\text{C}$ signature (-24‰) which is comparable to the signatures in the aquitard of site L (Fig. 6.1, Tab. 6.1).

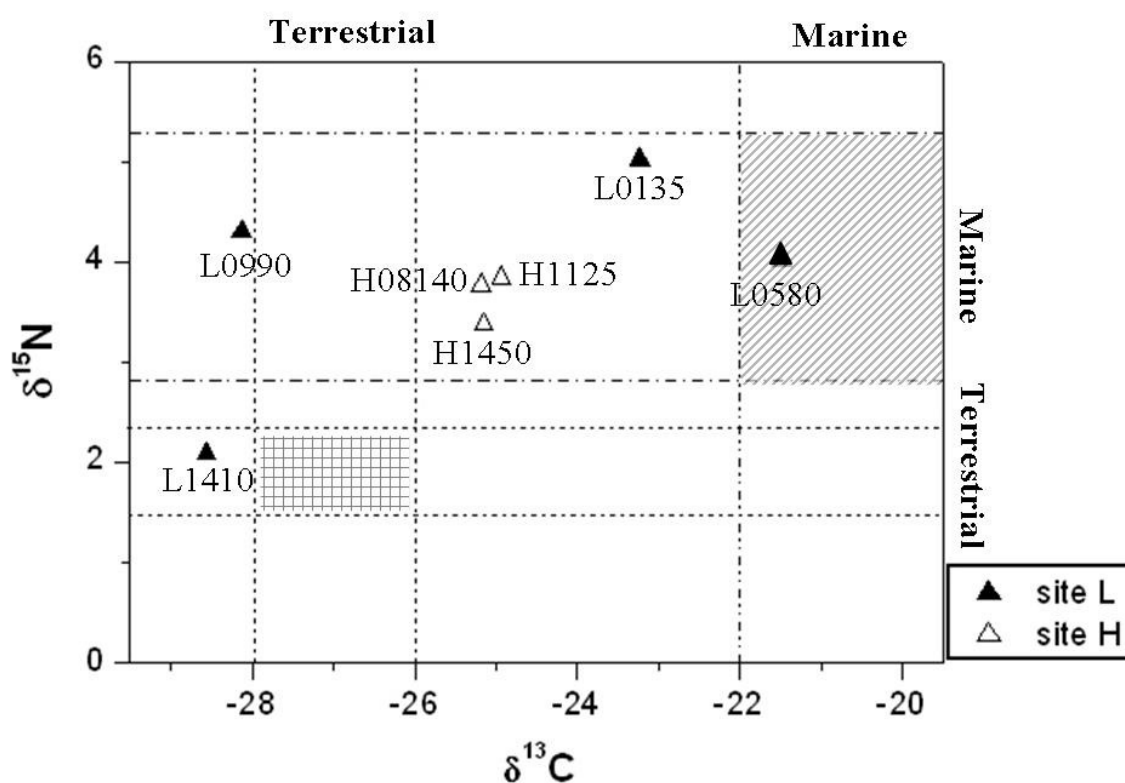


Fig. 6.5: Bivariate plots of $\delta^{13}\text{C}$ and $\delta^{15}\text{N}$ signatures delineating the sources of organic matter. Typical values for marine and terrestrial origin for $\delta^{13}\text{C}$ and $\delta^{15}\text{N}$ signatures were taken from literature (FRY & SHERR, 1984; WASER ET AL., 1998). In the case of $\delta^{15}\text{N}$ values, the dominance field was confined to a narrow range, which could be expanded with decreasing importance in both directions. The striped rectangle symbolizes the area where both signatures indicate marine origin whereas terrestrial origin is indicated by both signatures in the gridded area.

The fact that sand horizons in the Holocene aquitard are missing at site L, in addition to a low sedimentation rate (B. Weinman, personal communication) and clear $\delta^{13}\text{C}$ signatures, lead to the assumption that the area around site L was never directly influenced by the RR during Holocene but per-

sisted as paleointerfluvial. Therefore, only marine, tidal and terrigenous silts were deposited on top of the Pleistocene aquifer apart from the uppermost layers, which result from today's conditions. On the other hand, the aquifer at site L, mainly consisting of sandy material (Chapt. 5.3.1), has a fluvial origin. The constant $\delta^{13}\text{C}$ signature of $\sim -25.7 \pm 0.1\text{‰}$ (Tab. 6.1) is indicative for a predominance of terrestrial OM within the whole aquifer (FRY & SHERR, 1984). However, the signature is probably heavily influenced by reworking processes of the sediment by the RR also bringing in eroded surface material leading to the relatively homogeneous mixed marine/terrestrial $\delta^{13}\text{C}$ signals throughout the whole profile. MARTINOTTI ET AL. (1997) found $\delta^{13}\text{C}$ signatures of $-26 \pm 1.4\text{‰}$ in riverine environments.

At site H, all bulk parameters (e.g. TOC, TN, $\delta^{13}\text{C}$, $\delta^{15}\text{N}$, C/N) are equally distributed along the depth profile (Fig. 6.1/6.2). Therefore, a more or less constant source of OM is assumable. The whole sequence at site H is thought to be deposited during Holocene (B. Weinman, personal communication), comparable to the aquitard of site L. $\delta^{13}\text{C}$ and $\delta^{15}\text{N}$ signatures ($-24.8 \pm 0.4\text{‰}$, $3.7 \pm 0.3\text{‰}$) as well as C/N ratios (7.2 ± 0.5) suggest mixed input of terrestrial (C_3 plants) and marine sources throughout the whole depth profile (Fig. 6.5) probably resulting from riverine deposition because $\delta^{13}\text{C}$ signatures of current RR material are comparable to the ones at site H (Fig. 6.1). From these $\delta^{13}\text{C}$ values, in addition to the high sedimentation rate (B. Weinman, personal communication) it can be concluded, that the area next to site H was a former paleochannel occupied by the RR during Holocene in contrast to site L.

The results of the n-alkane distribution do not provide clear information about the origin of hydrocarbons in both cores. A relatively high ACL of ~ 30 in all but the lowest sample of site H is mainly seen as indicative for vascular land plants and emergent macrophytes (EGLINTON & HAMILTON, 1963). However, a missing odd-over-even predominance as expressed by a CPI close to unity in most of the samples is more indicative for n-alkanes derived from marine or reworked material (KENNICUTT ET AL., 1987). ROWLAND ET AL. (2006, 2007) and VAN DONGEN ET AL. (2008) interpreted a CPI of ~ 1 , in addition to characteristic hopane and sterane distribution patterns and the presence of an UCM, as indication for petroleum derived hydrocarbons which are naturally seeping into shallow sediments from a deeper source. From the current

data set, this conclusion does not seem to be valid for the Van Phuc sediments due to the absence of an UCM as well as hopanes and steranes. Furthermore, an even- or no predominance is also known from carbonates, evaporites and shales (TISSOT & WELTE, 1978) and, therefore, the CPI of Van Phuc sediments might be influenced by the original n-alkane pattern of outcropping rocks in the catchment area which were sedimented in the RRD over the course of time. The n-alkane distribution in Van Phuc most probably stands for a hydrocarbon mixture derived from various biogenic sources and, additionally, might be influenced by microbial reworking and diagenesis which is also known to influence the CPI (KVENVOLDEN, 1966).

CALCULATION OF MARINE AND TERRESTRIAL CONTRIBUTION

The total isotopic signature of organic carbon in the sediment consists of the isotopic signal of all contributing OM sources. Based on simple mixing models the proportion of each source can be quantified. Suitable values of end members have to be chosen which should be representative of the OC sources in the study area (BOLDRIN ET AL., 2005). No information about $\delta^{13}\text{C}$ signatures of possible end members in the RRD were obtained during the study. Therefore, not a single but a range of values was taken as end member for the calculation in order to give considerations to likely variations in isotopic signatures. End member signatures, chosen from typical values cited in literature, are in the range of -29 to -27‰ for C_3 and -14 to -12‰ for C_4 plants. For marine end members the selected range stretches from -20 to -22‰ (FRY & SHERR, 1984; MEYERS, 1994). The relative percentage of marine derived OM (f_m %) in each sample was calculated based on the equation developed by SCHULTZ AND CALDER (1976) :

$$f_m \text{ \%} = \frac{\delta^{13}\text{C}_{\text{terrestrial}} - \delta^{13}\text{C}_{\text{sample}}}{\delta^{13}\text{C}_{\text{terrestrial}} - \delta^{13}\text{C}_{\text{marine}}} \times 100 \quad (6.2)$$

$\delta^{13}\text{C}_{\text{terrestrial}}$ = carbon isotope signature of terrestrial end member

$\delta^{13}\text{C}_{\text{marine}}$ = carbon isotope signature of marine end member

$\delta^{13}\text{C}_{\text{sample}}$ = carbon isotope signature of the sample

The contribution of terrestrial material (f_t %) to the OM can be quantified with the following equation:

$$f_t = 1 - f \quad (6.3)$$

The results of the calculations show that there is no or only a limited percentage of marine material in the two peat layers at 12 ($3 \pm 3\%$) and 19 ($6 \pm 6\%$) m depth, respectively. The other layers in the aquitard of site L are dominated by marine OM contribution (median: 79%; Tab. 6.3) with exception of the sediment at 14 m depth with a high terrestrial proportion ($22 \pm 10\%$) originating from C_4 plants. Organic matter in the aquifer at site L mainly consist of terrestrial material from C_3 plants (marine proportion: $\sim 32 \pm 10\%$).

Tab. 6.3: Quantitative source estimation of OM in the sediments of site L and H. End member combinations were chosen as follows: (1) for C_3 plants as terrestrial source ($\delta^{13}C$): -20/-27, -20/-29, -22/-27, -22/-29‰; (2) for C_4 plants ($\delta^{13}C$): -20/-12, -20/-14, -22/-12, -22/-14‰ (only used for L10110). For each sample the mean value and standard deviation of all 4 possible end member combinations was calculated.

sample	depth [m]	mean marine contribution [%]	Std. dev.	sample	depth [m]	mean marine contribution [%]	Std. dev.
L0135	0.5	69	10	H0115	0.5	50	10
L0580	6	90	10	H08140	10	40	11
L0990	12	3	3	H1125	13	44	10
L10110	14	22	10	H1345	15	52	10
L1245	16	79	12	H1450	17	40	11
L1410	19	6	6	H3305	39	49	10
L2215	27	34	11	H37120	48	56	10
L3475	47	31	11				

At site H, the fraction of marine and terrestrial derived material seems to be about equally distributed with no significant trend towards depth. These calculations, however, give only a hint about the likely composition since the

model implies that the mixing between end members is conservative and no alteration occurs during decomposition (JASPER & GAGOSIAN, 1989).

6.4.2 REACTIVITY OF ORGANIC MATTER

For microbial processes not only the quantity but also the reactivity of the OM is of importance. Marine OM is mainly composed of relatively small, N-rich molecules, like proteins which is indicated by low C/N ratios (HEDGES ET AL., 1986). These compounds are more labile and, therefore, preferentially used by microorganisms under a variety of terminal electron acceptor processes (PRAHL ET AL., 1980; AECKERSBERG ET AL., 1991; MEYERS, 1997; ZENGLER ET AL., 1999; EHRENREICH ET AL., 2000). At site H, the C/N ratios of 6.7 to 7.7 (Tab. 6.1) are close to the Redfield ratio of 6.6 (REDFIELD, 1942) and, therefore, indicate the presence of relatively fresh marine dominated OM which is confirmed by the high percentage of marine material as suggested by the $\delta^{13}\text{C}$ signature (Tab. 6.3). Relatively low C/N ratios and a high contribution of marine material can also be found in some parts of the aquitard at site L indicating the presence of labile OM (Tab. 6.1/6.3).

Terrestrial OM is dominated by N-free macromolecules, like cellulose or lignin (C/N ratios >20) which are more difficult to decompose (HEDGES ET AL., 1986). In the peat layers a high contribution of terrestrial material is indicated by $\delta^{13}\text{C}$ signatures (Tab. 6.3), however, the C/N ratios of ~14 are relatively low for terrestrial origin (Tab. 6.1). Due to the high content of N-rich molecules, it could be assumed that the reactivity of the peat OM is reasonably good despite high proportion of terrestrial material (HEDGES ET AL., 1986). In the aquifer at site L a dominance of terrestrial OM especially in comparison to site H is indicated by the $\delta^{13}\text{C}$ signature (Tab. 6.3), however, no C/N ratio could have been measured. Still it can be assumed, that on the whole, OM at site H is more reactive, with exception of some layers in the aquitard at site L, and, therefore more suitable to fuel redox reactions in the aquifer. The reactivity of OM, however, is further influenced by the pH, T, oxidant concentration (VAN BERGEN ET AL., 1998) and physical protection mechanisms (e.g. accessibility, adsorption to surfaces) (KEIL ET AL., 1994; COLLINS ET AL., 1995).

N-alkanes can also be used as electron donors by microorganisms under aerobic and anaerobic conditions (FUCHS & SCHLEGEL, 2007) but MEYERS AND EADIE (1993) estimated that the rate of n-alkane remineralisation is only one fourth of total organic matter. However, ROWLAND ET AL. (2009) found indications in their experiments that degradation of n-alkanes, especially short chain n-alkanes, might have a considerable influence on the reduction of Fe(III) and, therefore, also on the release of As. The relatively low concentration of n-alkanes in relation to the TOC content and the absence of short chain n-alkanes in most of the samples indicate that n-alkanes only play a minor role as possible electron donor in the sediments of Van Phuc.

6.4.3 ROLE OF ORGANIC MATTER FOR ARSENIC MOBILISATION IN VAN PHUC

The natural reduction capacity of aquifer sediments is of general importance in controlling redox processes within groundwater environments and, therefore, heavily influences the As mobility (HARTOG ET AL., 2004). The results of the OM characterization suggest multiple sources of OC in the sediments of Van Phuc such as (1) OM accumulated at the time of deposition (silt, site L; Chapt. 6.4.1), and, (2) reworked sedimentary OM eroded from older unconsolidated sediment further upstream (aquifer site L, site H). Organic C from each source has the potential to act as electron donor needed for the microbial reduction of electron acceptors like O_2 , NO_3^- , Mn^{4+} or Fe^{3+} assuming their sufficient abundance. As a consequence, Fe- and Mn oxy-hydroxides will gradually dissolve leading to a release of As which is subsequently adsorbed on or incorporated into these oxy-hydroxide minerals (e.g. NICKSON ET AL., 2000; STÜBEN ET AL., 2003). The higher the reactivity of OM, the higher the stimulation of microbial communities leading to enhanced redox induced As release as demonstrated in laboratory (e.g. ISLAM ET AL., 2004) and field studies (HARVEY ET AL., 2002).

The similar composition of OM throughout the whole sediment profile at site H dominantly consisting of more labile OC from marine origin indicates a relatively high reactivity of the OM altogether. Consequently, the potential to induce redox conditions which might lead to the release of As is similar throughout site H based on the reactivity alone. With regard to the

quantity and accessibility, however, there are significant differences. Much higher contents of OC can be found in the fine fraction at site H (median: 0.1, max.: 0.8 wt-%), which would either indicate a hampered OM decomposition (ANDERSON ET AL., 1981) due to smaller pore sizes which slows down microbial activity (MCMAHON, 2001) or much higher OM deposition from the beginning. It was shown by MCMAHON (2001) that, in spite of the smaller turnover rates in silt layers, sufficient soluble OM degradation products like organic acids or humic substances could migrate into the aquifer, anyway, supporting microbial activity. There are clear indications from the hydrochemical profile (Fe^{2+} , NH_4^+ , PO_4^{3-} , HCO_3^- , DOC) at site H (Fig. 5.5) that some kind of leaching of electron donors into the aquifer takes place that might result from the surface layers which was also proposed by MCARTHUR ET AL. (2004) and BERG ET AL. (2008) for their study sites. The additional OC source could enhance the already higher reactivity of the aquifer and, therefore, stimulate further As release by means of reductive dissolution. However, there is no information about the composition of DOC that might leach from the surface layers. Degradation products like humic substances can also compete for As or serve as electron shuttle and enhance redox processes (LOVLEY, 1996).

At site L the situation is more complex. In the aquifer, the quantity of OC is comparable to site H (both 0.02 wt-%). However, the sediment can be considered as less reactive compared to site H due to the higher percentage of recalcitrant terrestrial OM. Consequently, the microbial activity is much smaller only inducing slightly reducing conditions at site L. Arsenic remains incorporated into Fe mineral phases which is also indicated by the results of the sequential extraction (Chapt. 5.3.4) as well as the μS -measurements (Chapt. 7.3.2) of sediment from the aquifer at site L. In contrast to site H, no additional reactive OM from above seems to be available which is suggested by the low concentrations of elements which are indicative for microbial induced redox processes (e.g. Fe^{2+} , NH_4^+ , PO_4^{3-} or HCO_3^-) throughout the whole depth profile (Fig. 5.4). In the aquitard of site L, there are punctually very high concentrations of OC (median: 0.12, max.: 4.5 wt-%), which mainly consist of terrestrial material in the lower peaty part. The C/N ratios, however, hint at a still high reactivity of the material. The occasionally grey colour of the sediment, the high percentage of adsorbed As typically occurring in re-

ducing environments in addition to pyrites that were found in some sediment horizons show that the aquitard is reducing at least in some parts, as well. The small grain size seems to slow down the microbial activity on the one hand, and, on the other hand, hamper a considerable migration of OC and dissolved As into the aquifer.

7 DISTRIBUTIONS AND ASSOCIATIONS OF ARSENIC WITHIN SEDIMENT GRAINS

7.1 INTRODUCTION

High As concentrations in many groundwater systems around the world have received much attention over the past few years. Much is known about the fixation and release of arsenic by now, even though there is still some dispute about the exact mechanisms (Chapt. 2.3). What seems to be clear is that the released As results from within the sediment itself. Known As containing constituents are silicates (e.g. biotite, chlorite, amphibole) as well as Fe/Mn oxy-hydroxides (e.g. goethite, hematite, magnetite) and carbonates (e.g. siderite) (Chapt. 2.2, e.g. ANAWAR ET AL., 2002; SENGUPTA ET AL., 2004; WAGNER ET AL., 2005; GUO ET AL., 2007). Fe oxy-hydroxides frequently occur as coatings on host grains (mainly on quartz and feldspars) precipitating in the course of diagenetic processes (REYNOLDS ET AL., 1999; HORNEMAN ET AL., 2004; SENGUPTA ET AL., 2004).

So far, not enough is known about where and in which associations As is present within mineral grains. This knowledge, however, is important to accurately predict As mobility in aquifers. So far, mainly sequential extractions are used in order to estimate the dominant associations of As (MCARTHUR ET AL., 2004). These methods are a very useful tool to get a first impression about possible associations and release mechanisms of As with little instrumental effort. However, the fractions are only operationally defined and, therefore, do not give insight into how and where As is bound within a mineral grain (KEON ET AL., 2001; HUDSON-EDWARDS ET AL., 2004). Furthermore, this approach does not reveal much about what actually happens to the sediment grains and the constituent minerals, respectively, during sequential extraction, although they are widely used (Chapt. 5.2.2).

Synchrotron radiation in association with well established X-ray based methods (e.g. μ S-XRF) allows high resolution measurements on a microme-

ter scale, which helps to get a more accurate insight into the above mentioned issues. The main aims of this chapter are (1) to get information about the enrichment, spatial distribution and associations of As within mineral grains of two sites differing considerably in their dissolved As concentration, and (2) to get insight into transformation of mineral grains and changes in the elemental associations, especially of As, that occur during sequential extraction schemes.

7.2 METHODS

7.2.1 SEDIMENT MATERIAL AND PREPARATION

The sediment used for scanning electron microscopy (SEM) as well as μ S-XRF measurements originates from Van Phuc (Vietnam) and was sampled at

Tab. 7.1: Samples chosen for μ S-XRF-analysis and the respective bulk As and Fe concentration measured with ED-XRF.

Sample	As [mg/kg]	Fe [g/kg]
L17045	20	5.7
L2640	5	7.0
L3350	5	8.6
H2020	6	9.5
H2910	11	6.7
H3305	8	4.4
H3515	30	5.2

two sites differing considerably in their As concentration in the groundwater. A detailed description of the hydrochemistry, the sampling method as well as the mineralogy and lithology of the sediment is given in Chapter 5.3.3. After sampling, the sediments were flushed with nitrogen and frozen until preparation in order to avoid oxidation and alteration of the sediment.

Five samples from each site were chosen for SEM based on their bulk As concentration, measured previously by means of

ED-XRF (Chapt. 5.3.3; Tab. 7.1). Before analysis, the sediment material was dispersed on a sample holder and coated with graphite in order to prevent electrostatic charging of the particles.

For μ S-XRF analysis samples were also chosen on the basis of bulk As concentrations (Tab. 7.1) and mineralogical characteristics. Quartz and feldspars are generally very low in solid As concentrations (BAUER & ONISHI, 1969) whereas mica, especially biotite, is known to considerably enrich As (WAGNER ET AL., 2005; SEDDIQUE ET AL., 2008). At site L, three samples were selected and can be characterized as follows: (1) As rich but relatively low quartz content (L17045), (2) low in As but rich in feldspar (L2640) (3) low in As but rich in quartz (L3350). The samples from site H can be characterized as follows: (1) low in As but rich in mica (H2020), (2) relatively high in As and mica (H2910), (3) relatively low in As, low in quartz (H3305), (4) highest As sample in both cores (H3515).

During preparation of sediment for μ S-XRF analysis, the samples were split into three parts of ~ 0.5 g, each. Two aliquots were transferred into centrifuge tubes in order to leach the sediments according to step 1 and 2 (referred to as PO_4 -leaching, LP), and, step 1 to 5 (dissolution of Fe oxyhydroxides, referred to as Fe dissolution step, LFe) of the sequential extraction scheme according to KEON ET AL. (2001) (Tab. 5.1); one aliquot was left untreated. After each step the samples were centrifuged at 4500 rpm for 20 min. Subsequently, the solution was decanted. The sediment material was washed with Mili-Q and dried at room temperature.

The untreated sediment as well as the material after leaching steps (LP and LFe) was embedded in Epotek resin and, subsequently, sliced and polished preparing thin sections of 60 - 100 μm thickness. Afterwards, the thin sections were attached to a piece of Mylar film as carrier material.

7.2.2 SCANNING ELECTRON MICROSCOPE (SEM)

The SEM (Zeiss DSM 960) was used in order to get an impression about the composition of the mineral grains and, especially, about their surface topography. Mineral grains were randomly chosen for SEM micrographs; however, special attention was paid to coated mineral grains which are thought to play an important role in the fixation of As (NICKSON ET AL., 2000; SWARTZ ET AL., 2004). For better identification of mineral phases, elemental concentrations were measured semi-quantitatively in situ with a connected energy

dispersive XRF (ED-XRF) device. The analysis was performed in the Laboratory of Electron Microscopy at the University of Karlsruhe (TH).

7.2.3 MICRO-SYNCHROTRON-XRF (μ S-XRF)

Synchrotron radiation is generated by the cyclic acceleration of electrons or positrons to relativistic energies (nearly to the speed of light) through magnetic fields in a so called storage ring. Part of the energy is transformed into electromagnetic radiation which is emitted tangentially to the storage ring, producing a continuous spectrum of radiation from infrared light to X-ray (SHAM & RIVERS, 2002). The main advantages of synchrotron radiation compared to X-rays produced by conventional X-ray tubes can be summarized as follows:

- High brightness (flux/vertical angle (ψ)) and high intensity
- High brilliance (brightness/source area), especially important for beamlines with focusing optics
- High collimation, i.e. small angular divergence of the beam
- Widely tunable in energy/wavelength by monochromatization

All these properties allow small scale measurements (e.g. XRF) with low detection limits.

The μ S-XRF measurements were performed at the FLUO-beamline of the Ångströmsource of the Forschungszentrum Karlsruhe (ANKA). For the analysis the emitted primary beam was monochromatized by a double multilayer monochromator (W-BC4, 3 nm period). In order to eliminate possible interferences of As with Pb the beam energy was adjusted to 12.5 keV, which is just below the adsorption edge of Pb. The beam was focused to a spot size of $2 \times 8 \mu\text{m}$ by means of refractive lenses. It penetrates the sample at an incident angle of 45° and, therefore, the characteristic X-rays emitted by the elements have a cylindrical form with the diameter of the spot size. Consequently, the signal corresponding to a measuring point always consists of an

average value of the characteristic X-rays emitted from the penetrated area. The signal was collected by a Vortex Silicon Multicathode Detector with a resolution of 142 eV at 5.9 keV. The measuring time in each spot was 10 - 20s.

The absorption of primary X-rays by the sample and afterwards the emission of the characteristic X-rays (fluorescence) depend on the thickness, density and major composition of the sample. Certified reference samples (STHS6-G; JOCHUM ET AL., 2000) have been used for calibration and quantification. The measurements were not carried out under vacuum; therefore, the Si content could not be quantified. However, its relative abundance within a grain is correct and can be used for statistical analysis.

The measured mineral grains were chosen according to their appearance under the optical microscope. In order to give justice to the variability of sediment samples, grains with obvious differences in appearance were selected. They can be grouped as follows: (1) coated mineral grains and (2) mafic minerals, including black, reddish and greenish minerals. Either a transect of a selected grain or a complete mapping was carried out.

7.2.4 STATISTICAL ANALYSIS

Due to the fact that some minerals and coatings are even thinner (nm to several μm) than the μS beam ($2 \times 8 \mu\text{m}$), each measuring point consists of a mixed signal. Therefore, a clear identification of minerals based on elemental associations is difficult. Multivariate statistical analysis, like factor analysis, helps to delineate these mixed signals. In order to apply multivariate approaches, the data set should be checked for normal distribution and should be cleaned from outliers, first. For the comparison of different data sets, the involved parameters have to have a similar scale. Therefore, they are standardized by means of z-transformation (STOYAN ET AL., 1997) which is done in STATISTICA (StatSoft, USA, Version 6) by default.

FACTOR ANALYSIS

Factor analysis is a statistical tool in order to group parameters based on mutual correlations among them. The algorithm allows the allocation of each

variable to independent groups, called factors. The main goal is to reduce the number of initial variables and to reveal patterns within the original data matrix which may originate, for example, from sharing the same “superordinate variable (cause)” which is responsible for the variance within the whole bundle of the variables grouped into a factor. Therefore, factor analysis can be seen as a heuristic approach, generating hypotheses which have to be verified (BORTZ, 2005).

Each factor, however, cannot fully explain the behaviour of such a superordinate variable but only to a certain extent which is expressed by the *factor loading*. It can be considered as the correlation of a variable with the factor it is allocated to. A factor loading of 0 means that the variable is not expressed by this factor, whereas a loading of +1 or -1 indicates a good positive or negative correlation with the factor, respectively.

The *communality* expresses to what extent the variance of a variable can be explained by all factors. Values of 1 indicate that the variance of a variable is completely explained by the factors. If a variable is not well modelled by the factor analysis its communality is close to 0 and should, therefore, be excluded.

For each case (e.g. measuring point) a so called *factor score* is calculated which shows the estimated value of each factor for the considered case. Factor scores are very convenient for data interpretation as they show, for example, where a special mineral phase, expressed by a factor, is dominant within an analysed grain.

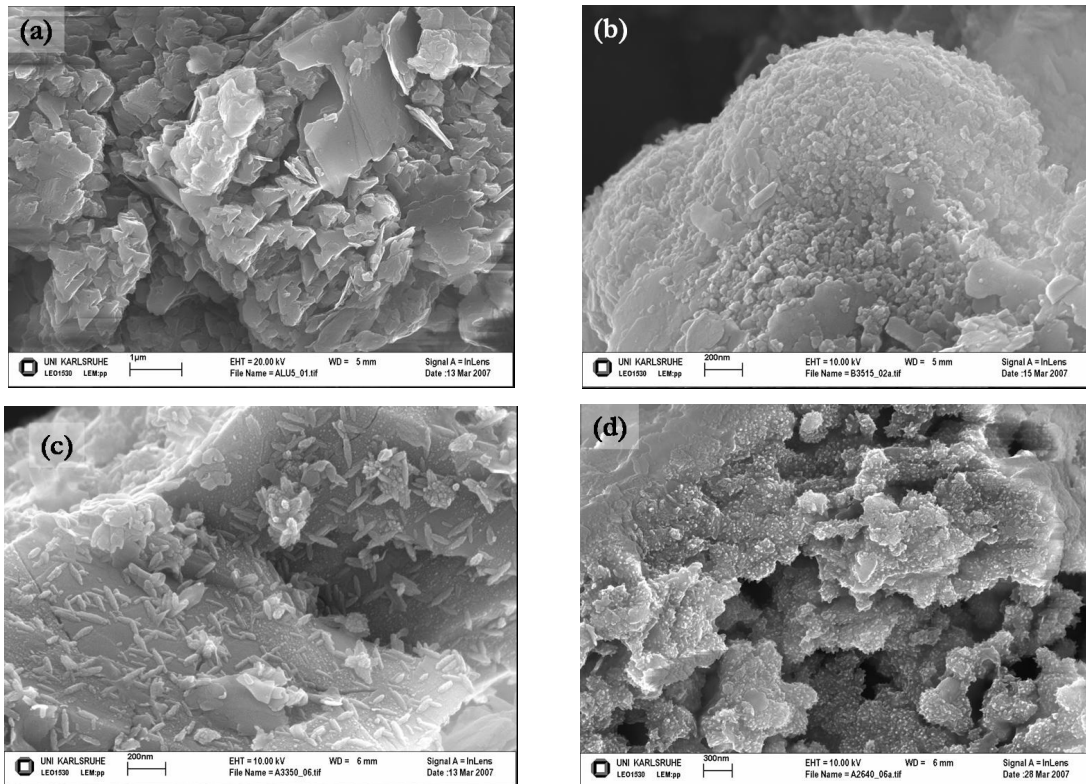
Before performing a factor analysis, it is advisable to pre-select suitable variables based on the analysis of the correlation matrix. Variables which show weak or no correlations with other variables will only lead to additional factors which most often explain a very low portion of the total variance (sometimes even less than an initial variable does). Such factors are difficult to interpret and the respective variables should better be excluded from the analysis. Elements which were considered for factor analysis are Si, K, Ca, V, Ti, Cr, Mn, Fe, Ni, Cu, Zn, Ga and As. Factor analysis was carried out using the STATISTICA program package (StatSoft, USA, Version 6). In a first step the program generates a correlation matrix based on which the factors are successively extracted. An eigenvalue of 1 is used as stop criterion

for the extraction. The rotation of the factor matrix (Varimax-procedure) maximizes the variance of the factor loadings for each factor transforming the loadings as close as possible to +1 and -1, respectively. More detailed descriptions as well as the mathematics of factor analysis can be taken from STOYAN ET AL. (1997) and BORTZ (2005).

7.3 RESULTS

7.3.1 SURFACE STRUCTURES

Different forms of minerals and surface precipitates, mainly consisting of Fe oxy-hydroxides or Fe carbonates, were detected by means of SEM-EDX analysis (Fig. 7.1). Iron sulphides (probably pyrites) were only found in the peat layer at 14 m depth at site L (L1410). In most of the samples precipitates do not cover the host minerals in form of a coherent coating (especially at site H), but more often occur as aggregates at preferential sites (Fig. 7.1c/e).



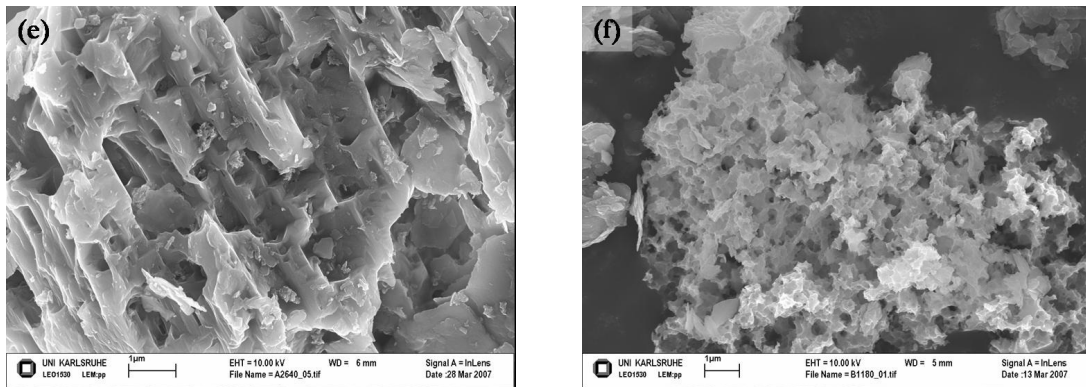


Fig. 7.1: Different habitus of surface precipitates: (a) triangular form consisting of Fe oxy-hydroxide or/and carbonate, (b) knob shaped Fe phases completely covering the surface, (c) elongated (rice grain) habitus consisting of Fe oxy-hydroxides, only scattered on the surface, (d) precipitates of Ti oxides and Fe carbonates. Strong weathering is visible on Al silicates at site L (e) and site H (f). In (e) Fe precipitates are visible, occasionally.

Different types of morphologies can be distinguished: (1) triangular structures (Fig. 7.1a), (2) knob forms (Fig. 7.1b) and (3) elongated habitus, much alike rice grains (Fig. 7.1c). The size of a precipitate is only a few tens of nanometres; therefore, an exact identification with EDX was not possible due to the interference with the simultaneously recorded signal from the underlying minerals. An identification based on specific mineral shapes was difficult because instead of well crystallized minerals amorphous phases are by far more common. Signs of strong weathering were visible on silicates at both sites; however, more deeply weathered structures could be seen at site H (Fig. 7.1e/f).

7.3.2 ELEMENTAL DISTRIBUTIONS WITHIN GRAINS

UNTREATED SAMPLES

The results of μ S-measurements of transects through grains and complete mappings of grains can be taken from Tab. 7.2 and are also listed in Appendix 4 in more detail. With elemental mappings of grains in a μ m range, As concentrations from below detection limit to more than 500 mg/kg could be detected. By far the highest concentrations occur in the two As rich samples from each core (L17045, H3515) both in coatings (<136 mg/kg, Fig. 7.2; Fig. 7.3) and mafic minerals (<514 mg/kg, Fig. 7.3d). In the other five samples,

the As concentrations are relatively low in the coatings (<11 mg/kg). Iron is considerably enriched in coatings (<71 g/kg) of the two As rich samples (L17045, H3515) as well as in the mica rich and quartz depleted samples of site H (H2020, H3305).

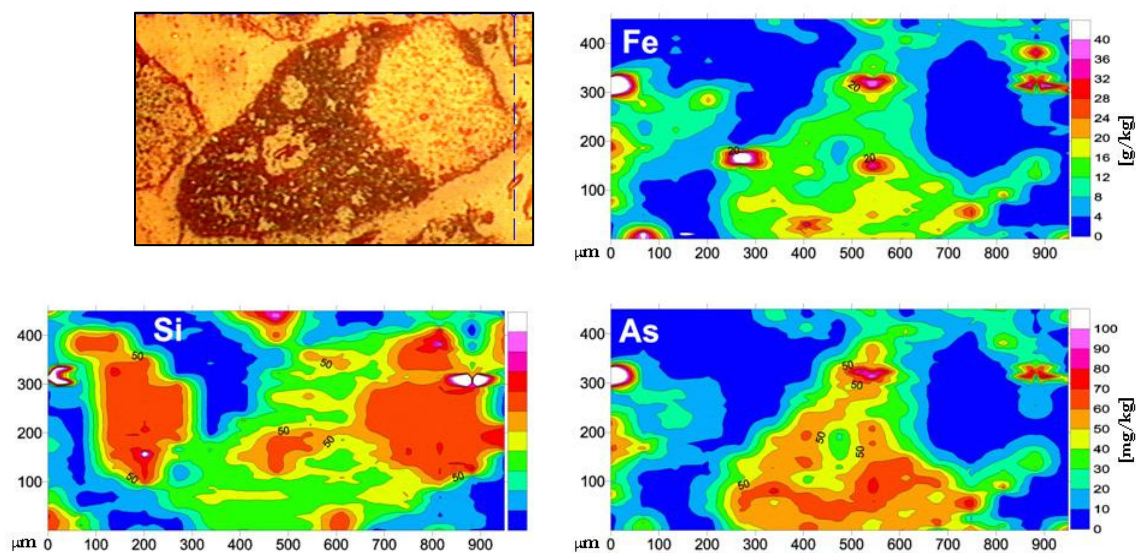


Fig. 7.2: Microscopic image and distribution of As, Fe and Si (not quantified) in a coated grain of the As rich sample of site H (H3515).

As a consequence, median Fe/As ratios are considerably different between the samples (Tab. 7.2). Mafic minerals generally have much higher median Fe/As ratios in all samples from both cores compared to coatings, which leads to the assumption that the precipitation of Fe oxy-hydroxide coatings leads to a relative enrichment of As compared to Fe. The very low median Fe/As ratios in the two As rich samples of 800 and 330, respectively, are worth mentioning (Tab. 7.2). There are clear correlations between As and Fe in coated mineral grains in most of the samples at both sites (Appendix A 5.1) with exception of the three samples which are low in As but rich in quartz, feldspar or mica (L2640, L3350, H2020). In coatings, As also often highly correlates with other elements like Mn, Ni, Cu, Zn. Associations of As with further elements will be described separately (Chapt. 7.3.5).

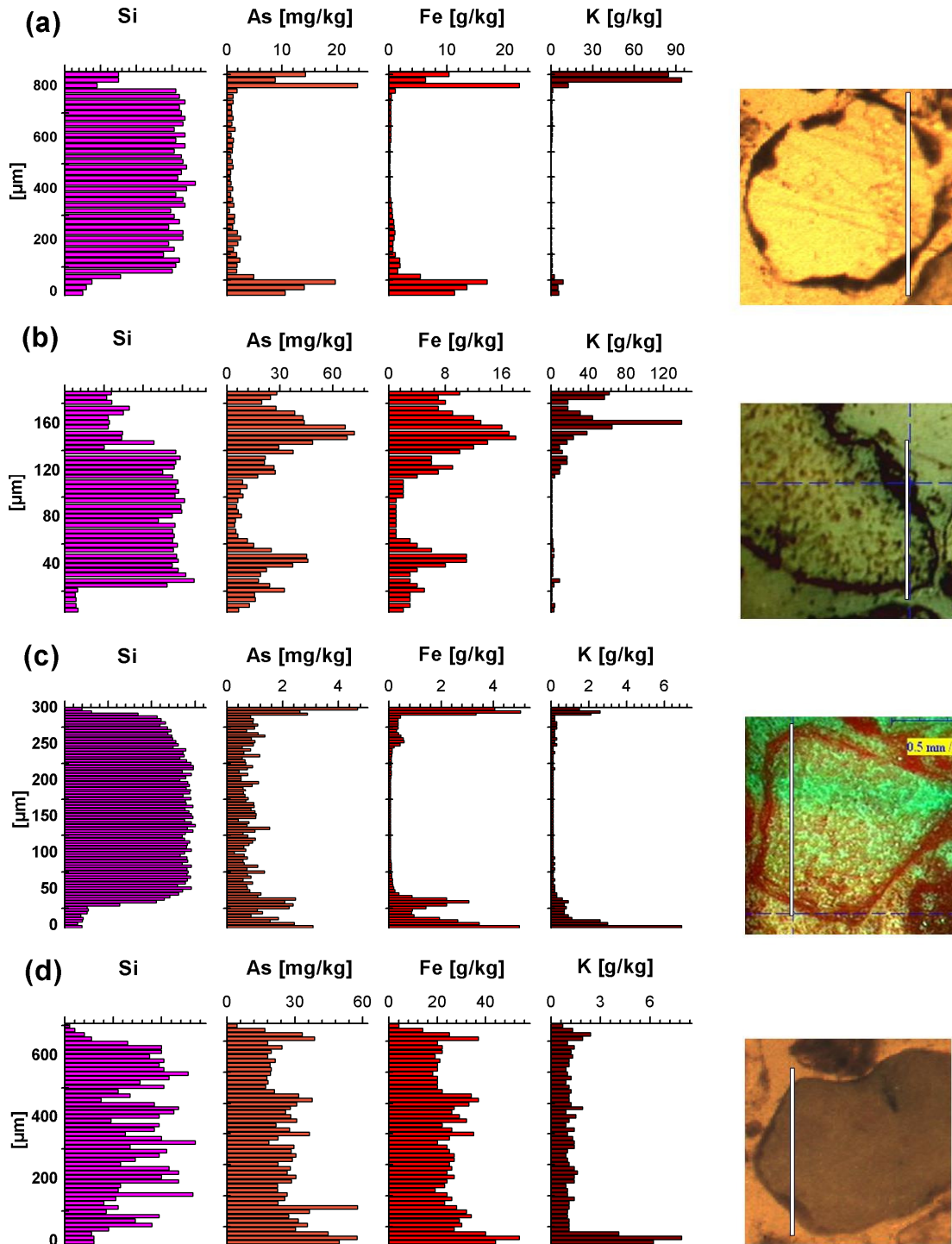


Fig. 7.3: Microscopic image and distribution of Si (not quantified), Fe, As and K in grains from different untreated samples (L17045 (a/d), H3515 (b), H2910 (c)) from both cores. (a) to (c) show coated grains with high (a + b) and low (c) As concentrations. In (d) the elemental distribution of a mafic mineral is illustrated.

AFTER PHOSPHATE LEACHING (LP)

After leaching with a 0.5 M Na-phosphate-solution, As concentrations remain more or less the same in most of the samples (Tab. 7.2). Considerable enrichment of As is still detectable above all in the in the As rich sample of site L (L17045LP, Fig. 7.4a) indicating that a substantial amount of As cannot be released by P-leaching. Arsenic concentrations are strongly reduced compared to measurements of untreated grains in the As rich (H3515LP) and quartz depleted samples (H3305LP) of site H (Tab. 7.2, Fig. 7.4b, c).

Tab. 7.2: Median concentrations of As and Fe as well as median Fe/As ratios calculated from the measurements of transects and discrete grains with μ S-XRF in the untreated samples, after leaching with 0.5 M Na-phosphate solution (LP) and after the dissolution of Fe oxy-hydroxides and carbonates (LFe). Included is also the number of measured grains in each sample.

Sample (depth)	Leaching step	As [mg/kg]	Fe [g/kg]	Fe/As	No. of measurements
L17045 (24 m)	original	4.6	9.8	800	12
	LP	6.7	6.6	1,200	10
	LFe	2.9	1.5	400	12
L2640 (33 m)	original	0.7	4.5	7,000	11
	LP	0.8	0.7	1,100	11
	LFe	0.7	2.7	19,400	11
L3350 (46 m)	original	0.8	17.0	14,900	12
	LP	0.9	11.0	9,600	10
	LFe	0.5	0.7	2,200	8
H2020 (23 m)	original	1.1	8.5	4,700	8
	LP	1.0	6.5	3,700	8
	LFe	0.6	0.9	1,800	8
H2910 (33 m)	original	5.2	8.8	1,600	9
	LP	10.0	8.5	1,000	13
	LFe	1.5	0.9	640	8
H3305 (39 m)	original	4.2	13.4	2,900	13
	LP	0.8	21	7,400	12
	LFe	0.7	4.5	5,100	8
H3515 (44 m)	original	20	3.7	330	18
	LP	5.8	4.1	600	14
	LFe	1.3	0.9	720	13

In the mica rich sample (H2910), the median As concentration of the measured grains is higher compared to the untreated sample which is probably caused by the heterogeneity of the sediments. As expectable, Fe concentrations are mainly similar to the concentrations in the untreated samples after P-leaching. The strong increase of Fe concentrations in the quartz depleted sample of site H (H3305) probably results from the much higher number of mafic grains (generally higher in Fe compared to coated minerals) that were analyzed.

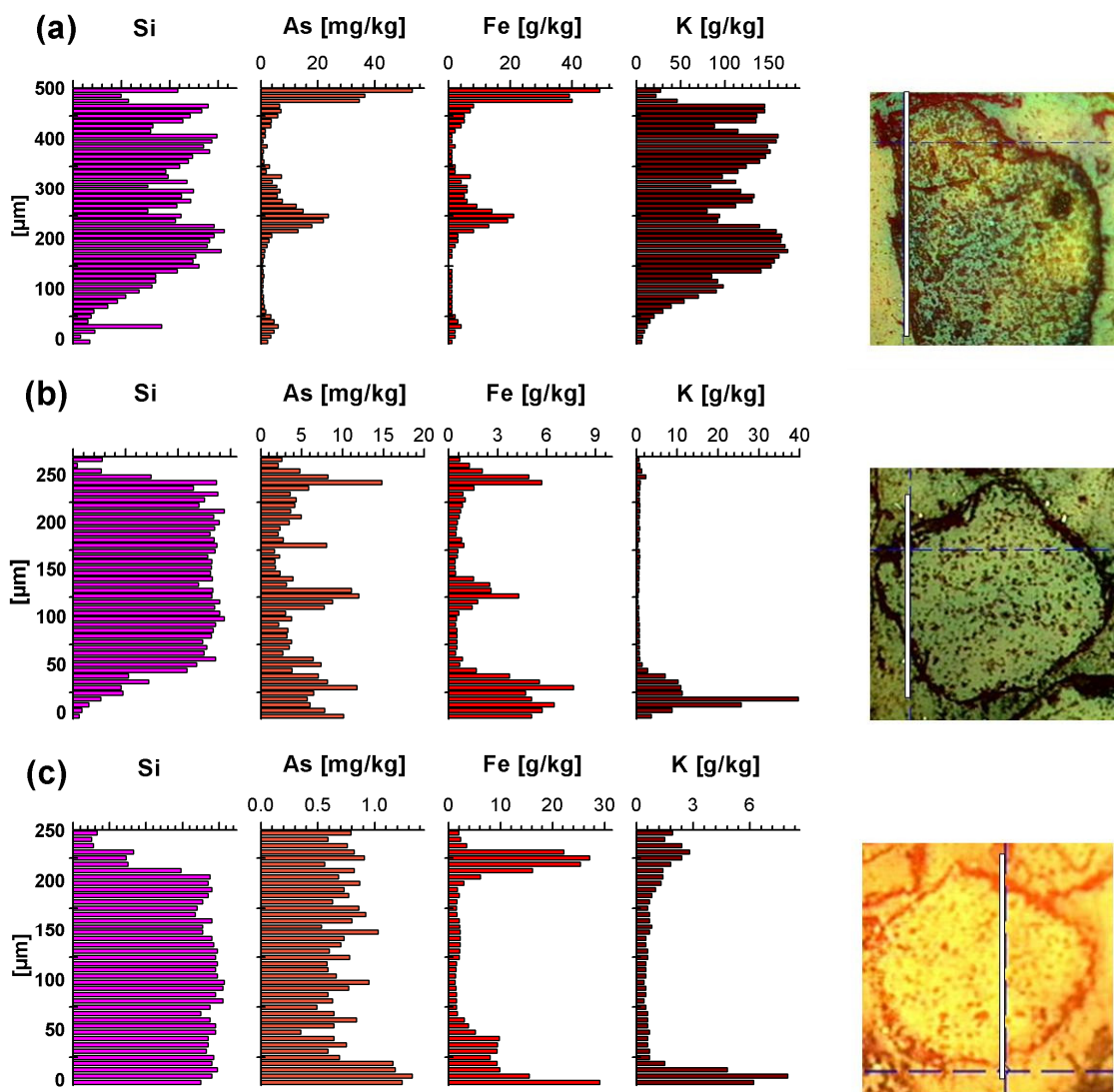


Fig. 7.4: Microscopic image and distribution of Si (not quantified), Fe, As and K in different coatings measured after leaching samples from both cores (L17045LP (a), H3515LP (b), H3305LP (c)) with 0.5 M Na-phosphate solution. Arsenic concentrations are still high after the leaching in (a) and (b), whereas in (c), As concentrations are mainly below detection limit.

In three samples, the two As rich (L17045LP, H3515LP) as well as the quartz depleted sample (H3305LP), the median Fe/As ratio is higher compared to the untreated materials (Tab. 7.2) indicating preferential release of As compared to Fe. A lower median Fe/As ratio occurs in the other four samples after P-leaching. This could, on the one hand, suggest preferential release of Fe compared to As or, on the other hand, re-precipitation of Fe and As. This will be discussed later in detail (Chapt. 7.4.2). High correlations between As and Fe exist in coated grains if As is still highly enriched even after P-leaching.

AFTER DISSOLUTION OF FE OXY-HYDROXIDES AND CARBONATES (LFE)

After dissolution of Fe oxy-hydroxides and carbonates, As concentrations are very low (<9 mg/kg, Fig. 7.5a, c) or even below detection limit (<1 mg/kg, Fig. 7.5b) in the coatings of all samples. Very high As concentrations can still be found in mafic minerals (Fig. 7.5d) with up to 200 mg/kg. Iron concentrations in coatings are also extremely low (<8 g/kg) compared to the untreated and P-leached material (<36 g/kg, Tab. 7.2) with high concentrations only occurring in mafic minerals (<550 g/kg). The remaining As and Fe in the coatings is always associated with K (Fig. 7.5a-c). However, there are no significant correlations between As and Fe or other elements apart from K in the coated grains. Consequently, it can be assumed that the dissolution of Fe oxy-hydroxide coatings has been successful. The median Fe/As ratios are lower compared to the measurements of untreated coatings in all samples with exception of the quartz depleted sample (H3305) which would suggest that higher amounts of Fe were released in this step compared to As (Tab. 7.2). The higher ratio in the quartz depleted sample could point out that only very low amounts of Fe were released compared to As or that re-precipitation of Fe and As took place.

It can be concluded from elemental mappings of untreated and leached grains that no major differences with regard to the amount of As or correlations with other measured elements occur between the two sites. Significant differences rather occur between the samples of one core and can probably be allocated to natural heterogeneities of fluvial material.

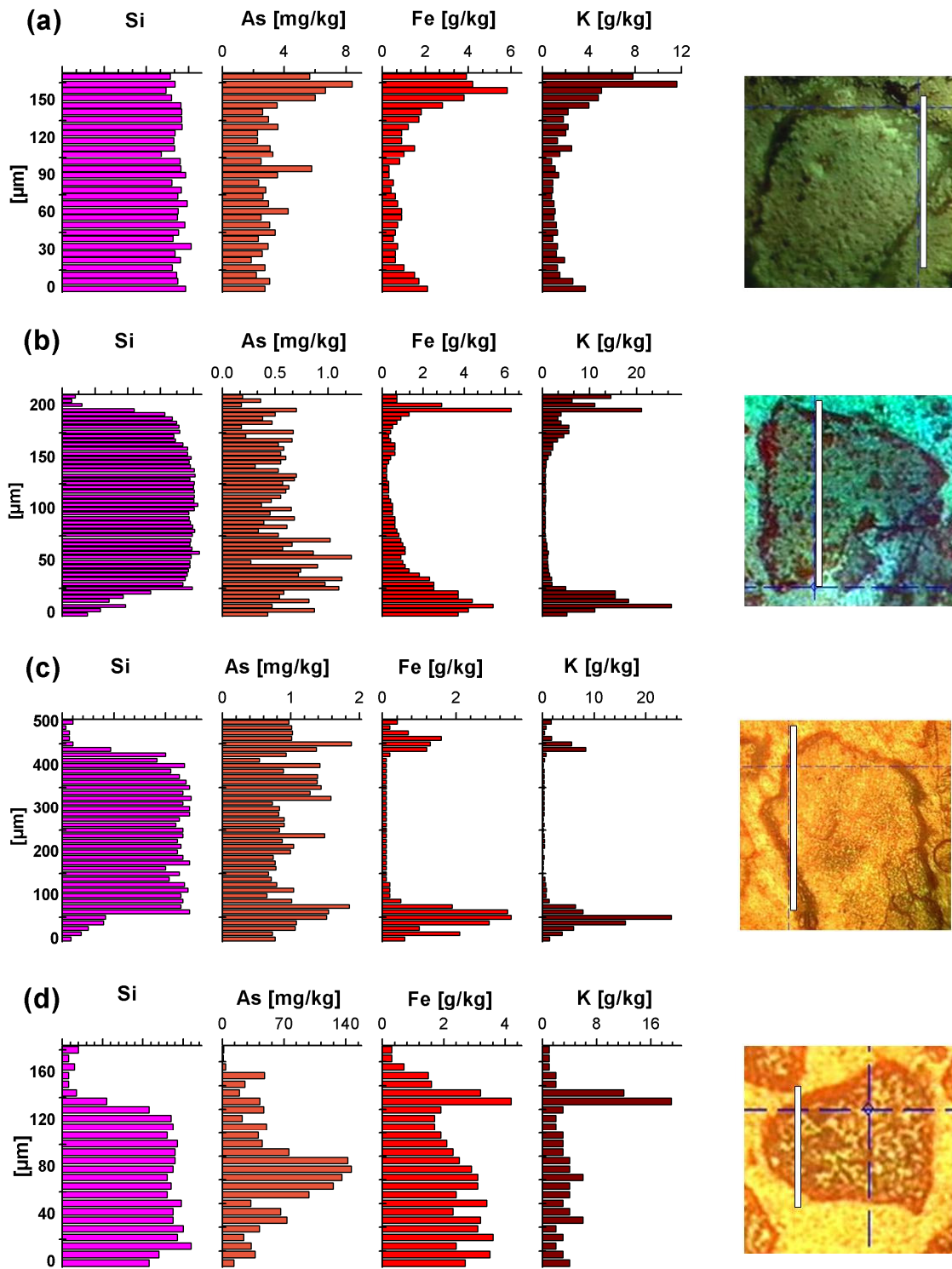


Fig. 7.5: Microscopic image and distribution of Si (not quantified), As, Fe and K of selected grains (L17045LFe (a), H2020 LFe (b), H3515 LFe (c), L2640 LFe (d)) measured after the dissolution of Fe oxy-hydroxides and carbonates. In (a) relatively high As concentrations remain, whereas in (b) and (c) the concentrations are mainly below detection limit of 1 mg/kg. In mafic minerals (d) very high As concentrations are present even after dissolution of Fe bearing oxy-hydroxides.

7.3.3 STATISTICAL ANALYSIS

Statistical analyses of selected measurements help to reveal associations of As with other elements. Additionally, multivariate statistics are a useful tool in order to delineate mixed signals caused by the fact that the μS beam is larger than the coatings itself. This is necessary to elucidate and locate possible As carrier phases within the aquifer sediments. Correlation matrices, factor loadings and factor scores of the statistical analysis are listed in Appendix 5.

UNTREATED SAMPLES

In the As rich sample of site L (L17045) the elemental composition of a coated mineral, probably quartz was measured along a transect (Fig. 7.3a). Two factors can be extracted from this data set by means of factor analysis. The first factor (F1) comprises Ca, Cr, Cu, Fe, Ni, As, Mn, Zn. Apart from Ca and Cr, which are lithophile, all other elements of F1 can be seen as siderophile or chalcophile. Consequently, F1 could probably be interpreted to represent an Fe oxy-hydroxide or sulphide in which the other elements are incorporated or adsorbed to. Due to some lithophile elements (Ca, Cr) in F1, it could also be possible, that this factor stands for a silicate phase. In the second factor (F2) mainly lithophile elements like K, V and Ga, and, Mn have high loadings which are typical for a (phyllo)silicate composition (Fig. 7.6).

The distribution of the factor scores along the transect suggests that F1 is mainly dominant in the upper and lower part of the transect which corresponds to the coating. The (phyllo)silicate represented by F2 is attached to the coating (Fig. 7.6). A closer look at the microscopic image (Fig. 7.3a) reveals a linear structure at the top of the transect which is probably represented by F2 and corresponds to a thin layer of phyllosilicate wrapping the core grain.

Similar to the previous grain, high As concentrations can be found in the coating of the central quartz grain of the quartz depleted sample (H3305). Two factors can be extracted from the recorded data (Fig. 7.7). F1 (high loadings of lithophile elements like K, Ca, Ga, Ti, V etc.) could be interpreted as a silicate and F2 (Mn, Cr, Fe, As) as an Fe oxy-hydroxide. Arsenic is included

in both factors with similar loadings (~0.7). Both coatings have in common that As highly correlates with Fe ($r = 0.98$, $n = 41 - 81$).

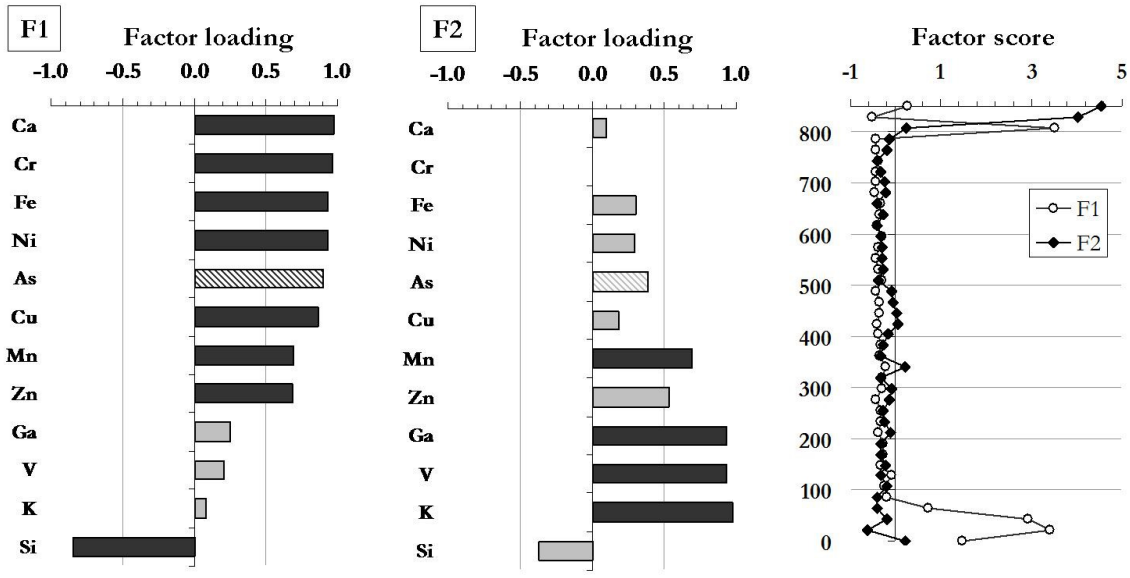


Fig. 7.6: Results of a factor analysis (factor loadings and factor scores) carried out on a data set collected along a transect through a grain of the As rich sample of site L (L17045). Ti was excluded from the analysis due to its low communality. The corresponding elemental distribution is shown in Fig. 7.3a.

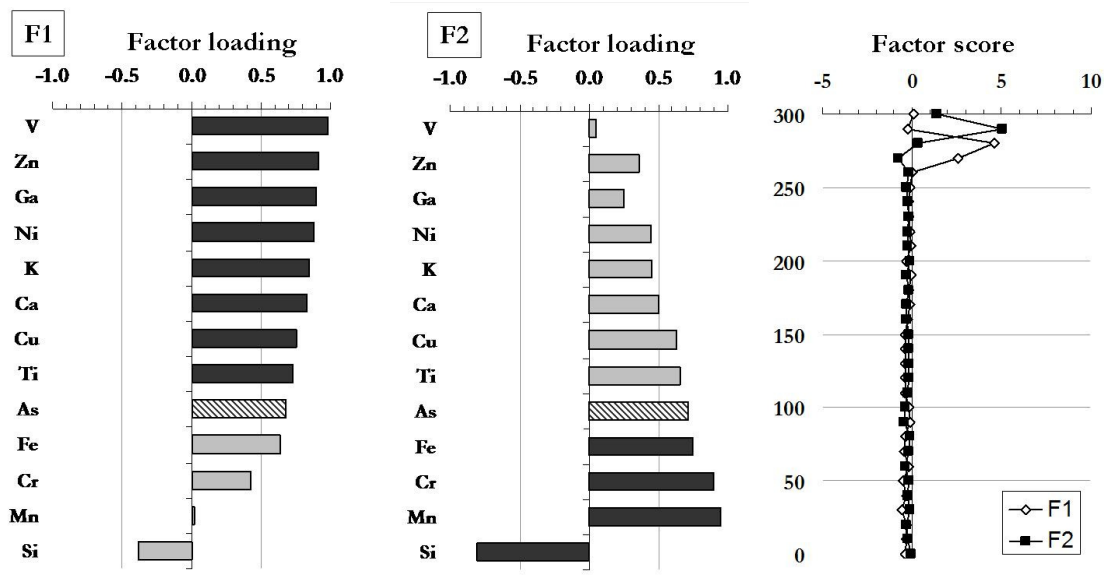


Fig. 7.7: Results of a factor analysis (factor loadings and factor scores) carried out on a data set collected along a transect through a grain in the sample with low quartz content of site H (H3305). The corresponding elemental distribution is given in Tab. A-19.

The results of factor analysis on the data from mafic minerals in general, mostly lead to numerous factors and low communalities for several elements and are, therefore, difficult to interpret. For a factor analysis based on the data of a mafic mineral from the As rich sample of site L (Fig. 7.3d), for example, several elements (Si, V, Ca, Ti, Cu) had to be excluded due to their low communalities. Two factors could be extracted which both have relatively high loadings for As (Fig. 7.8). In the first factor (F1), K groups together with Fe, As, Mn and Ni. Because K is a typical indicator for silicates this factor probably stands for a mafic (phyllo)silicate with impurities of Ni and As which is present at the rim of the grain. The second factor (F2) is stamped by high loadings for Zn, Ga, Cr as well as relatively high loadings for Fe, As and Ni. Except for Cr, these elements have a chalcophile character and, therefore, the factor could be interpreted to represent a sulphide phase which dominates the core of the grain.

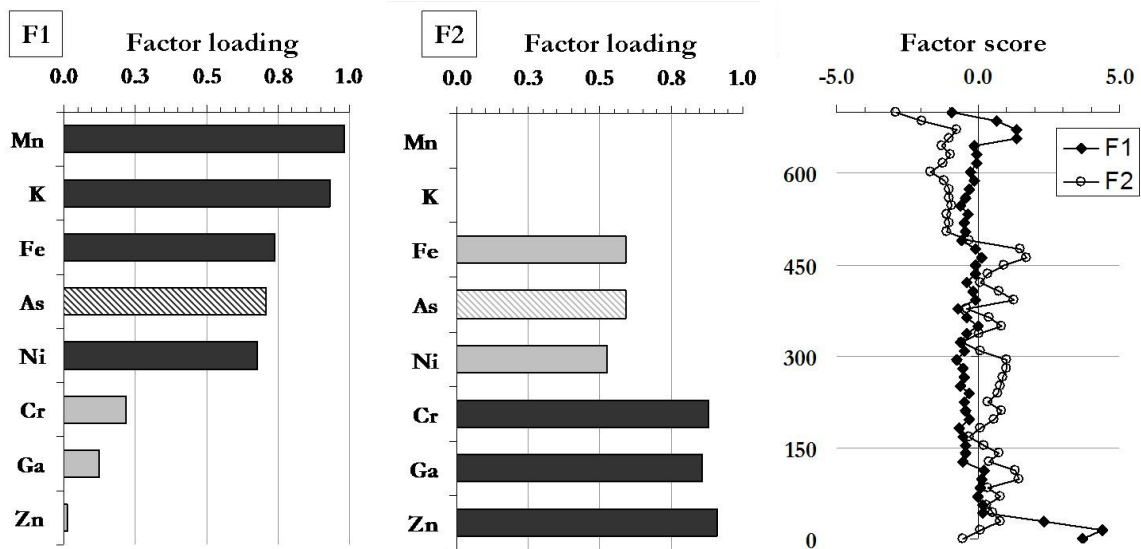


Fig. 7.8: Results of a factor analysis (factor loadings and factor scores) carried out on a dataset collected along a transect through a mafic grain in the As rich sample of site L (A17045). Si, Ca, Ti, V and Cu are excluded due to their low communalities. The corresponding elemental distribution is shown Fig. 7.3d.

AFTER PHOSPHATE LEACHING (LP)

From the data recorded by the mapping of a complete coated grain of the As rich sample of site L (Fig. 7.9) after P-leaching, two factors can be extracted. In the first factor, which dominates at the rim of the grain (Fig. 7.10) Fe, As,

Zn, Ni etc. are grouped, indicating an Fe oxy-hydroxide or sulphide, whereas in the second factor, lithophile elements (K, V, Si, Ga) have high loadings suggesting the presence of a silicate as core grain. Iron and As are strongly correlated with $r_s = 0.79$.

In the sample with low quartz content (H3305LP), As concentrations are mainly below detection limit with only slightly higher concentrations in the coating. Two factors can be extracted from the recorded data set by means of factor analysis. In the first factor (F1) both siderophile as well as chalcophile elements are grouped (Ga, Ni, Mn, Zn, Cr, V, Fe). For that reason, this factor could be interpreted as Fe oxy-hydroxide or sulphide. Arsenic is included in the second factor (F2) together with the lithophile elements K, Ti and Ca, suggesting that it is incorporated into a (phyllo)silicate. F2 dominates in the lower part (below F1, Fig. 7.11) and, therefore, probably can be seen as a (phyllo)silicate phase that is attached as coating around the core grain.

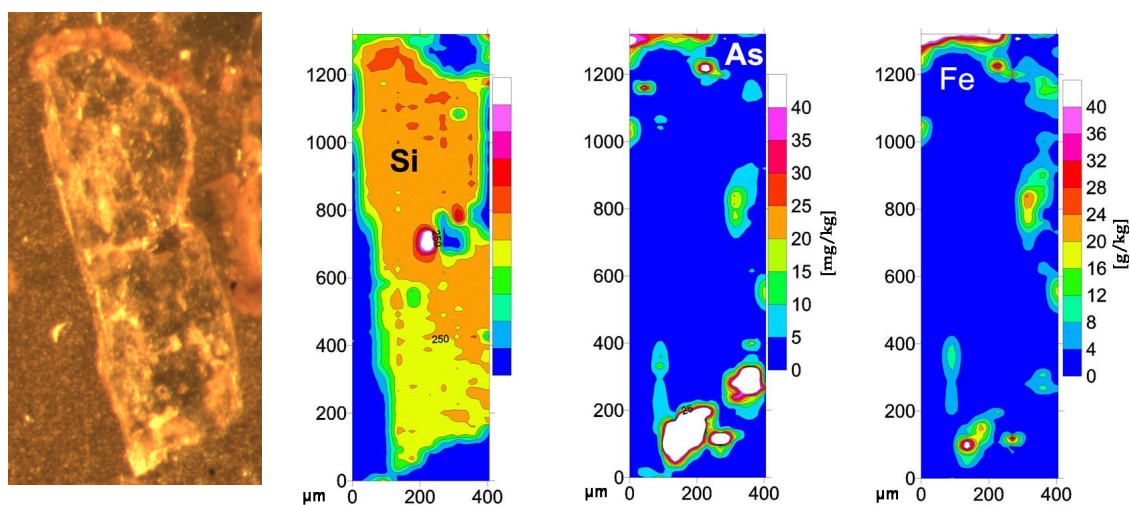


Fig. 7.9: Microscopic image and distribution of As, Fe and Si (not quantified) in a coated grain of sample L17045LP after leaching with 0.5 M Na-phosphate solution.

Factor analysis of data recorded along a transect through a grain of the As rich sample of site H (H3515LP) groups the elements into three factors (Fig. 7.12), the first of which (F1) is stamped by lithophile elements (K, V, Cr). The second factor has high loadings for As, Ga and Ni and, therefore, probably stands for a sulphide which is present as an inclusion in the host grain, as suggested by the distribution of the factor scores (Fig. 7.12).

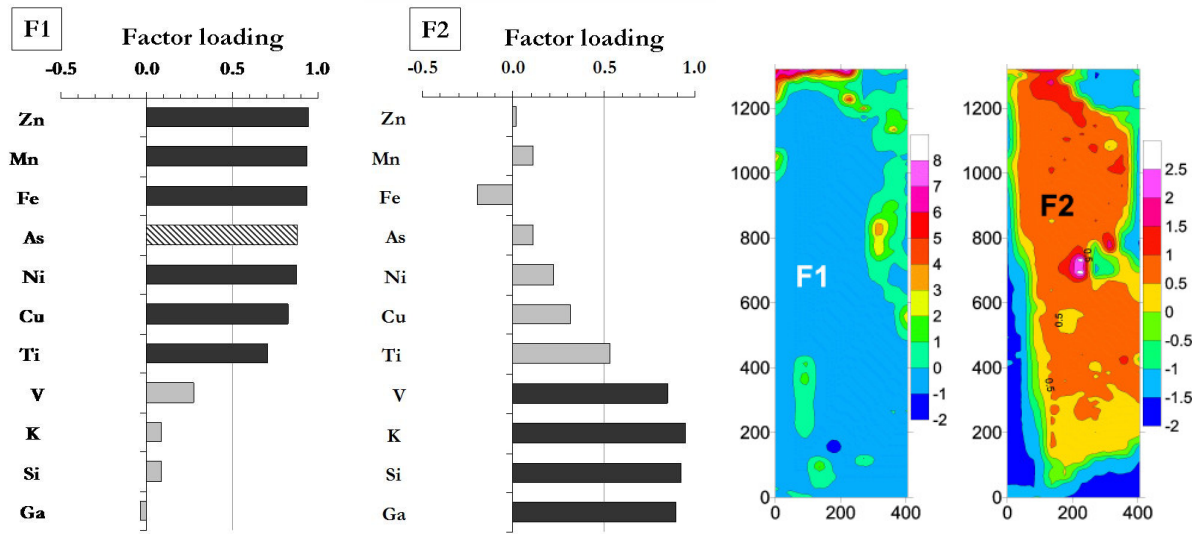


Fig. 7.10: Results of a factor analysis (factor loadings and factor scores) based on data recorded from the mapping of a grain of the As rich sample of site L after phosphate leaching (L17045LP). Silicon and Ca are excluded due to their low communalities. The corresponding elemental distribution is shown in Fig. 7.9.

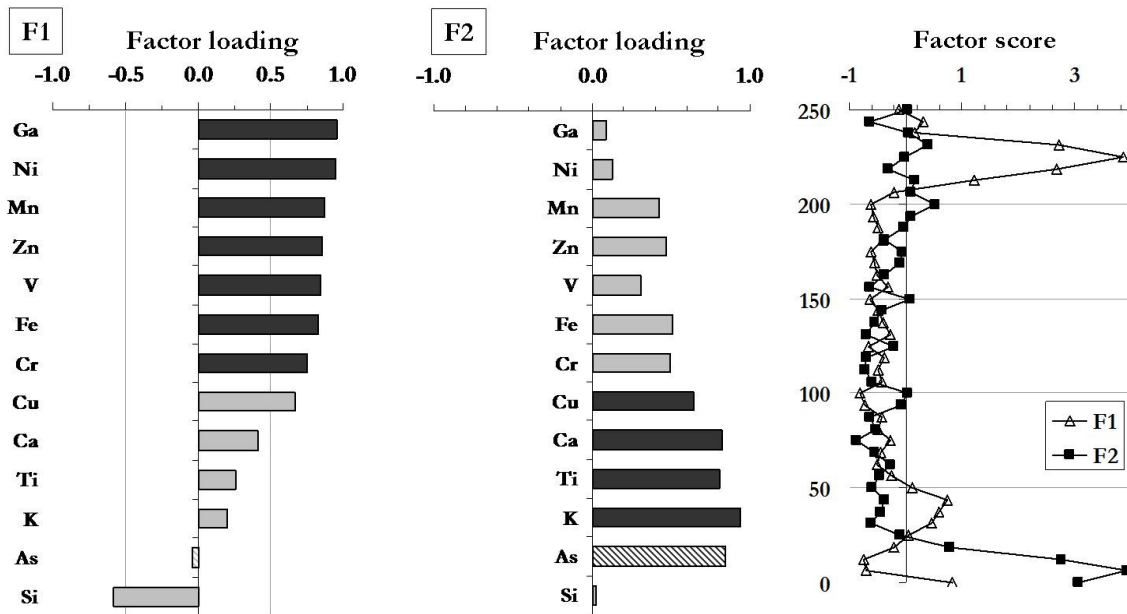


Fig. 7.11: Results of a factor analysis (factor loadings and factor scores) carried out on a dataset collected along a transect through a grain of the sample with low quartz content after phosphate leaching (H3305LP). The corresponding elemental distributions are shown in Fig. 7.4c.

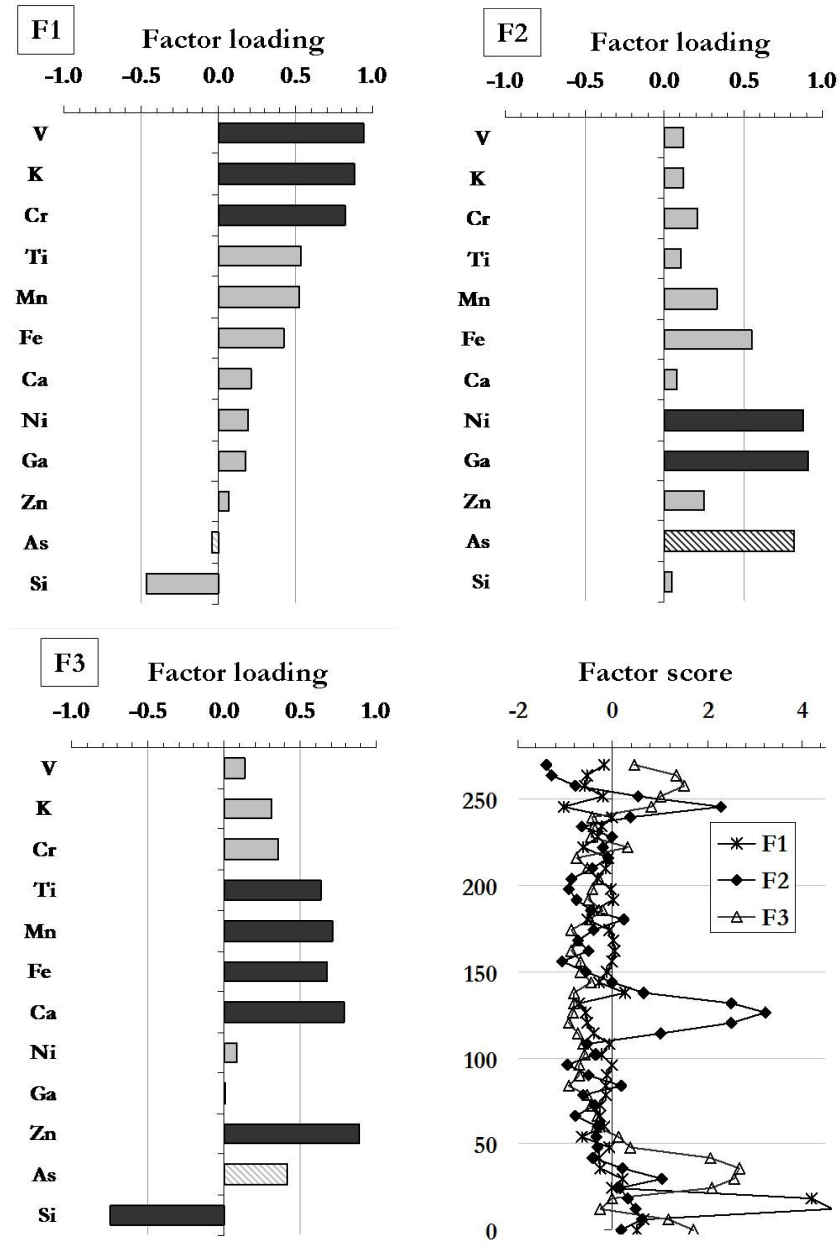


Fig. 7.12: Results of a factor analysis (factor loadings and factor scores) carried out on a dataset collected along a transect through a grain of the As rich sample of site H after phosphate leaching (H3515LP). Copper was excluded from factor analysis due to its low communality. The corresponding elemental distributions are shown in Fig. 7.4b.

The third factor (F3) comprises Fe, Mn, Zn, Ti and Ca and, therefore, might either be interpreted as carbonate or oxide phase, which makes up the coating of the mineral. The silicate, represented by F1, is attached to the coating of the mineral (Fig. 7.12). In the grain of the As rich sample (H3515LP), As and Fe still highly correlate ($r = 0.99$, respectively; $n = 50$), whereas there is no correlation in the sample with low quartz content (H3305LP).

AFTER DISSOLUTION OF FE OXY-HYDROXIDES AND CARBONATES (LFe)

After this second leaching step, As is mainly below detection limit in most of the coatings or does not show any correlations with other elements and was, therefore, excluded from the statistical analysis in many cases.

In the mica rich sample (H2020LFe) (Fig. 7.5b) As is below detection limit, whereas Fe is still present in the coating. Two factors could be extracted by factor analysis (Fig. 7.13). Factor 1 (F1) is stamped by high loadings for siderophile as well as chalcophile elements (Zn, Ni, Cr, Ga, Fe, Mn) and could, therefore, be interpreted as Fe dominated oxy-hydroxide or sulphide mainly present at the lower inner part of the transect in form of a coating around a core grain. High loadings of lithophile elements (K, Ti, V) characterize F2, suggesting the presence of a (phyllo)silicate at the bottom of the transect (Fig. 7.13).

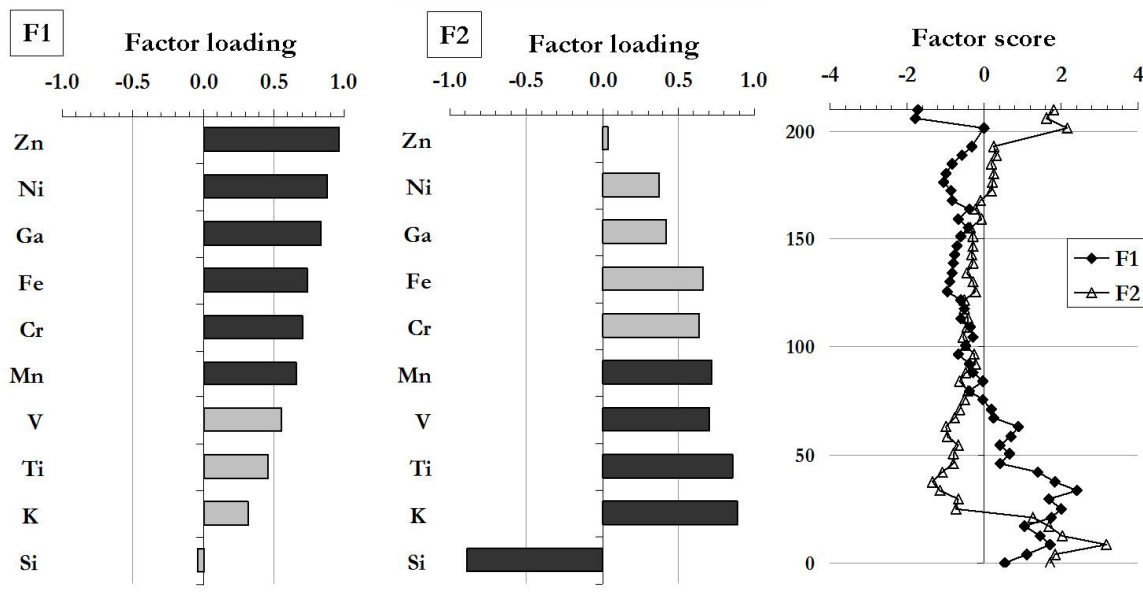


Fig. 7.13: Results of a factor analysis (factor loadings and factor scores) based on data recorded from a transect measurement through a grain of the mica rich sample (H2020LFe) after the dissolution of Fe oxy-hydroxides and carbonates. Arsenic, Cu and Ca were excluded from the analysis due to their low communalities. The corresponding elemental distributions are shown in Fig. 7.5b.

In the As rich sample of site L (L17045LFe, Fig. 7.5a) relatively high As concentrations are detectable, allowing to include As into the statistical analysis. Two factors were extracted, both including lithophile elements, and

therefore probably two different silicate phases occur as coatings of the central grain (Fig. 7.14).

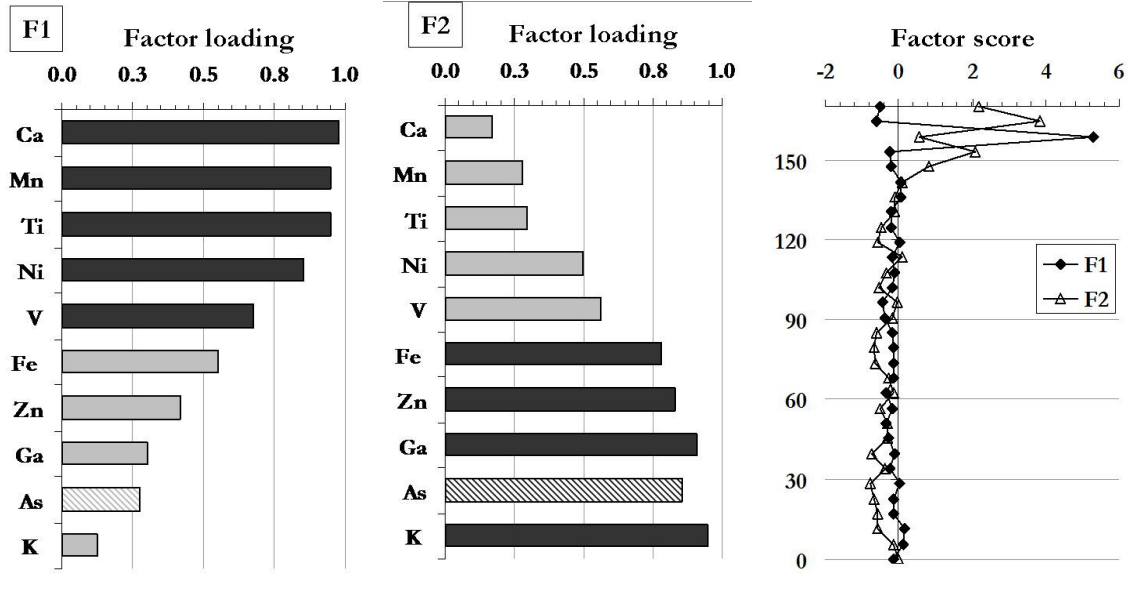
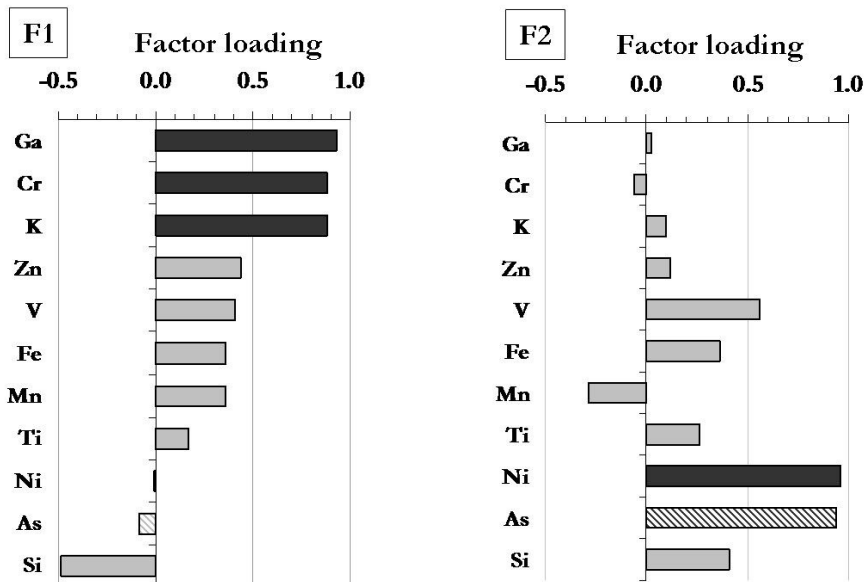


Fig. 7.14: Results of a factor analysis (factor loadings and factor scores) based on data recorded from a transect measurement through a grain of the As rich sample of site L (L17045Fe) after the dissolution of Fe oxy-hydroxides and carbonates. Silicon, Cu and Cr were excluded from the analysis due to their low communal-ity. The corresponding elemental distributions are shown in Fig. 7.5a.



to be continued on the following page

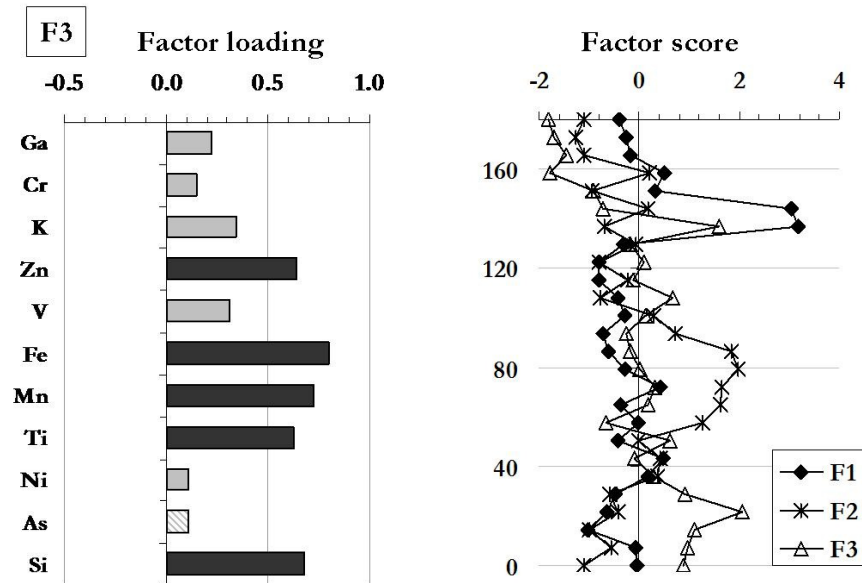


Fig. 7.15: Results of a factor analysis (factor loadings and factor scores) based on data recorded from a transect measurement through a mafic grain of the feldspar rich sample (L2640LFe) after the dissolution of Fe oxy-hydroxides and carbonates. Silicon and Cu were excluded from the analysis due to their low communalities. The corresponding elemental distributions are shown in Fig. 7.5d.

In mafic minerals, like in the feldspar rich sample (L2640LFe), high concentrations of As can still be measured after dissolution of Fe oxy-hydroxides and carbonates (Fig. 7.5d), but mainly in the core of the grain and not in the coating. Three factors can be extracted by factor analysis from the recorded data set among which F1 and F3 mainly consist of lithophile elements and suggest the presence of two different (phyllo)silicates (Fig. 7.15) making up the coating of the host grain. The second factor (F2), including As and Ni, could stand for a sulphide, which forms an inclusion in the mineral grain.

7.4 DISCUSSION

7.4.1 ARSENIC BEARING PHASES AND DIFFERENCES BETWEEN THE TWO SEDIMENT CORES

High As concentrations of up to 500 mg/kg were detected in discrete grains of the sediments from Van Phuc. A huge number of point measurements on particles in samples from different depth from both cores disclose great dif-

ferences in As concentrations and distributions of individual As bearing grains, but also reveal a very heterogeneous distribution of As within a single grain (Fig. 7.2). Hints for different As bearing phases of primary and secondary origin could be identified by means of statistical grouping methods. Typical primary phases which have a considerable As enrichment are probably mafic silicates or phyllosilicates as indicated by the grouping of As with K and other lithophile elements in one factor in several samples (Chapt. 7.3.3). In most of the cases, Fe is also associated in such factors (Fig. 7.7, Fig. 7.8, Fig. 7.11, Fig. 7.14), suggesting the presence of Fe bearing mafic phyllosilicates like biotite or chlorite. Maximum As concentrations in those parts where mafic phyllosilicates dominate vary from 6 - 60 mg/kg, which is about the range found by other authors for biotite or chlorite (5 - 50 mg/kg, SENGUPTA ET AL., 2004; SEDDIQUE ET AL., 2008). In one case, no Fe is included in such a factor (Fig. 7.6), suggesting that As (<14 mg/kg) might be associated with a phyllosilicate like illite that is also known to incorporate As in considerable amounts (10 - 41 mg/kg, PAL ET AL., 2002). Therefore, phyllosilicates seem to be important As carriers in Van Phuc but also elsewhere (ANAWAR ET AL., 2002; DOWLING ET AL., 2002; NATH ET AL., 2005; WAGNER ET AL., 2005; CHARLET ET AL., 2007). They frequently occur at the rim of a core grain in the sediments of both sites; however, they are no coatings in the actual sense, but rather attached to the surface of a host mineral possibly resulting from weathering of a central feldspar core grain.

Further minerals, which seem to be of importance for the As fixation in Van Phuc are sulphides, which mainly occur as distinct authigenic mineral grains (e.g. Fig. 7.15) but can also occur as surface precipitates or attached to quartz or feldspar mineral grains (e.g. Fig. 7.6). In a mafic mineral of the feldspar rich sample (A2640LFe), for example, there seems to be a NiAs sulphide present as small inclusion with As concentrations of up to 140 mg/kg (Fig. 7.15). In the As rich sample of site H (H3515LP), another sulphide with up to 14 mg/kg consisting mainly of Fe and Ni occurs as inclusion in a silicate phase but also as surface precipitate as indicated by the distribution of the factor scores (Fig. 7.12). Biogenic pyrite formation is considered to be very effective in scavenging As together with other elements like Ni or Cu from groundwater (SAUNDERS ET AL., 1997; ANAWAR ET AL., 2002; SMEDLEY & KINNIBURG, 2002; LOWERS ET AL., 2007). On the whole, the enrichment of As in

sulphides is relatively high compared to other minerals in the sediment but still rather low compared to sulphides mentioned in literature (100 - 77,000 in pyrites; Tab. 2.5; SMEDLEY & KINNIBURG, 2002). Sulphides are mainly associated with other minerals and rarely occur as distinct mineral grains. Their identification in surface precipitate is difficult due to the fact that the spot size of the μS beam ($2 \times 8 \mu\text{m}$) is still larger compared to the size of most of the investigated surface precipitates (few tens of nm), as indicated by the SEM-EDX analysis (Chapt. 7.3.1), therefore leading to mixed signals.

Iron oxy-hydroxides, frequently considered as one of the most important groups of minerals in controlling the As release (e.g. NICKSON ET AL., 2000; SWARTZ ET AL., 2004), were also found to contain considerable amounts of As (<140 mg/kg, Fig. 7.6; Fig. 7.10). However, these oxy-hydroxide phases could only be detected as coatings and not as discrete minerals. Additional to As, Fe oxy-hydroxides also incorporate or adsorb other heavy metals like Zn, Cu, Mn and Ni etc. There are also indications for carbonates precipitating onto the surface of grains, represented probably mainly by Ca and Fe carbonates (Fig. 7.12). Both, siderite and calcite are supersaturated at site H and, therefore, are likely to occur (Fig. 5.6). There are known As bearing calcites and siderites with concentrations of 9 - 40 mg/kg and 5 - 20 mg/kg, respectively (PAL ET AL., 2002; GUO ET AL., 2007). The occurrence of Fe oxy-hydroxide and carbonate surface precipitates was also proved by the SEM-EDX analysis (Chapt. 7.3.1).

High As concentrations occur in both mafic and coated minerals of the sediments of each site. On the whole, highest As concentrations can always be found in mafic minerals. It is generally assumed that As and Fe are closely associated in solids (HARVEY ET AL., 2002). In this investigation, clear correlations were found between As and Fe only if As is enriched in the coatings but not if present in mafic minerals. Based on this observation, it can be concluded that significant correlations between As and Fe are mainly expectable after dissolution of discrete primary minerals followed by the precipitation of Fe oxy-hydroxide coatings. The precipitation of Fe oxy-hydroxides further seems to lead to the enrichment of As relative to Fe as indicated by the much lower Fe/As ratio in coatings in comparison to mafic mineral phases (Chapt. 7.3.2). In the samples low in As but rich in feldspar,

quartz or mica (L2640, L3350, H2020) nearly no As enrichment in coatings is detectable. A very high Fe/As ratio (Tab. 7.2) as well as a lack of correlation between As and Fe are further characteristics of these samples. This leads to the assumption that either no enrichment of As took place due to low As concentrations during the precipitation of Fe oxy-hydroxides, or that only As has already been released but not Fe. Which of the assumptions is more appropriate cannot be answered based on the existing data. However, it can be assumed that the highly reducing conditions at site H already lead to a release of As. Low As concentrations in the coatings also occur in the quartz depleted as well as the mica rich samples (H3305, H2910). In contrast to the other samples, however, the Fe/As ratio is relatively low and a correlation between Fe and As exists in the coated grains which points towards a simultaneous release of Fe and As.

7.4.2 EFFECTS OF SEQUENTIAL EXTRACTION ON THE SEDIMENT COMPOSITION

In both As rich samples (L17045LP, H3515LP) still high As concentrations can be detected occasionally after the leaching with P-solution indicating that a certain amount of As is not present in an adsorptive way. However, the higher Fe/As ratio compared to the untreated samples indicate that more As relative to Fe has been released from the sample which is also supported by the much lower median As concentrations in the As rich sample of site H (H3515LP, Tab. 7.2). The results of the sequential extractions indicate that about 45 (L17045LP) and 35% (H3515LP) of As, respectively, is still present after the P-leaching (Tab. 7.2). In the quartz depleted sample (H3305LP) the As concentrations are much lower after P-leaching compared to the untreated material, which is in accordance to the indicated As release of >50% by the results of the sequential extraction (Tab. A-4; Tab. A-5). The much higher Fe/As ratio further supports the preferential release of adsorbed As from the quartz depleted sample (Tab. 7.2). In all three samples considerable correlations between As and Fe still occur if As is present in the coatings, therefore, it can be assumed that no major changes of the mineral structures took place.

Nearly no change occurred in the samples rich in feldspar, quartz and mica (L2640LP, L3305LP, H2020LP) where As concentrations in the coatings were already low in the untreated samples (Tab. 7.2). Considerable As enrichments are only visible in association with K and, therefore, As is probably present in (phyllo)silicate phases. In all three cases the Fe/As ratio is lower compared to the untreated samples which would indicate a preferential release of Fe. Additionally, re-precipitation of Fe minerals incorporating As or formation of Fe(II)-As(III) surface precipitates (DIXIT & HERING, 2006) could lead the lower Fe/As ratio.

After the dissolution of Fe oxy-hydroxides and carbonates, both As and Fe concentrations are considerably lower compared to the untreated and P-leached samples (Tab. 7.2). Fe-leaching leads to the break-up of the correlations between Fe and As in coatings. The correlation between As and Fe is preserved only in association with K, indicating the presence of both elements in silicate structures. Further elements which are associated with Fe oxy-hydroxide coatings like Mn or Cr have also lower concentrations and are probably also released by the dissolution of Fe oxy-hydroxides. Silicates do not seem to be affected, which is indicated by comparable concentrations of K, V and Ti in all three extraction steps (Tab. A-32; Tab. A-33). The more intensive release of Fe compared to As in this step should lead to a very low Fe/As ratio, at least lower compared to the P-leaching, which is the case in most of the samples with exception of the sample with low quartz content (H3305). The re-precipitation of Fe bearing phases, for example, could obliterate the ratio.

In the As rich and the quartz depleted sample of site H (H3515LP, H3305LP) it can be shown that considerable amounts of As can be released due to competition with PO_4^{3-} . High concentrations of PO_4^{3-} frequently occur in aquifers with high As concentrations (e.g. BGS & DPHE, 2001; DOWLING ET AL., 2002; SMEDLEY & KINNIBURG, 2002) as also at site H in Van Phuc, where the two samples are taken from (Fig. 5.4). Some authors postulated (e.g. DIXIT & HERING, 2003; SWARTZ ET AL., 2004) that a lack of sufficient free sorption sites in aquifer sediments might be responsible for high As concentrations in groundwater. However, this assumption can be refuted for Van Phuc because the As rich sample of site H has by far the lowest Fe concentration but

the highest enrichment of As in its coatings (Fe/As ratio ~300). Therefore, other processes have to be responsible for the As mobilization at this site. The dissolution of Fe oxy-hydroxides and carbonates lead to a complete release of As from the coatings. A change in the association of As with other elements indicates that re-precipitation processes could also play a role in the mobilization of As. Diagenetic remobilization and re-distribution of As from one phase to another was also suggested by ANAWAR ET AL. (2002). A complete dissolution of Fe oxy-hydroxides in Van Phuc under the currently prevailing redox-conditions, however, is not likely because the dissolution of Fe oxy-hydroxides is relatively slow (SCHWERTMANN, 1991) and phyllosilicates, attached to the surface of oxy-hydroxide coated mineral grains could further protect them from dissolution.

8 CONCEPTUAL MODEL FOR THE CURRENT DISSOLVED ARSENIC DISTRIBUTION IN VAN PHUC

Multiple geochemical processes along with special hydrological and sedimentological conditions seem to have an influence on the dissolved As distribution in Van Phuc as described in the previous chapters. Within this chapter all available data will be brought together in order to develop a conceptual model which possibly explains the current situation.

The most apparent differences between the two sites occur in water chemistry as well as the colour of the sediment, two characteristics which seem to be mutually influencing. The redox conditions at site L are less reducing (Mn reducing) in the aquifer compared to site H, resulting in low dissolved As concentrations ($< 10\mu\text{g/L}$), lower concentrations of most other dissolved ions compared to site H (Fig. 5.5) and brown sediments (Fig. 8.1). At site H, dissolved As concentrations (210 - 620 $\mu\text{g/L}$) are well above the current Vietnamese threshold value of 10 $\mu\text{g/L}$, the groundwater is highly reducing (no sulphate) and the aquifer sediment is mainly grey (Fig. 8.1).

The solid bulk As concentrations are similar at both sites but As is fixed in different ways. At site H, As is mainly adsorbed or partly incorporated into probably freshly formed amorphous Fe oxy-hydroxides or carbonates throughout the depth profile. A considerable release of As from Fe oxy-hydroxide coatings seem to have already occurred at some depth because only little enrichment of As was detected by the small scale elemental mappings of several mineral coatings (Chapt. 7.3.2). In the grey aquifer a high content of Fe(II) or mixed valence Fe(II/III) minerals is indicated by the low reflectance (ΔR) of < 0.5 (Fig. 8.1), which are thought to have a lower adsorption capacity for As compared to Fe(III) oxy-hydroxides (HORNEMAN ET AL., 2004; SWARTZ ET AL., 2004). In the aquifer at site L, As is mainly incorporated into amorphous and crystalline Fe oxy-hydroxides, with exception of the layer just below the transition from aquitard to aquifer where As is mostly adsorbed.

Site L	Sediment characteristics		GW characteristics
	clay/silt: <ul style="list-style-type: none"> • TOC: median 0.12, < 4.5 wt-% • OM: marine to terrestrial • CPI: 1.6-2.0 • As mainly adsorbed • $\Delta R < 0.5$ Fe(II/III) minerals • Fe/As 		no aquifer
	brown sand: <ul style="list-style-type: none"> • TOC: median 0.02 wt-% • As: 5 mg/kg • OM: ~33 % marine • CPI: ~ 1.6 • As incorporated in amorphous/crystalline oxides • $\Delta R > 0.5$ Fe(III) minerals • $r_{Fe/As}$: 0.71 • Fe/As: 4000 ± 1500 • Age: 17 kyr BP 		aquifer: <ul style="list-style-type: none"> • As: < 10 µg/L • Fe^{2+}, PO_4^{3-}, NH_4^+, HCO_3^-, DOC low • Mn high • no oxygen, nitrate • Fe/As >1000 • calcite/siderite: SI < 0 • water age >55a
	gravel: <ul style="list-style-type: none"> • Pleistocene 		<ul style="list-style-type: none"> • water age >55a • high sulphate • comparable to site H
Site H	Sediment characteristics		GW characteristics
	clay/silt: <ul style="list-style-type: none"> • TOC: median 0.1, < 0.8 wt-% • CPI: 2 • high n-alkane abundance 		no aquifer
	grey sand: <ul style="list-style-type: none"> • TOC: 0.02 wt-% • As: ~ 5 mg/kg • age 1 kyr BP • CPI ~ 1 • Fe/As: 3200 ± 2000 		Aquifer <ul style="list-style-type: none"> • As: 170-600 µg/L • Fe/As: ~100 • Fe^{2+}, PO_4^{3-}, NH_4^+, HCO_3^-, DOC high especially in upper part • no oxygen, no nitrate, no sulphate • $r_{Fe/Eh}$: 0.89 • calcite/siderite: SI >0 • water age: 15 to >55a
	brown sand: <ul style="list-style-type: none"> • $\Delta R > 0.5$ Fe(III) minerals 		brown sand: <ul style="list-style-type: none"> • water age: >55a
	gravel: <ul style="list-style-type: none"> • Pleistocene 		gravel aquifer: <ul style="list-style-type: none"> • water age >55a no sulphate

Fig. 8.1: Summary of the available results from sediment and groundwater analysis for site L and H in Van Phuc (GW = groundwater).

This exception will be discussed later in detail. The occasionally very low As enrichment in Fe oxy-hydroxide coatings mapped on a μm scale at site L indicates that either a considerable fraction of As had already been released and flushed away with time as proposed for other study sites (BGS & DPHE, 2001; VAN GEEN ET AL., 2008A) or As might still be incorporated in primary minerals and has never been released to a great extent in the past (Chapt. 7.3.2).

The question arises why the reducing conditions, which apparently seem to trigger the release of As, are so different between the two sites. All sources of OC have the potential to act as electron donor for microbial metabolism leading to reducing conditions, whereupon reactivity and quantity of OM are rate determining (HARTOG ET AL., 2004; ROWLAND ET AL., 2006; ROWLAND ET AL., 2007, VAN DONGEN ET AL., 2008).

In the aquifer of site L, the reactivity of OM seems to be lower compared to site H. Despite the higher reactivity at site H, the similar but low amount of TOC in the aquifer at both sites (Fig. 8.1) would probably only lead to slightly higher microbial turnover at site H. Therefore, a much lower As release due to reducing conditions in comparison to the current situation would be expectable. More important seems to be an additional supply of reactive OC from the upper sediment layers at site H leading to enhanced Fe oxy-hydroxide reduction, which is clearly indicated by the high concentrations of dissolved Fe and typical indicators of biodegradation (e.g. PO_4^{3-} , HCO_3^- , NH_4^+) in the groundwater in the upper part of the aquifer (Fig. 5.5). These upper layers are, in parts, high in TOC and deposited within silt to fine sand, probably allowing slow but sufficient percolation of electron donors into the aquifer. Infiltration of surface derived OC cannot be excluded at site H, especially due to the fact that the fields are fertilized with faecal matter. This possibility has to be further investigated; however, a strong influence is not conceivable due to the thickness and low permeability of the clay rich surface layers (Fig. 8.2).

In addition to OC, As might also be vertically transported within site H even though this is not as clearly indicated by the depth profile of dissolved As concentrations compared to the depth distribution of HCO_3^- , PO_4^{3-} etc. Co-precipitation, re-precipitation and transformation mainly of Fe bearing

minerals as well as competition with other ions (BGS & DPHE, 2001; MCARTHUR ET AL., 2001; DIXIT & HERING, 2003; HORNEMAN ET AL., 2004; SWARTZ ET AL., 2004; PEDERSEN ET AL., 2006) probably have a strong influence on the dissolved As distribution and, consequently, also could lead to a differing profile of dissolved As at both sites as discussed in Chapter 5.4.2.

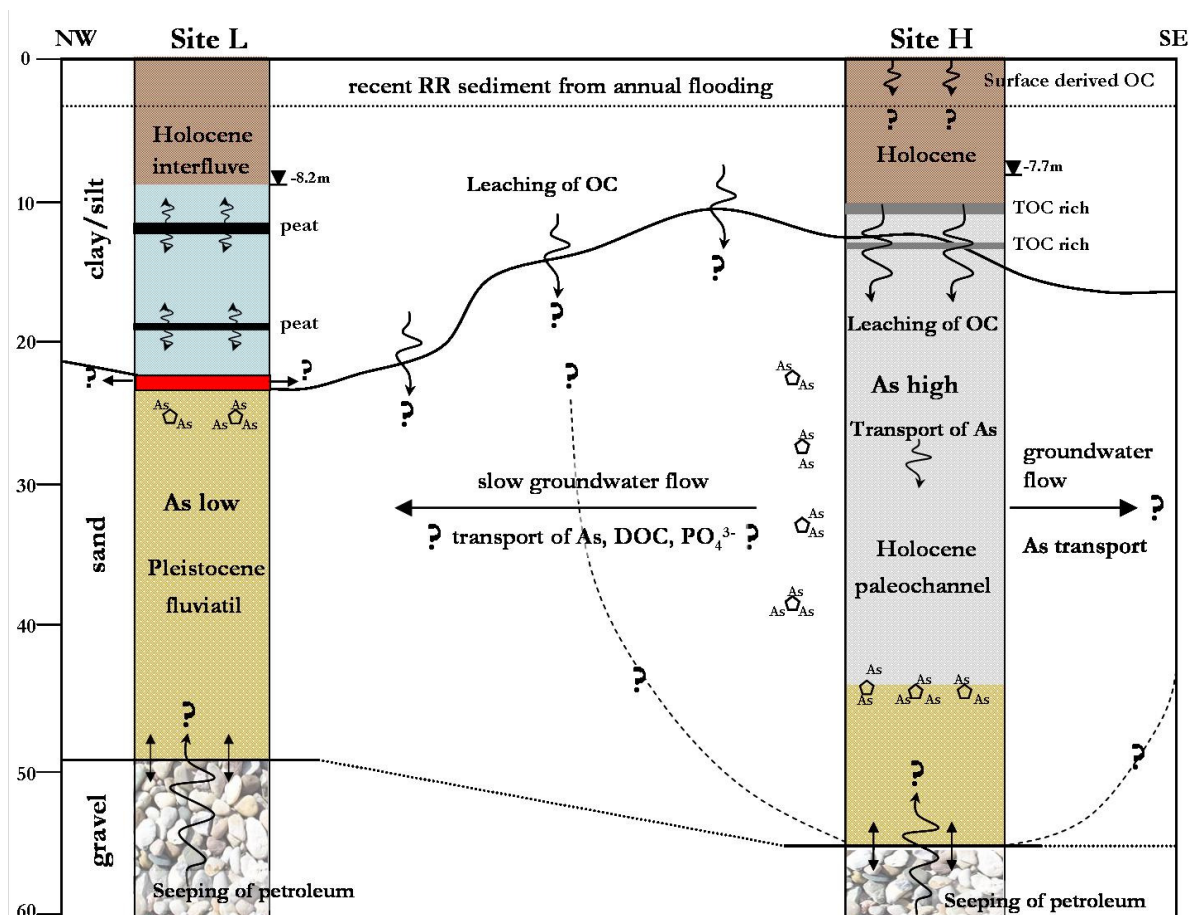


Fig. 8.2: Conceptual model for possible causes of the As distribution in Van Phuc based on the results from this thesis, on the transect measurements carried out by A. Van Geen (Lamont-Doherty Earth Observatory) and co-workers, and, previous studies in Van Phuc.

Indications for a downward transport of dissolved As at site H can be gained from the fact that highest As concentrations in the sediment occur at the transition from grey to brown sediments with high amounts of As in the adsorbed form. In this layer, Fe(III) bearing minerals are more dominant compared to the grey horizons, as shown by the reflectance measurement (Fig. 8.1), which have a higher adsorption capacity for As compared to Fe(II) dominated minerals. Therefore, downward percolating dissolved As could

be scavenged which would cause an enrichment of As in this layer (Fig. 8.2). It can be assumed that the whole reduction front is developing further downwards over time, but it might also be possible that an upwardly directed influence from the gravel layer maintains the redox front constant as discussed later.

The situation seems to be different at site L with regard to additional input of OC. Peat layers, very high in TOC, occur in the aquitard of site L (Fig. 8.2). The reducing power, emanating from these layers, does only seem to have a very local influence leading, on the one hand, to the dissolution and transformation of Fe(III) oxy-hydroxides ($\Delta R < 0.5$) and, on the other hand, to the adsorption of previously released As to the remaining Fe minerals (Fig. 8.1, Chapt. 5.3) in the aquitard. Percolation is sufficiently hindered due to the low grain size and the presence of an Fe concretion so that a considerable infiltration of electron donors into the aquifer, evoking strongly reducing conditions, does not appear to be of importance (Fig. 8.2). There are indications that dissolved As and Fe released in the upper aquitard might slowly move downwards. Dissolved Fe, for example, might have or still is precipitating at the transition from the reducing aquitard to the more oxidizing aquifer forming an Fe concretion ($\text{Fe}_2\text{O}_3 > 33 \text{ wt-}\%$). Dissolved and solid Fe concentrations further down are relatively low so no further migration is assumable. Dissolved As, on the other hand, could infiltrate into the aquifer despite the sealing property of the aquitard and the Fe concretion. This conclusion could be drawn from the fact that in the layer just below the Fe concretion, bulk As concentration are extremely high and mainly present in the adsorbed form (Chapt. 5.3). Therefore, this layer is supposed to be a barrier for downwards migrating As (Fig. 8.2). However, whether these processes are still active or mainly occurred in the past remains unclear.

The lowest part of the aquifer at both sites seems to be influenced by the fluctuation of the water table in the Pleistocene gravel aquifer as indicated in Fig. 8.2. The groundwater in the gravel aquifer, which is more oxidizing and controlled by a more regional flow could be pushed frequently into the overlying sandy aquifer during rainy season when the water table in the RR is much higher (up to 9 m) preventing the lower part of the sandy sediment at site H from considerable reduction. With regard to OM it can be summa-

rized that differences in the OM reactivity and availability could reasonably explain the differences in As release between the two sites which raises the question why these OM reactivity and availability are different. For both aspects the depositional environment appears to be a plausible explanation.

The aquifer at site L is of Pleistocene age, probably from paleofluviatil origin and dominated by a terrestrial signal (Tab. 6.3). Either marine OM, which is more easily degradable (HOLLERBACH, 1985; KILLOPS & KILLOPS, 1997), has preferentially been decomposed compared to land plant derived OM during the older sediment history or the OM source was more terrestrial from the beginning causing the currently lower reactivity. The aquitard of site L can be interpreted as paleointerfluvial deposit, which incorporates considerable amounts of highly reactive OM but does not have an influence on the lower aquifer as discussed above. This assumption is in accordance to MCARTHUR ET AL. (2008) who stated that areas beneath paleointerfluvial deposits are As free due to protection from downward migrating As and OM by paleosols formed after the last glacial maximum. Paleosols itself were not detected in Van Phuc perhaps because substantial changes occurred due to reducing conditions in the aquitard (Fig. 8.2) but some equivalents are proven to occur in the RRD (TANABE ET AL., 2003B; FUNABIKI ET AL., 2007). In contrast, there is strong evidence that the area around site H was part of a paleochannel system (Chapt. 6.4.1) in the Holocene, filled up with fluvial material bringing in a more reactive mixture of marine and terrestrial OM. The aquifer itself is not protected against infiltration of OM or dissolved As from more shallow organic rich layers by an impermeable layer at site H. Consequently, Fe oxy-hydroxide reduction is promoted releasing As into the aquifer. Probably only the upper two meter at both sites consists of recent fine material deposited by the RR during annual flooding and might prevent infiltration of surface derived OC (Fig. 8.2). SENGUPTA ET AL. (2004) also concluded from their study that the patchy distribution of dissolved As is correlated with the depositional environment in deltas; high As provinces preferentially occur in paleochannel systems.

The assumption that the area around site H might be stamped by the occurrence of a paleochannel is further supported by the distribution of dissolved As in a transect between the two sites recorded by A. van Geen and

co-workers (Lamont-Doherty Earth Observatory of Columbia University (LDEO)) with a needle sampler device (for more details about needle sampler see: VAN GEEN ET AL., 2006C). High dissolved As concentrations occur like

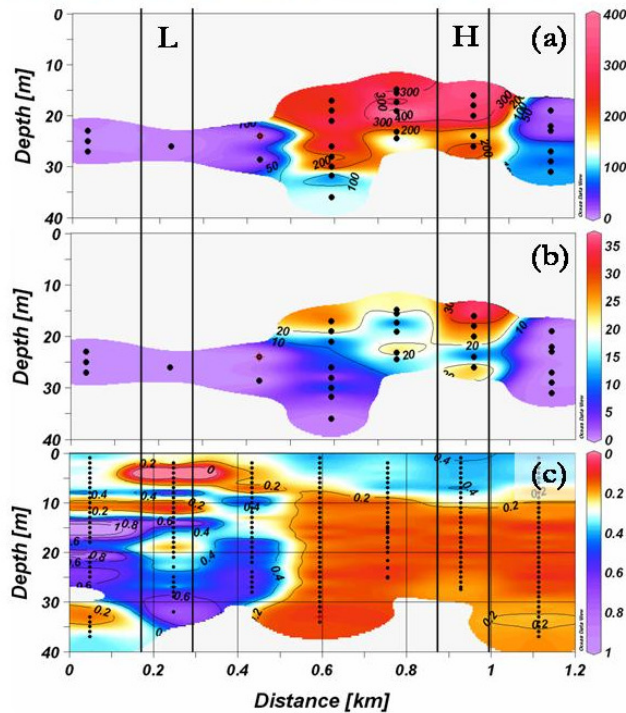


Fig. 8.3: Lateral distribution of dissolved As (a) and Fe^{2+} (b) concentrations as well as ΔR values of the sediment material (c) in Van Phuc measured along a transect which is indicated by a white line in the satellite image above (figures provided by courtesy of L. van Geen). ΔR values < 0.5 are indicative of high amounts of Fe(II) bearing minerals (HORNEMAN ET AL., 2004). The white area in the upper part of the figures results from the presence of clay from which no water samples could be obtained.

a pillow around site H and might, therefore, outline the extension of the paleo-channel (Fig. 8.3). The exact dimensions of such a paleo-channel are not known so far.

Fig. 8.3 also highlights the likely importance of an additional source of electron donors from above because both dissolved As and Fe have their highest concentration mainly in the upper part of the whole proposed paleo-channel. The exact position of the transition zone between high and low dissolved As concentrations, which is probably identical with the transition from Holocene to Pleistocene deposits between the two sites, is not known so far (Fig. 8.2) but indications can be gained from Fig. 8.3.

It is also unclear if the reducing front and, concurrently, the high As concentration is spreading over

the years. The paleointerfluvial might protect the aquifer of site L from horizontal influence due to reduction of hydraulic conductivity but lateral migration of dissolved As, DOC or even PO_4^{3-} , which might compete with As for sorption sites, is conceivable (Fig. 8.2). There are indications for a slow groundwater movement from site H towards site L due to differences in their hydraulic heads (Fig. 8.2) and in the groundwater age (site L: <55a; site H: 15 to >55a; Fig. 8.1) (FREI, 2006). Arsenic and other groundwater constituents, however, would migrate on a much slower scale towards site L compared to the water itself due to interactions with sediment particles like Fe oxy-hydroxides, which can considerably retard them (Fig. 8.2). MCARTHUR ET AL. (2008), for example, calculated that As only moves 0.2 to 1 m/yr due to sorption processes compared to a groundwater velocity of 30 m/yr at their study site. With the current data set it remains unclear if and in what time-frame site L might become polluted by lateral influence from the paleochannel area. No information also exists on the groundwater movement in southeasterly direction (Fig. 8.2). Concentrations of both dissolved As and Fe are currently low in this part but the results of reflectance measurements indicate a low redox state of the sediment ($\Delta R < 0.3$, Fig. 8.3). An extension of the As problem in this direction is, consequently, assumable and demands for frequent monitoring.

9 CONCLUSIONS

The studied distribution of dissolved As concentrations in aquifers of Van Phuc demonstrated that its patchy distribution is caused by a combination of special hydrological, sedimentological and geochemical features. The reducing conditions, which evoke differences in the partitioning of As between solid phase and solution and the redox state of Fe oxy-hydroxides, are the main difference between high and low As areas not only in Van Phuc but also in other affected delta regions (e.g. BGS & DPHE, 2001; SMEDLEY & KINNIBURG, 2002). This study has clearly shown that it is not only important to identify all relevant triggers for the onset of reducing conditions but also the range of their impact in order to delineate the patchy distribution of dissolved As concentrations in groundwater worldwide.

Important for the capacity of sediments to induce reducing conditions is the reactivity of OM along with its accessibility. The better availability of more reactive OM seems to trigger more strongly reducing conditions, which is accompanied by high As concentrations. The composition of OM (terrestrial or marine) and its bioavailability both seem to largely be influenced by the depositional environment of the sediment. Organic rich layers are often present within deposits of low grain size. The thickness and hydraulic conductivity of these layers determines its influence on surrounding aquifers with regard to redox conditions and the As release. This study has shown that spacious aquitards even though they are rich in reactive OM can protect underlying aquifers from infiltration of As or reactive OC and, therefore, prevent high dissolved As concentrations. Within delta environments paleointerfluves seem to be of importance because they mainly consist of material with low hydraulic conductivity preventing vertical migration.

The patchy distribution of dissolved As concentrations in deltas throughout the world, therefore, mainly depends on the lithology, which determines the hydrogeology and the composition of OM. In order to identify areas low in As for drilling of "save" wells it will be important to local-

ize layers rich in OM in a first step and determine its reactivity. In a second step the hydraulic properties of these layers have to be estimated in order to approximate their influence on the surrounding aquifers. In this context, the localization of paleointerfluvial and paleochannel structures would be helpful to distinguish low from high dissolved As regions.

OUTLOOK

This study provides some answers with regard to the fixation of As within mineral grains and the spatial distribution of dissolved As in Van Phuc. However, many questions still remain. In future, more has to be known about a possible lateral migration of dissolved As and reactive OC and the time frame this might occur. Where exactly is the border between Pleistocene and Holocene aquifer between the two sites and can the redox front cross this border? For that reason, it would be helpful to take further samples between the two sites and analyse them with regard to OM reactivity and availability as well as partitioning of As. Furthermore, geophysical methods could help to get a spatial impression about the underlying sediment and perhaps help to identify paleochannel structures. A detailed hydrological modelling of the groundwater flow which is of importance for the distribution of dissolved As and the supply of reactive OC is currently carried out at the LDEO.

For a better understanding of the fixation of As and to know more about As bearing phases, mineral identification of minerals by means of μ S-XRD or determination of the binding form and speciation of As by means of μ S-XAS analysis should be carried out. For a better overview and quantification of the processes involved during sequential extraction, it should be attempted to carry out extraction steps subsequently on the same grains and analyse the changes in elemental distribution after each step.

In future, it would be of important to verify if it is possible to delineate low from high As regions by localizing paleointerfluvial and paleochannel structures in addition to the determination of the reactivity and availability of OM in other As affected areas or if further steps are necessary.

ABBREVIATIONS

ACL	Average chain length	LDEO	Lamont Doherty Earth Observatory
ANKA	Ångströmquelle Karlsruhe	LFe	Leaching step which dissolves Fe oxy-hydroxides and carbonates
cal. BP	Calibrated years before present	LOD	Limit of detection
CAO	Chemoautotrophic arsenite oxidizers	LP	Phosphate leaching
CPI	Carbon preference index	MeOH	Methanol
CSA	Carbon sulphur analyser	MMA	Mono-methyl arsonic acid
CWA	Carbon water analyser	MS	Mass-spectrometry
DARP	Dissimilatory arsenate reducing prokaryotes	μS	Micro synchrotron
DCB	Dithionite-citrate-bicarbonate	NFL	Neutral lipid fraction
DCM	Dichlormethane	NGO	Non governmental organisation
DIRB	Dissimilatory iron reducing bacteria	NOM	Natural organic matter
DMA	Di-methyl arsenic acid	OC	Organic carbon
DOC	Dissolved organic carbon	OM	Organic matter
DOM	Dissolved organic matter	RRD	Red River Delta
EAWAG	Eidgenössische Anstalt für Wasserversorgung, Abwasserreinigung und Gewässerschutz	SEM	Scanning electron microscopy
EDTA	Ethylenediaminetetraacetic acid	SI	Saturation index
EDX	Energy dispersive XRF	SSA	Specific surface area
FLUO	Fluorescence	TIC	Total inorganic carbon
GC	Gas chromatography	TLF	Total lipid fraction
GIS	Geoinformation system	TMA	Tri-methyl arsine oxide
GW	Groundwater	TN	Total nitrogen
H	Site, high in dissolved arsenic	TOC	Total organic carbon
HAO	Heterotrophic arsenite oxidizers	TS	Total sulphur
HMW	High molecular weight n-alkane	AUS	Upper aquifer system
HR	High resolution	UCM	Unresolved Complex Mixture
ICP	Inductively-coupled-plasma	UNICEF	United Nations International Children's Emergency Fund
L	Site, low in dissolved arsenic	WDX	Wavelength dispersive XRF
LAS	Lower aquifer system	XAS	X-ray absorption spectroscopy
		XRD	X-ray diffraction analysis
		XRF	X-ray fluorescence analysis
		Yr	Year

LIST OF FIGURES

Fig. 2.1: Global distribution of known As affected regions in 2001, divided into As affected aquifers, geothermal groundwaters and some major mining related As problems (BGS & DPHE, 2001). In the meantime more areas suffering from natural As problems have been detected (see text).	9
Fig. 2.3: Effects of biotic and abiotic processes on the release of As. Fe(III) and As(V) can be microbially reduced using OC as electron donor, releasing Fe(II) and As(III) into the solution. Re-adsorption, competition and precipitation of secondary mineral phases can influence the As mobility (HERBEL & FENDORF, 2006).	17
Fig. 2.4: Speciation of As(V) and As(III) as a function of pH in a 0.01M NaCl medium at 25°C (SMEDLEY & KINNIBURG, 2002, modified).....	22
Fig. 2.5: Model for the reduction of Fe(III) through electron shuttling by humic substances (LOVLEY, 1996, modified). Fe reducing bacteria can use OC in order to transform already oxidized humic substances back into a reduced state. Each humic molecule can be re-oxidized several times.....	27
Fig. 2.6: Products of OM degradation in confining clay layers, rich in OC, can leach or diffuse into the aquifer fuelling redox reactions, here illustrated by the example of Fe(III) reduction (LOVLEY & CHAPELLE, 1995, modified).	28
Fig. 2.7: Model for OM degradation pathways and possible products in sedimentary environments in which Fe(III) reduction is predominating (LOVLEY, 2001, modified).....	29
Fig. 2.8: Gas chromatograms of crude oil. Visible are the changes from non-biodegraded to heavy biodegraded oil which is indicated by the presence of UCM (PETERS ET AL., 2005, modified).	34
Fig. 3.1: Generalized geological map of the Red River delta and the surrounding monotonous area (MATHERS ET AL., 1996).	42
Fig. 3.2: Distribution of lower (LAS) and upper (UAS) aquifer system in two transects through the city of Ha Noi. Included are the different hydraulic heads of the water table of each aquifer (AUTENRIETH, 2005, modified).	45
Fig. 3.3: Map depicting the study sites in Van Phuc village situated some 10 km south of the centre of Ha Noi city (modified map from BERG ET AL., 2007). Arsenic in groundwater shows a patchy distribution in this village. Site L (low) has particularly low levels of dissolved arsenic ($3 \pm 2 \mu\text{g/L}$), whereas site H (high) features very high arsenic concentrations ($400 \pm 135 \mu\text{g/L}$). The two sites are 700 m apart from each other. The satellite image was taken from google-earth (earth.google.com).....	46
Fig. 5.1: Depth distribution (left) of the nine multi-level wells at site L (green) and H (red). To protect the wells from infiltration of surface water, they were sealed with a concrete pad and a metal cap (right) (picture: M. Berg).	59

Fig. 5.2: Lithological logs of the boreholes drilled in April 2006 at (a) site L and (b) site H. Each site was equipped with a nest of nine monitoring wells. The labelling on the left side of each log marks the samples taken for sequential extraction procedure.....	65
Fig. 5.3: Depth profiles of grain size distribution in cumulative percentage of clay (<2 μm), silt (<63 μm), sand (>63 μm) and gravel (>2 mm), reflectance (ΔR at 520 nm) and concentration of arsenic, iron and total organic carbon (TOC) in the sediment at site L (3a) and site H (3b).	66
Fig. 5.5: Depth profile of dissolved arsenic, iron, manganese, dissolved organic carbon (DOC), total phosphorous, hydrogen carbonate, ammonium and total sulphur (zero values: below detection limit of 5 mg/L) analysed in the groundwater from site L (closed symbols) and site H (open symbols).	68
Fig. 6.2: Depth distribution of $\delta^{15}\text{N}$ values and C/N ratios as well as total organic carbon (TOC) and total nitrogen (TN) concentration at site L (a) and site H (b).	84
Fig. 6.3: Abundance of C_{21} to C_{36} n alkanes in dried sediments of site L (a)/(c) and site H (b)/(d).	87
Fig. 6.4: Depth distribution of $\delta^{13}\text{C}$ ratios and macroscopic indicators for the depositional environment in the silty part of site L acquired from visual sediment description.	88
Fig. 6.5: Bivariate plots of $\delta^{13}\text{C}$ and $\delta^{15}\text{N}$ signatures delineating the sources of organic matter. Typical values for marine and terrestrial origin for $\delta^{13}\text{C}$ and $\delta^{15}\text{N}$ signatures were taken from literature (FRY & SHERR, 1984; WASER ET AL., 1998). In the case of $\delta^{15}\text{N}$ values, the dominance field was confined to a narrow range, which could be expanded with decreasing importance in both directions. The striped rectangle symbolizes the area where both signatures indicate marine origin whereas terrestrial origin is indicated by both signatures in the gridded area.....	89
Fig. 7.1: Different habitus of surface precipitates: (a) triangular form consisting of Fe oxy-hydroxide or/and carbonate, (b) knob shaped Fe phases completely covering the surface, (c) elongated (rice grain) habitus consisting of Fe oxy-hydroxides, only scattered on the surface, (d) precipitates of Ti oxides and Fe carbonates. Strong weathering is visible on Al silicates at site L (e) and site H (f). In (e) Fe precipitates are visible, occasionally.....	104
Fig. 7.2: Microscopic image and distribution of As, Fe and Si (not quantified) in a coated grain of the As rich sample of site H (H3515).	105
Fig. 7.3: Microscopic image and distribution of Si (not quantified), Fe, As and K in grains from different untreated samples (L17045 (a/d), H3515 (b), H2910 (c)) from both cores. (a) to (c) show coated grains with high (a + b) and low (c) As concentrations. In (d) the elemental distribution of a mafic mineral is illustrated.	106
Fig. 7.4: Microscopic image and distribution of Si (not quantified), Fe, As and K in different coatings measured after leaching samples from both cores (L17045LP (a), H3515LP (b), H3305LP (c)) with 0.5 M Na-phosphate solution. Arsenic concentrations are still high after the leaching in (a) and (b), whereas in (c), As concentrations are mainly below detection limit.	108

Fig. 7.5: Microscopic image and distribution of Si (not quantified), As, Fe and K of selected grains (L17045LFe (a), H2020 LFe (b), H3515 LFe (c), L2640 LFe (d)) measured after the dissolution of Fe oxy-hydroxides and carbonates. In (a) relatively high As concentrations remain, whereas in (b) and (c) the concentrations are mainly below detection limit of 1 mg/kg. In mafic minerals (d) very high As concentrations are present even after dissolution of Fe bearing oxy-hydroxides.	110
Fig. 7.6: Results of a factor analysis (factor loadings and factor scores) carried out on a data set collected along a transect through a grain of the As rich sample of site L (L17045). Ti was excluded from the analysis due to its low communality. The corresponding elemental distribution is shown in Fig. 7.3a.	112
Fig. 7.7: Results of a factor analysis (factor loadings and factor scores) carried out on a data set collected along a transect through a grain in the sample with low quartz content of site H (H3305). The corresponding elemental distribution is given in Tab. A-19.	112
Fig. 7.8: Results of a factor analysis (factor loadings and factor scores) carried out on a dataset collected along a transect through a mafic grain in the As rich sample of site L (A17045). Si, Ca, Ti, V and Cu are excluded due to their low communalities. The corresponding elemental distribution is shown Fig. 7.3d.	113
Fig. 7.9: Microscopic image and distribution of As, Fe and Si (not quantified) in a coated grain of sample L17045LP after leaching with 0.5 M Na-phosphate solution.	114
Fig. 7.10: Results of a factor analysis (factor loadings and factor scores) based on data recorded from the mapping of a grain of the As rich sample of site L after phosphate leaching (L17045LP). Silicon and Ca are excluded due to their low communalities. The corresponding elemental distribution is shown in Fig. 7.9.	115
Fig. 7.11: Results of a factor analysis (factor loadings and factor scores) carried out on a dataset collected along a transect through a grain of the sample with low quartz content after phosphate leaching (H3305LP). The corresponding elemental distributions are shown in Fig. 7.4c.	115
Fig. 7.12: Results of a factor analysis (factor loadings and factor scores) carried out on a dataset collected along a transect through a grain of the As rich sample of site H after phosphate leaching (H3515LP). Copper was excluded from factor analysis due to its low communality. The corresponding elemental distributions are shown in Fig. 7.4b.	116
Fig. 7.13: Results of a factor analysis (factor loadings and factor scores) based on data recorded from a transect measurement through a grain of the mica rich sample (H2020LFe) after the dissolution of Fe oxy-hydroxides and carbonates. Arsenic, Cu and Ca were excluded from the analysis due to their low communalities. The corresponding elemental distributions are shown in Fig. 7.5b. ...	117
Fig. 7.14: Results of a factor analysis (factor loadings and factor scores) based on data recorded from a transect measurement through a grain of the As rich sample of site L (L17045Fe) after the dissolution of Fe oxy-hydroxides and carbonates. Silicon, Cu and Cr were excluded from the analysis due to their low communality. The corresponding elemental distributions are shown in Fig. 7.5a.	118

Fig. 7.15: Results of a factor analysis (factor loadings and factor scores) based on data recorded from a transect measurement through a mafic grain of the feldspar rich sample (L2640LFe) after the dissolution of Fe oxy-hydroxides and carbonates. Silicon and Cu were excluded from the analysis due to their low communality. The corresponding elemental distributions are shown in Fig. 7.5d.....	119
Fig. 8.1: Summary of the available results from sediment and groundwater analysis for site L and H in Van Phuc (GW = groundwater).	126
Fig. 8.2: Conceptual model for possible causes of the As distribution in Van Phuc based on the results from this thesis, on the transect measurements carried out by A. Van Geen (Lamont-Doherty Earth Observatory) and co-workers, and, previous studies in Van Phuc.....	128
Fig. 8.3: Lateral distribution of dissolved As (a) and Fe ²⁺ (b) concentrations as well as ΔR values of the sediment material (c) in Van Phuc measured along a transect which is indicated by a white line in the satellite image above (figures provided by courtesy of L. van Geen). ΔR values <0.5 are indicative of high amounts of Fe(II) bearing minerals (HORNEMAN ET AL., 2004). The white area in the upper part of the figures results from the presence of clay from which no water samples could be obtained.....	131

LIST OF TABLES

Tab. 2.3: Typical As concentrations of selected rocks, sediments and soils (BGS & DPHE, 2001, and references therein).	7
Tab. 2.4: Typical As concentrations in different water bodies (SMEDLEY & KINNIBURG, 2002, and references therein).	8
Tab. 2.5: As concentrations in different rock forming minerals.....	14
Tab. 2.6: Overview of different source indicators which allow differentiating between marine and terrestrial origin.	31
Tab. 5.1: Sequential extraction scheme used for the sediment leaching.	63
Tab. 5.2: Average partitioning of iron and arsenic in each fraction of the sequential extraction for all samples of site L and H.....	73
Tab. 6.1: Overview of the results of total organic carbon (TOC), total nitrogen (TN), $\delta^{13}\text{C}$ and $\delta^{15}\text{N}$ - isotopic signatures as well as calculated molar C/N ratios from selected samples at both sites and the Red River (n.d. = not determined).	84
Tab. 6.2: Total concentration of organic carbon (TOC), higher molecular weight (HMW) n-alkanes and indicative ratios calculated from the n-alkane distribution.	86
Tab. 6.3: Quantitative source estimation of OM in the sediments of site L and H. End member combinations were chosen as follows: (1) for C_3 plants as terrestrial source ($\delta^{13}\text{C}$): -20/-27, -20/-29, -22/-27, -22/-29‰; (2) for C_4 plants ($\delta^{13}\text{C}$): -20/-12, -20/-14, -22/-12, -22/-14‰ (only used for L10110). For each sample the mean value and standard deviation of all 4 possible end member combinations was calculated.	92
Tab. 7.2: Median concentrations of As and Fe as well as median Fe/As ratios calculated from the measurements of transects and discrete grains with $\mu\text{S-XRF}$ in the untreated samples, after leaching with 0.5 M Na-phosphate solution (LP) and after the dissolution of Fe oxy-hydroxides and carbonates (LFe). Included is also the number of measured grains in each sample.....	107

REFERENCES

- Aeckersberg et al., 1991** Aeckersberg, F., Bak, D., Widdel, f., 1991. Anaerobic oxidation of saturated hydrocarbons to CO₂ by a new type of sulfate reducing bacterium. *Archives of Microbiology* 156, 5-14.
- Agusa et al., 2006** Agusa, T., Kunito, T., Fujihara, J., Kubota, R., Minh, T.B., Trang, P.T.K., Iwata, H., Subramanin, A., Viet, O.H., Tanabe, S., 2006. Contamination by arsenic and other trace elements in tube-well water and its risk assessment to humans in Hanoi, Vietnam. *Environ. Poll.* 139, 95-106.
- Ahmann et al., 1994** Ahmann, D., Roberts, A.L., Krumholz, L.R., Morel, F.M.M., 1994. Microbe grows by reducing arsenic. *Nature*. 371, 750.
- Ahmed et al., 2004** Ahmed, K.L., Bhattacharya, P., Hasan, M.A., Akhter, S.H., Alam, S.M.M., Bhuyion, M.A.H., Imam, M.B., Khan, A.A., Sracek, O., 2004. Arsenic enrichment in groundwater of the alluvial aquifers in Bangladesh: an overview. *Appl. Geochem.* 19, 181-200.
- Ahmed, 2005** Ahmed, K.M., 2005. Management of the groundwater arsenic disaster in Bangladesh. In: Bundschuh, J., Bhattacharya, P., Chandrasekharam, D., (ed.) 2005. *Natural Arsenic in Groundwater: Occurrence, Remediation and Management*. S.283-296. A.A. Balkema Publishers. Leiden London New York.
- Ahmed et al., 2007** Ahmed, S., Sayed, M.H.S., Khan, M.H., Karim, M.N., Haque, M.A., Bhuiyan, M.S.A., Rahman, M.S., Faruquee, M.H., 2007. Sociocultural aspects of arsenicosis in Bangladesh: Community perspective. *Journal of Environmental Science and Health, Part A*, 42, 1945-1958.
- Ahuja, 2008** Ahuja, S., 2008. *Arsenic contamination of groundwater – Mechanism, Analysis, and Remediation*. Wiley & Sons.
- Anawar et al., 2002** Anawar, H.M., Komaki, K., Akai, J., Takada, J., Ishizuka, T., Takahashi, T., Yoshioka, Y., Kato, K., 2002. Diagenetic control on arsenic partitioning in sediments of the Meghna River delta, Bangladesh. *Environ. Geol.* 41, 816-825.
- Anawar et al., 2004** Anawar, H.M., Akai, J., Sakugawa, H., 2004. Mobilization of arsenic from subsurface sediments by effect of bicarbonate ions in groundwater. *Chemosphere* 54, 753-762.
- Anderson et al., 1981** Anderson, D.W., Saggar, S., Bettany, J.R., Stewart, J.W.B., 1981. Particle size fractions and their use in studies of soil organic matter: The nature and distribution of forms of carbon, nitrogen and sulfur. *Soil Sci. Soc. Am. J.* 45, 767-772.

- Andrews et al., 1998 Andrews, J.E., Greenaway, A.M., Dennis, P.F., 1998. Combined Carbon Isotope and C/N Ratios as Indicators of Source and Fate of Organic Matter in a Poorly Flushed, Tropical Estuary: Hunts Bay, Kingston Harbour, Jamaica. *Estuarine, Coastal and Shelf Science* 46, 743-756.
- Apello et al., 2002 Apello, C.A.J., Van der Weiden, M.J.J., Tournassat, C., Charlet, L., 2002. Surface complexation of ferrous iron and carbonate on ferrihydrite and the mobilization of arsenic. *Environ. Sci. Technol.* 36, 3096-3103.
- Arnosti & Holmer, 2003 Arnosti, C., Holmer, M., 2003. Carbon cycling in a continental margin sediment: contrasts between organic matter characteristics and remineralization rates and pathways. *Estuar. Coast. Shelf Sci.* 58, 197-208.
- Autenrieth, 2005 Autenrieth, M., 2005. Groundwater of Hanoi (Vietnam) – The groundwater system in the upper Red River Delta assessed using noble gases and hydrogeochemistry. Masters thesis. Department of Environmental Sciences. ETH Zürich.
- Azcue et al., 1995 Azcue, J.M., Murdoch, A., Rosa, F., Hall, G.E.M., Jackson, T.A., Reynoldson, T., 1995. Trace elements in water, sediments, pore-water, and biota polluted by tailings from an abandoned gold mine in British Columbia, Canada. *J. Geochem.* 52, 25-34.
- Balaji et al., 2000 Balaji, S., Gosh, B., Das, M.C., Gangopadhyay, A.K., Singh, K., Lal, S., Das, A., Chatterjee, S.K., Banerjee, N.N. 2000. Removal Kinetics of Arsenic from Aqueous Media on Modified Alumina. *Indian Journal of Chemical Technology* 7, 30-34.
- Bang et al., 2005 Bang, S., Patel, M., Lippincott, L., Meng, X., 2005. Removal of arsenic from groundwater by granular titanium dioxide adsorbent. *Chemosphere* 60, 389-397.
- Bauer & Blodau, 2006 Bauer, M., Blodau, C., 2006. Mobilization of arsenic by dissolved organic matter from iron oxides, soils and sediments. *Sci. Tot. Environ.* 354, 179-190.
- Bauer & Onishi, 1969 Bauer, W.O., Onishi, B.M.H., 1969. Arsenic. In Wedepohl, K.H. (ed). *Handbook of Geochemistry*. Springer, Berlin.
- Benson & Spencer, 1983 Benson, L.V., Spencer, R.J., 1983. Hydrochemical Reconnaissance Study of the Walter River Basin, California and Nevada. USGS Open File Rep. Denver, pp 83-740.
- Berg et al., 2001 Berg, M., Tran, H.C., Nguyen, T.C., Pham, H.V., Schertenleib, R., Giger, W., 2001. Arsenic contamination of groundwater and drinking water in Vietnam: A human health threat. *Environ. Sci. Technol.* 35, 2621-2626.
- Berg et al., 2006 Berg, M., Luzi, S., Trang, P.T.K., Viet, P.H., Giger, W., Stüben D., 2006. Arsenic removal from groundwater by household sand filters - comparative field study, model calculations, and health benefits. *Environ. Sci. Technol.* 40, 5567-5573.

- Berg et al., 2007** Berg, M., Stengel, C., Trang, P.T.K., Viet, P.H., Sampson, M.L., Leng, M., Samreth, S., Fredericks, D., 2007. Magnitude of Arsenic Pollution in the Mekong and Red River Deltas – Cambodia and Vietnam. *Sci. Total Environ.* 372, 413-425.
- Berg et al., 2008** Berg, M., Trang, P.T.K., Stengel, C., Buschmann, J., Viet, P.H., Giger, W., Stüben, D., 2008. Hydrological and sedimentary controls leading to arsenic contamination of groundwater in the Hanoi area, Vietnam: the impact of iron-arsenic ratios, peat, river bank deposits, and excessive groundwater abstraction. *Chem. Geol.* 249, 91-112.
- Beyer, 1964** Beyer, W., (1964). Zur Bestimmung der Wasserdurchlässigkeit von Kiesen und Sanden aus der Kornverteilungskurve. *Wasserwirtschaft-Wassertechnik* 14, 165-168.
- BGS & DPHE, 2001** BGS, DPHE, 2001. Arsenic contamination of groundwater in Bangladesh. In: Kinniburgh, D.G., Smedley, P.L. (Eds.), Vol. 2, Final Report, BGS Technical Report WC/00/19. British Geological Survey, Keyworth, U.K.
- Bhattacharya et al., 2003** Bhattacharya, R., Jana, J., Nath, B., Sahu, S.J., Chatterjee, D., Jacks, G., 2003. Groundwater As mobilization in the Bengal Delta Plain, the use of ferralite as a possible remedial measure - a case study. *Appl. Geochem.* 18, 1435-1451.
- Bhattacharya et al., 1997** Bhattacharya, P., Chatterjee, D., Jacks, G., 1997. Occurrence of arsenic contaminated groundwater in alluvial aquifers from Delta Plains, Eastern India: options for safe drinking water supply. *Water Resour. Dev.* 13, 79-92.
- Boldrin et al., 2005** Boldrin, A., Langone, L., Miserocchi, S., Turchetto, M., Acri, F., 2005. Po River plume on the Adriatic continental shelf: Dispersion and sedimentation of dissolved and suspended matter during different river discharge rates. *Marine Geology* 222-223, 135-158.
- Bortz, 2005** Bortz, J., 2005. *Statistik für Human- und Sozialwissenschaftler*. Springer, Berlin.
- Boyle & Jonasson, 1973** Boyle, R.W., Jonasson, I.R., 1973. The geochemistry of As and its use as an indicator element in geochemical prospecting. *J. Geochem. Explorer* 2, 251-296.
- Brannon & Patrick, 1987** Brannon, J.M., Patrick W.H., 1987. Fixation, transformation and mobilization of arsenic in sediments. *Environ. Sci. Technol.* 21, 450-459.
- Bray & Evans, 1961** Bray, E.E., Evans, E.D., 1961. Distribution of n-paraffins as a clue to recognition of sources beds. *Geochim. Cosmochim. Acta* 22, 2-15.
- Brewster, 1994** Brewster, M.D., 1994. Removing arsenic from contaminated water. *Water Environ. Techn.* 4, 54-57.

- Brooks & Smith, 1967** Brooks, J.D., Smith, J.W., 1967. The diagenesis of plant lipids during the formation of coal, petroleum and natural gas, I. Changes in the n-parafin hydrocarbons. *Geochim. Cosmochim. Acta* 31, 2389-2397.
- Bukau et al., 2000** Bukau, G., Artinger, R., Geyer, S., Wolf, M., Fritz, P., Kim, J.I., 2000. Groundwater in-situ generation of aquatic humic and fulvic acids and the mineralization of sedimentary organic carbon. *Appl. Geochem.* 15. 819-832.
- Buschmann et al., 2007** Buschmann, J., Berg, M., Stengel, C., Sampson M.L., 2007. Arsenic and manganese contamination of drinking water resources in Cambodia: coincidence of risk areas with low relief topography. *Environ. Sci. Technol.* 41, 2146-2152.
- Buschmann et al., 2008** Buschmann, J., Berg, M., Stengel, C., Winkel, L., Sampson, M.L., Trang, P.T.K., Viet, P.H., 2008. Contamination of drinking water resources in the Mekong delta floodplains: Arsenic and other trace metals pose serious health risks to population. *Environ. Int.* 34, 756-764.
- Calvert, 2004** Calvert, S.E., 2004. Beware Intercepts: interpreting compositional ratios in multi-component sediments and sedimentary rocks. *Org. Geochem.* 35, 981-987.
- Canfield, 1994** Canfield, D.E., 1994. Factors influencing organic carbon preservation in marine sediments. *Chem. Geol.* 114, 315-329.
- Cat et al., 2006** Cat, L.V., Joa, T.K., Lam, L.V., Ha, H.T.N., Hanh, P.T., Proeter, J., 2006. Arsenic removal from groundwater. Proceedings to national workshop on "Arsenic contamination in groundwater in Red River plain", 99-107.
- Challenger, 1945** Challenger, F., 1945. Biological methylation. *Chem. Rev.* 36, 315-362.
- Chapelle & Bradley, 1996** Chapelle, F.H., Bradley, P.B., 1996. Microbial acetogenesis as a source of organic acids in ancient Atlantic Coastal Plain sediments. *Geology* 24, 925-928.
- Charlet & Polya, 2006** Charlet, L., Polya, D.A., 2006. Arsenic in Shallow, Reducing Groundwaters in Southern Asia: An Environmental Health Disaster. *Elements* 2, 91-96.
- Charlet et al., 2007** Charlet, L., Chakraborty, S., Apello, C.A.J., Romen-Ross, G., Nath, B., Ansari, A.A., Lanson, M., Chatterjee, D., Basu Malik, S., 2007. Chemodynamics of an arsenic "hotspot" in a West Bengal aquifer: A field and reactive transport modelling study. *Appl. Geochem.* 22, 1273-1292.
- Cheng et al., 2004** Cheng, Z.Q., van Geen, A., Jing, C.Y., Seddique, A., Ahmed, K.M., 2004. Performance of Household-Level Arsenic Removal System During 4-month Deployments in Bangladesh. *Environ. Sci. Technol.* 38, 3442-3448.

- Cherry et al., 1979** Cherry, J.A., Shaikh, A.U., Tallman, D.E., Nicholson, R.V., 1979. Arsenic species as an indicator of redox conditions in ground-water. *J. Hydrol.* 43, 373-392.
- Chieu et al., 2006** Chieu, L.V., Duy, V.N., Ha, C.T., Tam, V.T.T., Mien, T.T., Berg, M., von Gunten, U., 2006. Application of kinetic study on arsenic-oxidation for improving arsenic removal in existing water plants in Hanoi. Proceedings to national workshop on "Arsenic contamination in groundwater in Red River plain", 108-113.
- Choong et al., 2007** Choong T.S.Y., Chuah, T.G., Robiah, Y., Gregory Koay, F.L., Azni, I., 2007. Arsenic toxicity, health hazards and removal techniques from water: an overview. *Desalination* 217, 139-166.
- Chowdhury et al., 1999** Chowdhury, T.R., Basu, G.K., Mandal, B.K., Biswas, B.K., Samanta, G., Chowdhury, U.K., Chanda, C.R., Lodh, D., Roy, S.L., Saha, K.C., Roy, S., Kabir, S., Quamruzzaman, Q., Chakraborti, D., 1999. Arsenic poisoning in the Ganges Delta. *Nature* 401, 545-546.
- Coker et al., 2006** Coker, V.S.; Gault, A.G.; Pearce, C.I.; van der Laan, G.; Telling, N.D.; Charnock, J.M.; Polya, D.A.; Lloyd, J.R, 2006. XAS and XMCD evidence for species-dependent partitioning of arsenic during microbial reduction of ferrihydrite to magnetite. *Environ. Sci. Technol.* 40, 7745-7750.
- Collins et al., 1995** Collins, M.J., Bishop, A.N., Farrimond, P., 1995. Sorption by mineral surfaces: Rebirth of the classical condensation pathway for kerogen formation? *Geochim. Cosmochim. Acta* 59, 2387-2391.
- Colombo et al., 1996** Colombo, J.C., Silverberg, N., Gearing, J.N., 1996. Biogeochemistry of organic matter in the Laurentian Trough, II. Bulk composition of the sediments and relative reactivity of major components during early diagenesis. *Mar. Geochem.* 51, 295-314.
- Cowie et al., 1992** Cowie, G.L., Hedges, J.I., Calvert, S.E., 1992. Sources and relative reactivities of amino acids, neutral sugars, and lignin in an intermittently anoxic marine environment. *Geochim. Cosmochim. Acta* 56, 1963-1978.
- Cowie & Hedges, 1994** Cowie, G.L., Hedges, J.I., 1994. Biochemical indicators of diagenetic alteration in natural organic matter mixtures. *Nature* 369, 304-307.
- Cranwell, 1982** Cranwell, P.A., 1982. Lipids of aquatic sediments and sedimenting particulates. *Progress in Lipid Research* 21, 271-308.
- Creelius, 1975** Creelius, E.A., 1975. The geochemical cycle of arsenic in Lake Washington and its relation to other elements. *Limnol. Oceanog.* 22, 441-451.
- Cullen & Reimer, 1989** Cullen, W.R., Reimer, K.J., 1989. Arsenic Speciation in the Environment. *Chemical Reviews* 89, 713-764.

- Cummings et al., 1999 Cummings, D.E., Caccavo, F., Fendorf, S., Rosenzweig, R.F., 1999. Arsenic mobilization by the dissimilatory Fe(III)-reducing bacterium *Shewanella alga* BrY. *Environ. Sci. Technol.* 33, 723-729.
- Dan & Ha, 2006 Dan, N.V., Ha, N.T., 2006. Distribution of arsenic level in qp aquifer in Red River Delta Plain. Proceedings to national workshop on "Arsenic contamination in groundwater in Red River plain", 32-36.
- Das et al., 1996 Das, D., Samanta, G., Mandal, B.K., Chowdhury, T.R., Chanda, C.R., Chowdhury, P.P., Basu, G.K., Chakraborti, D., 1996. Arsenic in groundwater in six districts of West-Bengal, India. *Environmental Geochemistry and Health* 18, 5-15.
- Del Razo et al., 1990 Del Razo, L.M., Arellano, M.A., Cebrián, M.E., 1990. The oxidation states of arsenic in well-water from a chronic arsenicism area of northern Mexico. *Environ. Pollut.* 64, 143-153.
- Dixit & Hering, 2003 Dixit, S., Hering, J.G., 2003. Comparison of Arsenic(V) and Arsenic(III) sorption onto iron oxide minerals: implications for arsenic mobility. *Environ. Sci. Technol.* 37, 4182-4189.
- Dixit & Hering, 2006 Dixit, S., Hering, J.G., 2006. Sorption of Fe(II) and As(III) on goethite in single- and dual-sorbate systems. *Chem. Geol.* 228, 6-15.
- Dowling et al., 2002 Dowling, C.B., Poreda, R.J., Basu, A.R., Peters, S.L., Aggarwal, P.K., 2002. Geochemical study of arsenic release mechanisms in the Bengal Basin groundwater. *Water Resour. Res.* 38, 1173.
- Driehaus et al., 1995 Driehaus, W., Seith, R., Jekel, M., 1995. Oxidation of Arsenate(III) with Manganese Oxides in Water-Treatment. *Water Research* 29, 297-305.
- Driehaus, 2005 Driehaus, W., 2005. Technologies for arsenic removal from portable water. In: Bundschuh, J., Bhattacharya, P., Chandrasekharan, D., (eds.) 2005. *Natural Arsenic in Groundwater: Occurrence, Remediation and Management*. S.133-144. A.A. Balkema Publishers. Leiden London New York.
- Dzombak & Morel, 1990 Dzombak, D.A., Morel, F.M.M., 1990. *Surface Complexation Modelling - Hydrous Ferric Oxide*. John Wiley. New York.
- Eary & Schramke, 1990 Eary, L.E., Schramke, J.A., 1990. Rates of inorganic oxidation reactions involving dissolved oxygen. In: Melchior, D.C., Bassett, R.L., (eds.). *Chemical modeling in aqueous systems II*. Vol. Am. Chem. Soc. Symp. Series 416, 379-396.
- Eglinton & Hamilton, 1963 Eglinton, G., Hamilton, R.J., 1963. The distribution of n-alkanes. In: Swain, T. (Ed.). *Chemical plant taxonomy*. Academic press, pp. 187-217.
- Ehrenreich et al., 2000 Ehrenreich, P., Behrends, A., Harder, J., Widdel, F., 2000. Anaerobic oxidation of alkanes by newly isolated denitrifying bacteria. *Archives of Microbiology* 173, 58-64.

- Ellis & Mahon, 1977 Ellis, A.J., Mahon, W.A.J., 1977. Chemistry and Geothermal Systems. Academic Press. New York.
- Ferguson & Gavis, 1972 Ferguson, J.F., Gavis, J., 1972. A review of the arsenic cycle in natural water. *Water Res.* 6, 1259-1274.
- Fergusson, 1990 Fergusson, J.E., 1990. The Heavy Elements: Chemistry, Environmental Impact and Health Effects. Pergamon Press. Great Britain
- Forqurean et al., 1997 Forqurean, J.W., Moore, T.O., Fry, B., Hollibaugh, J.T. 1997. Spatial and temporal variation in C:N:P ratios, $\delta^{15}\text{N}$ and $\delta^{13}\text{C}$ of eelgrass *Zostera marina* as indicators of ecosystem processes, Tomales bay, California, USA. *Marine Ecology-Progress Series* 147-157.
- Fredrickson et al., 1998 Fredrickson, J.K., Zchara, J.M., Kennedy, D.W., Don, H., Onstott, T.C., Hinman, N.W., Li, S.-M., 1998. Biogenic iron mineralization accompanying the dissimilatory reduction of hydrous ferric oxide by a groundwater bacterium. *Geochim. Cosmochim. Acta* 32, 3239-3257.
- Frei, 2006 Frei, F., 2006. Groundwater Dynamics and Arsenic Mobilization near Hanoi (Vietnam) Assessed Using Noble Gases and Tritium. Diploma thesis. Department of Environmental Sciences. ETH Zürich.
- Fry & Sherr, 1984 Fry, B., Sherr, E.B., 1984. $\delta^{13}\text{C}$ measurements as indicators of carbon flow in marine and freshwater ecosystems. *Contributions in Marine Science* 27, 13-47.
- Fuchs & Schlegel, 2007 Fuchs, G., Schlegel, H.-G., 2007. Allgemeine Mikrobiologie. 8. Auflage. Thieme Verlag Stuttgart, pp. 308-312.
- Funabiki et al., 2007 Funabiki, A., Haruyama, S., Quy, N.V., Hai, P.V., Thai, D.H., 2007. Holocene delta plain development in the Song Hong (Red River) delta, Vietnam. *Journal of Asian Earth Sciences* 30, 518-529.
- Gault et al., 2005 Gault, A.G., Islam, F.S., Polya, D.A., Charnock, J.M., Boothman, C., Chatterjee, D., Lloyed, J.R., 2005. Microcosm depth profiles of arsenic release in a shallow aquifer, West Bengal. *Mineralogical Magazine* 69, 855-863.
- Giger et al., 1980 Giger, W., Schaffner, C., Wakeham, S.G., 1980. Aliphatic and olefinic hydrocarbons in recent sediment of Greinfensee, Switzerland. *Geochim. Cosmochim. Acta* 44, 119-129.
- Goldberg & Glaubig, 1988 Goldberg, S., Glaubig, R.A., 1988. Anion sorption on a calcareous, montmorillonitic soil – arsenic. *Soil Sci. Soc. Am. J.* 52, 1297-1300.
- Goldsmith et al., 1972 Goldsmith, J.R., Deane, M., Thom, J., Gentry, G., 1972. Evaluation of elevated arsenic in well waters. *Water Res.* 6, 1133-1136.

- Gough & Rowland, 1990 Gough, M.A., Rowland, S.J., 1990. Characterization of unresolved complex mixtures of hydrocarbons in petroleum. *Nature* 344, 648-650.
- Grafe et al., 2001 Grafe, M., Eich, M.J., Grossl, P.R., Saunders, A.M., 2001. Adsorption of As(V) and As(III) on goethite in presence and absence of dissolved organic carbon. *Soil Sci. Soc. Amer. J.* 65, 1680-1687.
- Guo et al., 2007 Guo, H., Stüben, D., Berner, Z., 2007. Removal of arsenic from aqueous solution by natural siderite and hematite. *Appl. Geochem.* 22, 1039-1051.
- Harmelin-Vivien et al., 2008 Harmelin-Vivien, M., Loizeau, V., Mellon, C., Beker, B., Arlhac, D., Bodiguel, X., Ferraton, F., Hermand, R., Phillipon, X., Salen-Picard, C., 2008. Comparison of C and N stable isotope ratios between surface particulate organic Matter and microphytoplankton in the Gulf of Lions (NW Mediterranean). *Continental Shelf Research* 28, 1911-1919.
- Hartog et al., 2004 Hartog, N., Van Bergen, P.F., De Leeuw, J.W., Griffioen, J., 2004. Reactivity of organic matter in aquifer sediment: geological and geochemical controls. *Geochim. Cosmochim. Acta.* 68, 1281-1292.
- Harvey et al., 2002 Harvey, C.F., Swartz, C.H., Badruzzaman, A.B.M., Keon-Blute, N., Yu, W., Ashraf Ali, M., Jay, J., Beckie, R., Niedan, V., Brabander, D., Oates, P.M., Ashfaq, K.N., Islam, S., Hemond, H.F., Ahmed, M.F., 2002. Arsenic mobility and groundwater extraction in Bangladesh. *Science* 298, 1602-1606.
- Harvey et al., 2006 Harvey, C.H., Ashfaq, K.N., Yu, W., Badruzzaman, A.B.M., Ali, M.A., Oates, P.M., Micheal, H.A., Neumann, R.B., Beckie, R., Islam, S., Ahmed, M.F., 2006. Groundwater dynamics and arsenic contamination in Bangladesh. *Chemical Geol.* 228, 112-136.
- Hassan, 2005 Hassan, M.M., 2005. Arsenic poisoning in Bangladesh: spatial mitigation planning with GIS and public participation. *Health Policy* 74, 247-260.
- Hayes, 1993 Hayes, J.M., 1993. Factors controlling ^{13}C content of sedimentary organic compounds: Principles and evidence. *Mar. Geol.* 113, 111-125.
- Hedges et al., 1986 Hedges, J.I., Clark, W.A., Quay, P.D., Richey, J.E., Devol, A.H., Santos, U.D., 1986. Composition and fluxes of particulate organic material in Amazon River. *Limnol. Oceanogr.* 31, 717-738.
- Herbel & Fendorf, 2006 Herbel, M., Fendorf, S., 2006. Biogeochemical processes controlling the speciation and transport of arsenic within iron coated sands. *Chem. Geol.* 228, 16-32.
- Hering & Kneebone, 2002 Hering, J., Kneebone, P.E., 2002. Biogeochemical controls on arsenic occurrence and mobility in water supplies. In: Frankenberg, W. (ed.), 2002. *Environmental Chemistry of Arsenic*. Dekker, New York, p. 155-181.

- Hirner et al., 2000 Hirner, A.V., Rehage, H., Sulkowski, M., 2000. Umweltgeochemie. Herkunft, Mobilität und Analyse von Schadstoffen in der Pedosphäre. Steinkopf. Darmstadt.
- Hoefs, 1987 Hoefs, J., 1987. Stable isotope geochemistry. Springer. Berlin, Heidelberg, New York. pp. 52-54.
- Hollerbach, 1985 Hollerbach, A., 1985. Grundlagen der organischen Geochemie. Springer Verlag. Berlin Heidelberg New York Tokyo.
- Horneman et al., 2004 Horneman, A., Van Geen, A., Kent, D.V., Mathe, P.E., Zheng, Y., Dhar, R.K., O'Connell, S.O., Hoque, M.A., Aziz, Z., Shamsudduha, M., Seddique, A.A., Ahmed, K.M., 2004. Decoupling of As and Fe release to Bangladesh groundwater under reducing conditions. Part I: Evidence from sediment profiles. *Geochim. Cosmochim. Acta.* 68, 3459-3473.
- Hu et al., 2006 Hu, J., Peng, P., Jia, G., Mai, B., Zhang, G., 2006. Distribution and sources of organic carbon, nitrogen and their isotopes in sediments of the subtropical Pear River estuary and adjacent shelf, Southern China. *Marine Chemistry* 98, 274-285.
- Hudson-Edwards et al., 2004 Hudson-Edwards, K.A., Houghton, S.L., Osborn, A., 2004. Extraction and analysis of arsenic in soils and sediments. *Trends Anal. Chem.* 23, 745-752.
- Hutchinson, 1887 Hutchinson, J., 1887. Arsenic cancer. *British Medical Journal* 2, 1280-1281.
- Islam et al., 2004 Islam, F.S., Gault, A.G., Boothman, C., Polya, D.A., Charnock, J.M., Chatterjee, D., Lloyd, J.R., 2004. Role of metal-reducing bacteria in arsenic release from Bengal delta sediments. *Nature.* 430, 68-71.
- Islam et al., 2005 Islam, F.S., Pederick, R.L., Gault, A.G., Adams, L.K., Polya, D.A., Charnock, J.M., Lloyd, J.R., 2005. Interactions between Fe(III)-Reducing Bacterium *Geobacter sulfurreducens* and Arsenate, and Capture of the Metalloid by Biogenic Fe(II). *Applied And Environmental Microbiology* 71, 8642-8648.
- Islam et al., 2007 Islam, F.S., Lawson, M., Lythgoe, P.R., Wogelius, R.A., Thinnpan, V., Lloyd, J.R., Charnock, J.M., Polya, D.A., 2007. Adsorption of As(III) and As(V) onto vivianite – Evaluation as a sink for arsenic in Bengali aquifers. *Geochim. Cosmochim. Acta*, 71, A432.
- Jaffé et al., 2001 Jaffé, R., Mead, R., Hernandez, M.E., Peralba, M.C., DiGuida, O.A., 2001. Origin and transport of sedimentary organic matter in two subtropical estuaries: a comparative, biomarker-based study. *Org. Geochem.* 32, 507-526.
- Jain & Ali, 2000 Jain, C.K., Ali, I., 2000. Arsenic: Occurrence, toxicity and speciation techniques. *Wat. Res.* 34, 4304-4312.
- Jain & Loeppert, 2000 Jain, A., Loeppert, R.H., 2000. Effect of competing anions on the adsorption of arsenate and arsenite by ferrihydrite. *J. Environ.*

- Qual. 29, 1422-1430.
- Jakariya & Bhattacharya, 2007** Jakariya, MD., Bhattacharya, P., 2007. Use of GIS in local level participatory planning for arsenic mitigation: A case study from Matlab Upazila, Bangladesh. *Journal of Environmental Science and Health, Part A*, 42, 1933-1944.
- Jasper & Gagosian, 1989** Jasper, J.P., Gagosian, R.B., Glacial-interglacial climatically forced delta ¹³C variations in sedimentary organic matter. *Nature* 342, 60-62.
- Jeckel, 1994** Jeckel, M.R., 1994. Removal of arsenic in drinking water treatment. In: Nriagu, J.O. (ed.), 1994. *Arsenic in the environment. Part I: Cycling and characterization*. Wiley. New York.
- Jochum et al., 2000** Jochum, K. P., Dingwell, D.B., Rocholl, A., Stoll, B., Hofmann, A. W., and 31 others, 2000. The preparation and preliminary characterisation of eight geological MPI-DING reference glasses for In-Situ microanalysis, *Geostand. Newslet.* 24, 87133.
- Kabir & Howard, 2007** Kabir, A., Howard, G., 2007. Sustainability of arsenic mitigation in Bangladesh: Results of functionality survey. *International Journal of Environmental Health Research* 17, 207-218.
- Kapaj et al., 2006** Kapaj, S., Peterson, H., Libar, K., Bhattacharya, P., 2006. Human health effects from chronic arsenic poisoning - A review. *Journal of Environmental Science and Health, Part A* 41, 2399-2428.
- Kartinen & Martin, 1995** Kartinen, E.O., Martin, C.J., 1995. An overview of arsenic removal processes. *Desalination* 103, 78-88.
- Keil et al., 1994** Keil, R.G., Tsamakis, E., Fuh, C.B., Giddings, J.C., Hedges, J.I., 1994. Mineralogical and textural controls on the organic composition of coastal marine Sediments: Hydrodynamic separation using SPLITT-fraction. *Geochim. Cosmochim. Acta* 58, 879-893.
- Kennedy et al., 2004** Kennedy, H., Gacia, E., Kennedy D.O., Papadimitriou, S., Duarte, C.M., 2004. Organic carbon sources to SE Asian coastal sediments. *Estuarine, Coastal and Shelf Science* 60, 59-68.
- Kennicutt et al., 1987** Kennicutt, M.C., Barker, C., Brooks, J.M., DeFreitas, D.A., Zhu, G.H., 1987. Selected organic matter source indicators in Orinoco, Nile and Changjiang deltas. *Organ. Geochem.* 11, 41-51.
- Keon et al., 2001** Keon, N.E., Swartz, C.H., Brabander, D.J., Harvey, C., Hemond, H.F., 2001. Validation of an arsenic sequential extraction method for evaluating mobility in sediments. *Environ. Sci. Technol.* 35, 2778-2784.
- Killops & Killops, 1997** Killops, S.D., Killops, V.J., 1997. *Einführung in die organische Geochemie*. Enke Verlag Stuttgart.
- Kim et al., 2000** Kim, M., Nriagu, J., Haack, S., 2000. Carbonate ions and arsenic dissolution by groundwater. *Environ. Sci. Technol.* 34, 3094-3100.
- Kocar et al., 2006** Kocar, B.D., Herbel, M.J., Tufano, K.J., Fendorf, S., 2006. Contrasting effects of dissimilatory iron(III) and arsenic(V) on arsenic retention and transport. *Environ. Sci. Technol.* 40, 6715-6721.
- Korte & Fernando, 1991** Korte, M.S., Fernando, Q., 1991. A review of Arsenic(III) in

- 1991 Groundwater. *Crit. Rev. Environ. Contr.* 21, 1-39.
- Kvenvolden, 1966** Dvenvolden, K.A., 1966. Evidence for transformation of normal fatty acids in sediments. In: Hobson, G.D. (Ed.). *Advances in Organic Geochemistry*. Pp. 335-366.
- Larsen et al., 2008** Larsen, F., Pham, N.Q., Dang, N.D., Postma, D., Jessen, S., Pham, V.H., Nguyen, T.B., Trieu, H.D., Nguyen, H., Chambon, J., Nguyen, H.V., Ha, D.H., Hue, N.T., Duc, M.T., 2008. Controlling geological and hydrogeological processes in an arsenic contaminated aquifer on the Red River flood plain, Vietnam. *Appl. Geochem.* 23, 3099-3115.
- Laverman et al., 1995** Laverman, A.M., Blum, J.S., Schaefer, J.K., Phillips, E.J.P., Lovely, D.R., Oremland, R.S., 1995. Growth of strain SES-3 with arsenate and other diverse electron acceptors. *Appl. Environ. Microbiol.* 61/10, 3556-3561.
- Lenoble et al., 2004** Lenoble, W., Laclautre, C., Serpaud, B., Deluchat, V., Bollinger, J.C., 2004. As(V) retention and As(III) simultaneous oxidation and removal on MnO₂-loaded Polystyrene Resin. *Science of Total Environment* 326, 197-207.
- Li et al., 2006** Li, Z., Saito, Y., Matsumoto, E., Wang, Y., Tanabe, S., Vi, Q.L., 2006. Climate change and human impact on the Song Hong (Red River) Delta, Vietnam, during the Holocene. *Quaternary International* 144, 4-28.
- Lovley, 1992** Lovley, D.R., 1992. Microbial oxidation of organic matter coupled to the reduction of Fe(III) and Mn(IV)-oxides. *Catena supplement* 21, 101-114.
- Lovley & Chapelle, 1995** Lovley, D.R., Chapelle, F.H., 1995. Deep subsurface microbial processes. *Rev. of Geoph.* 33, 365-381.
- Lovley, 1996** Lovley, D.R., Coates, J.D., Blunt-Harris, E.L., Phillips, E.J.P., Woodward, J. C., 1996. Humic substances as electron acceptors for microbial respiration. *Nature.* 382, 1996.
- Lovley, 2001** Lovley, D.R., 2001. Reduction of iron and humics in subsurface environments. In: Frederickson, J.K., Fletcher, M., (eds.). *Subsurface microbiology and biogeochemistry*. Wiley & Sons. New York.
- Lowers et al., 2007** Lowers, H.A., Breit, G.N., Forster, A.L., Whitney, J., Yount, J., Uddin, M.N., Muneem. A.A., 2007. Arsenic incorporation into authigenic pyrite, Bengal Basin sediment, Bangladesh. *Geochim. Cosmochim. Acta* 71, 2699-2717.
- Luo et al., 1997** Luo, Z.D, Uhang, Y.M., Ma, L., Zhang, G.Y., He, X., Wilson, R., Byrd, D.M., Griffiths, J.G., Lai, S., He, L., Grumski, K., Lamm, S.H., 1997. Chronic arsenicism and cancer in Inner Mongolia - consequences of well-water arsenic levels greater than 50 µg/L. In: Abernathy, C.O., Calderon, R.L., Chapell, W.L. (eds.). *Arsenic exposure and health effects*. Chapman Hall. London, pp. 55-68.
- Luzi et al., 2004** Luzi, S., Berg, M., Trang, P.T.K., Viet, P.H., Schertenleib, R.,

2004. Household Sand-Filters for Arsenic Removal - An option to mitigate arsenic from iron-rich groundwater. Swiss Federal Institute for Environmental Science and Technology (EAWAG).
- Macur et al., 2001** Macur, R.E., Wheeler, J.T., McDermott, T.R., Inskip, W.P., 2001. Microbial populations associated with the reduction and enhanced mobilization of arsenic in mine tailings. *Environ. Sci. Technol.* 35, 3676-3682.
- Maksymowska et al., 2000** Maksymowska, D., Rechar, P., Piekarek-Jankowska, H., Riera, P., 2000. Chemical and isotopic composition of organic matter sources in the Gulf of Gdansk (Southern Baltic Sea). *Estuarine, Coastal and Shelf Science* 51, 585-598.
- Mandal & Suzuki, 2002** Mandal, B.K., Suzuki, K.T., 2002. Arsenic around the world: a review. *Talanta* 58, 201-235.
- Manning et al., 1998** Manning, B.A., Fendorf, S.E., Goldberg, S., 1998. Surface structure and stability of As(III) on Goethite: spectroscopic evidence for inner-sphere complexes. *Environ. Sci. Technol.* 32, 2383-2388.
- Martinotti et al., 1997** Martinotti, W., Camusso, M., Guzzi, L., Patrolecco, L., Pettine, M., 1997. C, N and their stable isotopes in suspended and sedimented matter from the Po Estuary (Italy). *Water Air and Soil Pollution* 99, 325-332.
- Masscheleyn et al., 1991** Masscheleyn, P.H., DeLaune, R.D., Patrick, W.H., 1991. Effect of redox potential and pH on arsenic speciation and solubility in a contaminated soil. *Environ. Sci. Technol.* 25, 1414-1419.
- Mathers et al., 1996** Mathers, S., Davies, J., McDonald, A., Zalasiewicz, J., Marsh, S., 1996. The Red River delta of Vietnam: A demonstration of the applicability of sedimentology to the investigation of unconsolidated sedimentary aquifers. BGS Technical Report, WC/96/02. British Geological Survey. Keyworth. UK.
- Mathers & Zalasiewicz, 1999** Mathers, S., Zalasiewicz, J., 1999. Holocene sedimentary architecture of the Red River Delta, Vietnam. *J. Coastal Res.* 15, 314-325.
- Matschullat, 1999** Matschullat, J., 1999. Arsenic in der Geosphere. Arsenic in the Geosphere. *Schriftenreihe der Deutschen Geologischen Gesellschaft* 6, 5-20.
- Mayer, 1994** Mayer, L.M., 1994. Surface area control of organic carbon accumulation in continental shelf sediments. *Geochim. Cosmochim. Acta* 58, 1271-1284.
- McArthur et al., 2001** McArthur, J.M., Ravenscroft, P., Safiulla, S., Thirlwall, M.F., 2001. Arsenic in groundwater: Testing pollution mechanisms for sedimentary aquifers in Bangladesh. *Water Resources Research* 37, 109-117.
- McArthur et al., 2004** McArthur, J.M., Banerjee, D.M., Hudson-Edwards, K.A., Mishra, R., Purohit, R., Ravenscroft, P., Cronin, A., Howarth, R.J., Chatterjee, A., Talukder, T., Lowry, D., Houghton, S., Chadha, D.K., 2004. Natural organic matter in sedimentary basins and its rela-

- tion to arsenic in anoxic ground water: the examples of West Bengal and its worldwide implications. *Appl. Geochem.* 19, 1255-1293.
- McArthur et al., 2008** McArthur, J.M., Ravenscroft, P., Banerjee, d.M., Milsom, J., Hudson-Ewards, K.A., Sengupta, S., Bristow, C., Sarkar, A., Tonkin, S., Purohit, R., 2008. How paleosols influence groundwater flow and arsenic pollution: A model from the Bengal Basin and its worldwide implication. *Water Resources Research* 44, W11411.
- McMahon, 2001** McMahon, P.B., 2001. Aquifer/aquitard interfaces: mixing zones that enhance biogeochemical reactions. *Hydrog. J.* 9, 34-43.
- Mead, 2005** Mead, M.N., 2005. Arsenic: in search of an Antidote to a Global Poison. *Environ Health Perspect.* 113, A378-86.
- Meharg et al., 2006** Meharg, A.A., Scrimgeour, C., Hossain, S.A., Ruller, K., Cruickshank, K, Williams, P.N., Kinniburgh, D.G., 2006. Codeposition of organic carbon and arsenic in Bengal Delta Aquifers. *Environ. Sci. Technol.* 40, 4928-4935.
- Meng et al., 2000** Meng, X., Bang, S., Korfiatis, G.P., 2000. Effects of silicate, sulfate and carbonate on arsenic removal by ferric chloride. *Wat. Res.* 34, 1255-1261.
- Meng et al., 2001** Meng, X., Korfiatis, G.P., Jing, C., Christodoulatos, C., 2001. Redox transformations of arsenic and iron in water treatment sludge during aging and TCLP extraction. *Environ. Sci. Technol.* 35, 3476-3481.
- Meyers & Benson, 1988** Meyers, P.A., Benson, L.V., 1988. Sedimentary Biomarker and Isotopic Indicators of the Paleoclimatic History of the Walter Lake Basin, Western Nevada. *Org. Geochem.* 13, 807-813.
- Meyers & Eadie, 1993** Meyers, P.A., Eadie, J., 1993. Sources, degradation and recycling of organic matter associated with sinking particles in Lake Michigan. *Organic Geochemistry* 20, 47-56.
- Meyers, 1994** Meyers, P.A., 1994. Preservation of elemental and isotopic source identification of sedimentary organic matter. *Chem. Geol.* 114, 289-302.
- Meyers, 1997** Meyers, P.A., 1997. Organic geochemical proxies of paleoceanographic, paleolimnologic, and paleoclimatic processes. *Org. Geochem.* 27, 213-250.
- Milton et al., 2007** Milton, A.H., Smith, W., Dear, K., Ng, J., Sim, M., Ranmuthugala, G., Lokuge, K., Caldwell, B., Rahmann, A., Rahman, H., Shraim, A., Huang, D., Shahidullah, S.M., 2007. A randomised intervention trial to assess two arsenic mitigation options in Bangladesh. *Journal of Environmental Science and Health, Part A*, 42, 1897-1908.
- Misrocchi et al., 2007** Misrocchi, S., Langone, L., Tesi, T., 2007. Content and isotopic composition of organic carbon within a flood layer in the Po River prodelta (Adriatic Sea). *Continental Shelf Research* 27, 388-358.
- Mukhopadhyay et** Mukhopadhyay, R., Rosen, B.P., Phung, L.T., Silver, S., 2002. Mi-

- al., 2002 microbial arsenic: from geocycles to genes and enzymes. *Fems Microbiology Reviews* 26, 311-325.
- Müller & Voss, 1999 Müller, A., Voss, M., 1999. The paleoenvironments of coastal lagoons in the southern Baltic Sea: II $\delta^{13}\text{C}$ and $\delta^{15}\text{N}$ ratios of organic matter-sources and sediments. *Paleogeography, Paleoclimatology, Paleoecology* 135, 17-32.
- Nagy & Korom, 1983 Nagy, G., Korom, I., 1983. Late skin symptoms of arsenic poisoning observations in arsenic endemy at Bugag-Alsomonostor. *Z. Hautkr.* 58, 961-964.
- Nath et al., 2005 Nath, B., Berner, Z., Basu Malik, S., Chatterjee, D., Charlet, L., Stueben, D., 2005. Characterization of aquifers conducting groundwaters with low and high arsenic concentrations: a comparative case study from West Bengal, India. *Mineralogical Magazine* 69, 841-854.
- Ngoc et al., 2006 Ngoc, D.M., Hai, N.K., Hoa, N.Q., 2006. The adversed affects of arsenic contamination in groundwater to public health. *Proceedings to national workshop on "Arsenic contamination in groundwater in Red River plain"*, 74-80.
- Nhan et al., 2006 Nhan, D.D., Minh, D.A., Hoan, N.V., Thin, N.T.H., Lieu, D.T.B., Anh, V.T., Anh, N.T.L., 2006. Mobilization of arsenic in groundwater in the southern part of Hanoi city. *Proceedings to national workshop on "Arsenic contamination in groundwater in Red River plain"*, 37-46.
- NHEGD, 2002 NHEGD, 2002. Annual Report 2001, Northern Hydrogeological and Engineering Geological Division, Vietnam Geological Survey, Hanoi, Vietnam.
- Nickson et al., 2000 Nickson, R.T., McArthur, J.M., Ravenscroft, P., Burgess, W.G., Ahmed, K.M., 2000. Mechanisms of arsenic release to groundwater, Bangladesh and West Bengal. *Appl. Geochem.* 15, 403-413.
- Nicolli et al., 1989 Nicolli, H.B., Suriano, J.M., Peral., M.A.G., Ferpozzi, L.H., Baleani, O.A., 1989. Groundwater contamination with arsenic and other trace-elements in an area of the Pampa, province of Córdoba, Argentina. *Environ. Geol. Wat. Sci.* 14, 3-6.
- Norrman et al., 2008 Norrman, J., Sparrenbom, C.J., Berg, M., Nhan, D.D., Nhan, P.Q., Rosqvist, H., Cakcs, G., Sigvardsson, E., Baric, D., Moreskog, J., Harms-Ringdahl, P., Hoan, N.V., 2008. Arsenic mobilisation in a new well field for drinking water production along the Red River, Nam Du, Hanoi. *Appl. Geochem.* 23, 3127-3142.
- O'Day, 2006 O'Day, P.A., 2006. Chemistry and Mineralogy of Arsenic. *Elements* 2, 77-83.
- Oberacker et al., 2002 Oberacker, F., Maier, D., Maier, M., 2001. Arsenic and Drinking Water, Part 1 – A. Review of the Source, Distribution and Behaviour of Arsenic in the Environment. *Vom Wasser* 99, 79-110.

- Oremland et al., 2000
Oremland, R.S., Dowdle, P.R., Hoefft, S., Sharp, J.O., Schaefer, J.K., Miller, L.G., Blum, J.S., Smith, R.L., Bloom N.S., Wallschlaeger, D., 2000. Bacterial dissimilatory reduction of arsenate and sulfate in meromictic Mono Lake, California. *Geochim. Cosmochim. Acta.* 64, 3073-3084.
- Oremland & Stolz, 2003
Oremland, R.S., Stolz, J.F., 2003. The ecology of Arsenic. *Science* 300, 939-944.
- Oscarson et al., 1981
Oscarson, D.W., Huang, P.M., Defosse, D., Herbillion, A., 1981. Oxidative power of Mn(IV) and Fe(III) oxides with respect to As(III) in terrestrial and aquatic environments. *Nature* 291, 50-51.
- Ostrom et al., 1998
Ostrom, N.E., Knoke, K.E., Hedin, L.O., Robertson, G.P., Smucker, A.J.M., 1998. Temporal trends in nitrogen isotope values of nitrate leaching from an agricultural soil. *Chemical Geology* 146, 219-227.
- Pal et al., 2002
Pal, T., Mukherjee, P.K., Sengupte, S., 2002. Nature of arsenic pollutants in groundwater of Bengal Delta – A case study from Baruipur area, West Bengal, India. *Current Science* 82, 554-561.
- Parkhurst & Appello, 1999
Parkhurst, D.L., Appello, C.A., 1999. User's guide to PHREEQC (version 2) – A computer program for speciation, reaction-path, 1D-transport, and inverse geochemical calculations. U.S. Geol. Sur. Water Resour. Inv. Rep., 99-4259.
- Pedersen et al., 2006
Pedersen, H.D., Postma, D., Jakobsen, R., 2006. Release of arsenic associated with the reduction and transformation of iron oxides. *Geochim. Cosmochim. Acta.* 70, 4116-4129.
- Penrose, 1974
Penrose, W.R., 1974. Arsenic in the marine and aquatic environments. Analysis, occurrence and significance. *CRC Crit. Rev. Environ. Control.* 4, 465-482.
- Perdue & Koprivnjak, 2007
Perdue, E.M., Koprivnjak, J.-F., 2007. Using the C/N ratio to estimate terrigenous inputs of organic matter to aquatic environments. *Estuarine, Coastal and Shelf Science* 73, 65-72.
- Peters et al., 2005
Peters, K.E., Walters, C.C., Moldowan, J.M., 2005. *The Biomarker Guide – Volume 2. Biomarkers and Isotopes in Petroleum Exploration and Earth History.* Cambridge University Press.
- Peterson & Carpenter, 1983
Peterson, M.L., Carpenter, R., 1983. Biogeochemical processes affecting total arsenic and arsenic species distribution in an intermittently anoxic Fjord. *Mar. Chem.* 12, 295-321.
- Petrack et al., 2000
Petrack, J.S., Ayala-Fierro, F., Cullen, W.R., Carter, D.E., Aposhian, H.V., 2000. Monomethylarsonous acid (MMA(III)) is more toxic than arsenite in Chang human hepatocytes. *Toxicol. Appl. Pharmacol.* 163, 203-207.
- Petrusevski et al., 2008
Petrusevski, B., Sharma, S., van der Meer, W.G., Kruijs, F., Khan, M., Barua, M., Schippers, J.C., 2008. Four years of development and field-testing of IHE arsenic removal filter in rural Bangladesh. *Water, Science & Technology* 58, 53-58.

- Philip, 1985** Philip, R.P., 1985. Biological markers in fossil fuel production. *Mass Spectrom. Rev.* 4, 1-54.
- Pietrogrande et al., 2009** Pietrogrande, M.C., Mercuriali, M., Pasti, L., Dondi, F., 2009. Data handling of complex GC-MS chromatograms: characterization of n-alkane distribution as chemical marker in organic input source identification. *Analyst* 134, 671-680.
- Plant et al., 2005** Plant, J.A., Kinniburgh, D.G., Smedley, P.L., Fordyce, F.M., Klinck, B.A., 2005. Arsenic and Selenium. In: Lollar, B.S., 2005. *Treatise on Geochemistry. Volume 9 – Environmental Geochemistry.* Elsevier Amsterdam Heidelberg, p. 17-66.
- Polizzotto et al., 2006** Polizzotto, M.L., Harvey, C.F., Li, G., Badruzzman, B., Ali, A., Newville, M., Sutton, S., Fendorf, S., 2006. Solid-phases and desorption processes of arsenic within Bangladesh sediments. *Chem. Geol.* 228, 97-111.
- Polizzotto et al., 2008** Polizzotto, M.L., Kocar, B.D., Benner, S.G., Sampson, M., Fendorf, S., 2008. Near-surface wetland sediments as a source of arsenic release to ground water in Asia. *Nature* 454, 505-508.
- Polya et al., 2005** Polya, D.A., Gault, A.G., Diebe, N., Feldmann, P., Rosenboom, J.W., Gilligan, E., Fredericks, D., Milton, A.H., Sampson, M., Rowland, H.A.L., Lythgoe, P.R., Jones, J.C., Middleton, C., Cooke, D.A., 2005. Arsenic hazard in shallow Cambodian groundwaters. *Mineralogical Magazine* 69, 807-823.
- Postma, 1982** Postma, D., 1982. Pyrite and siderite formation in brackish and freshwater swamp sediments. *Amer. J. Sci.* 282, 1151-1183.
- Postma et al., 2007** Postma, D., Larsen, F., Hue, N.T.M., Duc, M.T., Viet, P.H., Nhan, P.Q., Jessen, S., 2007. Arsenic in groundwater of the Red River floodplain, Vietnam: controlling geochemical processes and reactive transport modelling. *Geochim. Cosmochim. Acta* 71, 5054-5071.
- Poynter et al., 1990** Poynter, J.G., Eglinton, G., 1990. Molecular composition of three sediments from hole 171C: The Bengal Fan. In: Cochran, J.R., Stow, D.A.V., et al., (eds.). *Proceedings of the Ocean Drilling Program Scientific Results. Vol 116*, pp. 155-161.
- Prahl et al., 1980** Prahl, F.G., Bennett, J.T., Carpenter, R., 1980. The early diagenesis of aliphatic hydrocarbons and organic matter in sedimentary particulates from Dabob Bay, Washington. *Geochim. Cosmochim. Acta* 44, 1967-1976.
- Puttemans & Massart, 1982** Puttemans, F., Massart, D.L., 1982. Solvent extraction procedures for the differential determination of arsenic (V) and arsenic (III) species by electrothermal atomic absorption spectrometry. *Anal. Chim. Acta* 141, 225-232.
- Quicksall et al., 2008** Quicksall, A.N., Bostick, B.C., Sampson, M.L., 2008. Linking organic matter deposition and iron mineral transformations to groundwater arsenic levels in the Mekong Delta, Cambodia. *Appl. Geochem.* 23, 3088-3098.

- Radloff et al., 2007** Radloff, K.A., Cheng, Z., Rahman, M.W., Ahmed, K.M., Mailoux, B.J., Juhl, A.R., Schlosser, P., Van Geen, A., 2007. Mobilization of arsenic during one-year incubations of grey aquifer sands from Araihasar, Bangladesh. *Environ. Sci. Technol.* 41, 3639-3645.
- Radu et al., 2005** Radu, T., Subacz, J., Phillippi, J.M., Barnett, M.O., 2005. Effects of dissolved carbonate on arsenic adsorption and mobility. *Environ. Sci. Technol.* 39, 7875-7882.
- Rangin et al., 1995** Ranging, C., Klein, M., Roques, D., LePichon, X., Trong, L.V., 1995. The Red River fault system in the Tonkin Gulf, Vietnam. *Tectonophysics* 243, 209-222.
- Ravenscroft et al., 2001** Ravenscroft, P., McArthur, J.M., Hoque, B.A., 2001. Geochemical and paeohydrological controls on pollution of groundwater by arsenic. In: Chappell, W., Abernathy, C.O., Calderon, R., (eds.). *Arsenic exposure and health effects IV*. Elsevier. Oxford, pp. 83-78.
- Redfield, 1942** Redfield, A.C., 1942. The processes determining the concentrations of oxygen, phosphate and other organic derivatives within the depth of the Atlantic Ocean. *Papers on Physical Oceanography and Meteorology* 9.
- Redman et al., 2002** Redman, A.D., Macalady, D.L., Ahmann, D., 2002. Natural organic matter affects arsenic speciation and sorption onto hematite. *Environ. Sci. Technol.* 36, 2889-2896.
- Reynolds et al., 1999** Reynolds, J.G., Naylor, D.V., Fendorf, S.E., 1999. Arsenic Sorption in Phosphate-Amended Soils during Flooding and Subsequent Aeration. *Soil Sci. Soc. Am. J.* 63, 1149-1156.
- Rieley, et al., 1991** Rieley, G., Collier, R.J., Jones, D.M., Eglinton, G., 1991. The biogeochemistry of Ellesmere Lake, UK-I: source correlation of leaf wax inputs to the sedimentary lipid record. *Organ. Geochem.* 17, 901-912.
- Robertson, 1989** Robertson, F.N., 1989. Arsenic in groundwater under oxidizing conditions, south-west United States. *Environmental Geochemistry and Health* 11, 171-176.
- Robinson et al., 1995** Robinson, B., Outred, H., Brooks, R., Kirkman, J., 1995. The distribution and fate of arsenic in Waikato River System, North Island, New Zealand. *Chem. Spec. Bioavail.* 7, 89-96.
- Rochette et al., 2000** Rochette, E.A., Bostick, B.C., Li, G.C., Fendorf, S., 2000. Kinetics of arsenate reduction by dissolved sulphide. *Environ. Sci. Technol.* 34, 4714-4720.
- Routh et al., 1999** Routh, J., McDonald, T.J., Grossman, E.L., 1999. Sedimentary organic matter sources and depositional environment in the Yegua formation (Brazos County, Texas). *Org. Geochem.* 30, 1437-1453.
- Rowland et al.,** Rowland, H.A.L., Polya, D.A., Lloyed, J.R., Pancost, R.D., 2006.

- 2006 Characterisation of organic matter in shallow, reducing, arsenic-rich aquifer, West Bengal. *Org. Geochem.* 37, 1101-1114.
- Rowland et al., 2007 Rowland, H.A.L., Pederick, R.L., Polya, D.A., Pancost, R.D., van Dongen, B.E., Gault, A.G., Vaughan, D.J., Bryant, C., Aderson, B., Lloyed, J.R., 2007. The control of organic matter on microbially mediated iron reduction and arsenic release in shallow alluvial aquifers, Cambodia. *Geobiology* 5, 281-292.
- Rowland et al. 2009 Rowland, H.A.L., Boothman, C., Pancost, R., Gault, A.G., Pola, D.A., Lloyed, J.R., 2009. The Role of indigenous microorganisms in the biodegradation of naturally occurring petroleum, the reduction of iron, and the mobilization of arsenite from West Bengal aquifer sediments. *J. Environ. Qual.* 38, 1598-1607.
- Saha et al., 1999 Saha, J.C., Dikshit, A.K., Bandyopadhyay, M., Saha, K.C., 1999. A review of arsenic poisoning and its effects on human health. *Crit. Rev. Environ. Sci. Technol.* 29, 281-313.
- Sarkar et al., 2008 Sarkar, S., Blaney, L.M., Gupta, A., Gosh, D., Sengupta, A.K., 2008. Arsenic Removal from Groundwater and Its Safe Containment in a Rural Environment: Validation of a Sustainable Approach. *Environ. Sci. Technol.* 42, 4268-4273.
- Saunders et al., 1997 Saunders, J.A., Pritchett, M.A., Cook, R.B., 1997. Geochemistry of biogenic pyrite and ferromanganese stream coatings: A bacterial connection? *Geomicrobiol. J.* 14, 203-217.
- Scholz & Neumann, 2007 Scholz, F., Neumann, T., 2007. Trace element diagenesis in pyrite-rich sediments of the Achterwasser lagoon, SW Baltic Sea. *Marine Chemistry* 107, 516-532.
- Schultz & Calder, 1976 Schultz, D., Calder, J.A., 1976. Organic carbon $^{13}\text{C}/^{12}\text{C}$ variations in estuarine sediments. *Geochim. Cosmochim. Acta* 40, 381-385.
- Schwedt & Rieckhoff, 1996 Schwedt, G., Rieckhoff, M., 1996. Analysis of oxothio arsenic species in soil and water. *J. Praktische Chemie* 388, 55-59.
- Schwertmann, 1991 Schwertmann, U., 1991. Solubility and dissolution of iron oxides. *Plant and Soil* 130, 1-25.
- Seddique et al., 2008 Seddique, A.A., Masuda, H., Mitamura, M., Shinoda, K., Ymanaka, T., Ita, T., Maruoka, T., Uesugi, K., Ahmed, K.M., Biswas, D.K., 2008. Arsenic release from biotite into a Holocene groundwater aquifer in Bangladesh. *Appl. Geochem.* 23, 2236-2248.
- Sengupta et al., 2004 Sengupta, S., Mukherjee, P-K., Pal, T., Shome, S., 2004. Nature and origin of arsenic carriers in shallow aquifer sediments of Bengal Delta, India. *Environ. Geology* 45, 1071-1081.
- Sham & Rivers, 2002 Sham, T.K., Rivers, M.L., 2002. A Brief Overview of Synchrotron Radiation. IN: Fenter, P.A., Rivers, M.L., Sturchio, N.C., Sutton, S.R. (eds.). *Applications of synchrotron radiation in low-temperature geochemistry and environmental science. Reviews in Mineralogy & Geochemistry* 49, 117-147.

- Shibasaki et al., 2007** Shibasaki, N., Lei, P., Kamata, A., 2007. Evaluation of deep groundwater development for arsenic mitigation in western Bangladesh. *Journal for Environmental Science and Health, Part A*, 42, 1919-1932.
- Singh & Plant, 2004** Singh, T.S., Plant, K.K., 2004. Equilibrium, Kinetics and Thermodynamic Studies for Adsorption of As(III) and Activated Alumina. *Separation and Purification Technology* 36, 139-147.
- Smedley & Kinniburgh, 2002** Smedley, P.L., Kinniburgh, D.G., 2002. A review of the source, behaviour and distribution of arsenic in natural waters. *Appl. Geochem.* 17, 517-568.
- Smedley et al., 1996** Smedley, P.L., Edmunds, W.M., Pelig-Ba, K.B., 1996. Mobility of arsenic in groundwater in the Obuasi area of Ghana. In: Appleton, J.D., Fuge, R., McCall, G.J.H. (eds.). *Environmental Geochemistry and Health*. Geol. Soc. Spec. Publ. 113. Geological Society. London, pp. 163-181.
- Smedley, 2005** Smedley, 2005. Arsenic Occurrence in Groundwater in South and East Asia – Scale, Causes and Mitigation (paper 1). In: *Towards a More Effective Operational Response – Arsenic Contamination of Groundwater in South and East Asian Countries*. World Bank Technical Report II.
- Smith et al, 1992** Smith, A.H., Hopenhayn-Rich, C., Bates, M.N., Goeden, H.M., Hertz-Picciotto, I., Duggan, H.M., Wood, R., Kosnett, M.J., Smith, M.T., 1992. Cancer risk from arsenic drinking water. *Env. Health Perspect.* 97, 259-267.
- Smith et al., 2000** Smith, A.H., Lingas, E.O., Rahman, M., 2000. Contamination of drinking water by arsenic in Bangladesh: a public health emergency. *Bull. World Health Org.* 78, 1093-1103.
- Smith et al., 2003** Smith, M.M.H., Hore, T., Chakraborty, P., Chakraborty, D.K., Savarimuthu, X., Smith, A.H., 2003. A Dugwell Program to Provide Arsenic-Safe Water in West Bengal, India: Preliminary Results. *Journal of Environmental Science and Health, Part A*, 38, 289-299.
- Snyder & Bish, 1989** Snyder, R.L., Bish, D.L., 1989. Quantitative analysis. In: Bish, D.L., Post, J.E. (Eds.), *Modern Powder Diffraction*. Reviews in Mineralogy 20. Mineralogical Society of America, pp. 101-144.
- Son & Hoa, 2006** Son, L.T., Hoa, N.Q., 2006. Arsenic mitigation activities in safe water supply in rural Vietnam. *Proceedings to national workshop on "Arsenic contamination in groundwater in Red River plain"*, 91-98.
- Stauder et al., 2005** Stauder, S., Raue, B., Sacher, F., 2005. Thioarsenates in Sulfidic Waters. *Environ. Sci. Technol.* 39, 5933-5939.
- Stollenwerk et al., 2007** Stollenwerk, K.G., Breit G.N., Welch A.H., Yount, J.C., Whitney, J.W., Foster, A.L., Uddin, M.N., Majumder, R.K., Ahmed, N., 2007. Arsenic attenuation by oxidized aquifer sediments in Bangladesh. *Science of the Total Environment* 379, 133-150.

- Stoyan et al., 1997** Stoyan, D., Stoyan, H., Jansen, U., 1997. Umweltstatistik - Statistische Verarbeitung und Analyse von von Umweltdaten. Teubner, Stuttgart, Leipzig.
- Stollenwerk, 2003** Stollenwerk, K.G. (2003). Geochemical processes controlling transport of arsenic in groundwater: A review of adsorption. In: Welch, A.H., Stollenwerk, K.G., (eds.) 2003. Arsenic in groundwater - geochemistry and occurrence. Kluwer, Dordrecht, 67-100.
- Stüben et al., 2003** Stüben, D., Berner, Z., Chandrasekharam, D., Karmarkar, J., 2003. Arsenic enrichment in groundwater of West Bengal, India: geochemical evidence for mobilization of As under reducing conditions. *Appl. Geochem.* 18, 1417-1434.
- Stute et al., 2007** Stute, M., Zheng, Y., Schlosser, P., Horneman, A., Dhar, R.K., Datta, S., Hoque, M.A., Seddique, A.A., Shamsudduha, Ahmed, K.M., Van Geen, A., 2007. Hydrological control of As concentrations in Bangladesh groundwater. *Water Resour. Res.* 43, W09417.
- Styblo et al., 2000** Styblo, M., Del Razo, L.M., Vega, L., Germolec, D.R., LeClyse, E.L., Hamilton, G.A., Wang, C., Cullen, W.R., Thomas, D.J., 2000. Comparative toxicity of trivalent and pentavalent inorganic and methylated arsenicals in human cells. *Arch. Toxicol.* 74, 289-299.
- Su & Pulse, 2001** Su, C., Pulse, R.W., 2001. Arsenate and arsenite removal by zerovalent iron: effects of phosphate, silicate, carbonate, borate, sulphate, chromate, molybdate and nitrate, relative to chloride. *Environ. Sci. Technol.* 35, 4562-4568.
- Swartz et al., 2004** Swartz. C.H., Blute, N.K., Badruzzman, B., Ali, A., Barbander, D., Jay, J., Besancon, J., Islam, S., Hemnond, H.F., Harvey, C.D., 2004. Mobility of arsenic in a Bangladesh aquifer: Inferences from geochemical profiles, leaching data and mineralogical characterisation. *Geochim. Cosmochim. Acta* 68, 4539-4557.
- Tanabe et al., 2003a** Tanabe, S., Hori, K., Saito, Y., Haruyama, S., Doanh, L.Q., Sato, Y., Hiraide, S., 2003a. Sedimentary facies and radiocarbon dates of the Nam Dinh-1 core from the Song Hong (Red River) delta, Vietnam. *Journal of Asian Earth Sciences* 21, 503-513.
- Tanabe et al., 2003b** Tanabe, S., Hori, K., Saito, Y., Haruyama, S., Vu, V.P., Kitamura, A., 2003b. Song Hong (Red River) delta evolution related to millennium-scale Holocene sea-level changes. *Quaternary Science Reviews* 22, 2345-2361.
- Tanabe et al., 2006** Tanabe, S., Saito, Y., Vu, Q.L., Hanebuth, T.J.J., Ngo, Q.L., Kitamura, A., 2006. Holocene evolution of the Song Hong (Red River) delta system, northern Vietnam. *Sed. Geol.* 187, 29-61.
- Thornton & McManus, 1994** Thornton, S.F., McManus, J., 1994. Application of organic carbon and nitrogen stable isotope and C/N ratios as source indicators of organic matter provenance in estuarine systems: evidence from the Tay Estuary, Scotland. *Estuarine, Coastal and Shelf Science* 38, 219-233.

- Tissot & Welte, 1978** Tissot, B.P., Welte, D.H., 1978. Petroleum formation and occurrence. Springer Verlag Berlin Heidelberg New York.
- Tong, 2002** Tong, N.T., 2002. Arsenic pollution in groundwater in the Red River Delta. Geological Survey of Vietnam, Northern Hydrogeological-Engineering Geological Division.
- Trafford et al., 1996** Trafford, J.M., Lawrence, A.R., Macdonald, D.M.J., Nguyen, V.D., Tran, D.N., Nguyen, T.H., 1996. The effect of urbanisation on groundwater quality beneath the city of Hanoi, Vietnam. BGS Technical Report WC/96/22. British Geological Survey, Keyworth, UK.
- Trang et al., 2005** Trang, P.K., Berg, M., Viet, P.H., Van Mui, N., van der Meer, J.R., 2005. Bacterial bioassay for rapid and accurate analysis of arsenic in highly variable groundwater samples. Environ. Sci. Technol. 39, 7625-7630.
- Trang et al., 2006** Trang, P.T.K., Lan, V.T.M., Kubota, R., Agusa, T., Hue, N.T.M., Hao, T.T., Nhat, B.H., Dau, P.T., Phu, D.M., Berg, M., Viet, P.H., Tamabe, S., 2006. Arsenic pollution in groundwater in Red River Delta, Vietnam: situation and human exposure. Proceedings to national workshop on "Arsenic contamination in groundwater in Red River plain", 67-70.
- Umweltbundesamt, 1999** Umweltbundesamt (1999). Arsen und Verbindungen. In: Berechnung von Prüfwerten zur Bewertung von Altlasten: Ableitung und Berechnung von Prüfwerten der Bundesbodenschutz- und Altlastenverordnung für den Wirkungspfad Boden – Mensch aufgrund der Bekanntmachung der Ableitungsmethoden und -maßstäbe im Bundesanzeiger Nr. 161a vom 25.August 1999. F095, Erich Schmidt, Berlin.
- USEPA, 2002** USEPA, 2002. National primary drinking water regulation. Current drinking water regulations. Environmental Protection Agency. Office of water.
- Vahter & Marafante, 1988** Vahter, M., Marafante, E., 1988. In vivo methylation and detoxification of arsenic. In: Craig, P.J., Glockli, F. (eds.). The Biological Alkylation of Heavy Elements, Royal Society of Chemistry, London.
- van Bergen et al., 1998** Van Bergen, P.F., Nott, C.J., Bull, I.D., Poulton, P.R., Evershed, R.P., 1998. Organic geochemical studies of soils from Rothamsted Classical Experiments-IV. Preliminary results from a study of the effect of soil pH on organic matter decay. Org. Geochem. 29, 1779-1795.
- van Dongen et al., 2008** van Dongen, B.A., Rowland, H.A.L., Gault, A.G., Polya, D.A., Bryant, C., Pancost, R.D., 2008. Hopane, sterane and n-alkane distributions in shallow sediments hosting high arsenic groundwaters in Cambodia. Appl. Geochem. 23, 3047-3058.
- van Geen et al., 2003** van Geen, A., Zheng, Y., Versteeg, R., Stute, M., Horneman, A., Dhar, R., Steckler, M., Gelman, A., Small, C., Ahsan, H., Graiano,

- J.H., Hussain, I., Ahmed, K.M., 2003. Spatial variability of arsenic in 6000 tube wells in a 25 km² area of Bangladesh. *Water Resour. Res.* 39, 1140.
- van Geen et al., 2004 van Geen, A., Rose, J., Thorai, S., Garnier, J.M., Zheng, Y., Bottero, J.Y., 2004. Decoupling of As and Fe release to Bangladesh groundwater under reducing conditions. Part II: Evidence from sediment incubations. *Geochim. Cosmochim. Acta* 68, 3475-3486.
- van Geen et al., 2006a van Geen, A., Zheng, Y., Cheng, Z., Aziz, Z., Horneman, A., Dhar, R.K., Mailloux, B., Stute, M., Weinman, B., Goodbred, S., Seddique, A.A., Hoque, M.A., Ahmed, K.M., 2006a. A transect of groundwater and sediment properties in Araihasar, Bangladesh: Further evidence of decoupling between As and Fe mobilization. *Chem. Geol.* 228, 85-96.
- van Geen et al., 2006b van Geen, A., Trevisani, M., Immel, J., Jakariya, Md., Osman, N., Cheng, Z., Gelman, A., Ahmed, K.M., 2006b. Targeting Low-arsenic Groundwater with Mobile-phone Technology in Araihasar, Bangladesh. *J. Health Popul. Nutr.* 24, 282-297.
- van Geen et al., 2006c van Geen, A., Aziz, Z., Horneman, A., Weinman, B., Dhar, R.K., Zheng, Y., Goodbred, S., Versteeg, R., Seddique, A.A., Hoque, M.A., Ahmed, K.M., 2006c. Preliminary evidence of a link between surface soil properties and the arsenic content of shallow groundwater in Bangladesh. *Journal of Geochemical Exploration* 88, 157-161.
- van Geen et al., 2007 van Geen, A., Cheng, Z., Jia, Q., Seddique, A.A., Rahman, M.W., Rahman, M.M., Ahmed, K.M., 2007. Monitoring 51 community wells in Araihasar, Bangladesh, for up to 5 years: Implications for arsenic mitigation. *Journal for Environmental Science and Health, Part A*, 42, 1729-1740.
- van Geen et al., 2008a van Geen, A., Zheng, Y., Goodbred Jr., S., Horneman, A., Aziz, Z., Cheng, Z., Stute, M., Mailloux, B., Weinman, B., Hoque, M.A., Seddique, A.A., Hossain, M.S., Chowdhury, S.H., Ahmed, K.M., 2008a. Flushing history as a hydrogeological control on the regional distribution of arsenic in shallow groundwater of the Bengal Basin. *Environ. Sci. and Technol.*, 42, 2283-2288.
- van Geen et al., 2008b van Geen, A., Radloff, K., Aziz, Z., Cheng, Z., Huq, M. R., Ahmed, K. M., Weinman, B., Goodbred, S., Jung, H. B., Zheng, Y., Berg, M., Trang, P. T. K., Charlet, L., Metral, J., Tisserand, D., Guillot, S., Chakraborty, S., Gajurel, A. P., Upreti, B. N. 2008b. Comparison of arsenic concentrations in simultaneously-collected groundwater and aquifer particles from Bangladesh, India, Vietnam, and Nepal. *Appl. Geochem.* 23, 3244-3251.
- van Herreweghe et al., 2003 van Herreweghe, S., Swennen, R., Vandecasteele, C., Cappuyns, V., 2003. Solid phase speciation of arsenic by sequential extraction in standard reference materials and industrially contaminated soil samples. *Environ. Pollution* 122, 323-342.
- Vaughan, 2006 Vaughan, D.J., *Arsenic. Elements* 2, 71-75.

- Volkman et al., 1992 Volkman, J.K., Holdsworth, D.G., Neill, G.P., Bavor Jr, H.J., 1992. Identifiacion of natural, anthropogenic and petroleum hydrocarbons in aquatic sediments. *Sci. Tot. Environ.* 112, 203-219.
- Volkman et al., 1998 Volkman, J.K., Barrett, S.M., Blackburn, S.I., Mansour, M.P., Sikes, E.L., Gelin, F., 1998. Microalgal biomarkers: A review of recent research developments. *Org. Geochem.* 29, 1163—1176.
- Voss et al., 2001 Voss, M., Dippner, J.W., Montoya, J.P., 2001. Nitrogen isotope patterns in the oxygen-deficient waters of Eastern Tropical North Pacific Ocean. *Deep-Sea Research I* 48, 1905-1921.
- Wagner et al., 2005 Wagner, F., Berner, Z., Stüben, D. 2005. Arsenic in groundwater of the Bengal Delta Plain: Geochemical evidences for small scale redox zonation in the aquifer. In: Bundschuh, J., Bhattacharya, P., Chandrasekharam, D. (eds.). *Natural Arsenic in Groundwater: Occurrences, remediation and management*. Taylor and Francis, Balkema. p. 3-15.
- Waser et al., 1998 Waser, N.A., Yin, K.D., Yu, Z.M., Tada, K., Harrison, P.J., Turpin, D.H., Calvert, S.E., 1998. Nitrogen isotope fractionation during nitrate, ammonium and urea uptake by marine diatoms and coccolithophores under various conditions of N availability. *Marine Ecology-Progress Series* 169, 29-41.
- Waychunas et al., 1993 Waychunas, G.A., Rea, B.A., Fuller, C.C., Davis, J.A., 1993. Surface chemistry of ferrihydrite: Part1. EXAFS studies of the geometry of coprecipitated and adsorbed arsenate. *Geochim. Cosmochim. Acta.* 57, 2251-2269.
- Welch et al., 1988 Welch, A.H., Lico, M.S., Huges, J.L., 1988. Arsenic in groundwater of Western United States. *Ground Water* 26, 333-347.
- Welch et al., 2000 Welch, A.H., Westjohn, D.B., Helsel, D.R., Wanty, R.B., 2005. Arsenic in groundwater of the United States: occurrence and geochemistry. *Ground Water* 38, 589-604.
- Wenzel et al., 2001 Wenzel, W.W., Kirchbaumr, N., Prohaska, T., Stingeder, G., Lombic, E., Adriano, D.C., 2001. Arsenic fractionation in soils using an improved sequential extraction procedure. *Anal. Chim. Acta* 436, 309-323.
- White et al., 1963 White, D.E., Hem, J.D., Waring, G.A., 1963. *Data of Geochemistry*. 6th edition. Chapter F. Chemical Composition of Sub-Surface Waters. *Us Geol. Surv. Prof. Pap.*
- WHO, 2003 WHO, 2003. Arsenic in drinking water. Background Document for development of WHO Guidelines for drinking-water quality. WHO/SDE/WSH/03.04/75. World Health Organisation.
- Williams, 2001 Williams, I., 2001. *Environmental Chemistry*. Wiley. London, p. 388.
- Winkel et al., 2008 Winkel, L., Berg, M., Amini, M., Hug, S.J., Johnson, C.A., 2008. Predicting groundwater arsenic contamination in Southeast Asia from surface parameters. *Nature geoscience* 1, 536-542.

- Worldbank, 2005** Worldbank, 2005. Arsenic Contamination of Groundwater in South and East Asian Countries - Towards a More Effective Operational Response. Volume II: Technical Report.
- Xu et al., 1988** Xu, H., Allard, B., Grimvall, A., 1988. Influence of pH and organic substances on the adsorption of As(V) on geological materials. *Water Air Soil Poll.* 40, 293-305.
- Yamauchi & Fowler, 1994** Yamauchi, H., Fowler, B.A., 1994. Toxicity and metabolism of inorganic and methylated arsenicals. In: Nriagu, J.O. (ed.). *Arsenic in the Environment. Part II: Human Health and Ecosystem Effects.* Wiley. New York., pp. 35-43.
- Zengler et al., 1999** Zengler, K., Richnow, H.H., Rosselló-Mora, R., Michaelis, W., Widdel, F., 1999. Methane formation from long-chain alkanes by anaerobic microorganisms. *Nature* 401, 266-269.
- Zheng et al., 2004** Zheng, Y., Stute, M., Van Geen, A., Gavrieli, I., Dhar, R., Simpson, H.J., Schlosser, P., Ahmed, K.M., 2004. Redox control of arsenic mobilization in Bangladesh groundwater. *Appl. Geochem.* 19, 201-214.
- Zheng et al., 2005** Zheng, Y., van Geen, A., Stute, M., Dhar, R., Mo, Z., Cheng, Z., Horneman, A., Gavrieli, I., Simpson, H.J., Versteeg, R., Steckler, M., Grazioli-Venier, A., Goodbred, S., Shahnewaz, M., Shamsudduha, M., Hoque, M.A., Ahmed, K.M., 2005. Geochemical and hydrogeological contrasts between shallow and deeper aquifers in two villages of Araihasar, Bangladesh: Implications for deeper aquifers as drinking water sources. *Geochim. Cosmochim. Acta* 69, 5203-5218.
- Zhou et al., 2006** Zhou, J., Wu, Y., Zhang, J., Kang, Q., Liu, Z., 2006. Carbon and nitrogen composition and stable isotope as potential indicators of source and fate of organic matter in the salt marsh of the Changjiang Estuary, China. *Chemosphere* 65, 310-317.
- Zobrist et al., 2000** Zobrist, J., Dowdle, P.R., Davis, J.A., Oremland, R.S., 2000. Mobilization of arsenite by dissimilatory reduction of adsorbed arsenate. *Environ. Sci. Technol.* 34, 4747-4753.

APPENDIX

A.1 GROUNDWATER CHEMISTRY

A.2 SEQUENTIAL EXTRACTION

A.3 GRAIN SIZE ANALYSIS

A.4 GEOCHEMICAL AND MINERALOGICAL SEDIMENT CHARACTERIZATION

A.4.1 BULK ANALYSIS

A.4.2 MEASUREMENTS OF INDIVIDUAL GRAINS

A.5 FACTOR ANALYSIS BASED ON RESULTS OF μ S-XRF MEASUREMENTS

A.5.1 CORRELATION MATRICES

A.5.2 FACTOR LOADINGS AND COMMUNALITY

A.5.3 FACTOR SCORES

A.6 CHARACTERIZATION OF ORGANIC MATTER

A.1 GROUNDWATER CHEMISTRY

Tab. A-1: Results of the hydrochemical analysis of the nine wells at each site and the Red River (part I) measured with IPC-MS (Element 2, Thermo Fisher)(ML = multi level; n.d. = not determined, LOD = limit of detection).

well	dept h [m]	As- tot [µg/L]	As (III) [µg/L]	Fe [mg/L]	Mn [mg/L]	Na [mg/L]	K [mg/L]	Ca [mg/L]	Mg [mg/L]	Sr [µg/L]	Ba [µg/L]
ML-L-1	24	0.8	0.6	0.1	2.56	30.9	2.0	8	8.9	57	28
ML-L-2	27	1.1	0.7	0.1	0.64	35.5	2.3	10	12.2	75	35
ML-L-3	30	0.6	0.5	0.02	0.55	36.5	2.3	11	13.1	86	31
ML-L-4	33	0.7	0.6	0.04	0.41	28.1	2.6	21	22.2	166	54
ML-L-5	36.5	0.6	0.4	0.03	0.25	20.9	2.7	25	28.9	230	77
ML-L-6	39	0.8	0.2	<LOD	0.50	20.4	3.0	33	33.3	280	92
ML-L-7	41	1.7	0.5	0.1	0.45	22.0	2.9	32	31.2	267	94
ML-L-8	45	0.8	0.4	0.04	2.76	33.4	3.6	38	31.6	279	121
MLC-L	54	7.6	6.8	10.2	0.59	33.2	3.8	22	20.2	173	103
ML-H- 1	17	330	n.d.	15.9	0.25	14.1	4.1	128	37.1	560	461
ML-H- 2	21	441	443	14.2	0.38	10.7	3.4	109	32.7	365	618
ML-H- 3	24	311	333	16.9	0.15	14.2	1.6	127	25.4	293	506
ML-H- 4	27	218	n.d.	13.0	0.38	12.4	2.2	127	25.0	317	532
ML-H- 5	34	340	358	16.2	0.14	12.6	1.5	121	24.0	276	472
ML-H- 6	36	615	597	12.2	0.43	10.3	2.5	130	27.0	419	873
ML-H- 7	41	207	196	10.7	1.86	12.4	3.8	86	39.4	404	522
ML-H- 8	45	306	n.d.	8.3	1.45	13.5	3.1	98	34.8	424	499
MLC- H	57	8	2.6	2.0	0.98	12.3	2.6	119	26.6	374	142
Red River	0	4	n.d.	<LOD	0.02	3.4	1.4	25	4.1	n.d.	30

Tab. A-2: Results of the hydrochemical analysis of the nine wells at each site and the Red River (part II) measured with a portable system YSI 556 and a WTW Multi 340i (John Morris Scientific Pty Ltd.) for temperature (T), pH, electrical conductivity (EC), redox-potential (Eh) and dissolved oxygen (O₂), with ICP-MS (Element 2, Thermo Fisher) for P(tot), ICP-OES (Spectro Ciros CCD) for Si(tot), photometry for ammonium (NH₄-N), TOC 5000 Analyser (Shimadzu, Switzerland) for dissolved organic carbon (DOC), and, ion chromatography (IC) (Dionex, Switzerland) for NO₃⁻, SO₄²⁻ and Cl⁻ (LOD = limit of detection, ML = multi level).

well	depth [m]	T [°C]	pH	Diss. O ₂ [mg/L]	EC [µS/cm]	Eh [mV]	P (tot) [µg/L]	Si (tot) [mg/L]	HCO ₃ ⁻ [mg/L]	Cl ⁻ [mg/L]	SO ₄ ²⁻ [mg/L]	NH ₄ -N [mg/L]	DOC [mg/L]
ML-L-1	24	26.0	6.2	0.3	217	109	30	18.1	140	4.6	9.9	0.2	2.2
ML-L-2	27	26.1	6.5	1.2	251	77	28	18.2	171	3.8	8.1	0.1	1.5
ML-L-3	30	26.8	6.4	0.6	267	144	25	18.5	183	3.9	8.6	0.1	<LOD
ML-L-4	33	27.0	6.5	0.5	322	106	30	18.3	232	3.6	5.6	0.1	<LOD
ML-L-5	36.5	26.1	6.5	0.5	359	84	27	18.0	264	3.3	5.0	0.1	<LOD
ML-L-6	39	27.2	6.4	0.6	414	60	6	18.7	311	3.5	<LOD	0.1	<LOD
ML-L-7	41	27.6	6.6	0.7	413	85	26	19.0	305	4	<LOD	0.2	<LOD
ML-L-8	45	26.9	6.7	0.3	462	94	20	19.3	352	3.5	<LOD	0.2	<LOD
MLC-L	54	27.0	7.2	0.5	341	-148	387	17.8	241	5.3	5.7	0.7	2.1
ML-H-1	17	25.9	6.8	0.4	825	-164	657	21.5	650	8.2	<LOD	23.2	3.9
ML-H-2	21	25.3	7.0	0.6	481	-130	620	15.6	554	8.8	<LOD	18.6	2.3
ML-H-3	24	26.7	7.0	1.0	721	-160	526	17.1	550	9.9	<LOD	9.1	2.6
ML-H-4	27	25.9	7.1	0.8	357	-117	201	17.5	509	9.7	<LOD	4.4	<LOD
ML-H-5	34	25.6	7.0	0.7	686	-125	183	16.1	521	10.2	<LOD	4.1	1.7
ML-H-6	36	25.1	7.2	0.5	708	-114	385	14.3	541	10.6	<LOD	6.0	1.6
ML-H-7	41	26.8	6.9	1.5	605	-139	455	18.0	464	3.1	<LOD	2.3	1.6
ML-H-8	45	25.8	6.9	1.3	622	-135	371	18.6	473	3.8	<LOD	2.8	1.6
MLC-H	57	27.6	6.9	1.1	646	-98	158	20.3	486	3.1	<LOD	3.8	1.7
Red River	0	n.d.	8.0 4	n.d.	140	2	n.d.	4.7	101	1.4	5.9	0.2	2.7

Tab. A-3: Calculated saturation index (SI) based on the result of the hydrochemical analysis for siderite, vivianite, calcite and dolomite from different depth at both sites (ML = multi level).

well	depth [m]	SI _{siderite} FeCO ₃	SI _{vivianite} Fe ₃ (PO ₄) ₂ ·x8H ₂ O	SI _{calcite} CaCO ₃	SI _{dolomite} CaMg(CO ₃)
ML-L-1	24	-0.4	-4.8	-2.0	-3.5
ML-L-2	27	-0.3	-4.5	-1.5	-2.6
ML-L-3	30	-0.6	-5.8	-1.7	-2.8
ML-L-4	33	0.3	-3.0	-0.8	-1.2
ML-L-5	36.5	0.01	-4.2	-1.0	-1.5
ML-L-6	39	0.2	-4.0	-0.7	-1.0
ML-L-7	41	0.2	-3.4	-0.7	-1.0
ML-L-8	45	0.1	-3.4	-0.4	-0.6
MLC-L	54	0.5	-0.4	-0.5	-1.2
ML-H-1	17	0.3	0.5	1.6	2.3
ML-H-2	21	0.5	0.9	1.8	2.3
ML-H-3	24	0.4	0.6	1.7	2.5
ML-H-4	27	0.4	0.4	1.7	2.3
ML-H-5	34	0.4	0.5	1.7	2.2
ML-H-6	36	0.4	0.5	1.6	1.6
ML-H-7	41	0.03	0.1	1.3	1.0
ML-H-8	45	0.2	0.4	1.4	1.4
MLC-H	57	0.3	0.4	0.6	-1.4

A.2 SEQUENTIAL EXTRACTION

Tab. A-4: Results of sequential extractions on selected samples of site L according to KEON ET AL. (2001, slightly modified) (LOD = limit of detection).

sample	As [mg/kg]	Fe [mg/kg]	Mn [mg/kg]	Al [mg/kg]	Ti [mg/kg]	Ni [mg/kg]	Cu [mg/kg]	Pb [mg/kg]
L08120 (11 m)								
L08120 F1	2.4	419	33.2	1626	23	2.4	2.0	<LOD
L08120 F2	24.8	2,045	17.9	2,547	<LOD	11.1	3.8	<LOD
L08120 F3	12.5	9,261	3.2	870	60	15.7	78	24
L08120 F4	1.7	1,615	<LOD	558	15	3.7	10.9	0.8
L08120 F5	3.2	1,943	10.5	1,181	62	6.4	1.2	0.03
L08120 F6	0.4	8,856	33.6	54,550	811	24.3	12.4	7.8
L08120 F7	11.8	10,449	0.1	218	85	3.7	10.7	1.5
L1410 (19 m)								
L1410 F1	1.0	201	31.6	13	0.2	27.3	0.3	<LOD
L1410 F2	11.0	1,180	3.4	634	17	22.4	1.3	0.1
L1410 F3	3.1	1,371	2.3	266	41	3.7	7.4	9.5
L1410 F4	0.1	366	<LOD	252	6.8	1.8	1.4	0.5
L1410 F5	2.1	674	3.1	807	29	5.0	0.3	<LOD
L1410 F6	0.2	5,435	49.9	33,253	9,54.0	12.7	5.7	4.3
L1410 F7	7.7	1,443	<LOD	159	67.6	0.7	5.3	0.2
L17045 (24 m)								
L17045 F1	0.1	41	137.4	32	0.6	0.6	0.3	<LOD
L17045 F2	5.0	480	154.8	243	0.3	2.0	7.2	0.1
L17045 F3	0.7	412	89.7	139	6.5	0.9	3.1	2.2
L17045 F4	1.8	811	59.4	65	8.0	1.1	1.2	0.6
L17045 F5	1.1	5,538	50.4	267	46.3	5.3	0.1	0.05
L17045 F6	<LOD	1,763	18.4	17,381	2,58.8	6.3	1.2	7.4
L17045 F7	0.02	<LOD	<LOD	84	0.2	<LOD	2.2	<LOD
L2215 (27 m)								
L2215 F1	<LOD	360	91	32	6.3	1.2	0.6	<LOD
L2215 F2	<LOD	1,120	7.6	1042	<LOD	1.1	0.5	0.1
L2215 F3	0.3	16,969	188	454	11.3	1.1	3.1	7.8
L2215 F4	<LOD	3,012	63.5	424	22.5	1.7	1.1	0.7
L2215 F5	0.5	4,478	8.4	714	128	1.4	<LOD	0.1
L2215 F6	<LOD	9,108	59	60,505	1,438	24	10.8	5.7
L2215 F7	0.01	<LOD	<LOD	145	14.6	0.2	3.6	0.1

to be continued on the following page

sample	As [mg/kg]	Fe [mg/kg]	Mn [mg/kg]	Al [mg/kg]	Ti [mg/kg]	Ni [mg/kg]	Cu [mg/kg]	Pb [mg/kg]
L 2640 (32 m)								
L2640 F1	<LOD	4	2.1	4	0.1	0.1	0.1	<LOD
L2640 F2	<LOD	104	2.2	220	<LOD	<LOD	<LOD	<LOD
L2640 F3	0.2	474	5.0	665	9.6	1.3	1.2	1.0
L2640 F4	<LOD	349	<LOD	201	2.9	2.0	0.8	0.2
L2640 F5	0.3	5,407	10.5	363	78	3.0	<LOD	0.1
L2640 F6	<LOD	7,572	46	35,165	650	11.7	5.5	6.4
L2640 F7	<LOD	<LOD	<LOD	191	6.1	0.1	1.7	<LOD
L 29130 (40 m)								
L29130 F1	<LOD	1	6.1	2	0.1	0.1	0.1	<LOD
L29130 F2	<LOD	135	8.2	199	<LOD	<LOD	<LOD	<LOD
L29130 F3	0.1	548	19	617	6.9	1.2	1.2	1.2
L29130 F4	<LOD	362	7.1	173	2.9	1.5	0.7	0.5
L29130 F5	0.1	4,639	10.4	348	79	2.7	<LOD	0.1
L29130 F6	<LOD	6,064	39	27,504	503	7.6	3.8	7.2
L29130 F7	<LOD	<LOD	<LOD	154	1.9	0.01	1.5	<LOD
L3350 (46 m)								
L3350 F1	0.01	44	11.2	32	1.2	0.1	0.02	0.04
L3350 F2	<LOD	849	14.0	267	<LOD	0.7	<LOD	<LOD
L3350 F3	0.7	1,037	6.7	628	9.8	1.0	0.7	<LOD
L3350 F4	<LOD	993	45	264	13.1	1.0	0.6	0.2
L3305 F5	<LOD	11,637	18	969	142	4.4	0.7	0.3
L3350 F6	0.6	9,698	105	26,733	1,840	11.0	5.1	7.1
L3350 F7	0.03	73	1.3	5	27	0.2	1.4	<LOD
L 3475 (47 m)								
L3475 F1	0.1	70	10.2	56	1.3	1.4	0.2	<LOD
L3475 F2	<LOD	1,190	64	369	<LOD	6.5	2.3	<LOD
L3475 F3	0.3	1,548	21	500	10.5	3.3	2.9	3.0
L3475 F4	<LOD	1,559	26	297	8.6	7.0	1.1	0.4
L3475 F5	0.2	6,826	13	383	74	17.5	<LOD	0.1
L3475 F6	<LOD	6,463	46	25,593	657	19.2	4.3	5.8
L3475 F7	0.03	7	<LOD	101	8.9	0.1	2.4	0.04

Tab. A-5: Results of sequential extractions on selected samples of site H according to KEON ET AL. (2001, slightly modified) (LOD = limit of detection). To check reproducibility, three samples were analysed from a depth of 39 m (H3305).

sample	As [mg/kg]	Fe [mg/kg]	Mn [mg/kg]	Al [mg/kg]	Ti [mg/kg]	Ni [mg/kg]	Cu [mg/kg]	Pb [mg/kg]
H1450 (17 m)								
H1450 F1	0.2	81	153	94	1	0.1	0.2	0.1
H1450 F2	6.6	838	325	636	<LOD	4.0	2.7	0.2
H1450 F3	1.7	10,419	192	2,010	85	4.4	14.5	21.8
H1450 F4	0.1	1,606	95	780	32	1.7	1.0	0.3
H1450 F5	0.5	9,698	19	1,659	96	2.0	1.2	0.2
H1450 F6	0.6	10,763	90	49,262	1,047	21.2	10.9	6.9
H1450 F7	0.3	208	1	103	145	1.5	5.8	0.4
H2020 (23 m)								
H2020 F1	0.03	110	14	38	1	0.2	<LOD	<LOD
H2020 F2	1.8	703	42	296	<LOD	2.7	11.4	<LOD
H2020 F3	0.9	4,801	73	1,187	64	2.4	0.3	<LOD
H2020 F4	0.1	1,190	84	385	20	1.0	0.3	0.2
H2020 F5	<LOD	2,450	10	716	34	0.8	0.2	0.05
H2020 F6	0.4	5,008	55	27,351	473	7.5	1.9	6.2
H2020 F7	<LOD	16	0.5	<LOD	1	1.1	1.6	0.01
H2750 (30 m)								
H2750 F1	0.05	37	1	41	1	0.1	0.2	0.04
H2750 F2	1.7	567	4	126	<LOD	<LOD	<LOD	<LOD
H2750 F3	0.5	424	3	277	7	0.7	<LOD	<LOD
H2750 F4	0.4	500	87	190	8	0.8	0.2	0.1
H2750 F5	<LOD	725	3	405	19	0.5	0.1	<LOD
H2750 F6	0.4	1,971	15	14,823	203	2.8	1.1	7.1
H2750 F7	<LOD	2	<LOD	20	2	0.01	0.1	<LOD
H3305-1 (39 m)								
H3305-1 F1	0.1	36	70	17	0.1	0.5	0.8	0.2
H3305-1 F2	3.9	968	181	624	<LOD	5.6	0.5	<LOD
H3305-1 F3	1.3	5,040	103	1,189	42	5.5	6.3	4.9
H3305-1 F4	0.4	2,627	110	573	30	4.8	1.5	0.5
H3305-1 F5	0.1	9,224	41	2,935	101	17.2	1.3	0.2
H3305-1 F6	0.9	9,524	85	39,304	998	21.4	5.7	9.6
H3305-1 F7	0.04	50	2	34	51	0.5	2.5	0.03

to be continued on the following page

sample	As [mg/kg]	Fe [mg/kg]	Mn [mg/kg]	Al [mg/kg]	Ti [mg/kg]	Ni [mg/kg]	Cu [mg/kg]	Pb [mg/kg]
H3305-2 (39 m)								
H3305-2 F1	0.1	42	72	21	0.2	0.5	0.6	0.2
H3305-2 F2	3.5	986	181	757	<LOD	6.8	0.7	0.3
H3305-2 F3	1.4	4,894	130	1,156	44	5.3	6.1	4.8
H3305-2 F4	0.2	2,295	124	552	28	4.1	1.1	0.4
H3305-2 F5	0.2	8,775	41	2,688	90	16.5	1.2	0.2
H3305-2 F6	0.4	9,188	83	33,776	939	20.0	5.0	7.0
H3305-2 F7	0.1	52	1	143	35	0.6	1.0	0.04
H3305-3 (39 m)								
H3305-3 F1	0.1	26	79	13	0.1	2.1	0.4	0.1
H3305-3 F2	3.4	859	150	588	<LOD	6.0	13.3	<LOD
H3305-3 F3	1.3	4,615	105	1,073	40	5.0	5.3	4.3
H3305-3 F4	0.1	2,332	137	543	26	4.3	1.1	0.5
H3305-3 F5	<LOD	7,979	34	2,416	78	16.1	1.1	0.2
H3305-3 F6	0.5	9,686	86	35,150	933	20.9	5.2	7.5
H3305-3 F7	0.1	45	2	42	39	1.3	3.4	0.1
H3515 (44 m)								
H3515 F1	1.0	98	11	80	2	0.3	0.3	0.1
H3515 F2	15.3	636	46	611	<LOD	1.2	5.0	<LOD
H3515 F3	5.8	1,871	21	653	22	1.8	2.6	<LOD
H3515 F4	2.5	1,014	106	230	13	1.2	0.2	0.2
H3515 F5	0.4	2,981	10	883	46	2.3	0.8	0.1
H3515 F6	0.5	4,215	50	20767	635	5.4	2.3	6.8
H3515 F7	0.01	21	1	<LOD	8	0.1	1.8	0.04

A.3 GRAIN SIZE ANALYSIS

Tab. A-6: Results of grain size analysis by means of laser granulometry (Mastersizer 2000, Malvern) and calculated K-values according to BEYER (1964) of site L.

sample	depth [m]	clay [%]	silt [%]	sand [%]	K-value
L0135	0.4	7.9	84.0	8.1	5.06E-08
L0225	0.9	7.7	71.2	21.1	4.56E-08
L0245	1.3	7.7	79.9	12.4	5.42E-08
L0275	1.8	14.2	82.7	3.1	1.63E-08
L0360	3.1	14.2	82.9	2.9	1.61E-08
L0445	4.1	2.1	24.6	73.4	9.06E-07
L0490	4.6	9.5	86.9	3.6	3.57E-08
L0580	5.9	15.4	78.6	6.0	1.46E-08
L0650	7.3	6.2	81.8	12.1	9.31E-08
L06100	8.0	18.9	79.6	1.4	1.15E-08
L0760	9.5	18.4	80.5	1.2	1.28E-08
L0860	10.1	12.5	81.2	6.4	3.55E-08
L08120	10.8	10.2	82.6	7.2	2.91E-08
L0990	12.0	7.8	77.7	14.5	4.97E-08
L1025	12.8	6.7	80.5	12.8	7.25E-08
L10110	13.8	14.1	71.5	14.4	1.43E-08
L11105	15.1	15.1	72.5	12.4	1.46E-08
L1245	16.4	10.3	76.7	13.0	2.66E-08
L1335	17.9	8.0	72.4	19.5	4.11E-08
L1410	18.6	10.4	81.2	8.4	2.95E-08
L14100	19.7	15.8	77.9	6.4	1.37E-08
L1540	20.4	15.6	76.8	7.6	1.45E-08
L15140	21.4	8.8	62.9	28.3	3.57E-08
L1640	21.9	7.8	60.3	31.9	4.52E-08
L1690	22.4	8.8	67.8	23.4	3.63E-08
L16140	22.9	6.9	49.6	43.5	5.56E-08
L17045	23.8	4.1	26.3	82.3	1.48E-06
L1805	24.9	3.6	30.3	66.1	2.06E-07
L1905	25.0	4.3	37.3	58.4	1.28E-07
L2215	27.1	8.8	64.4	26.8	3.55E-08
L2250	27.5	3.8	34.3	61.9	1.65E-07
L2460	30.2	2.5	25.7	71.8	4.39E-07
L2540	31.5	5.6	41.4	53.0	7.39E-08
L2640	32.4	1.9	22.9	75.2	8.94E-07
L2870	36.5	1.0	15.1	83.9	6.92E-06
L2960	38.1	0.8	10.9	88.3	1.89E-05
L29130	38.8	5.0	37.5	57.6	9.47E-08
L3190	43.0	4.2	37.5	58.3	1.77E-07
L3290	44.6	3.7	35.9	60.5	4.26E-06
L3350	45.6	1.2	14.1	84.6	1.28E-07
L3430	46.8	1.0	17.4	81.6	6.20E-06
L3475	47.3	3.7	38.7	57.6	1.76E-07

Tab. A-7: Results of grain size analysis by means of laser granulometry (Mastersizer 2000, Malvern) and calculated K-values according to BEYER (1964) of site H.

sample	depth [m]	clay [%]	silt [%]	sand [%]	K-value
H0115	0.3	3.6	35.6	60.8	1.96E-07
H0240	1.3	11.8	87.4	0.8	2.27E-08
H0380	2.8	11.5	86.0	2.4	2.45E-08
H0440	4.1	5.9	64.9	29.2	8.43E-08
H0530	5.2	12.6	86.2	1.2	2.08E-08
H0670	6.3	11.5	83.0	5.5	2.42E-08
H0750	7.1	4.3	47.4	48.3	1.56E-07
H07100	7.7	4.2	64.5	31.3	1.60E-07
H0860	8.7	6.8	68.6	24.6	6.45E-08
H08140	9.4	6.5	76.7	16.8	7.24E-08
H0970	10.9	8.4	83.5	8.1	4.44E-08
H1030	11.7	2.9	33.6	19.5	6.64E-08
H1090	12.4	6.6	73.9	63.5	3.50E-07
H1125	12.8	6.6	72.4	21.0	6.22E-08
H1150	13.2	1.3	20.4	78.2	1.66E-06
H1180	13.6	12.3	83.1	4.5	2.12E-08
H1345	15.7	1.9	18.1	80.0	1.13E-06
H1425	16.1	0.6	9.7	89.7	2.75E-05
H1450	16.6	6.5	78.1	15.4	8.09E-08
H1530	17.3	5.0	43.0	52.0	9.69E-08
H1610	18.2	0.6	9.7	89.7	1.87E-05
H1860	20.8	5.5	38.1	56.4	8.73E-08
H1960	22.3	6.3	30.7	63.0	7.61E-08
H2020	23.2	3.8	45.6	50.6	1.52E-07
H2220	26.0	2.2	26.6	71.2	8.60E-07
H2320	26.4	0.0	7.2	92.8	1.99E-04
H2450	27.3	0.9	16.8	82.3	3.84E-06
H2655	28.8	5.6	23.2	71.2	7.96E-08
H2750	29.8	3.2	25.1	71.7	2.83E-07
H2850	31.1	1.4	26.4	72.2	1.88E-06
H2910	32.0	2.5	44.7	52.8	5.62E-07
H2960	33.4	2.4	30.2	67.5	6.50E-07
H3030	34.2	3.1	32.7	64.2	2.44E-07
H3055	35.0	3.8	40.1	56.1	1.56E-07
H3180	36.1	2.4	24.8	72.8	4.93E-07

to be continued on the following page

APPENDIX

sample	depth [m]	clay [%]	silt [%]	sand [%]	K-value
H31120	36.6	5.9	47.6	46.5	6.56E-08
H3250	39.2	4.3	37.9	57.8	1.28E-07
H3305	39.0	4.6	46.5	48.9	1.03E-07
H3330	39.8	2.6	30.5	66.9	4.92E-07
H3360	41.2	7.0	45.0	48.0	5.05E-08
H3415	41.6	3.2	37.7	59.1	2.24E-07
H3445	42.2	8.2	48.7	43.1	4.10E-08
H3515	44.1	5.4	39.3	55.2	9.51E-08
H3535	44.3	2.2	31.0	66.8	5.34E-07
H3615	44.9	1.6	19.0	79.3	1.48E-06
H3680	45.9	1.9	30.3	67.8	7.76E-07
H3740	46.8	1.9	32.5	65.7	6.57E-07
H37120	47.6	3.9	43.6	52.5	1.42E-07
H3815	49.2	2.7	37.4	59.9	3.17E-07
H3930	49.9	1.2	22.1	76.7	1.92E-06
H4025	51.0	0.8	22.8	76.4	3.00E-06
H4090	52.1	1.8	27.3	70.8	6.98E-07
H40140	52.9	10.0	50.9	39.1	2.60E-08
H41535	53.4	0.0	10.6	89.4	2.51E-05
H4165	54.9	5.4	44.7	49.9	8.41E-08
H42	55.0	7.5	76.1	16.4	5.22E-08

A.4 GEOCHEMICAL AND MINERALOGICAL SEDIMENT CHARACTERIZATION

A.4.1 BULK ANALYSIS

Tab. A-8: Elemental concentrations of bulk sediment samples of site L measured with energy dispersive X-ray fluorescence analysis (EDX) (LOD = limit of detection) – part I.

sample	depth [m]	As [ppm]	Fe ₂ O ₃ [wt-%]	CaO [wt-%]	TiO ₂ [wt-%]	MnO [wt-%]	Ni [ppm]	Cu [ppm]	Zn [ppm]	Rb [ppm]	Sr [ppm]
L0135	0.4	29	5.8	1.6	0.6	0.11	53	63	116	123	86
L0225	0.9	15	5.1	1.4	0.6	0.10	30	34	82	114	84
L0245	1.3	19	6.0	0.8	0.8	0.07	30	38	106	122	69
L0275	1.8	21	7.4	1.3	0.7	0.15	39	44	106	153	87
L0360	3.1	20	6.8	1.0	0.7	0.09	45	35	110	152	82
L0445	4.1	10	3.0	0.8	0.4	0.02	30	21	54	81	71
L0490	4.6	16	5.5	1.2	0.7	0.07	38	38	89	127	78
L0580	5.9	20	6.7	0.8	0.7	0.08	56	40	110	160	90
L0650	7.3	13	4.5	1.5	0.6	0.06	35	34	72	98	77
L06100	8.0	19	6.7	0.6	0.7	0.03	56	46	129	182	91
L0760	9.5	12	5.0	0.5	0.7	<LOD	55	35	139	161	86
L08120	10.8	24	3.2	0.6	0.6	<LOD	45	54	101	154	87
L0990	12.0	22	8.1	0.6	0.7	<LOD	42	41	120	167	75
L1025	12.8	19	2.4	0.3	0.6	<LOD	15	20	48	71	47
L10110	13.8	8	2.9	0.2	0.6	<LOD	15	17	42	80	41
L11105	15.1	18	6.2	0.3	0.7	<LOD	23	34	60	135	56
L1245	16.4	15	5.2	0.3	0.6	<LOD	47	42	69	125	58
L1335	17.9	14	3.2	0.2	0.5	<LOD	23	34	57	116	63
L1410	18.6	18	2.5	0.2	0.5	<LOD	38	30	98	129	62
L14100	19.7	9	6.0	0.4	0.7	0.04	27	31	78	141	60
L1540	20.4	7	5.9	0.4	0.7	0.04	25	41	73	133	63
L15140	21.4	5	4.7	0.3	0.6	0.03	22	26	64	108	51
L1640	21.9	5	4.6	0.3	0.5	0.04	31	18	63	109	51
L1690	22.4	5	1.6	0.2	0.4	<LOD	27	20	51	111	49
L16125	22.8	5	33.8	0.2	0.4	0.08	2	58	91	73	31
L16140	22.9	4	4.3	0.2	0.5	0.04	18	25	58	102	49
L17045	23.7	20	1.6	0.1	0.1	0.08	22	11	22	62	27
L185	24.9	3	1.3	0.2	0.2	<LOD	31	14	32	64	40
L195	25.0	3	1.3	0.2	0.2	<LOD	17	18	32	70	42
L2215	27.1	6	4.1	0.3	0.5	0.05	28	37	62	120	51
L2250	27.6	3	1.3	0.2	0.2	<LOD	16	16	43	73	47
L2440	30.2	3	1.5	0.2	0.2	<LOD	22	14	34	72	45
L2540	31.2	3	1.7	0.2	0.2	<LOD	14	12	36	85	53
L2640	32.5	5	2.0	0.2	0.3	<LOD	16	15	42	92	58
L2870	36.5	3	1.8	0.2	0.2	<LOD	16	11	33	79	51
L2960	38.1	3	1.8	0.2	0.2	0.02	20	10	32	81	53
L29130	38.8	4	1.7	0.2	0.2	<LOD	18	17	34	76	55

to be continued on the following page

sample	depth [m]	As [ppm]	Fe ₂ O ₃ [wt-%]	CaO [wt-%]	TiO ₂ [wt-%]	MnO [wt-%]	Ni [ppm]	Cu [ppm]	Zn [ppm]	Rb [ppm]	Sr [ppm]
L3190	43.0	2	2.4	0.3	0.3	<LOD	22	19	42	81	60
L3290	44.6	4	2.2	0.2	0.2	<LOD	17	17	37	85	56
L3350	45.6	5	2.5	0.3	0.3	<LOD	17	13	38	69	59
L3430	46.8	3	2.8	0.3	0.3	<LOD	18	14	43	90	64
L3475	47.3	6	3.2	0.4	0.3	0.02	147	30	50	77	58
L34130	47.7	3	0.7	0.2	0.1	<LOD	23	24	19	50	22
L35	48.0	3	1.2	0.9	0.1	<LOD	6	6	16	<LOD	25

Tab. A-9: Elemental concentrations of bulk sediment samples of site L measured with energy dispersive X-ray fluorescence analysis (EDX) (LOD = limit of detection) – part II.

sample	depth [m]	Y [ppm]	Zr [ppm]	Nb [ppm]	Sn [ppm]	Ba [ppm]	La [ppm]	Ce [ppm]	Pb [ppm]
L0135	0.4	32	211	15	8	520	42	96	67
L0225	0.9	28	235	15	7	439	43	88	29
L0245	1.3	57	519	57	7	421	86	199	17
L0275	1.8	37	199	15	6	515	48	98	31
L0360	3.1	35	191	13	6	541	53	100	33
L0445	4.1	21	237	10	3	374	39	72	16
L0490	4.6	33	225	14	6	469	53	105	28
L0580	5.9	35	209	14	6	535	41	113	34
L0650	7.3	29	251	12	3	385	51	77	21
L06100	8.0	35	173	15	6	630	57	121	35
L0760	9.5	35	196	16	7	648	61	100	31
L08120	10.8	54	186	15	7	526	66	139	27
L0990	12.0	33	146	15	5	476	54	90	27
L1025	12.8	24	298	17	3	227	30	65	18
L10110	13.8	23	328	16	3	227	29	56	12
L11105	15.1	27	243	17	5	377	40	86	22
L1245	16.4	32	252	16	5	375	48	89	18
L1335	17.9	36	232	15	3	412	74	154	30
L1410	18.6	36	283	19	5	411	51	112	27
L14100	19.7	26	220	18	5	453	47	78	17
L1540	20.4	26	228	16	5	444	51	80	20
L15140	21.4	25	239	14	5	409	47	92	18
L1640	21.9	25	302	15	3	402	49	92	17
L1690	22.4	27	337	18	3	421	54	92	13
L16125	22.8	18	148	8	<LOD	205	21	61	42
L16140	22.9	25	408	15	4	396	40	91	16
L17045	23.7	7	74	7	<LOD	330	12	24	14
L185	24.9	11	88	7	<LOD	312	13	38	8
L195	25.0	11	93	7	<LOD	331	19	36	8
L2215	27.1	25	254	19	4	409	43	80	24
L2250	27.6	13	123	10	2	354	28	42	10

to be continued on the following page

sample	depth [m]	Y [ppm]	Zr [ppm]	Nb [ppm]	Sn [ppm]	Ba [ppm]	La [ppm]	Ce [ppm]	Pb [ppm]
L2440	30.2	12	124	9	<LOD	353	21	44	10
L2540	31.2	13	105	8	3	404	19	41	12
L2640	32.5	15	130	10	6	410	25	60	11
L2870	36.5	14	120	8	2	373	20	31	13
L2960	38.1	14	113	9	3	408	25	53	10
L29130	38.8	13	114	9	2	382	31	54	9
L3190	43.0	13	123	9	<LOD	378	23	54	11
L3290	44.6	14	111	9	3	412	19	46	9
L3350	45.6	13	126	12	2	316	30	61	12
L3430	46.8	15	155	11	3	375	20	64	12
L3475	47.3	17	149	12	3	349	33	57	15
L34130	47.7	12	149	14	<LOD	189	14	28	5
L35	48.0	8	81	2	5	15	22	37	4

Tab. A-10: Elemental concentrations of bulk sediment samples of site H measured with energy dispersive X-ray fluorescence analysis (EDX) (LOD = limit of detection) – part I.

sample	depth [m]	As [ppm]	Fe ₂ O ₃ [wt-%]	CaO [wt-%]	TiO ₂ [wt-%]	MnO [wt-%]	Ni [ppm]	Cu [ppm]	Zn [ppm]	Rb [ppm]	Sr [ppm]
H0115	0.3	14	4.8	1.4	0.6	0.08	38	33	81	111	82
H0240	1.3	23	6.9	1.1	0.7	0.14	48	39	108	154	84
H0380	2.8	19	6.3	1.1	0.7	0.10	41	37	101	141	82
H0440	4.1	12	4.8	1.3	0.6	0.07	31	35	69	105	74
H0530	5.2	16	7.1	0.6	0.7	0.11	43	39	108	165	85
H0670	6.3	16	6.3	1.6	0.7	0.10	46	41	100	128	87
H0750	7.1	11	3.9	1.2	0.5	0.07	26	26	64	93	78
H07100	7.7	10	5.0	1.4	0.6	0.09	31	27	80	109	73
H0860	8.7	8	5.4	1.7	0.6	0.09	25	25	78	101	82
H08140	9.6	12	6.1	1.4	0.7	0.11	42	43	102	131	83
H0970	10.9	15	5.9	1.8	0.7	0.11	33	36	92	125	80
H1030	11.7	11	4.7	1.5	0.6	0.07	29	28	74	107	82
H1090	12.4	7	3.1	1.0	0.4	0.03	20	18	54	83	81
H1125	12.8	14	6.3	1.7	0.7	0.12	34	34	79	120	86
H1150	13.2	5	2.6	0.6	0.3	0.03	24	14	45	100	94
H1180	13.6	27	5.9	1.4	0.7	0.11	40	36	103	142	101
H1345	14.7	7	2.9	0.8	0.4	0.03	21	19	41	83	84
H1425	16.1	6	2.3	0.5	0.3	0.03	24	13	38	86	82
H1450	16.6	13	5.3	1.6	0.6	0.08	35	27	81	106	88
H1530	17.3	5	2.2	0.5	0.3	0.03	22	19	40	93	83
H1610	18.2	5	2.3	0.6	0.3	0.02	21	10	40	82	84
H1860	20.8	5	2.2	0.5	0.3	0.02	16	19	38	78	74
H1960	22.3	5	2.1	0.4	0.2	<LOD	11	16	31	75	68
H2020	23.2	6	2.7	0.4	0.2	0.03	18	10	43	105	77
H2220	26.0	5	2.4	0.5	0.3	0.03	21	17	36	80	78
H2320	26.4	1	1.9	0.4	0.2	<LOD	12	10	31	86	78

to be continued on the following page

APPENDIX

sample	depth [m]	As [ppm]	Fe ₂ O ₃ [wt-%]	CaO [wt-%]	TiO ₂ [wt-%]	MnO [wt-%]	Ni [ppm]	Cu [ppm]	Zn [ppm]	Rb [ppm]	Sr [ppm]
H2450	27.4	4	2.3	0.5	0.3	0.02	15	14	34	84	81
H2535	28.2	6	1.3	0.3	0.1	<LOD	11	13	22	65	41
H2655	28.8	4	0.7	0.2	0.1	<LOD	13	13	23	92	46
H2750	29.8	10	0.5	0.1	0.1	<LOD	13	8	25	54	30
H2850	31.1	7	1.6	0.3	0.2	<LOD	23	16	30	73	50
H2910	32.0	11	1.9	0.2	0.3	<LOD	17	10	36	87	40
H2960	33.2	9	1.4	0.2	0.2	<LOD	13	17	32	66	37
H3030	34.2	8	2.0	0.3	0.2	<LOD	11	16	41	80	57
H3055	34.8	6	1.7	0.2	0.2	<LOD	19	17	51	85	58
H3180	36.1	4	1.1	0.2	0.2	<LOD	18	10	31	68	46
H31120	36.6	4	2.0	0.3	0.3	<LOD	26	18	51	96	63
H3250	38.2	3	1.1	0.2	0.2	<LOD	11	10	26	65	47
H3305	39.0	8	3.0	0.7	0.3	0.03	42	18	48	82	69
H3330	39.8	4	2.2	0.4	0.4	<LOD	21	15	60	109	76
H3360	41.2	4	0.9	0.2	0.2	<LOD	15	34	32	74	52
H3415	41.6	8	1.9	0.3	0.3	<LOD	32	12	44	89	56
H3445	42.4	2	0.5	0.1	0.1	<LOD	16	38	25	48	30
H3515	44.1	30	1.5	0.3	0.2	<LOD	12	21	32	71	65
H3535	44.3	10	1.8	0.2	0.2	<LOD	11	9	42	88	55
H36540	45.0	4	1.8	0.3	0.2	<LOD	24	12	39	72	59
H3680	45.9	3	1.6	0.3	0.3	<LOD	19	15	48	93	86
H3740	46.8	2	2.0	0.3	0.4	<LOD	22	13	62	115	69
H37120	47.6	2	1.5	0.3	0.3	<LOD	21	16	37	83	64
H3815	49.3	4	1.7	0.3	0.3	<LOD	20	13	42	76	59
H4025	51.0	3	1.6	0.3	0.3	<LOD	23	13	53	103	76
H4090	52.1	4	2.1	0.4	0.4	<LOD	28	15	45	76	73
H40140	53.0	3	2.1	0.3	0.3	<LOD	22	47	49	78	67
H41535	53.6	3	2.0	0.3	0.3	<LOD	19	14	43	92	74
H4165	54.9	4	1.9	0.3	0.2	<LOD	11	17	27	66	51
H42	55.0	4	2.6	0.3	0.3	<LOD	22	23	43	71	40

Tab. A-11: Elemental concentrations of bulk sediment samples of site H measured with energy dispersive X-ray fluorescence analysis (EDX) (LOD = limit of detection) – part II.

sample	depth [m]	Y [ppm]	Zr [ppm]	Nb [ppm]	Sn [ppm]	Ba [ppm]	La [ppm]	Ce [ppm]	Pb [ppm]
H0115	0.3	29	264	14	7	460	47	108	31
H0240	1.3	39	202	16	6	555	55	122	39
H0380	2.8	34	193	14	7	504	45	104	32
H0440	4.1	29	239	13	4	402	52	72	24
H0530	5.2	35	180	16	4	569	49	104	38
H0670	6.3	37	245	17	4	479	37	102	42
H0750	7.1	24	232	13	3	415	38	74	26
H07100	7.7	30	256	16	4	447	52	97	31
H0860	8.7	28	227	14	4	410	46	95	40
H08140	9.6	37	241	17	5	507	60	106	45

to be continued on the following page

sample	depth [m]	Y [ppm]	Zr [ppm]	Nb [ppm]	Sn [ppm]	Ba [ppm]	La [ppm]	Ce [ppm]	Pb [ppm]
H0970	10.9	37	245	18	5	501	50	94	37
H1030	11.7	31	246	14	3	426	43	90	36
H1090	12.4	18	178	12	3	385	31	70	19
H1125	12.8	34	366	16	4	475	55	111	33
H1150	13.2	16	128	10	<LOD	461	14	47	20
H1180	13.6	41	201	15	4	469	52	109	59
H1345	14.7	20	242	13	2	387	44	80	16
H1425	16.1	15	144	10	2	437	28	51	15
H1450	16.6	30	238	15	4	417	38	92	44
H1530	17.3	16	156	9	3	445	26	60	16
H1610	18.2	16	155	11	3	408	30	70	15
H1860	20.8	14	140	11	3	390	23	50	15
H1960	22.3	13	121	9	2	366	36	50	11
H2020	23.2	14	106	11	4	486	23	50	17
H2220	26.0	18	142	13	3	385	37	53	13
H2320	26.4	13	108	8	5	500	59	105	109
H2450	27.4	14	107	11	4	423	25	46	11
H2535	28.2	14	118	8	4	287	24	40	11
H2655	28.8	13	88	6	3	471	20	39	32
H2750	29.8	10	65	4	<LOD	247	18	24	60
H2850	31.1	12	109	8	<LOD	338	21	32	9
H2910	32.0	17	145	13	3	341	19	65	16
H2960	33.2	16	94	6	2	312	24	63	17
H3030	34.2	17	111	9	3	394	27	59	11
H3055	34.8	17	117	8	3	406	28	49	12
H3180	36.1	12	113	7	2	354	21	37	10
H31120	36.6	17	138	11	3	430	26	63	14
H3250	38.2	12	88	8	<LOD	344	17	28	10
H3305	39.0	16	141	10	3	389	24	64	17
H3330	39.8	20	145	11	4	470	25	45	13
H3360	41.2	12	132	10	2	371	31	41	10
H3415	41.6	26	209	12	3	402	48	72	15
H3445	42.4	8	64	5	<LOD	230	12	28	9
H3515	44.1	13	140	9	<LOD	336	24	45	14
H3535	44.3	18	118	10	2	382	36	49	12
H36540	45.0	17	126	11	<LOD	355	30	58	11
H3680	45.9	18	128	11	3	484	34	52	14
H3740	46.8	23	175	15	4	442	32	65	21
H37120	47.6	18	136	12	3	395	28	56	11
H3815	49.3	15	113	9	3	369	33	52	10
H4025	51.0	18	122	11	3	510	37	70	14
H4090	52.1	18	144	14	6	630	57	121	12
H40140	53.0	17	149	13	2	351	28	52	11
H41535	53.6	16	144	12	4	415	44	62	15
H4165	54.9	13	113	9	<LOD	313	16	40	10
H42	55.0	18	130	9	3	256	30	60	16

Tab. A- 12: Elemental concentrations of sediment material of selected samples of both sites after total acid digestion measured with ICP-MS part -I.

sample	depth [m]	Na	Mg	Al	K	Ca	Ti	Mn	Fe
L0135	0.4	6.3	11.6	64	22	13.4	5.2	1.1	44
L0650	7.3	6.5	8.5	45	18	9.7	4.6	0.6	32
L08120	10.8	4.7	5.0	48	24	2.6	5.1	0.1	19
L10110	13.8	0.9	2.9	43	10	0.8	3.5	0.2	23
L1640	21.9	1.7	5.2	56	19	1.1	4.6	0.4	33
L17045	23.8	1.3	0.8	18	14	0.4	0.7	0.9	15
L2250	27.5	2.0	2.5	28	16	0.8	2.0	0.1	12
L2640	32.4	2.8	3.7	37	18	1.0	2.4	0.1	17
L29130	38.8	2.9	2.9	30	17	1.1	1.9	0.1	14
L3475	47.2	3.4	5.2	34	15	2.8	2.6	0.2	21
H0380	2.8	5.8	10.5	64	24	7.9	5.1	1.0	41
H0860	8.7	5.8	8.9	49	19	13.0	4.7	0.9	38
H1180	13.6	4.0	9.9	63	24	10.6	5.4	1.0	38
H1345	14.6	6.3	5.7	35	17	6.9	3.4	0.4	20
H1860	20.8	6.0	4.3	29	17	4.6	2.3	0.3	17
H2450	27.3	6.2	4.9	32	18	4.4	2.3	0.3	17
H2750	29.8	1.4	1.0	17	13	0.6	0.9	0.04	5
H2910	32.0	1.9	2.5	32	16	1.0	2.2	0.1	15
H3250	37.2	3.4	2.3	25	14	1.4	1.5	0.1	10
H3515	41.6	3.7	2.0	21	15	2.2	1.5	0.1	12
H36540	44.9	3.3	2.6	27	15	2.0	2.1	0.1	15
H3740	46.8	3.6	4.2	36	20	2.0	2.8	0.2	16
H3930	49.9	4.3	5.1	41	22	2.4	3.0	0.2	16
H41535	53.5	4.2	3.7	34	18	2.3	2.7	0.1	17

Tab. A- 13: Elemental concentrations of sediment material of selected samples of both sites after total acid digestion measured with ICP-MS part -II.

sample	depth [m]	V	Cr	Co	Ni	Cu	Zn	As	Rb	Pb
		[mg/kg]								
L0135	0.4	130	107	20	64	64	149	23.8	127	68
L0650	7.3	99	77	16	39	35	106	8.0	99	24
L08120	10.8	141	83	11	47	54	143	10.6	145	31
L10110	13.8	66	57	5	18	21	62	3.4	88	18
L1640	21.9	100	61	7	32	24	76	2.6	117	21
L17045	23.8	21	28	4	21	13	26	24.6	65	16
L2250	27.5	38	30	3	18	17	48	1.7	78	13
L2640	32.4	55	40	5	22	11	53	2.5	93	15
L29130	38.8	43	38	6	19	10	39	1.7	78	13
L3475	47.2	58	127	15	152	23	53	4.5	81	17
H0380	2.8	135	94	20	49	40	113	9.9	120	32
H0860	8.7	100	80	16	39	34	96	6.9	111	40
H1180	13.6	130	80	19	47	37	120	17.9	84	61
H1345	14.6	61	57	10	25	13	55	5.3	89	22
H1860	20.8	46	42	8	20	19	58	4.3	89	16
H2450	27.3	46	43	9	20	8	43	4.3	95	16
H2750	29.8	21	17	4	9	6	23	10.2	59	53
H2910	32.0	56	44	15	25	11	57	11	89	17
H3250	37.2	33	30	7	16	8	49	2.2	72	13
H3515	41.6	27	36	5	16	15	32	35.3	77	13
H36540	44.9	41	48	6	18	8	41	1.6	73	14
H3740	46.8	58	52	8	25	11	131	1.3	108	21
H3930	49.9	61	50	9	28	13	73	1.9	122	18
H41535	53.5	55	48	6	19	9	47	1.4	91	17

Tab. A-14: Elemental concentrations of selected bulk sediment samples of both sites measured with wavelength dispersive X-ray fluorescence analysis (WDX).

sample	depth [m]	Na ₂ O [wt-%]	Al ₂ O ₃ [wt-%]	SiO ₂ [wt-%]	P ₂ O ₅ [wt-%]	K ₂ O [wt-%]	V [ppm]	Cr [ppm]	Co [ppm]
L0135	0.4	0.7	15	60	0.13	2.6	109	108	23
L0360	3.1	0.6	17	59	0.12	3.1	119	105	24
L0445	4.1	0.7	9	78	0.07	2.0	70	82	18
L0650	7.6	0.7	12.	69	0.11	2.2	89	89	17
L06100	8.0	0.4	21	54	0.06	3.2	147	116	22
L08120	10.8	0.5	17	55	0.05	2.9	121	102	15
L10110	13.8	0.1	9	76	0.02	1.2	72	82	10
L11105	15.1	0.2	16	63	0.07	2.3	111	108	15
L1410	18.6	0.3	13	71	0.04	2.3	92	91	44
L1640	21.9	0.2	12	71	0.05	2.3	82	86	10
L17045	23.8	0.2	4	90	0.05	1.8	12	33	6
L2250	27.5	0.3	6	87	0.03	2.0	34	54	7
L2640	32.4	0.3	8	83	0.03	2.1	45	63	10
L29130	38.8	0.4	7	86	0.03	2.0	44	58	9
L3475	47.3	0.4	8	80	0.05	1.8	2	182	16
H0380	2.8	0.6	16	62	0.12	2.9	114	96	23
H0440	4.1	0.8	12	70	0.10	2.3	96	88	18
H0640	6.3	0.7	15	62	0.13	2.6	103	111	21
H0860	8.7	0.7	12	65	0.12	2.3	93	92	18
H0970	10.9	0.6	14	61	0.14	2.6	104	98	21
H1150	13.2	0.9	9	80	0.05	2.5	44	57	14
H1180	13.6	0.5	16	58	0.12	2.8	118	97	22
H1345	14.7	0.8	8	80	0.05	2.1	55	70	13
H1450	16.6	0.7	12	64	0.11	2.3	88	93	21
H1870	20.8	0.7	7	84	0.05	2.1	31	52	14
H2450	27.3	0.8	7	83	0.05	2.3	34	59	13
H2750	29.8	0.2	3	93	0.03	1.5	19	36	11
H2910	32.0	0.2	7	84	0.04	2.1	48	62	15
H3120	36.1	0.4	6	88	0.02	1.9	33	46	11
H3250	38.2	0.4	5	89	0.02	1.9	29	44	9
H3250	38.2	0.4	5	88	0.02	1.9	28	42	12
H3415	41.6	0.5	9	81	0.05	2.2	68	324	20
H3515	44.1	0.5	5	91	0.03	1.9	22	54	10
H36540	44.8	0.4	6	85	0.04	1.9	37	59	12
H3740	46.8	0.4	9	80	0.04	2.5	47	83	12
H3930	49.8	0.5	9	75	0.03	2.5	55	74	11
H4105	53.6	0.3	6	6	0.03	1.9	32	51	8

Tab. A-15: Results of X-ray diffraction analysis (XRD) of bulk sediment samples of site L (LOD =limit of detection).

sample	depth [m]	Quartz [%]	Plagioclase [%]	Kalifeld-spar [%]	Mica [%]	Kaolinite [%]	Dolomite [%]	Calcite [%]	further phases [%]
L0135	0.4	45	2	2	32	10	0.5	3	5.5
L0225	0.9	45	4	2	17	6	0	3	23.0
L0245	1.3	41	3	3	24	11	0	<LOD	18.0
L0360	3.1	31	2	<LOD	21	10	0	0.5	35.5
L0445	4.1	65	4	5	21	6	<LOD	0.5	0.0
L0490	4.6	43	3	1	17	9	1	1	25.0
L0580	5.9	35	2	<LOD	17	9	<LOD	<LOD	37.0
L0650	7.3	52	2	2	18	5	0.5	1	19.5
L06100	8.0	26	1	<LOD	20	10	0.5	<LOD	42.5
L0760	9.5	27	1	2	19	10	0.5	<LOD	40.5
L0860	10.1	40	2	3	19	8	0.3	<LOD	27.8
L08120	10.8	32	2	<LOD	26	7	0.6	0.5	31.9
L0990	12.0	19	1	<LOD	25	7	0.5	<LOD	47.5
L1025	12.8	63	<LOD	<LOD	<LOD	<LOD	<LOD	<LOD	37.0
L10110	13.8	66	<LOD	<LOD	<LOD	<LOD	<LOD	<LOD	34.0
L11105	15.1	38	1	2	15	10	<LOD	<LOD	34.0
L1245	16.4	45	<LOD	<LOD	15	3	<LOD	<LOD	37.0
L1335	17.9	48	1	3	23	5	0.4	<LOD	19.6
L1410	18.6	58	<LOD	3	18	9	0.4	<LOD	11.6
L14100	19.7	38	1	<LOD	23	8	0.6	<LOD	29.4
L1540	20.4	38	<LOD	2	10	2	0.4	<LOD	47.6
L15140	21.4	52	<LOD	4	29	7	0.2	<LOD	7.8
L1640	21.9	52	<LOD	<LOD	17	10	<LOD	<LOD	21.0
L1690	22.4	52	<LOD	7	32	8	<LOD	<LOD	1.0
L16140	22.9	55	<LOD	<LOD	15	6	0.4	<LOD	23.7
L17045	23.7	82	1	15	<LOD	<LOD	<LOD	<LOD	2.0
L1805	24.9	80	1	11	8	<LOD	<LOD	<LOD	0.0
L1905	25.0	80	<LOD	15	<LOD	<LOD	<LOD	<LOD	5.0
L2215	27.1	47	0.4	9	18	<LOD	<LOD	<LOD	25.6
L2250	27.6	78	1	16	12	<LOD	0.5	<LOD	0.0
L2460	30.2	80	1	18	18	4	0.5	<LOD	0.0
L2540	31.2	70	3	14	21	4	0.5	<LOD	0.0
L2640	32.5	68	2	15	16	3	0.5	<LOD	0.0
L2870	36.5	78	6	16	16	<LOD	0.5	<LOD	0.0
L2960	38.1	78	1	10	10	<LOD	<LOD	<LOD	1.0
L29130	38.8	75	<LOD	11	17	3	<LOD	<LOD	0.0
L3190	43.0	74	2	7	16	<LOD	0.4	<LOD	0.6
L3290	44.6	73	2	15	19	<LOD	0.4	<LOD	0.0
L3350	45.6	75	2	5	16	<LOD	<LOD	<LOD	2.0
L3430	46.8	90	<LOD	14	<LOD	<LOD	0.4	0.5	0.0
L3475	47.3	60	<LOD	8	20	4	<LOD	<LOD	8.0
L34120	47.7	90	<LOD	14	<LOD	<LOD	0.4	0.5	0.0

Tab. A-16: Results of X-ray diffraction analysis (XRD) of bulk sediment samples of site H (LOD =limit of detection).

sample	depth [m]	Quartz [%]	Plagioclase [%]	Kalifeld-spar [%]	Mica [%]	Kaolinite [%]	Dolomite [%]	Calcite [%]	further phases [%]
H0115	0.3	45	4	3	25	7	0.35	1	14.6
H0240	1.3	32	2	<LOD	27	9	1	1	28.0
H0380	2.8	36	3	<LOD	35	10	0.5	1	14.5
H0440	4.1	45	2	2	31	8	0.3	1	10.7
H0530	5.2	31	3	<LOD	25	10	1	<LOD	30.0
H0670	6.3	36	2	2	16	6	0.5	1	36.5
H0750	7.1	55	4	4	8	5	0.5	1	22.5
H0860	8.7	42	4	2	22	8	0.5	1	20.5
H0970	10.9	37	1	2	15	<LOD	0.3	1	43.7
H1030	11.7	45	5	<LOD	24	8	<LOD	1	17.0
H1090	12.4	60	3	6	25	9	0.3	0.5	0.0
H1150	13.2	60	7	11	13	5	0.3	0.5	3.2
H1180	13.6	36	9	18	7	<LOD	1	<LOD	29
H1345	14.7	55	4	10	15	5	<LOD	0.3	10.7
H1450	16.6	38	3	2	10	5	0.25	1	40.8
H1610	18.2	60	2	6	9	5	<LOD	<LOD	18.0
H1860	20.8	55	6	21	15	4	0.3	<LOD	0.0
H2020	23.2	55	3	13	15	4	0.6	<LOD	9.4
H2220	26.0	60	2	10	11	3	<LOD	<LOD	14.0
H2450	27.4	55	3	13	14	5	0.2	<LOD	9.8
H2535	28.2	75	<LOD	14	<LOD	<LOD	0.24	<LOD	10.8
H2750	29.8	85	1	9	<LOD	<LOD	0.39	<LOD	4.6
H2850	31.1	80	1	8	10	3	0.4	<LOD	0.0
H2910	32.0	60	<LOD	14	13	5	0.2	<LOD	7.8
H2960	33.2	87	2	8	10	<LOD	0.4	<LOD	0.0
H3030	34.2	77	0	11	18	3	0.3	<LOD	0.0
H3055	34.8	55	0	16	18	3	0.5	<LOD	7.5
H3180	36.1	68	2	15	16	<LOD	0.2	<LOD	0.0
H31120	36.6	63	2	9	23	5	0.4	<LOD	0.0
H3250	38.2	70	<LOD	24	9	<LOD	<LOD	<LOD	0.0
H3305	39.0	52	2	8	8	3	0.4	<LOD	26.3
H3330	39.8	85	<LOD	16	<LOD	<LOD	<LOD	<LOD	0.0
H3360	41.2	88	<LOD	12	<LOD	<LOD	<LOD	<LOD	0.0
H3415	41.6	70	<LOD	10	10	<LOD	0.5	<LOD	9.5
H3445	42.4	60	<LOD	9	12	<LOD	0.23	<LOD	18.8
H3515	44.1	79	2	9	10	<LOD	0.32	<LOD	0.0
H3535	44.3	55	2	12	13	<LOD	0.32	<LOD	17.7
H3740	46.8	53	3	13	25	<LOD	0.46	<LOD	5.5
H37120	47.6	60	2	18	19	<LOD	0.32	<LOD	0.7
H3815	49.3	58	5	11	13	<LOD	0.44	<LOD	12.6
H3930	49.9	50	3	18	39	4	0.3	<LOD	0.0
H4025	51.0	55	<LOD	17	24	<LOD	0.3	<LOD	3.7
H4090	52.1	70	2	10	16	4	0.3	<LOD	0.0
H41535	53.6	75	<LOD	9	16	3	0.3	<LOD	0.0
H4165	54.9	63	<LOD	12	19	4	<LOD	<LOD	2.0

Tab. A-17: Content of total organic (TOC) and inorganic carbon (TIC) as well total sulphur (TS) in bulk sediment samples of site L and Red River sediment.

sample	depth [m]	TOC [wt-%]	TIC [wt-%]	TS [wt-%]
L0135	0.4	0.38	0.67	0.013
L0225	0.9	0.14	0.48	0.033
L0245	1.3	0.20	0.41	0.030
L0275	1.8	0.17	0.61	0.040
L0360	3.1	0.15	0.45	0.016
L0445	4.1	0.09	0.25	0.051
L0490	4.6	0.21	0.59	0.026
L0580	5.9	0.27	0.55	0.014
L0650	7.3	0.20	0.49	0.011
L06100	8.0	0.22	0.42	0.013
L0760	9.5	0.09	0.19	0.006
L0860	10.1	0.11	0.27	0.084
L08120	10.8	3.78	0.68	0.581
L0990	12.0	4.55	0.75	4.049
L1025	12.8	3.10	0.66	0.893
L10110	13.8	0.12	0.45	0.009
L11105	15.1	0.08	0.57	0.016
L1245	16.4	0.06	0.49	0.006
L1335	17.9	0.05	0.19	0.009
L1410	18.6	0.69	0.25	0.272
L14100	19.7	0.10	0.74	0.010
L1540	20.4	0.08	0.67	0.010
L15140	21.4	0.07	0.53	0.007
L1640	21.9	0.06	0.42	0.005
L1690	22.4	0.04	0.05	0.008
L16125	22.8	0.01	0.10	0.083
L16140	22.9	0.02	0.04	0.005
L17045	23.7	0.02	0.03	0.009
L1805	24.9	0.02	0.04	0.014
L1905	25.0	0.01	0.03	0.011
L2215	27.1	0.05	0.43	0.009
L2250	27.6	0.03	0.01	0.006
L2460	30.2	0.01	0.04	0.011
L2540	31.2	0.03	0.02	0.010
L2640	32.5	0.02	0.01	0.006
L2870	36.5	< LOD	0.04	0.007
L2960	38.1	< LOD	0.05	0.005
L29130	38.8	0.00	0.02	0.009
L3190	43.0	0.02	0.03	0.008
L3290	44.6	0.01	0.02	0.007
L3350	45.6	0.03	0.02	0.012
L3430	46.8	0.01	0.02	0.007
L3475	47.3	0.06	0.19	0.039
L34120	47.7	0.03	0.03	0.011
L35	>58	0.01	0.04	0.008
RR	0	0.08	0.18	0.013

Tab. A-18: Content of total organic (TOC) and inorganic carbon (TIC) as well total sulphur (TS) in bulk sediment samples of site H.

sample	depth [m]	TOC [wt-%]	TIC [wt-%]	TS [wt-%]
H0115	0.3	0.11	0.47	0.010
H0240	1.3	0.08	0.39	0.007
H0380	2.8	0.05	0.36	0.006
H0440	4.1	0.06	0.37	0.005
H0530	5.2	0.10	0.23	0.008
H0670	6.3	0.08	0.47	0.006
H0750	7.1	0.06	0.30	0.006
H07100	7.7	0.56	0.76	0.039
H0860	8.7	0.40	0.89	0.014
H08140	9.6	0.82	0.91	0.029
H0970	10.9	0.79	0.98	0.017
H1030	11.7	0.43	0.75	0.014
H1090	12.4	0.06	0.32	0.007
H1125	12.8	0.58	0.96	0.017
H1150	13.2	0.03	0.17	0.009
H1180	13.6	0.80	0.77	0.018
H1345	14.7	0.13	0.18	0.006
H1425	16.1	0.02	0.12	0.007
H1450	16.5	0.43	0.74	0.016
H1530	17.3	0.03	0.09	0.005
H1610	18.2	0.03	0.08	0.006
H1860	20.8	0.02	0.07	0.003
H1960	22.3	0.03	0.05	0.004
H2020	23.2	0.03	0.13	0.004
H2220	26.0	0.03	0.08	0.006
H2320	26.4	0.02	0.06	0.005
H2450	27.4	0.03	0.07	0.005
H2535	28.0	0.01	0.09	0.005
H2655	28.8	<LOD	0.05	0.004
H2750	29.8	0.01	0.02	0.004
H2850	31.1	0.03	0.08	0.009
H2910	32.0	0.01	0.03	0.004
H2960	33.2	0.01	0.03	0.007
H3030	34.2	0.02	0.02	0.005
H3055	34.8	0.02	0.01	0.004

to be continued on the following page

sample	depth [m]	TOC [wt-%]	TIC [wt-%]	TS [wt-%]
H3180	36.1	0.01	0.01	0.004
H31120	36.6	0.02	0.01	0.006
H3250	38.2	0.02	0.02	0.005
H3305	39.0	0.04	0.21	0.004
H3330	39.8	0.02	0.04	0.004
H3360	41.2	<LOD	0.05	0.005
H3415	41.6	0.02	0.03	0.004
H3445	42.4	0.01	0.01	0.004
H3515	44.1	0.02	0.05	0.005
H3535	44.3	0.02	0.02	0.004
H3605	45.0	0.01	0.02	0.004
H3680	45.9	0.02	0.01	0.005
H3740	46.8	0.02	0.03	0.004
H37120	47.8	0.10	0.02	0.005
H3815	49.3	0.03	0.07	0.005
H3930	49.9	0.03	0.03	0.005
H4025	51.0	0.03	0.03	0.005
H4090	52.1	0.02	0.04	0.006
H40140	53.0	0.01	0.03	0.003
H415-35	53.6	0.04	0.03	0.009
H4165	54.9	0.02	0.02	0.004
H42	55.0	0.04	0.09	0.005

A.4.2 MEASUREMENTS OF INDIVIDUAL GRAINS

A.4.2.1 GRAINS OF UNTREATED SAMPLES

Tab. A-19: Elemental concentrations recorded by means of μ S-XRF analysis through an untreated coated grain of L17045 (No. 90).

μm	As	Fe	K	Mn	Ca	Ti	V	Cr	Ni	Cu	Zn	Ga
	[mg/kg]	[g/kg]	[mg/kg]									
850	14.3	10.3	84.6	2908	196	1653	126	8	16	6	32	7.3
829	8.7	6.3	94.0	1534	71	1987	112	14	9	4	18	6.5
808	23.7	22.5	12.4	2075	610	1971	56	56	36	7	29	1.9
786	1.8	1.1	1.1	84	15	993	12	5	2	1	8	0.8
765	1.1	0.4	0.7	30	33	901	11	5	2	2	7	0.9
744	1.1	0.3	0.6	22	45	763	0	5	2	2	5	0.7
723	0.8	0.3	0.4	19	33	861	7	6	2	1	6	0.7
701	0.9	0.3	0.6	19	33	803	5	4	1	1	11	0.7
680	1.1	0.3	0.8	17	44	759	7	5	2	1	7	0.9
659	0.9	0.3	0.9	14	43	727	1	9	3	2	7	0.7
638	1.4	0.3	1.0	21	65	708	11	7	2	2	7	0.7
616	0.7	0.3	1.0	19	31	758	0	5	2	2	5	0.5
595	1.2	0.3	0.5	22	100	768	10	6	2	2	5	0.7
574	1.0	0.2	0.4	13	98	972	15	7	2	1	6	0.7
553	0.9	0.2	0.2	20	22	1202	2	3	2	2	6	0.9
531	0.7	0.2	0.1	6	35	1798	6	6	2	2	9	0.8
510	1.0	0.2	0.2	5	63	2351	1	3	1	3	11	0.5
489	1.1	0.1	0.1	22	65	3066	23	8	2	1	8	0.9
468	0.7	0.2	0.2	8	63	3816	23	8	2	2	10	1.1
446	0.6	0.2	0.2	11	49	3587	34	10	2	2	14	0.7
425	0.8	0.2	0.3	11	86	2365	38	6	1	2	15	0.5
404	1.0	0.2	0.3	21	50	2588	16	6	2	2	9	0.8
383	0.7	0.2	0.1	19	72	2386	11	6	2	2	9	0.7
361	1.0	0.3	0.3	21	57	2137	0	4	1	1	11	0.5
340	1.3	0.4	0.3	28	58	2346	32	10	2	2	28	0.8
319	0.5	0.5	0.4	36	116	2253	5	5	2	1	9	0.7
298	1.4	0.6	0.2	41	73	2404	23	8	3	2	9	1.0
276	1.3	0.8	0.5	70	68	1638	18	5	2	1	7	0.9
255	1.0	0.9	0.4	76	33	1430	5	5	2	2	9	0.7
234	1.9	1.0	0.4	81	58	1707	9	9	3	1	7	1.0
213	2.5	0.9	0.3	73	74	1583	23	3	2	2	8	0.6
191	2.0	0.7	0.3	60	54	1541	13	8	2	2	6	0.4
170	1.2	0.7	0.3	42	54	1537	1	7	2	2	8	0.9
149	1.8	1.1	0.5	97	40	1515	10	2	3	2	6	0.7
128	2.3	1.8	0.8	132	78	1156	2	4	5	3	12	0.6
106	1.8	1.9	1.0	181	30	1372	17	15	3	2	6	0.9
85	1.7	1.5	0.8	111	19	988	0	12	4	2	7	0.7
64	4.8	5.4	2.3	458	164	1185	5	23	7	3	13	0.8
43	19.7	16.9	8.8	1620	399	4344	41	66	21	8	24	1.1
21	14.0	13.4	4.8	1456	524	1477	4	68	21	16	25	3.0
0	10.6	11.3	5.4	965	291	1032	32	22	15	5	18	2.1

Tab. A-20: Elemental concentrations recorded by means of μ S-XRF analysis through an untreated coated grain of H3515 (No. 100).

μm	As	Fe	K	Mn	Ca	Ti	V	Cr	Ni	Cu	Zn	Ga
	[mg/kg]	[g/kg]	[mg/kg]									
210	13.0	5	88	48	328	1303	19	8	5	5	15	1.5
206	10.0	3	171	14	74	1199	27	18	2	3	12	1.8
202	7.8	2	267	15	205	1392	63	13	2	4	9	2.2
197	9.2	2	204	4	408	1333	39	2	1	3	13	2.6
193	17.3	6	124	50	1077	1850	36	5	5	6	18	3.5
189	28.3	10	62	70	1670	2143	41	41	6	9	24	2.8
185	24.8	7	57	69	2576	2494	21	8	40	7	21	2.9
181	19.8	8	18	96	1475	1805	25	15	7	7	25	1.8
176	27.8	7	18	79	2489	2302	10	17	7	10	27	2.5
172	38.5	9	31	78	2968	2147	0	21	13	12	37	3.9
168	43.1	12	44	110	1380	2803	145	42	13	14	34	4.9
164	43.7	13	139	69	1065	2232	61	25	19	16	52	7.7
160	67.1	16	65	102	1729	3340	47	24	18	20	52	7.3
155	72.4	17	38	140	2195	3019	20	63	17	19	47	8.2
151	68.1	18	24	161	2032	3814	8	54	13	17	39	5.2
147	48.5	14	17	148	1807	4041	7	46	13	13	33	5.3
143	29.4	12	9	97	1781	2013	80	23	10	11	23	3.8
139	37.6	10	12	89	2605	2901	6	34	8	9	21	3.1
134	21.8	6	17	46	1219	1513	36	20	8	6	17	2.0
130	21.2	6	17	58	1463	1615	13	34	8	7	18	2.3
126	26.7	9	10	79	2766	1900	34	21	11	7	26	2.8
122	27.5	7	9	80	759	1700	53	29	5	7	17	2.0
118	17.4	4	4	35	730	1307	9	8	4	7	14	2.1
113	8.8	2	1	17	213	1035	20	0	4	3	12	1.6
109	11.2	2	1	13	43	1035	24	2	2	4	12	1.7
105	7.6	2	1	12	168	1024	16	3	2	11	12	1.4
101	9.0	2	1	19	150	983	31	0	3	6	11	0.7
97	6.0	1	1	2	82	953	25	7	3	4	11	1.6
92	5.5	1	1	6	125	948	25	3	3	3	9	1.2
88	6.4	1	1	15	54	945	14	2	2	3	11	1.0
84	8.3	1	1	8	70	1024	24	3	3	4	11	1.3
80	4.7	1	1	12	147	1106	21	2	3	3	10	0.7
76	4.3	1	1	5	147	1133	15	6	2	2	11	1.4
71	5.0	1	1	16	228	1167	8	8	2	3	12	0.7
67	6.2	1	1	12	329	1188	48	8	3	3	11	1.1
63	11.5	3	2	27	640	1152	26	6	6	6	15	0.9
59	15.2	4	2	29	621	1300	40	2	5	6	17	2.1
55	25.0	6	3	58	642	1385	29	13	10	11	29	2.6
50	45.2	11	3	72	417	1566	19	23	21	16	52	4.9

to be continued on the following page

APPENDIX

μm	As	Fe	K	Mn	Ca	Ti	V	Cr	Ni	Cu	Zn	Ga
	[mg/kg]	[g/kg]	[mg/kg]									
46	45.8	11	2	60	516	1380	15	9	23	17	55	5.1
42	37.2	8	2	78	407	1220	29	1	15	13	37	6.4
38	22.5	4	2	41	345	1108	8	1	7	8	20	2.3
34	19.0	3	2	23	345	1208	31	3	4	8	20	2.1
29	18.0	3	9	22	537	1238	30	8	5	9	19	1.9
25	24.1	4	3	38	556	1115	6	20	6	7	26	1.3
21	32.5	5	1	21	189	1029	21	2	5	12	47	2.2
17	15.6	3	1	28	222	1065	13	1	3	8	36	1.3
13	16.0	3	1	19	230	1026	22	1	4	9	29	1.0
8	12.7	3	4	27	376	1102	26	11	5	14	32	0.7
4	6.5	2	3	22	570	1144	2	0	3	9	19	0.7
0	36.9	24	26	341	6584	2752	6	72	24	24	49	4.6

Tab. A-21: Elemental concentrations recorded by means of μ S-XRF analysis through an untreated coated grain of H2910 (No. 90).

μm	As	Fe	K	Mn	Ca	Ti	V	Cr	Ni	Cu	Zn	Ga
	[mg/kg]	[g/kg]		[mg/kg]								
0	3.1	5.0	6.9	30	913	1567	41	42	6	4	22	2.7
4	2.4	3.5	3.0	26	703	1304	20	31	5	4	17	1.6
8	1.6	2.6	2.6	17	723	887	20	20	3	5	16	1.7
11	1.8	1.9	1.1	7	568	694	9	18	3	3	16	0.9
15	0.9	1.0	0.9	7	694	560	7	8	2	2	7	0.9
19	1.3	0.9	0.7	7	296	555	8	9	2	1	7	0.5
23	1.1	0.9	0.7	7	333	493	4	6	2	2	6	0.6
26	2.2	1.4	0.8	10	325	474	15	7	2	3	8	1.3
30	2.4	2.2	0.7	7	207	457	13	16	4	3	16	1.3
34	2.1	3.1	0.9	16	850	559	18	10	6	1	13	1.7
38	2.5	2.2	0.6	12	264	426	15	8	5	2	10	1.5
41	1.1	0.9	0.3	8	250	385	6	6	2	0	6	1.1
45	1.2	0.4	0.3	6	294	389	12	9	2	1	5	0.9
49	0.8	0.2	0.2	4	140	366	6	6	2	1	6	0.5
53	0.7	0.2	0.2	4	183	373	5	3	2	1	7	0.8
56	0.7	0.1	0.2	4	185	386	4	7	1	1	5	0.6
60	0.9	0.1	0.1	3	208	376	1	5	1	0	6	0.9
64	0.6	0.1	0.2	3	185	373	0	5	1	0	6	0.8
68	0.9	0.1	0.1	5	278	380	1	6	1	1	5	0.7
71	0.7	0.1	0.1	4	138	370	4	5	2	1	6	0.9
75	1.3	0.1	0.1	4	104	351	1	5	2	1	5	0.9
79	0.7	0.1	0.2	3	127	357	4	4	1	1	5	0.7
83	1.1	0.1	0.1	3	238	363	4	5	2	1	7	0.9
86	0.6	0.1	0.2	4	233	341	2	6	2	1	6	0.6
90	0.6	0.1	0.1	4	420	291	9	3	2	1	5	0.9
94	0.7	0.1	0.2	4	737	314	5	6	1	1	6	0.5
98	0.6	0.1	0.1	5	276	259	7	5	1	1	5	1.1
101	0.3	0.1	0.1	4	267	347	0	4	1	1	5	0.6
105	0.7	0.1	0.1	4	347	255	6	3	1	1	6	0.8
109	0.6	0.1	0.1	4	189	297	5	3	2	1	4	0.9
113	0.8	0.1	0.1	4	65	255	1	4	1	1	6	1.0
116	0.9	0.1	0.1	3	135	240	1	5	1	1	6	0.6
120	1.0	0.1	0.1	4	242	229	2	8	2	1	5	0.9
124	0.7	0.1	0.1	4	192	236	0	4	1	1	7	1.0
128	0.6	0.1	0.1	3	81	240	3	5	1	1	6	0.6
131	1.0	0.1	0.1	4	78	155	3	6	2	1	6	0.9
135	1.5	0.1	0.1	5	337	189	7	5	2	1	6	0.7
139	0.7	0.1	0.1	6	84	193	2	6	1	1	8	0.9
143	0.8	0.1	0.1	2	49	187	9	6	1	1	6	0.9
146	0.4	0.1	0.1	5	89	136	9	4	1	1	4	0.8

to be continued on the following page

APPENDIX

μm	As	Fe	K	Mn	Ca	Ti	V	Cr	Ni	Cu	Zn	Ga
	[mg/kg]	[g/kg]						[mg/kg]				
150	1.0	0.0	0.1	4	75	194	0	5	1	1	6	0.8
154	1.0	0.1	0.1	6	61	183	3	6	2	1	7	0.9
158	1.0	0.1	0.1	4	76	153	11	7	1	1	5	0.7
161	0.9	0.1	0.1	3	78	153	3	6	1	1	5	0.9
165	1.0	0.1	0.1	3	77	186	6	5	2	1	6	0.9
169	1.0	0.1	0.1	3	129	149	10	4	2	1	5	0.8
173	0.7	0.1	0.1	5	47	177	3	6	2	1	5	0.9
176	0.8	0.1	0.1	5	66	168	8	5	1	1	6	0.9
180	0.6	0.1	0.1	3	93	175	10	4	1	1	5	1.1
184	0.6	0.1	0.1	4	145	168	7	4	1	1	4	0.8
188	0.7	0.1	0.1	4	99	166	4	5	2	1	5	0.9
191	0.6	0.1	0.1	3	68	181	12	6	1	1	5	0.5
195	0.9	0.1	0.1	5	85	163	4	4	1	1	5	0.8
199	1.1	0.1	0.1	3	88	199	0	6	2	1	4	1.0
203	0.5	0.1	0.1	3	90	180	9	3	2	1	5	0.9
206	0.5	0.1	0.1	4	90	219	14	4	2	1	5	0.8
210	0.7	0.1	0.1	3	78	205	9	5	2	1	4	0.8
214	0.4	0.1	0.1	2	94	167	4	5	1	1	7	0.6
218	0.7	0.1	0.2	2	68	164	2	4	1	1	7	0.9
221	0.9	0.1	0.1	3	106	221	9	5	2	1	7	0.7
225	0.7	0.1	0.1	4	77	189	4	4	1	2	4	0.9
229	0.6	0.1	0.1	5	107	208	6	4	1	1	5	0.8
233	0.5	0.1	0.1	3	65	208	10	3	1	0	3	0.7
236	1.2	0.1	0.1	3	165	226	6	4	1	1	4	0.8
240	0.6	0.1	0.2	4	137	228	5	5	1	1	6	1.4
244	0.8	0.1	0.1	5	118	200	12	5	2	1	4	1.0
248	0.5	0.2	0.1	5	109	212	1	5	2	1	5	1.0
251	0.9	0.4	0.3	4	144	205	5	9	2	0	5	0.7
255	1.0	0.6	0.2	5	142	276	15	7	1	0	6	1.0
259	0.9	0.6	0.3	4	134	233	5	8	2	0	6	1.1
263	1.4	0.4	0.2	4	140	242	2	8	2	1	7	1.0
266	1.1	0.4	0.2	4	152	218	9	7	1	0	5	0.9
270	0.7	0.3	0.2	6	173	220	10	6	2	0	5	0.8
274	1.0	0.3	0.3	4	200	301	3	6	2	1	4	0.6
278	1.1	0.4	0.3	4	219	363	4	9	2	1	5	0.7
281	0.9	0.3	0.3	4	205	323	1	6	1	0	7	0.8
285	0.9	0.3	0.2	6	301	369	7	5	2	0	6	0.9
289	0.8	0.4	0.2	3	148	320	1	5	1	1	5	0.9
293	2.9	3.3	2.1	17	535	477	16	15	9	2	14	1.9
296	2.6	5.0	2.6	30	421	774	21	29	6	4	16	2.6
300	4.7	4.0	1.5	30	398	604	42	22	4	4	11	2.1

Tab. A-22: Elemental concentrations recorded by means of μ S-XRF analysis through an untreated coated grain of H3305 (No. 64).

μm	As	Fe	K	Mn	Ca	Ti	V	Cr	Ni	Cu	Zn	Ga
	[mg/kg]	[g/kg]	[mg/kg]									
300	2.9	24.1	2.6	58	1034	713	14	61	9	4	9	0.8
290	5.5	45.7	5.9	4712	1484	1568	11	197	20	12	18	1.6
280	6.0	47.7	7.9	320	2869	1623	103	100	39	14	32	2.6
270	2.2	9.4	7.4	73	787	999	55	50	15	7	23	2.3
260	1.1	2.7	1.3	22	242	457	1	11	3	3	9	1.1
250	1.2	1.9	1.1	17	129	352	14	3	2	2	6	0.8
240	0.5	1.8	1.1	10	146	345	12	15	3	2	5	0.7
230	1.1	2.2	1.0	12	178	392	3	10	3	2	5	0.9
220	1.1	2.7	1.0	16	110	334	7	11	4	2	6	0.8
210	0.8	2.9	1.0	14	192	360	8	22	3	2	6	1.0
200	0.9	2.9	1.1	13	296	412	8	11	4	2	4	0.4
190	0.8	2.7	0.8	15	187	420	8	13	3	2	6	1.1
180	0.8	2.1	0.9	8	275	394	6	9	4	2	6	0.6
170	0.6	1.1	0.7	10	138	446	17	15	2	2	6	0.8
160	0.8	1.0	0.6	10	108	439	4	6	3	2	4	0.8
150	0.8	0.8	0.5	5	55	486	3	9	2	2	4	0.7
140	0.8	0.8	0.4	7	80	464	1	7	3	2	5	0.6
130	0.7	0.8	0.4	7	114	509	0	7	2	3	5	0.7
120	0.8	0.9	0.5	6	67	372	0	5	2	3	5	0.6
110	0.7	1.0	0.5	5	126	339	5	7	2	2	4	0.6
100	0.8	1.0	0.4	8	110	393	5	4	1	2	5	1.0
90	0.6	1.1	0.5	9	142	342	12	8	4	2	5	0.9
80	1.1	1.3	0.6	8	122	290	1	6	3	2	5	0.6
70	0.8	1.0	0.6	10	75	269	5	10	3	2	3	0.6
60	0.9	0.9	0.7	6	152	288	11	9	1	2	5	0.7
50	0.6	0.9	0.5	7	46	317	4	3	3	2	3	0.5
40	0.5	0.9	0.5	10	66	278	9	10	2	3	3	0.7
30	0.7	0.8	0.6	10	88	247	3	10	2	1	3	0.4
20	0.7	0.9	0.6	10	135	275	1	9	1	2	3	0.9
10	0.9	0.8	0.7	6	113	324	8	4	2	2	6	0.6
0	0.8	0.9	0.6	9	142	314	4	11	2	3	4	0.8

Tab. A-23: Elemental concentrations recorded by means of μ S-XRF analysis through an untreated mafic grain of L17045 (No. 84).

μm	As	Fe	K	Mn	Ca	Ti	V	Cr	Ni	Cu	Zn	Ga
	[mg/kg]	[g/kg]						[mg/kg]				
700	4.4	4	0.7	166	187	1	23	11	9	3	7	1.0
686	16.7	14	1.3	751	734	6	87	45	29	4	18	3.3
672	33.3	25	2.4	919	475	16	281	99	31	9	33	4.8
658	38.7	37	1.9	865	1314	7	155	74	20	16	29	3.6
644	18.0	20	1.0	507	813	16	36	77	16	6	23	5.3
630	24.2	22	1.4	468	739	31	35	90	14	3	24	6.7
616	19.5	22	1.2	437	1075	21	274	85	17	4	25	2.9
602	17.9	19	1.3	384	1246	18	67	33	11	3	24	3.7
588	21.3	21	1.1	408	870	16	257	89	17	3	24	3.5
574	19.0	20	1.1	353	1154	11	99	58	17	4	27	6.2
560	19.5	20	0.9	327	1086	16	297	42	16	4	31	5.3
546	19.3	18	1.0	305	1278	8	118	46	14	4	31	7.1
532	17.6	20	1.2	320	752	8	116	57	18	5	28	5.1
518	18.1	20	0.9	332	850	23	518	54	15	5	28	6.3
504	17.0	20	1.1	331	743	11	167	64	15	5	26	5.8
490	21.0	22	1.2	332	862	12	194	83	15	2	35	8.7
476	31.7	34	1.1	495	668	18	33	159	27	5	50	12.1
462	37.6	37	1.1	531	662	10	249	180	29	7	50	11.7
448	30.7	33	1.2	466	723	16	92	150	23	4	45	9.7
434	27.9	27	1.9	368	1016	19	140	121	21	3	42	8.4
420	25.8	26	0.9	371	1136	13	229	127	17	3	35	7.9
406	28.1	29	1.5	359	670	14	8	177	23	5	40	8.5
392	30.9	32	1.1	419	957	16	315	187	29	4	47	8.7
378	21.6	22	0.9	267	1050	7	174	94	13	3	36	5.4
364	27.7	26	1.4	326	812	11	197	156	16	5	35	9.8
350	36.3	35	1.0	438	1062	37	613	158	22	3	42	8.3
336	22.6	25	1.3	301	1232	28	56	144	19	3	33	7.3
322	18.5	20	1.4	245	1264	11	78	97	15	5	31	6.1
308	29.6	24	1.4	301	1003	20	172	115	13	3	40	7.5
294	28.3	25	1.0	288	1206	14	209	142	20	3	46	11.3
280	30.4	27	0.9	339	1049	30	242	139	22	4	43	12.2
266	28.9	27	1.0	330	717	23	324	124	22	5	42	12.4
252	22.6	25	1.1	280	800	15	194	131	25	3	44	10.7
238	28.0	26	1.4	350	929	12	272	128	24	4	39	12.0
224	26.5	24	1.6	317	1094	11	277	75	18	3	47	10.1
210	30.4	27	1.4	336	1776	18	93	120	19	5	43	13.0
196	28.5	24	1.4	345	894	13	258	109	23	3	36	14.2
182	22.4	23	0.9	295	772	10	126	140	17	2	32	8.5
168	22.4	19	1.0	272	653	8	177	97	20	3	28	9.4

to be continued on the following page

μm	As	Fe	K	Mn	Ca	Ti	V	Cr	Ni	Cu	Zn	Ga
	[mg/kg]	[g/kg]	[mg/kg]									
154	26.5	24	1.0	329	988	12	189	98	21	3	36	10.9
140	25.5	26	1.4	379	864	15	195	123	21	6	43	12.3
126	22.5	23	1.1	331	433	16	104	117	22	5	36	12.0
112	57.7	28	1.1	404	806	39	115	160	26	1	36	14.0
98	36.5	32	1.0	512	631	8	173	165	32	3	39	15.5
84	27.3	34	1.0	567	821	20	473	125	21	4	34	11.7
70	31.5	29	1.1	509	904	19	138	136	26	2	35	14.4
56	35.5	30	1.1	587	733	32	424	103	20	4	34	12.7
42	30.3	27	1.1	581	548	24	194	105	29	3	34	14.8
28	44.7	40	4.1	1084	571	22	134	176	39	3	37	13.5
14	57.4	54	7.9	1529	658	15	178	161	32	7	38	11.9
0	49.5	44	6.2	1378	635	18	297	111	36	1	34	9.7

Tab. A-24: Elemental concentrations recorded by means of μ S-XRF analysis through an untreated mafic grain of H3515 (No. 110).

μm	As	Fe	K	Mn	Ca	Ti	V	Cr	Ni	Cu	Zn	Ga
	[mg/kg]	[g/kg]	[mg/kg]									
400	5.2	1	111	21	8	0.8	113	5	7	2	3	4.0
390	17.7	3	109	25	41	0.6	42	6	3	3	4	5.7
380	50.6	9	37	72	668	0.9	52	35	4	8	13	2.2
370	27.8	26	23	225	1190	5.5	36	34	6	10	22	3.8
360	37.9	53	29	208	4939	2.6	91	3843	9	7	30	3.7
350	44.7	36	48	482	6225	5.6	226	151	43	22	62	9.7
340	53.6	44	31	259	3430	2.2	84	141	35	32	83	4.8
330	49.7	23	31	165	2429	2.2	140	105	49	24	51	6.1
320	53.1	23	25	258	1804	2.1	73	111	29	20	88	7.9
310	69.7	26	31	262	1899	2.5	116	126	30	24	41	6.3
300	51.1	21	25	141	1975	2.1	69	104	29	22	38	5.3
290	46.9	29	16	333	4411	1.7	51	147	25	27	84	9.1
280	61.9	26	17	182	3783	3.3	102	180	29	25	53	13.0
270	48.7	21	15	144	3110	1.7	49	90	19	21	43	12.0
260	66.8	28	23	153	3037	4.9	176	137	26	29	55	15.6
250	61.7	27	21	214	3356	2.8	58	168	28	64	51	10.8
240	70.9	36	45	252	3021	3.6	91	178	29	37	64	11.5
230	58.9	25	33	160	1883	3.4	64	154	22	22	46	10.5
220	64.7	29	42	166	2737	4.3	133	198	34	33	54	13.1
210	39.1	19	17	148	1277	1.8	21	211	14	16	32	5.2
200	17.2	18	28	132	1572	1.7	51	86	24	17	33	3.5
190	17.4	12	24	104	2505	3.0	16	81	11	10	24	3.3
180	23.4	13	14	87	1619	1.5	24	85	13	14	17	3.6
170	26.3	16	22	110	1711	2.1	34	93	16	16	22	3.1
160	29.4	18	16	132	2597	2.2	37	78	24	19	33	4.9
150	24.2	15	15	115	3183	8.3	102	67	17	45	25	3.7
140	17.4	11	12	75	1600	7.0	53	71	11	10	19	3.4
130	44.4	18	15	361	4363	2.1	32	91	23	20	26	2.8
120	26.5	15	15	100	4794	2.5	18	66	13	13	25	3.6
110	32.4	21	18	117	2375	3.7	107	215	16	23	36	7.0
100	49.7	32	18	176	2767	2.9	148	111	23	19	54	5.1
90	43.2	22	16	139	1895	2.0	130	181	23	18	42	7.2
80	46.5	20	14	141	2542	2.5	140	107	23	18	42	7.0
70	45.6	17	11	114	995	2.8	123	133	19	19	39	6.3
60	44.4	23	14	152	1520	2.5	139	136	28	16	79	6.8
50	35.9	15	10	95	1569	1.9	100	109	20	15	30	5.5
40	37.3	18	13	91	1791	2.1	152	143	20	15	35	7.0
30	35.9	15	15	103	1229	2.8	91	142	12	15	24	4.8
20	28.9	15	18	105	1522	2.3	58	91	18	13	28	3.9
10	26.3	20	19	150	1731	2.3	54	78	14	15	41	4.5
0	18.9	11	14	73	986	1.5	24	60	8	8	16	2.7

A.4.2.2 GRAINS AFTER P-LEACHING

Tab. A-25: Elemental concentrations recorded by means of μ S-XRF analysis through a coated grain of H3305LP (No. 119) after P-leaching.

μm	As	Fe	K	Mn	Ca	Ti	V	Cr	Ni	Cu	Zn	Ga
	[mg/kg]	[g/kg]						[mg/kg]				
250	0.8	2	1.9	9	196	765	17	4	5	2	4	1.6
244	0.6	2	1.5	20	175	575	34	5	3	3	5	2.0
238	0.8	3	2.4	48	194	652	19	17	3	4	9	2.0
231	0.8	22	2.8	390	939	754	80	96	19	5	40	10.1
225	0.9	27	2.4	436	985	636	108	108	27	6	53	13.5
219	0.6	25	1.8	396	511	726	93	58	15	5	44	6.7
213	0.8	16	1.4	278	339	757	59	37	14	4	26	3.8
206	0.7	6	1.4	82	275	716	15	14	5	2	12	1.5
200	0.9	3	1.3	30	320	720	23	9	2	3	8	1.1
194	0.7	2	1.0	22	185	693	17	6	2	2	5	0.9
188	0.8	2	0.8	28	169	618	24	6	2	2	4	0.9
181	0.6	2	0.7	15	130	591	22	15	1	2	4	0.9
175	0.9	2	0.6	21	217	555	7	11	2	2	4	0.6
169	0.9	2	0.7	15	148	495	21	10	2	2	3	0.7
163	0.8	2	0.7	28	177	399	4	3	3	2	5	0.9
156	0.5	2	0.8	33	216	477	5	9	2	2	6	1.2
150	1.0	2	0.7	35	200	471	12	14	2	2	4	1.1
144	0.7	2	0.5	39	159	467	8	14	1	1	5	1.0
138	0.7	2	0.5	30	130	426	15	17	2	1	4	0.7
131	0.6	2	0.6	39	126	444	17	12	3	1	5	1.2
125	0.8	2	0.6	23	314	480	3	6	2	1	4	0.8
119	0.6	2	0.5	14	94	443	7	10	2	2	4	0.9
113	0.6	1	0.5	19	95	448	1	6	2	1	3	0.7
106	0.7	1	0.5	13	150	431	24	8	2	1	3	0.7
100	0.9	1	0.4	13	146	526	11	6	2	2	3	0.7
94	0.8	1	0.5	15	234	598	6	7	2	1	4	0.8
88	0.6	1	0.5	18	165	478	12	10	2	1	4	0.5
81	0.6	1	0.4	14	241	467	8	9	3	1	4	0.7
75	0.5	1	0.5	22	142	433	15	11	2	1	4	0.5
69	0.6	2	0.6	18	185	438	2	6	2	2	5	0.8
63	0.8	3	0.6	40	178	454	4	10	3	1	7	0.7
56	0.6	4	0.6	42	210	503	1	16	3	2	10	1.6
50	0.4	5	0.7	87	324	541	5	25	3	3	13	1.5
44	0.6	10	0.6	158	373	519	15	37	8	5	18	4.7
38	0.7	9	0.6	147	303	421	33	33	7	4	15	4.0
31	0.6	9	0.7	108	161	508	18	22	6	3	17	3.5
25	0.7	8	0.7	85	467	484	35	9	2	3	19	1.6
19	1.2	9	1.5	110	499	491	36	25	4	4	18	1.5
13	1.2	10	4.8	108	1124	1038	63	16	3	4	19	1.5
6	1.3	16	8.0	194	1548	912	23	50	6	6	26	2.0
0	1.2	29	6.2	429	753	947	44	143	6	7	47	2.7

Tab. A-26: Elemental concentrations recorded by means of μ S-XRF analysis through a coated grain of L17045LP (No. 30) after P-leaching.

μm	As	Fe	K	Mn	Ca	Ti	V	Cr	Ni	Cu	Zn	Ga
	[mg/kg]	[g/kg]		[mg/kg]								
500	53.2	49	27	1768	718	1876	118	602	82	23	112	13
490	36.5	39	22	1496	899	2362	110	153	74	17	51	11
480	34.5	40	46	1743	1285	3734	101	139	61	16	48	12
470	6.5	8	145	301	492	911	112	29	13	3	12	11
460	7.0	7	145	270	261	734	84	55	9	4	13	10
450	5.9	5	136	208	567	681	64	21	8	3	9	9
440	3.6	5	135	194	721	684	53	17	7	2	7	10
430	3.5	4	88	156	622	1170	76	22	4	2	7	9
420	1.5	2	115	78	341	439	56	8	3	2	4	10
410	1.5	1	160	45	597	368	76	2	1	1	4	11
400	0.7	1	158	39	529	326	60	5	2	1	3	12
390	2.1	2	148	62	522	414	56	11	4	2	4	11
380	0.8	1	151	39	385	361	71	2	2	1	3	12
370	0.6	1	146	36	371	411	63	5	2	1	3	10
360	1.1	1	139	53	280	292	72	5	2	1	4	11
350	3.0	2	124	113	349	354	73	7	5	2	7	10
340	1.9	2	115	110	466	347	57	7	5	3	8	10
330	7.1	7	97	265	545	522	72	33	9	4	11	9
320	4.0	4	112	163	394	487	62	18	7	2	8	9
310	5.5	6	84	236	615	422	38	20	9	4	12	9
300	6.6	6	118	240	474	427	62	22	10	5	9	9
290	5.7	5	133	176	439	472	64	28	11	11	9	10
280	7.4	6	131	266	323	473	69	10	12	5	11	9
270	12.3	9	112	323	438	878	73	32	18	7	17	9
260	14.8	14	80	520	1767	1066	105	46	27	9	22	10
250	23.7	21	94	759	1407	1329	74	472	35	13	36	9
240	22.0	19	92	703	703	2670	67	80	38	9	30	9
230	17.8	13	139	522	570	819	102	37	54	8	21	11
220	13.0	8	158	267	849	748	102	22	16	4	15	11
210	3.8	3	164	124	569	606	73	23	6	3	23	11
200	2.8	3	163	97	385	657	83	10	6	2	7	11
190	2.1	2	168	75	405	448	106	6	6	1	4	11
180	1.3	1	171	50	436	424	96	5	3	1	4	12
170	1.2	1	161	32	595	379	96	1	2	1	4	11
160	0.6	0	156	27	475	327	89	0	1	2	2	10
150	0.6	0	152	20	395	339	80	1	2	1	3	12
140	0.8	1	141	22	310	366	83	0	2	1	3	10
130	1.0	1	85	32	5381	447	60	0	1	1	4	15
120	0.7	1	92	28	1186	244	61	1	1	1	3	12

to be continued on the following page

μm	As	Fe	K	Mn	Ca	Ti	V	Cr	Ni	Cu	Zn	Ga
	[mg/kg]	[g/kg]	[mg/kg]									
110	0.7	1	98	24	500	304	69	2	1	1	2	11
100	0.6	1	90	30	422	233	59	1	2	1	3	10
90	0.9	1	70	29	635	246	46	3	1	1	3	9
80	0.8	1	54	31	288	173	44	4	2	1	4	9
70	1.1	1	39	36	200	157	33	5	3	2	4	8
60	1.7	1	30	35	185	70	29	7	2	1	4	7
50	3.4	2	20	59	127	103	25	8	4	2	6	6
40	4.6	3	15	90	135	81	3	11	6	3	8	6
30	6.0	4	12	118	165	82	14	10	7	3	8	5
20	4.5	2	9	78	127	73	20	15	6	2	7	5
10	3.5	2	7	63	78	58	3	6	4	2	5	4
0	2.3	1	6	30	59	34	6	4	3	2	3	3

Tab. A-27: Elemental concentrations recorded by means of μ S-XRF analysis through a coated grain of H3515LP (No. 31) after P-leaching.

μm	As	Fe	K	Mn	Ca	Ti	V	Cr	Ni	Cu	Zn	Ga
	[mg/kg]	[g/kg]		[mg/kg]								
270	2.6	0.7	0.6	2	98	372	5	2	2	2	11	0.7
264	2.1	1.3	0.9	7	337	433	5	1	1	3	23	1.2
258	4.8	2.0	1.2	12	614	479	10	1	3	3	24	1.2
252	8.2	4.9	2.3	16	845	548	19	12	5	6	18	1.7
246	14.8	5.7	0.9	28	178	293	5	9	6	8	22	2.7
240	5.8	1.5	0.9	8	96	240	14	8	4	6	11	2.0
234	3.6	0.9	0.7	3	77	135	2	5	2	4	8	0.9
228	4.3	1.0	0.7	1	175	162	0	5	5	3	9	1.3
222	4.2	0.8	0.8	9	1124	138	0	1	3	5	12	1.6
216	3.6	0.7	0.8	6	77	82	5	3	3	3	6	1.7
210	4.9	0.6	0.7	7	135	80	5	6	2	5	5	1.2
204	3.4	0.5	0.6	6	237	87	2	1	1	2	7	0.8
198	2.3	0.5	0.8	7	497	68	8	1	2	2	4	0.7
192	2.1	0.4	0.6	8	347	84	6	5	2	2	5	1.2
186	2.7	0.8	0.7	7	348	79	0	0	2	2	11	1.5
180	8.0	0.9	0.4	3	46	59	1	2	3	2	7	1.5
174	1.7	0.6	0.7	1	46	91	2	0	4	3	5	1.2
168	2.3	0.5	0.8	4	26	73	5	1	2	2	4	1.0
162	1.7	0.4	0.7	2	53	95	4	4	3	2	5	1.4
156	1.8	0.4	0.7	2	28	81	2	4	2	2	3	0.6
150	2.3	0.4	0.6	2	82	71	3	2	2	3	6	1.3
144	3.9	1.5	0.6	0	117	93	2	7	4	2	11	1.5
138	3.1	2.5	0.5	7	21	113	21	4	10	4	9	1.0
132	11.1	2.6	0.6	6	39	71	1	0	9	2	10	3.2
126	12.0	4.3	0.4	6	24	111	7	6	10	2	13	4.0
120	8.8	1.8	0.3	14	58	88	1	1	11	4	10	3.3
114	7.7	1.4	0.6	2	122	93	5	3	5	4	8	2.4
108	3.0	0.6	0.5	5	109	80	6	5	4	2	6	0.8
102	3.7	0.5	0.6	3	129	76	4	1	2	2	7	1.3
96	2.2	0.4	0.7	2	164	101	3	3	2	2	3	0.7
90	3.3	0.5	0.8	1	171	74	5	1	2	4	5	1.4
84	3.2	0.5	0.6	2	91	95	0	1	4	7	5	1.9
78	3.7	0.5	0.7	3	56	87	5	2	2	3	6	0.9
72	3.5	0.5	0.7	3	143	102	4	2	2	2	9	1.5
66	2.6	0.4	0.7	2	106	99	2	3	2	6	10	0.9
60	6.4	0.8	0.8	6	91	120	10	9	2	2	9	1.1
54	7.3	0.7	1.4	3	200	153	1	1	3	2	12	0.8
48	3.8	1.7	2.7	16	671	221	9	15	3	3	15	1.5
42	7.0	3.7	7.1	26	1216	513	26	6	4	4	29	1.1
36	8.1	5.5	10.2	37	2086	1471	1	24	6	5	24	1.5
30	11.7	7.6	10.9	31	2664	643	16	60	7	4	26	2.0
24	6.4	4.7	11.2	23	2609	682	11	23	6	6	21	1.9
18	5.7	5.1	39.6	40	1061	1453	80	51	6	5	15	2.6
12	6.0	6.4	25.6	32	854	1202	98	100	7	5	16	2.3
6	7.8	5.7	8.7	34	676	714	12	36	6	6	15	2.0
0	10.1	5.1	3.7	32	124	2407	21	16	4	3	15	1.7

A.4.2.3 GRAINS AFTER FE-DISSOLUTION

Tab. A-28: Elemental concentrations recorded by means of μ S-XRF analysis through a coated grain of L17045LFe (No. 56) after Fe-dissolution.

μm	As	Fe	K	Mn	Ca	Ti	V	Cr	Ni	Cu	Zn	Ga
	[mg/kg]	[g/kg]	[mg/kg]									
170	5.6	3.9	7.8	27	648	1401	18	41	20	8	28	7.2
164	8.4	4.2	11.6	20	1315	1821	65	62	33	8	31	11.3
159	6.7	5.8	5.1	153	1565 ₉	7498	85	332	81	9	35	8.4
153	6.0	3.8	4.8	29	439	1476	22	43	25	7	38	7.4
147	3.5	2.8	4.0	18	252	1003	14	41	20	5	21	4.9
142	2.6	1.8	2.2	17	325	972	20	344	19	5	21	3.2
136	3.0	1.7	1.8	21	555	860	7	57	17	5	17	2.9
130	3.6	1.2	2.2	8	39	744	8	42	14	5	15	1.6
125	2.3	0.9	2.0	7	147	726	4	32	9	3	13	1.5
119	2.3	0.9	1.3	12	1090	753	14	22	7	3	13	2.0
113	3.1	1.5	2.5	13	104	761	27	26	9	5	14	3.4
108	3.3	1.0	1.5	9	70	976	12	20	10	3	11	1.9
102	2.5	0.8	0.8	9	83	832	0	15	7	4	11	2.9
96	5.8	0.3	1.1	1	40	642	20	14	5	3	9	1.8
91	3.6	0.3	1.4	5	429	811	0	2	7	5	10	4.2
85	2.3	0.5	0.9	7	157	705	11	3	5	1	9	2.5
79	2.8	0.4	0.9	4	85	779	12	8	7	4	8	1.5
74	2.6	0.6	0.8	5	30	926	4	6	7	5	10	1.8
68	3.0	0.7	1.0	1	130	879	20	2	13	6	11	3.5
62	4.2	0.9	1.1	3	54	1078	2	8	8	5	11	3.1
57	2.5	0.9	1.0	3	177	786	11	18	6	5	10	2.3
51	3.1	0.7	1.2	4	53	695	2	9	6	5	10	3.1
45	3.4	0.6	1.3	10	129	647	3	11	9	5	10	3.0
40	2.3	0.5	0.9	9	115	799	3	19	8	5	9	1.7
34	3.0	0.7	1.3	8	122	687	9	11	7	4	13	2.1
28	2.6	0.6	1.2	18	342	783	6	26	7	4	7	1.5
23	1.9	0.6	1.9	9	165	689	6	31	8	4	10	1.3
17	2.8	1.0	1.3	1	577	696	11	33	7	7	9	1.0
11	2.2	1.5	1.5	10	590	873	28	28	9	9	10	1.1
6	3.1	1.7	2.6	19	173	875	38	24	13	4	11	2.0
0	2.7	2.1	3.7	13	119	1042	12	34	11	4	12	1.8

Tab. A-29: Elemental concentrations recorded by means of μ S-XRF analysis through a coated grain of H2020LFe (No. 75) after Fe-dissolution.

μm	As	Fe	K	Mn	Ca	Ti	V	Cr	Ni	Cu	Zn	Ga
	[mg/kg]	[g/kg]	[mg/kg]									
0	0.4	3.7	5.2	48	280	1144	22	19	5	2	12	3
4	0.9	4.2	11.1	49	631	1340	33	19	5	3	16	4
8	0.5	5.4	27.3	64	874	1611	64	35	6	3	15	6
13	0.8	4.4	18.2	52	832	1324	30	25	5	2	16	6
17	0.5	3.7	15.4	53	551	961	30	22	5	1	14	4
21	0.6	3.7	15.4	52	763	1163	37	20	6	2	17	4
25	1.1	2.5	4.9	27	971	458	14	18	4	1	18	4
29	1.0	2.5	2.0	26	316	307	24	12	5	1	16	4
34	1.1	2.3	1.9	23	254	286	12	16	6	2	18	6
38	0.7	1.8	1.5	16	187	239	11	3	5	2	19	4
42	0.7	1.3	1.3	16	157	193	13	8	4	2	16	3
46	0.9	1.1	1.2	12	143	194	4	4	2	2	11	3
50	0.3	1.0	1.1	13	123	175	11	9	2	1	13	3
55	1.2	0.9	1.1	12	166	171	12	6	3	1	11	2
59	0.9	1.1	1.3	10	178	159	10	9	2	2	14	3
63	0.6	1.1	0.9	15	238	131	12	6	3	2	14	2
67	0.7	1.0	0.9	13	135	149	7	4	2	1	12	1
71	1.0	0.9	0.7	11	142	172	8	7	3	2	10	2
76	0.5	0.8	0.6	12	119	149	7	8	3	1	7	2
80	0.3	0.7	0.5	9	137	155	11	5	1	1	7	1
84	0.6	0.6	0.6	7	132	196	7	5	2	1	8	2
88	0.4	0.6	0.6	5	138	195	9	7	2	1	9	1
92	0.7	0.6	0.6	10	102	188	12	10	2	1	6	1
97	0.4	0.5	0.6	7	183	182	10	5	1	1	6	1
101	0.6	0.5	0.5	6	156	170	7	4	1	1	8	1
105	0.4	0.5	0.6	8	256	199	13	3	1	1	9	1
109	0.5	0.4	0.7	8	276	185	8	6	2	1	7	1
113	0.5	0.3	0.7	7	224	195	8	3	1	1	7	1
118	0.6	0.3	0.7	3	207	180	6	4	2	1	7	1
122	0.6	0.3	0.6	7	193	190	1	2	1	1	8	1
126	0.6	0.3	0.6	5	215	159	10	2	1	1	4	1
130	0.7	0.2	0.6	6	236	194	2	3	2	1	4	0
134	0.7	0.2	0.7	2	270	159	0	3	1	1	5	1
139	0.5	0.2	0.6	5	234	122	9	4	1	2	4	1
143	0.3	0.2	0.8	5	209	146	4	6	2	1	5	1
147	0.5	0.3	0.8	10	296	143	9	2	1	1	6	1
151	0.6	0.4	1.2	15	286	242	6	3	1	2	7	1
155	0.6	0.6	1.8	9	365	252	9	3	1	4	9	1
160	0.6	0.6	2.2	13	371	298	10	4	1	4	6	1

to be continued on the following page

μm	As	Fe	K	Mn	Ca	Ti	V	Cr	Ni	Cu	Zn	Ga
	[mg/kg]	[g/kg]	[mg/kg]									
164	0.5	0.6	2.2	13	391	225	7	5	1	10	7	2
168	0.7	0.4	3.2	5	412	215	2	4	1	1	6	1
172	0.2	0.3	4.5	12	557	219	11	3	2	1	5	1
176	0.7	0.4	5.6	12	790	331	4	3	1	1	5	1
181	0.2	0.5	5.6	8	2421	389	8	1	2	0	4	1
185	0.5	0.7	3.9	8	5655	292	7	6	1	1	4	2
189	0.4	0.9	3.3	13	4601	294	23	5	2	1	5	2
193	0.5	1.3	3.9	15	3251	454	7	11	1	1	8	2
197	0.7	6.3	21.0	80	2617	3767	68	50	7	3	21	5
202	0.2	2.9	11.1	39	1754	774	45	16	3	2	11	3
206	0.4	0.7	6.3	10	1297	387	11	4	1	1	4	2
210	0.2	0.7	14.5	8	1314	404	1	4	2	1	4	2

Tab. A-30: Elemental concentrations recorded by means of μ S-XRF analysis through a coated grain of H3515LFe (No. 182) after Fe-dissolution.

μm	As	Fe	K	Mn	Ca	Ti	V	Cr	Ni	Cu	Zn	Ga
	[mg/kg]	[g/kg]	[mg/kg]									
500	1.0	415	1.7	8	199	165	5	7	2	1	7	0.7
488	1.0	207	0.7	3	69	120	4	3	3	4	6	0.7
475	1.0	688	0.4	5	124	147	1	5	2	3	8	0.9
463	1.0	1635	1.8	8	85	178	12	12	4	4	9	1.8
450	1.9	1250	5.6	7	335	1789	0	21	3	4	8	2.1
438	1.4	1187	8.4	7	367	1148	14	20	4	3	18	1.3
425	0.9	160	0.7	3	130	152	5	7	3	3	7	1.2
413	0.5	87	0.4	3	89	104	1	7	4	3	5	1.2
400	1.4	75	0.2	4	63	83	6	8	3	3	5	1.0
388	0.9	91	0.3	4	101	116	10	5	2	3	5	0.6
375	1.4	109	0.3	5	104	87	18	7	3	4	6	1.5
363	1.4	90	0.3	3	137	110	11	6	3	3	6	1.1
350	1.4	130	0.3	4	109	120	5	8	3	3	7	1.6
338	1.3	91	0.3	4	69	136	2	3	3	3	5	1.0
325	1.6	65	0.3	7	98	122	5	6	3	3	4	1.1
313	0.7	98	0.3	3	98	122	9	5	2	2	6	1.0
300	0.8	97	0.3	5	125	151	1	7	3	3	6	0.8
288	0.8	76	0.3	3	123	173	9	5	2	3	6	1.0
275	0.9	90	0.2	6	101	147	5	5	2	3	5	0.8
263	0.9	64	0.3	6	92	183	4	3	3	2	6	1.1
250	0.8	87	0.2	3	57	173	3	8	3	3	7	1.1
238	1.5	60	0.3	2	347	198	9	8	3	2	5	1.1
225	0.9	59	0.4	2	122	247	4	7	3	3	4	0.9
213	1.0	62	0.4	3	87	208	4	7	2	3	4	0.9
200	1.0	60	0.1	3	132	256	9	7	2	2	5	0.9
188	0.7	64	0.3	5	123	241	8	6	3	2	5	1.2
175	0.8	68	0.2	5	112	304	0	3	2	2	5	0.9
163	0.8	55	0.2	3	124	275	1	5	1	2	5	1.0
150	0.7	75	0.1	3	100	300	3	5	3	2	5	0.6
138	0.7	122	0.5	3	171	313	2	6	3	3	6	0.5
125	0.8	209	0.6	4	339	383	1	7	4	2	7	1.1
113	1.0	216	0.8	7	238	351	2	6	4	3	9	0.6
100	0.6	153	0.7	5	115	406	14	6	3	3	6	1.2
88	1.0	484	1.3	6	204	612	0	14	3	3	12	0.9
75	1.9	1875	6.4	16	318	1081	8	10	3	6	13	3.2
63	1.5	3385	7.8	19	990	984	13	16	5	3	18	2.6
50	1.5	3501	24.9	23	1538	1619	80	29	6	4	20	3.9
38	1.1	2864	16.0	9	1068	1175	3	39	3	4	14	3.3
25	1.1	978	6.0	7	438	463	14	7	2	2	10	1.5
13	0.7	2051	3.8	18	521	463	11	5	6	3	16	1.6
0	0.8	599	1.4	5	1187	437	5	7	3	2	9	1.2

Tab. A-31: Elemental concentrations recorded by means of μ S-XRF analysis through a mafic grain of L2640LFe (No. 169) after Fe-dissolution.

μm	As	Fe	K	Mn	Ca	Ti	V	Cr	Ni	Cu	Zn	Ga
	[mg/kg]	[g/kg]						[mg/kg]				
180	1.5	0.3	1.2	2	289	361	6	3	2	2	3	0.9
173	1.2	0.3	1.1	4	253	398	1	8	2	2	3	0.7
166	3.7	0.7	1.3	5	253	442	14	4	3	2	3	1.5
158	47.9	1.5	1.5	1	235	570	28	10	33	4	4	2.6
151	25.3	1.6	1.9	8	229	520	9	16	17	2	5	1.7
144	19.1	3.2	11.6	7	203	757	89	35	21	1	7	5.9
137	42.3	4.2	18.9	20	539	1045	37	38	31	4	10	6.6
130	46.7	1.9	3.1	6	174	719	32	4	29	3	5	2.1
122	22.4	1.7	2.2	8	89	595	24	6	12	2	4	1.0
115	50.1	1.7	1.9	5	94	571	25	4	22	3	5	1.1
108	40.8	1.9	2.7	13	161	682	27	15	22	2	6	1.0
101	45.0	2.1	3.0	6	120	716	61	12	34	2	6	1.1
94	75.2	2.3	3.1	1	84	735	33	6	43	0	5	0.6
86	142.2	2.5	3.5	8	90	719	40	1	86	2	4	1.4
79	146.1	2.9	3.9	5	59	715	55	5	80	3	7	1.4
72	135.3	3.1	5.6	7	600	858	49	16	75	3	8	2.5
65	125.5	3.1	3.8	6	119	928	43	4	75	2	5	1.9
58	97.9	2.4	3.8	2	57	620	46	11	57	1	5	2.0
50	32.2	3.4	3.0	4	119	681	38	9	32	2	7	1.5
43	65.8	2.3	3.7	10	150	478	63	28	41	2	5	1.8
36	73.2	3.2	5.5	6	190	542	34	20	41	3	8	1.6
29	42.0	3.1	2.3	15	9	568	41	13	23	2	4	1.6
22	23.9	3.6	2.7	11	64	1583	66	1	14	3	5	2.3
14	32.6	2.4	1.9	10	83	603	2	3	20	4	7	1.6
7	36.9	3.5	3.2	12	142	519	42	12	22	3	7	2.0
0	13.1	2.7	4.3	9	285	572	19	13	13	4	10	1.7

Tab. A-32: Mean elemental concentrations of selected samples of site L measured by means of μ S-XRF analysis in untreated material, after leaching of the sediment with 0.5M Na-phosphate solution (LP) and after dissolution of Fe oxy-hydroxides and carbonates (LFe). The mean is calculated from the elemental concentrations in each analysed individual grain. The number of grains considered for the mean is given in the last column.

Sample	Leaching step	As	Fe	K	Ca	Ti	V	Mn	Ni	Cu	Zn	Ga	Cr	Fe/As	No. of measurements
		[mg/kg]	[g/kg]				[mg/kg]								
L17045	un-treated	4.6	9.8	2.2	0.4	1.0	28	248	6.4	5.0	13	2.0	28	800	12
	LP	6.7	6.6	3.7	0.3	1.1	28	127	94.0	4.2	14	2.3	19	1,200	10
	LFe	2.9	1.5	1.5	0.2	1.0	15	8.4	8.6	5.1	14	1.8	7.3	400	12
L2640	un-treated	0.7	4.5	4.6	0.2	0.7	25	19	4.0	3.2	13	2.9	15	7,000	11
	LP	0.8	0.7	1.3	0.4	0.5	11	8	2.1	3.1	35	1.8	10	1,100	11
	LFe	0.7	2.4	5.4	0.1	0.7	32	9	5.8	3.5	7	2.2	9.4	19,400	11
L3350	un-treated	0.8	17.0	5.0	0.6	2.1	80	43	9.0	5.5	19	7.0	100	14,900	12
	LP	0.9	11.0	1.8	0.4	1.2	38	60	6.0	6.0	15	3.7	48	9,600	10
	LFe	0.5	0.7	1.2	0.4	0.6	7	6	1.5	1.4	19	0.7	12	2,200	8

Tab. A-33: Mean elemental concentrations of selected samples of site H measured by means of μ S-XRF analysis in untreated material, after leaching of the sediment with 0.5M Naphosphate solution (LP) and after dissolution of Fe oxy-hydroxides and carbonates (LFe). The mean is calculated from the elemental concentrations in each analysed individual grain. The number of grains considered for the mean is given in the last column.

Sample	Leaching step	As	Fe	K	Ca	Ti	V	Mn	Ni	Cu	Zn	Ga	Cr	Fe/As	No. of measurements
		[mg/kg]	[g/kg]				[mg/kg]								
H2020	un-treated	1.1	8.5	2.9	0.5	0.7	29	100	4.8	3.5	27	2.6	16	4,700	8
	LP	1.0	6.5	5.5	0.5	1.2	34	80	4.9	4.3	18	2.4	24	3,700	8
	LFe	0.6	0.9	1.3	0.3	0.5	11	15	1.8	3.8	7	1.9	5.7	1,800	8
H2910	un-treated	5.2	8.8	4.1	1.1	1.0	50	27	7.3	9.0	25	2.5	45	1,600	9
	LP	10.0	8.5	3.1	0.7	0.7	116	29	21.0	12.0	20	2.8	33	1,000	13
	LFe	1.5	0.9	1.3	1.2	0.6	9	5	3.2	2.7	17	1.7	4.3	640	8
H3305	un-treated	4.2	13.4	7.8	0.4	0.9	19	80	6.5	8.1	20	4.3	36	2,900	13
	LP	0.8	21.0	10.2	0.6	2	31	83	7.7	3.2	39	5.3	38	7,400	12
	LFe	0.7	4.5	3.0	0.5	1.6	22	13	4.2	4.5	50	2.3	25	5,100	8
H3515	un-treated	20.0	3.7	6.0	0.9	1.3	34	54	7.7	9.0	20	2.6	29	330	18
	LP	5.8	4.1	4.0	0.3	0.9	33	24	4.1	4.2	14	3.4	8.35	600	14
	LFe	1.3	0.9	2.8	0.5	0.4	6.4	9	2.9	4.2	15	1.5	8	720	13

A.5 FACTOR ANALYSIS BASED ON RESULTS OF μ S-XRF MEASUREMENTS

A.5.1 CORRELATION MATRICES

A.5.1.1 UNTREATED SAMPLES

Tab. A-34: Correlation matrix based on the results of an elemental mapping by means of μ S-XRF of a transect through an untreated coated grain of L17045 (No. 90).

	Si	K	Ca	Ti	V	Cr	Mn	Fe	Ni	Cu	Zn	Ga	As
Si	1.00												
K	-0.45	1.00											
Ca	-0.84	0.17	1.00										
Ti	-0.12	0.06	0.21	1.00									
V	-0.49	0.89	0.31	0.30	1.00								
Cr	-0.81	0.10	0.92	0.28	0.21	1.00							
Mn	-0.84	0.73	0.74	0.16	0.78	0.65	1.00						
Fe	-0.91	0.37	0.94	0.20	0.49	0.88	0.87	1.00					
Ni	-0.88	0.36	0.95	0.18	0.48	0.87	0.86	0.99	1.00				
Cu	-0.80	0.28	0.84	0.16	0.28	0.87	0.71	0.78	0.78	1.00			
Zn	-0.70	0.52	0.72	0.38	0.68	0.64	0.83	0.77	0.77	0.68	1.00		
Ga	-0.58	0.96	0.33	0.05	0.87	0.25	0.82	0.49	0.48	0.47	0.61	1.00	
As	-0.90	0.45	0.91	0.22	0.57	0.86	0.91	0.99	0.98	0.77	0.80	0.56	1.00

Tab. A-35: Correlation matrix based on the results of an elemental mapping by means of μ S-XRF of a complete untreated coated grain of H3515 (No. 100).

	Si	K	Ca	Ti	V	Cr	Mn	Fe	Ni	Cu	Zn	Ga	As
Si	1.00												
K	0.05	1.00											
Ca	0.12	0.75	1.00										
Ti	0.06	0.85	0.77	1.00									
V	0.11	0.64	0.60	0.68	1.00								
Cr	-0.07	0.62	0.66	0.67	0.55	1.00							
Mn	0.06	0.78	0.75	0.83	0.72	0.74	1.00						
Fe	0.05	0.78	0.77	0.85	0.73	0.77	0.95	1.00					
Ni	0.08	0.61	0.72	0.70	0.64	0.78	0.81	0.85	1.00				
Cu	0.07	0.51	0.61	0.62	0.58	0.65	0.78	0.81	0.79	1.00			
Zn	0.06	0.70	0.67	0.79	0.69	0.69	0.90	0.94	0.81	0.78	1.00		
Ga	0.13	0.76	0.68	0.80	0.70	0.63	0.84	0.88	0.74	0.66	0.87	1.00	
As	0.07	0.77	0.69	0.84	0.71	0.69	0.88	0.92	0.75	0.71	0.90	0.90	1.00

Tab. A-36: Correlation matrix based on the results of an elemental mapping by means of μ S-XRF of a transect through an untreated coated grain of H3305 (No. 64).

	Si	K	Ca	Ti	V	Cr	Mn	Fe	Ni	Cu	Zn	Ga	As
Si	1.00												
K	-0.67	1.00											
Ca	-0.78	0.88	1.00										
Ti	-0.77	0.92	0.92	1.00									
V	-0.44	0.84	0.85	0.73	1.00								
Cr	-0.86	0.79	0.79	0.90	0.46	1.00							
Mn	-0.64	0.48	0.44	0.66	0.06	0.88	1.00						
Fe	-0.89	0.84	0.95	0.94	0.67	0.93	0.68	1.00					
Ni	-0.69	0.92	0.98	0.93	0.89	0.76	0.43	0.91	1.00				
Cu	-0.75	0.92	0.94	0.96	0.76	0.88	0.63	0.95	0.95	1.00			
Zn	-0.61	0.97	0.91	0.92	0.90	0.72	0.39	0.83	0.95	0.92	1.00		
Ga	-0.49	0.92	0.82	0.83	0.86	0.64	0.32	0.72	0.86	0.84	0.94	1.00	
As	-0.85	0.87	0.95	0.96	0.71	0.91	0.66	0.99	0.93	0.96	0.87	0.77	1.00

Tab. A-37: Correlation matrix based on the results of an elemental mapping by means of μ S-XRF of a transect through an untreated mafic grain of L17045 (No. 84).

	Si	K	Ca	Ti	V	Cr	Mn	Fe	Ni	Cu	Zn	Ga	As
Si	1.00												
K	-0.34	1.00											
Ca	0.58	-0.19	1.00										
Ti	0.05	0.03	0.06	1.00									
V	0.03	0.00	0.03	0.34	1.00								
Cr	-0.13	0.20	-0.11	0.33	0.10	1.00							
Mn	-0.53	0.88	-0.28	0.10	0.10	0.20	1.00						
Fe	-0.25	0.68	-0.06	0.30	0.26	0.70	0.73	1.00					
Ni	-0.49	0.54	-0.37	0.17	0.12	0.60	0.70	0.71	1.00				
Cu	-0.25	0.16	0.07	-0.23	-0.02	-0.05	0.33	0.26	0.09	1.00			
Zn	0.12	0.07	0.17	0.22	0.22	0.74	0.01	0.58	0.43	0.00	1.00		
Ga	-0.02	0.13	-0.11	0.32	0.15	0.67	0.13	0.53	0.57	-0.21	0.68	1.00	
As	-0.31	0.62	-0.10	0.44	0.19	0.66	0.68	0.87	0.72	0.14	0.51	0.59	1.00

A.5.1.2 AFTER P-LEACHING

Tab. A-38: Correlation matrix based on the results of an elemental mapping by means of μ S-XRF of a transect through a coated grain of H3515LP (No.31) after P-leaching.

	Si	K	Ca	Ti	V	Cr	Mn	Fe	Ni	Cu	Zn	Ga	As
Si	1.00												
K	-0.58	1.00											
Ca	-0.52	0.52	1.00										
Ti	-0.76	0.64	0.46	1.00									
V	-0.55	0.87	0.28	0.57	1.00								
Cr	-0.59	0.82	0.55	0.60	0.83	1.00							
Mn	-0.70	0.74	0.68	0.81	0.61	0.73	1.00						
Fe	-0.65	0.62	0.66	0.71	0.55	0.74	0.89	1.00					
Ni	-0.15	0.29	0.22	0.24	0.29	0.35	0.43	0.62	1.00				
Cu	-0.28	0.32	0.35	0.27	0.25	0.32	0.49	0.48	0.29	1.00			
Zn	-0.70	0.38	0.69	0.53	0.30	0.41	0.71	0.75	0.31	0.39	1.00		
Ga	-0.09	0.30	0.13	0.20	0.26	0.31	0.39	0.54	0.77	0.33	0.28	1.00	
As	-0.22	0.19	0.31	0.38	0.14	0.31	0.56	0.73	0.63	0.34	0.55	0.71	1.00

Tab. A-39: Correlation matrix based on the results of an elemental mapping by means of μ S-XRF of a transect through a coated grain of H3305LP (No.119) after P-leaching.

	Si	K	Ca	Ti	V	Cr	Mn	Fe	Ni	Cu	Zn	Ga	As
Si	1.00												
K	-0.21	1.00											
Ca	-0.15	0.86	1.00										
Ti	-0.31	0.82	0.71	1.00									
V	-0.51	0.42	0.61	0.53	1.00								
Cr	-0.30	0.61	0.65	0.51	0.69	1.00							
Mn	-0.37	0.55	0.67	0.53	0.84	0.93	1.00						
Fe	-0.35	0.62	0.72	0.58	0.83	0.93	0.99	1.00					
Ni	-0.52	0.30	0.54	0.35	0.84	0.75	0.87	0.83	1.00				
Cu	-0.45	0.76	0.78	0.68	0.70	0.81	0.84	0.87	0.67	1.00			
Zn	-0.36	0.59	0.73	0.56	0.85	0.91	0.98	0.99	0.85	0.87	1.00		
Ga	-0.52	0.26	0.53	0.29	0.83	0.74	0.84	0.80	0.97	0.67	0.83	1.00	
As	0.02	0.70	0.64	0.56	0.28	0.39	0.32	0.38	0.13	0.46	0.35	0.09	1.00

Tab. A-40: Correlation matrix based on the results of an elemental mapping by means of μ S-XRF of a complete coated grain of A17045LP (No.34) after P-leaching.

	Si	K	Ca	Ti	V	Cr	Mn	Fe	Ni	Cu	Zn	Ga	As
Si	1.00												
K	0.92	1.00											
Ca	0.59	0.62	1.00										
Ti	0.52	0.54	0.73	1.00									
V	0.72	0.79	0.64	0.66	1.00								
Cr	-0.18	-0.18	0.18	0.37	-0.04	1.00							
Mn	0.18	0.19	0.48	0.69	0.34	0.65	1.00						
Fe	-0.07	-0.08	0.29	0.55	0.08	0.73	0.87	1.00					
Ni	0.27	0.28	0.51	0.68	0.41	0.58	0.87	0.74	1.00				
Cu	0.34	0.35	0.61	0.73	0.45	0.51	0.78	0.65	0.80	1.00			
Zn	0.11	0.11	0.44	0.67	0.26	0.64	0.86	0.88	0.80	0.75	1.00		
Ga	0.75	0.78	0.53	0.40	0.69	-0.26	0.08	-0.22	0.21	0.26	-0.01	1.00	
As	0.19	0.19	0.42	0.65	0.34	0.53	0.77	0.79	0.73	0.71	0.83	0.06	1.00

A.5.1.3 AFTER FE-DISSOLUTION

Tab. A-41: Correlation matrix based on the results of an elemental mapping by means of μ S-XRF of a transect through a coated grain of L17045LFe (No.56) after Fe-dissolution.

	Si	K	Ca	Ti	V	Cr	Mn	Fe	Ni	Cu	Zn	Ga	As
Si	1.00												
K	-0.26	1.00											
Ca	-0.37	0.28	1.00										
Ti	-0.40	0.40	0.98	1.00									
V	-0.36	0.65	0.74	0.78	1.00								
Cr	-0.20	0.28	0.68	0.68	0.59	1.00							
Mn	-0.41	0.39	0.97	0.98	0.76	0.71	1.00						
Fe	-0.40	0.83	0.65	0.74	0.79	0.57	0.76	1.00					
Ni	-0.36	0.58	0.91	0.95	0.84	0.73	0.95	0.87	1.00				
Cu	-0.14	0.58	0.41	0.47	0.55	0.35	0.45	0.68	0.57	1.00			
Zn	-0.32	0.79	0.53	0.63	0.67	0.55	0.65	0.93	0.79	0.61	1.00		
Ga	-0.25	0.87	0.46	0.57	0.68	0.37	0.54	0.84	0.71	0.59	0.87	1.00	
As	-0.26	0.79	0.44	0.54	0.68	0.28	0.49	0.74	0.64	0.51	0.76	0.87	1.00

Tab. A-42: Correlation matrix based on the results of an elemental mapping by means of μ S-XRF of a transect through a coated grain of H2020LFe (No. 75) after Fe-dissolution.

	Si	K	Ca	Ti	V	Cr	Mn	Fe	Ni	Cu	Zn	Ga	As
Si	1.00												
K	-0.74	1.00											
Ca	-0.25	0.23	1.00										
Ti	-0.73	0.89	0.15	1.00									
V	-0.55	0.79	0.13	0.84	1.00								
Cr	-0.53	0.78	0.05	0.87	0.85	1.00							
Mn	-0.63	0.82	0.05	0.94	0.88	0.93	1.00						
Fe	-0.62	0.80	0.06	0.92	0.87	0.94	0.98	1.00					
Ni	-0.41	0.61	-0.10	0.71	0.71	0.83	0.84	0.89	1.00				
Cu	-0.10	0.16	-0.14	0.20	0.18	0.17	0.22	0.19	0.12	1.00			
Zn	-0.14	0.34	-0.21	0.47	0.53	0.66	0.66	0.74	0.85	0.14	1.00		
Ga	-0.47	0.67	0.12	0.72	0.71	0.83	0.82	0.89	0.89	0.21	0.83	1.00	
As	0.27	-0.14	-0.28	-0.01	-0.04	0.19	0.12	0.20	0.35	0.05	0.52	0.33	1.00

Tab. A-43: Correlation matrix based on the results of an elemental mapping by means of μ S-XRF of a transect through a mafic grain of L2640LFe (No. 169) after Fe-dissolution.

	Si	K	Ca	Ti	V	Cr	Mn	Fe	Ni	Cu	Zn	Ga	As
Si	1.00												
K	-0.14	1.00											
Ca	-0.46	0.52	1.00										
Ti	0.30	0.38	0.04	1.00									
V	0.29	0.40	-0.13	0.52	1.00								
Cr	-0.24	0.78	0.47	0.03	0.41	1.00							
Mn	0.18	0.53	0.20	0.33	0.14	0.49	1.00						
Fe	0.51	0.60	0.03	0.62	0.62	0.41	0.56	1.00					
Ni	0.46	0.15	-0.03	0.25	0.43	-0.04	-0.11	0.42	1.00				
Cu	0.08	0.29	0.37	0.28	-0.02	0.12	0.46	0.35	0.02	1.00			
Zn	0.27	0.64	0.41	0.33	0.24	0.49	0.47	0.72	0.22	0.56	1.00		
Ga	-0.33	0.90	0.49	0.40	0.45	0.75	0.47	0.53	0.03	0.34	0.50	1.00	
As	0.49	0.09	-0.05	0.23	0.37	-0.10	-0.11	0.37	0.98	0.03	0.18	-0.04	1.00

A.5.2 FACTOR LOADINGS AND COMMUNALITY

A.5.2.1 UNTREATED SAMPLES

Tab. A-44: Results of a factor analysis based on elemental concentration recorded from μ S-XRF transect-measurements through a coated grain of L17045 (No. 90).

	F1	F2	commu- nality
Ca	0.97	0.10	0.96
Cr	0.96	0.00	0.95
Fe	0.93	0.30	1.00
Ni	0.93	0.29	0.99
As	0.90	0.39	1.00
Cu	0.86	0.18	0.95
Mn	0.70	0.70	0.98
Zn	0.69	0.53	0.81
Ga	0.25	0.94	0.98
V	0.21	0.93	0.93
K	0.08	0.98	0.97
Si	-0.85	-0.37	0.96
Expl. Var.	6.95	3.98	
Prp. Totl	0.58	0.33	

Tab. A-45: Results of a factor analysis based on elemental concentration recorded from μ S-XRF transect-measurements through a coated grain of H3305 (No. 64).

	F1	F2	commu- nality
V	0.98	0.05	0.96
Zn	0.92	0.36	0.99
Ga	0.90	0.25	0.93
Ni	0.88	0.45	0.99
K	0.85	0.45	0.98
Ca	0.83	0.51	0.99
Cu	0.75	0.63	0.97
Ti	0.73	0.66	0.97
As	0.68	0.71	0.99
Fe	0.63	0.75	1.00
Cr	0.42	0.90	1.00
Mn	0.02	0.95	0.99
Si	-0.39	-0.80	0.96
Expl. Var.	7.08	5.10	
Prp. Totl	0.54	0.39	

Tab. A-46: Results of a factor analysis based on elemental concentration recorded from μ S-XRF transect-measurements through a mafic grain of L17045 (No. 84).

	F1	F2	commu- nality
Mn	0.98	0.00	0.96
K	0.93	0.00	0.80
Fe	0.74	0.59	0.93
As	0.71	0.59	0.81
Ni	0.68	0.53	0.86
Cr	0.22	0.88	0.81
Ga	0.12	0.86	0.67
Zn	0.01	0.91	0.79
Expl. Var.	3.41	3.31	
Prp. Totl	0.43	0.41	

A.5.2.2 AFTER P-LEACHING

Tab. A-47: Results of a factor analysis based on elemental concentration recorded from μ S-XRF transect-measurements through a coated grain of H3305LP (No. 119) after P-leaching.

	F1	F2	commu- nality
Ga	0.96	0.09	0.98
Ni	0.95	0.13	0.97
Mn	0.87	0.43	1.00
Zn	0.85	0.47	0.99
V	0.85	0.31	0.87
Fe	0.83	0.51	1.00
Cr	0.75	0.49	0.96
Cu	0.66	0.64	0.91
Ca	0.41	0.82	0.96
Ti	0.26	0.81	0.77
K	0.20	0.93	0.97
As	-0.03	0.85	0.63
Si	-0.59	0.02	0.78
Expl. Var.	6.33	4.35	
Prp. Totl	0.49	0.33	

Tab. A-48: Results of a factor analysis based on elemental concentration recorded from μ S-XRF transect-measurements through a coated grain of H3515LP (No. 31) after P-leaching

	F1	F2	F3	commu- nality
V	0.94	0.12	0.14	0.90
K	0.88	0.13	0.31	0.90
Cr	0.82	0.21	0.36	0.89
Ti	0.54	0.11	0.64	0.80
Mn	0.52	0.33	0.71	0.91
Fe	0.42	0.55	0.68	0.95
Ca	0.22	0.08	0.79	0.81
Ni	0.19	0.87	0.08	0.73
Ga	0.18	0.91	0.01	0.74
Zn	0.07	0.26	0.89	0.85
As	-0.04	0.82	0.42	0.84
Si	-0.47	0.05	-0.74	0.81
Expl. Var.	3.43	2.85	3.75	
Prp. Totl	0.29	0.24	0.31	

Tab. A-49: Results of factor analysis based on elemental concentrations recorded from a complete μ S-XRF mapping of a coated grain of L17045LP (No. 34) after P-leaching.

	F1	F2	commu- nality
Zn	0.95	0.01	0.86
Mn	0.94	0.11	0.88
Fe	0.94	-0.20	0.90
As	0.88	0.11	0.74
Ni	0.88	0.23	0.81
Cu	0.82	0.31	0.73
Ti	0.71	0.53	0.74
V	0.27	0.85	0.72
K	0.09	0.95	0.88
Si	0.09	0.92	0.84
Ga	-0.04	0.89	0.70
Expl. Var.	5.46	3.76	
Prp. Totl	0.50	0.34	

A.5.2.3 AFTER FE-DISSOLUTION

Tab. A-50: Results of a factor analysis based on elemental concentration recorded from μ S-XRF transect-measurements through a coated grain of H2020LFe (No. 75) after Fe-dissolution.

	F1	F2	commu- nality
Zn	0.97	0.04	0.90
Ni	0.88	0.38	0.89
Ga	0.84	0.42	0.90
Fe	0.74	0.66	0.99
Cr	0.70	0.64	0.92
Mn	0.66	0.72	0.97
V	0.55	0.70	0.83
Ti	0.46	0.85	0.97
K	0.32	0.88	0.88
Si	-0.04	-0.89	0.70
Expl. Var.	4.50	4.48	
Prp. Totl	0.45	0.45	

Tab. A-52: Results of a factor analysis based on elemental concentration recorded from μ S-XRF transect-measurements through a mafic grain of L2640LFe (No. 169) after Fe-dissolution.

	F1	F2	F3	commu- nality
Ga	0.93	0.02	0.22	0.92
Cr	0.88	-0.06	0.15	0.86
K	0.88	0.10	0.34	0.91
Zn	0.44	0.12	0.64	0.72
V	0.41	0.56	0.31	0.79
Fe	0.36	0.36	0.80	0.88
Mn	0.36	-0.29	0.73	0.67
Ti	0.17	0.26	0.63	0.69
Ni	-0.01	0.96	0.11	0.98
As	-0.09	0.94	0.11	0.98
Si	-0.49	0.41	0.68	0.82
Expl. Var.	3.30	2.61	2.74	
Prp. Totl	0.30	0.24	0.25	

Tab. A-51: Results of a factor analysis based on elemental concentration recorded from μ S-XRF transect-measurements through a coated grain of L17045LFe (No. 56) after Fe-dissolution.

	F1	F2	commu- nality
Ca	0.98	0.17	0.99
Mn	0.95	0.28	0.98
Ti	0.95	0.29	0.99
Ni	0.86	0.50	0.98
V	0.68	0.56	0.81
Fe	0.55	0.78	0.97
Zn	0.42	0.83	0.94
Ga	0.30	0.91	0.90
As	0.27	0.86	0.81
K	0.13	0.95	0.92
Expl. Var.	4.60	4.52	
Prp. Totl	0.46	0.45	

A.5.3 FACTOR SCORES

A.5.3.1 UNTREATED SAMPLES

Tab. A-53: Factor scores corresponding to the results of factor analysis of sample L17045 (No. 90).

μm	F1	F2
850	0.26	4.54
829	-0.51	4.03
808	3.53	0.23
786	-0.43	-0.15
765	-0.44	-0.20
744	-0.38	-0.41
723	-0.43	-0.32
701	-0.42	-0.25
680	-0.47	-0.23
659	-0.33	-0.40
638	-0.34	-0.27
616	-0.41	-0.41
595	-0.31	-0.34
574	-0.37	-0.29
553	-0.44	-0.30
531	-0.39	-0.27
510	-0.31	-0.38
489	-0.43	-0.09
468	-0.36	-0.06
446	-0.35	0.03
425	-0.42	0.06
404	-0.38	-0.17
383	-0.34	-0.26
361	-0.37	-0.34
340	-0.22	0.20
319	-0.29	-0.34
298	-0.30	-0.08
276	-0.42	-0.13
255	-0.33	-0.28
234	-0.32	-0.24
213	-0.38	-0.12
191	-0.29	-0.32
170	-0.28	-0.33
149	-0.32	-0.22
128	-0.10	-0.32
106	-0.24	-0.18
85	-0.20	-0.40
64	0.72	-0.40
43	2.92	-0.18
21	3.42	-0.61
0	1.47	0.21

Tab. A-54: Factor scores corresponding to the results of factor analysis of sample H3305 (No. 64).

	F1	F2
300	0.09	1.41
290	-0.23	5.07
280	4.56	0.37
270	2.59	-0.79
260	0.05	-0.17
250	-0.08	-0.31
240	-0.20	-0.22
230	-0.19	-0.18
220	-0.13	-0.22
210	-0.07	-0.26
200	-0.31	-0.09
190	-0.04	-0.33
180	-0.19	-0.20
170	-0.10	-0.28
160	-0.25	-0.28
150	-0.34	-0.20
140	-0.39	-0.19
130	-0.34	-0.16
120	-0.39	-0.15
110	-0.40	-0.23
100	-0.18	-0.39
90	-0.09	-0.44
80	-0.38	-0.13
70	-0.41	-0.20
60	-0.20	-0.34
50	-0.47	-0.19
40	-0.31	-0.27
30	-0.59	-0.13
20	-0.33	-0.27
10	-0.30	-0.22
0	-0.37	-0.01

Tab. A-55: Factor scores corresponding to the results of factor analysis of sample L17045 (No. 84).

μm	F1	F2
700	-0.91	-2.91
686	0.68	-1.96
672	1.34	-0.73
658	1.38	-1.01
644	-0.13	-1.26
630	-0.05	-0.97
616	-0.03	-1.23
602	-0.27	-1.68
588	-0.11	-1.18
574	-0.32	-1.00
560	-0.46	-1.02
546	-0.59	-0.91
532	-0.34	-1.08
518	-0.49	-1.00
504	-0.44	-1.10
490	-0.55	-0.31
476	-0.10	1.48
462	0.11	1.70
448	-0.10	0.92
434	-0.10	0.33
420	-0.41	0.09
406	-0.18	0.73
392	-0.11	1.29
378	-0.71	-0.41
364	-0.40	0.41
350	0.02	0.83
336	-0.41	0.04
322	-0.59	-0.59
308	-0.50	0.10
294	-0.73	1.01
280	-0.51	1.03
266	-0.50	0.86
252	-0.60	0.81
238	-0.30	0.69
224	-0.48	0.33
210	-0.46	0.85
196	-0.32	0.58
182	-0.64	0.09
168	-0.52	-0.32
154	-0.43	0.23

μm	F1	F2
140	-0.44	0.75
126	-0.53	0.39
112	0.21	1.33
98	0.14	1.45
84	0.08	0.37
70	0.02	0.80
56	0.19	0.32
42	0.19	0.54
28	2.34	0.79
14	4.38	0.07
0	3.68	-0.50

to be continued

A.5.3.2 AFTER P-LEACHING**Tab. A-56: Factor scores corresponding to the results of factor analysis of sample H3515LP (No. 31).**

μm	F1	F2	F3
270	-0.17	-1.38	0.45
264	-0.54	-1.27	1.36
258	-0.60	-0.79	1.53
252	-0.20	0.55	1.01
246	-1.02	2.28	0.81
240	-0.01	0.39	-0.41
234	-0.22	-0.64	-0.41
228	-0.32	-0.01	-0.44
222	-0.61	-0.19	0.32
216	-0.10	-0.08	-0.77
210	-0.14	-0.42	-0.53
204	-0.30	-0.86	-0.30
198	-0.04	-0.93	-0.44
192	0.01	-0.76	-0.51
186	-0.40	-0.44	-0.20
180	-0.53	0.24	-0.47
174	-0.05	-0.41	-0.88
168	0.01	-0.73	-0.72
162	0.05	-0.52	-0.85
156	0.00	-1.06	-0.68
150	-0.13	-0.56	-0.66
144	-0.29	-0.01	-0.45
138	0.26	0.66	-0.80
132	-0.69	2.50	-0.81
126	-0.55	3.23	-0.83
120	-0.52	2.52	-0.92
114	-0.40	1.03	-0.74
108	-0.06	-0.53	-0.62
102	-0.24	-0.38	-0.59
96	-0.01	-0.96	-0.69
90	-0.13	-0.52	-0.69
84	-0.16	0.18	-0.93
78	-0.15	-0.63	-0.52
72	-0.26	-0.36	-0.45
66	-0.26	-0.79	-0.31
60	-0.17	-0.32	-0.35
54	-0.65	-0.34	0.12
48	-0.07	-0.32	0.38
42	-0.28	-0.42	2.07
36	-0.25	0.20	2.67
30	0.21	1.05	2.57
24	-0.02	0.16	2.09
18	4.21	0.33	-0.01
12	4.63	0.50	-0.26
6	0.65	0.61	1.18
0	0.53	0.19	1.69

Tab. A-57: Factor scores corresponding to the results of factor analysis of sample H3305LP (No. 119).

μm	F1	F2
250	-0.12	0.02
244	0.32	-0.63
238	0.15	0.06
231	2.71	0.40
225	3.84	-0.01
219	2.68	-0.32
213	1.21	0.15
206	-0.20	0.08
200	-0.60	0.52
194	-0.58	0.09
188	-0.49	-0.04
181	-0.40	-0.38
175	-0.61	-0.05
169	-0.56	-0.10
163	-0.51	-0.38
156	-0.31	-0.63
150	-0.64	0.08
144	-0.49	-0.41
138	-0.39	-0.54
131	-0.28	-0.69
125	-0.66	-0.21
119	-0.38	-0.71
113	-0.48	-0.72
106	-0.42	-0.60
100	-0.80	0.02
94	-0.72	-0.08
88	-0.43	-0.64
81	-0.49	-0.52
75	-0.27	-0.87
69	-0.44	-0.55
63	-0.51	-0.27
56	-0.25	-0.47
50	0.11	-0.59
44	0.73	-0.38
38	0.60	-0.44
31	0.45	-0.60
25	0.05	-0.10
19	-0.20	0.79
13	-0.74	2.76
6	-0.71	3.91
0	0.83	3.06

A.5.3.3 AFTER FE-DISSOLUTION

Tab. A-58: Factor scores corresponding to the results of factor analysis of sample H3515LFe (No. 182).

μm	F1
500	-0.27
488	-0.65
475	-0.33
463	0.26
450	1.09
438	1.18
425	-0.39
413	-0.54
400	-0.55
388	-0.65
375	-0.40
363	-0.50
350	-0.30
338	-0.63
325	-0.50
313	-0.57
300	-0.51
288	-0.55
275	-0.58
263	-0.51
250	-0.45
238	-0.44
225	-0.59
213	-0.59
200	-0.52
188	-0.46
175	-0.53
163	-0.54
150	-0.63
138	-0.54
125	-0.25
113	-0.26
100	-0.33
88	0.18
75	1.44
63	2.23
50	3.83
38	2.61
25	0.38
13	1.00
0	0.35

Tab. A-59: Factor scores corresponding to the results of factor analysis of sample H2020LFe (No. 75).

μm	F1	F2
0	0.54	1.71
4	1.11	1.84
8	1.72	3.18
13	1.46	2.03
17	1.06	1.68
21	1.76	1.27
25	1.99	-0.72
29	1.68	-0.65
34	2.41	-1.15
38	1.85	-1.33
42	1.38	-1.08
46	0.41	-0.79
50	0.65	-0.78
55	0.40	-0.68
59	0.70	-0.94
63	0.90	-0.99
67	0.26	-0.76
71	0.18	-0.63
76	-0.03	-0.50
80	-0.37	-0.41
84	-0.02	-0.62
88	-0.27	-0.49
92	-0.39	-0.22
97	-0.68	-0.25
101	-0.49	-0.49
105	-0.28	-0.54
109	-0.33	-0.46
113	-0.60	-0.40
118	-0.51	-0.50
122	-0.62	-0.50
126	-0.96	-0.21
130	-0.88	-0.29
134	-0.82	-0.43
139	-0.79	-0.30
143	-0.75	-0.32
147	-0.69	-0.30
151	-0.59	-0.30
155	-0.42	-0.35
160	-0.68	-0.05
164	-0.38	-0.21
168	-0.83	-0.09
172	-0.87	0.19

to be continued on the following page

APPENDIX

176	-1.04	0.23
181	-0.98	0.26
185	-0.82	0.19
189	-0.56	0.31
193	-0.31	0.26
202	-0.01	2.16
206	-1.78	1.62
210	-1.71	1.80

Tab. A-60: Factor scores corresponding to the results of factor analysis of sample L17045LFe (No. 56).

μm	F1	F2
170	-0.51	2.17
164	-0.62	3.83
159	5.31	0.57
153	-0.25	2.10
147	-0.20	0.81
142	0.07	0.10
136	0.05	-0.11
130	-0.22	-0.09
125	-0.20	-0.47
119	0.03	-0.56
113	-0.16	0.10
108	-0.10	-0.35
102	-0.19	-0.53
96	-0.43	-0.05
91	-0.38	-0.19
85	-0.16	-0.61
79	-0.14	-0.67
74	-0.15	-0.65
68	-0.13	-0.26
62	-0.33	-0.14
57	-0.19	-0.50
51	-0.35	-0.32
45	-0.27	-0.32
40	-0.10	-0.76
34	-0.22	-0.37
28	0.02	-0.77
23	-0.13	-0.67
17	-0.14	-0.58
11	0.15	-0.56
6	0.13	-0.13
0	-0.16	-0.01

Tab. A-61: Factor scores corresponding to the results of factor analysis of sample L2640LFe (No. 169).

μm	F1	F2	F3
180	-0.39	-1.09	-1.82
173	-0.26	-1.27	-1.69
166	-0.17	-1.09	-1.46
158	0.50	0.21	-1.78
151	0.32	-0.94	-0.90
144	3.04	0.18	-0.70
137	3.17	-0.70	1.60
130	-0.30	-0.07	-0.17
122	-0.80	-0.80	0.11
115	-0.80	-0.23	-0.11
108	-0.42	-0.76	0.67
101	-0.29	0.29	0.13
94	-0.72	0.72	-0.26
86	-0.62	1.84	-0.18
79	-0.28	1.99	0.01
72	0.43	1.65	0.31
65	-0.37	1.63	0.18
58	-0.01	1.27	-0.66
50	-0.43	0.00	0.61
43	0.48	0.44	-0.10
36	0.18	0.37	0.29
29	-0.48	-0.58	0.91
22	-0.65	-0.41	2.05
14	-1.02	-1.00	1.10
7	-0.06	-0.55	0.98
0	-0.05	-1.09	0.88

A.6 CHARACTERIZATION OF ORGANIC MATTER

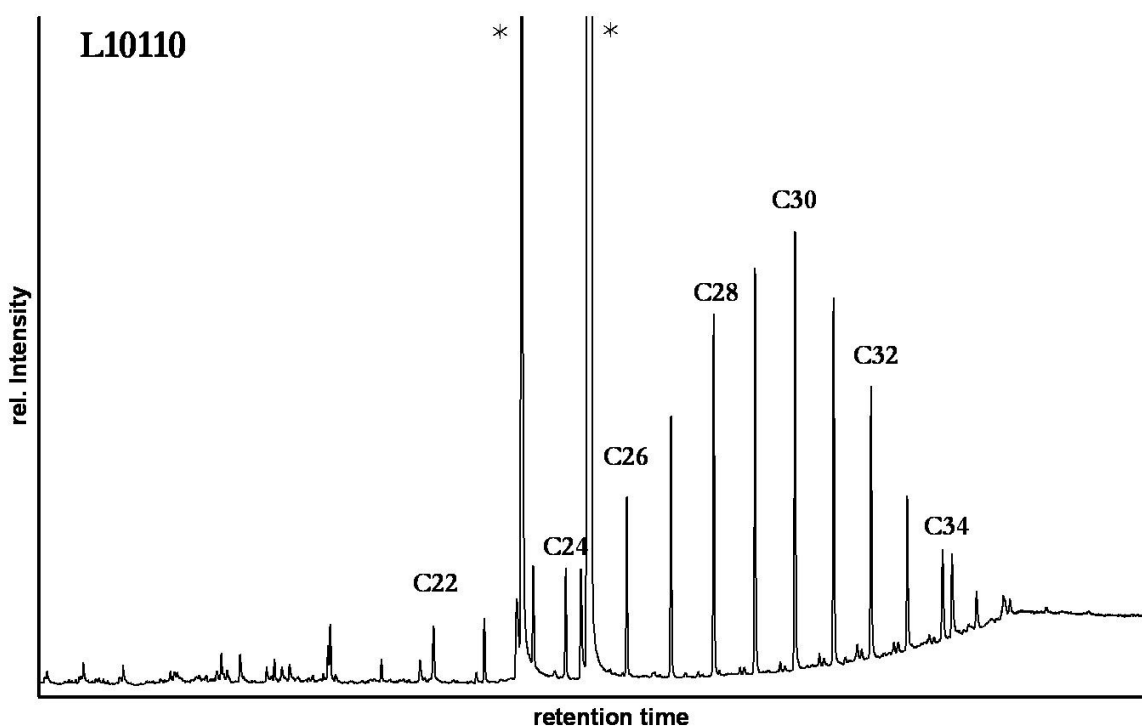


Fig. A-1: Selected ion monitoring (SIM) gas chromatogram of n-alkanes ($m/z = 57$) of sample L10110 of site L. * denotes contamination (phthalates) from the chemicals used. Adrostan (internal standard) is visible in the SIM of steranes ($m/z = 217$) or in the total ion chromatogram (both not displayed).

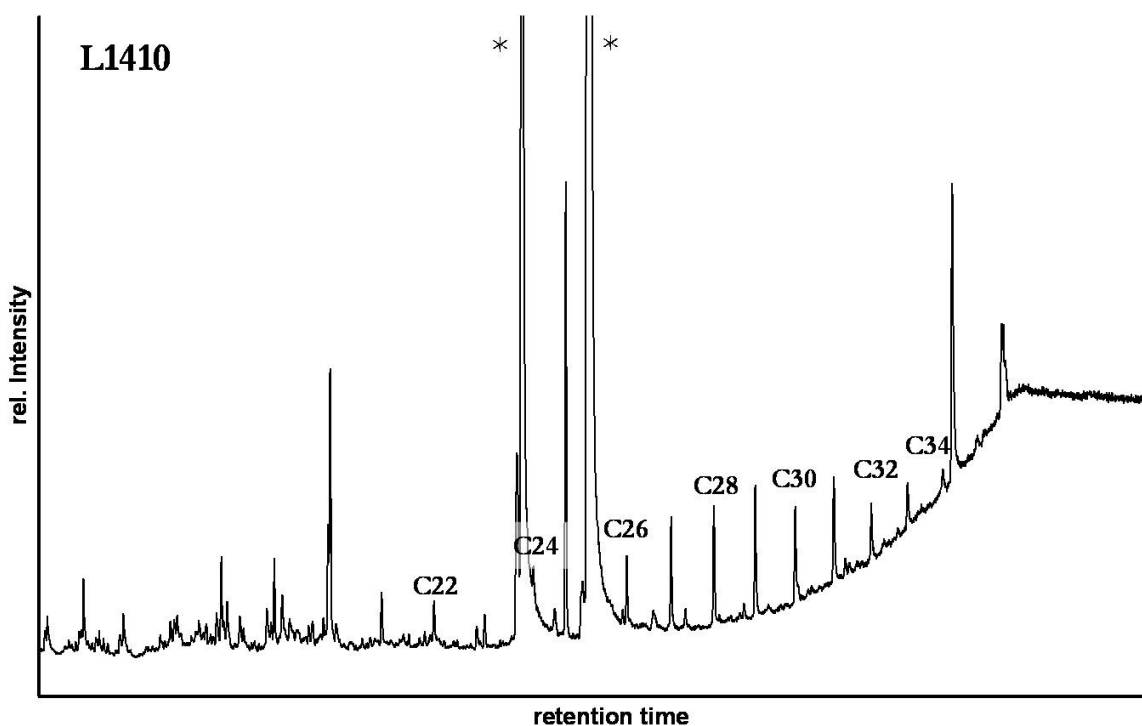


Fig. A-2: Selected ion monitoring gas chromatogram of n-alkanes ($m/z = 57$) of sample L1410 of site L. * denotes contamination (phthalates) from the chemicals used. Adrostan (internal

standard) is visible in the SIM of steranes ($m/z = 217$) or in the total ion chromatogram (both not displayed).

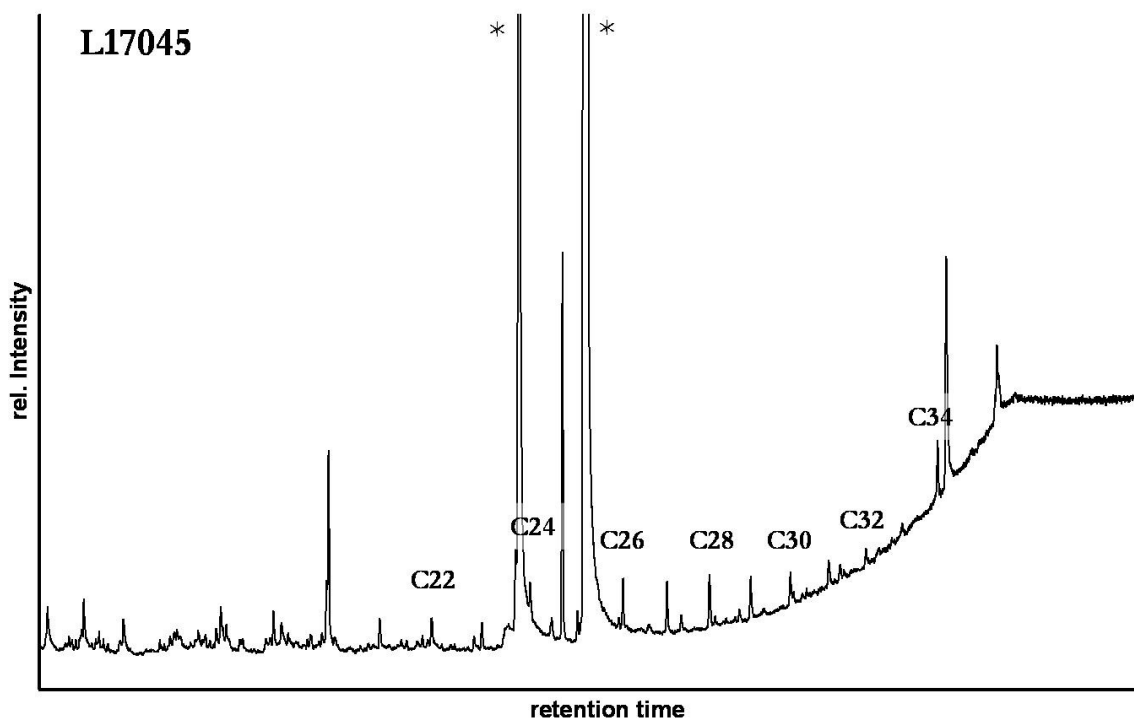


Fig. A-3: Selected ion monitoring gas chromatogram of n-alkanes ($m/z = 57$) of sample L17045 of site L. * denotes contamination (phthalates) from the chemicals used. Adrostan (internal standard) is visible in the SIM of steranes ($m/z = 217$) or in the total ion chromatogram (both not displayed).

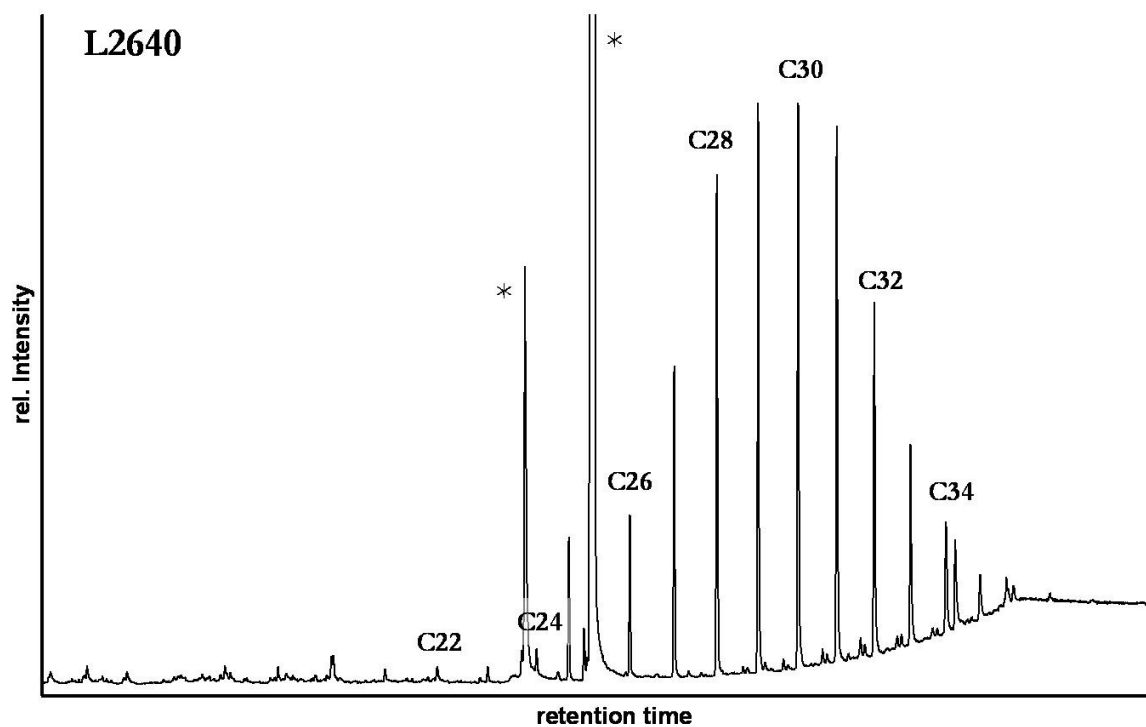


Fig. A-4: Selected ion monitoring gas chromatogram of n-alkanes ($m/z = 57$) of sample L2640 of site L. * donates contamination (phthalates) from the chemicals used. Adrostan (internal standard) is visible in the SIM of steranes ($m/z = 217$) or in the total ion chromatogram (both not displayed).

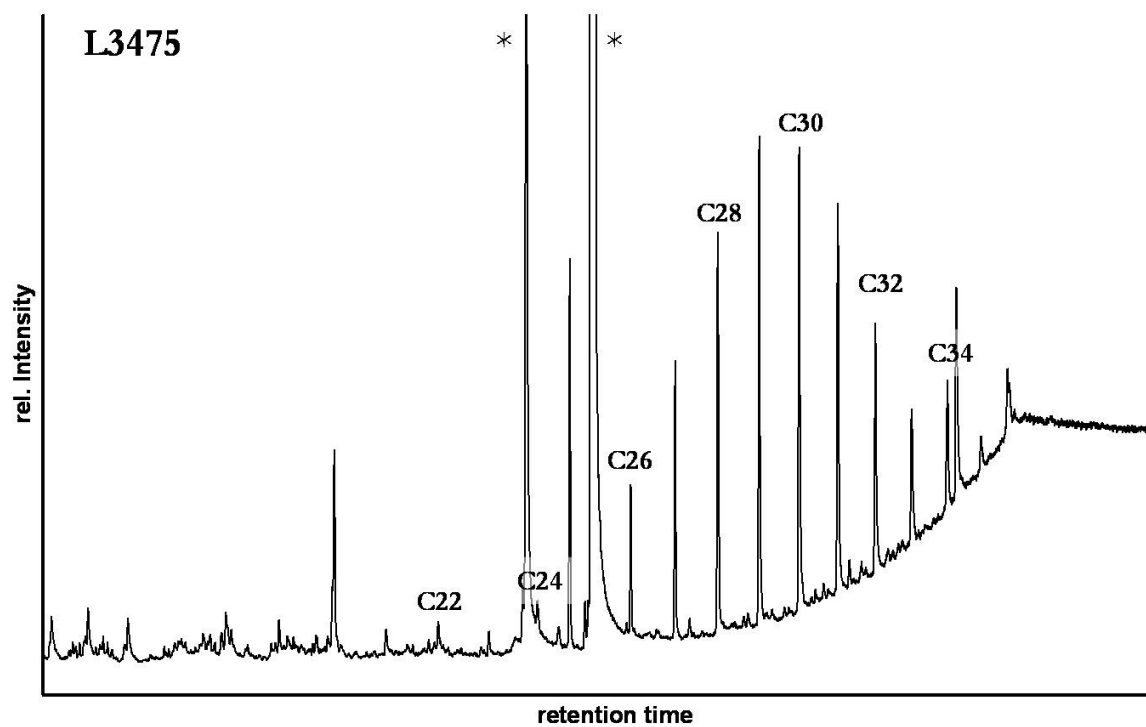


Fig. A-5: Selected ion monitoring gas chromatogram of n-alkanes ($m/z = 57$) of sample L3475 of site L. * donates contamination (phthalates) from the chemicals used. Adrostan (internal standard) is visible in the SIM of steranes ($m/z = 217$) or in the total ion chromatogram (both not displayed).

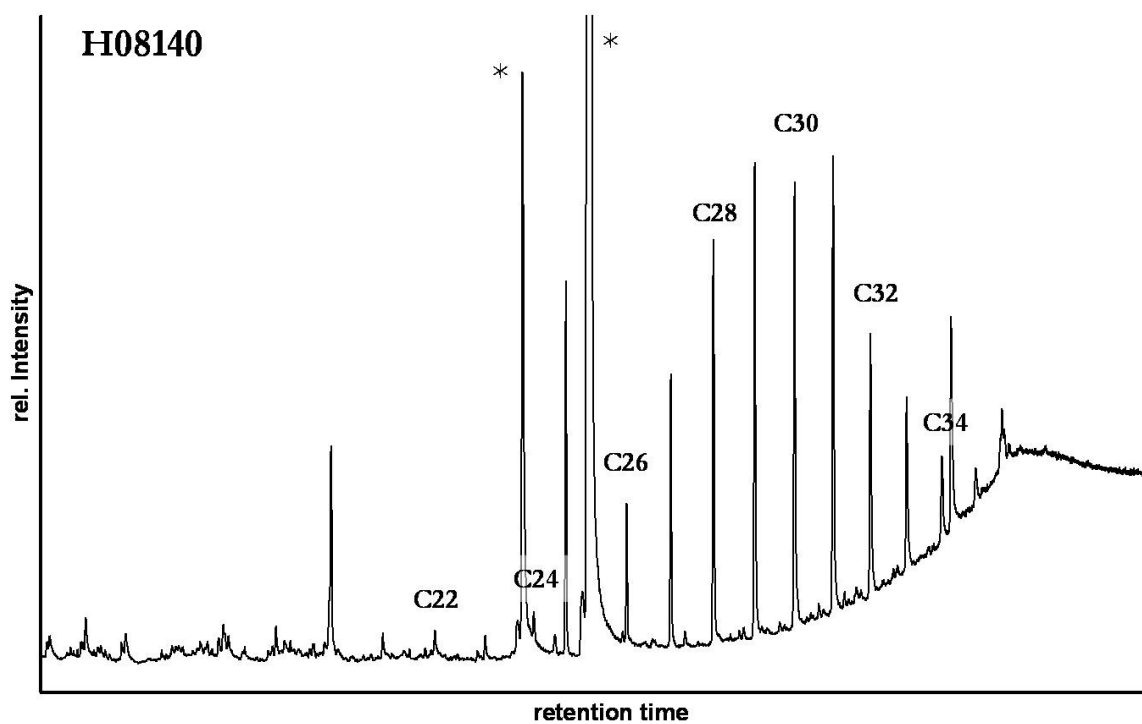


Fig. A-6: Selected ion monitoring gas chromatogram of n-alkanes ($m/z = 57$) of sample H08120 of site H. * donates contamination (phthalates) from the chemicals used. Adrostan (internal standard) is visible in the SIM of steranes ($m/z = 217$) or in the total ion chromatogram (both not displayed).

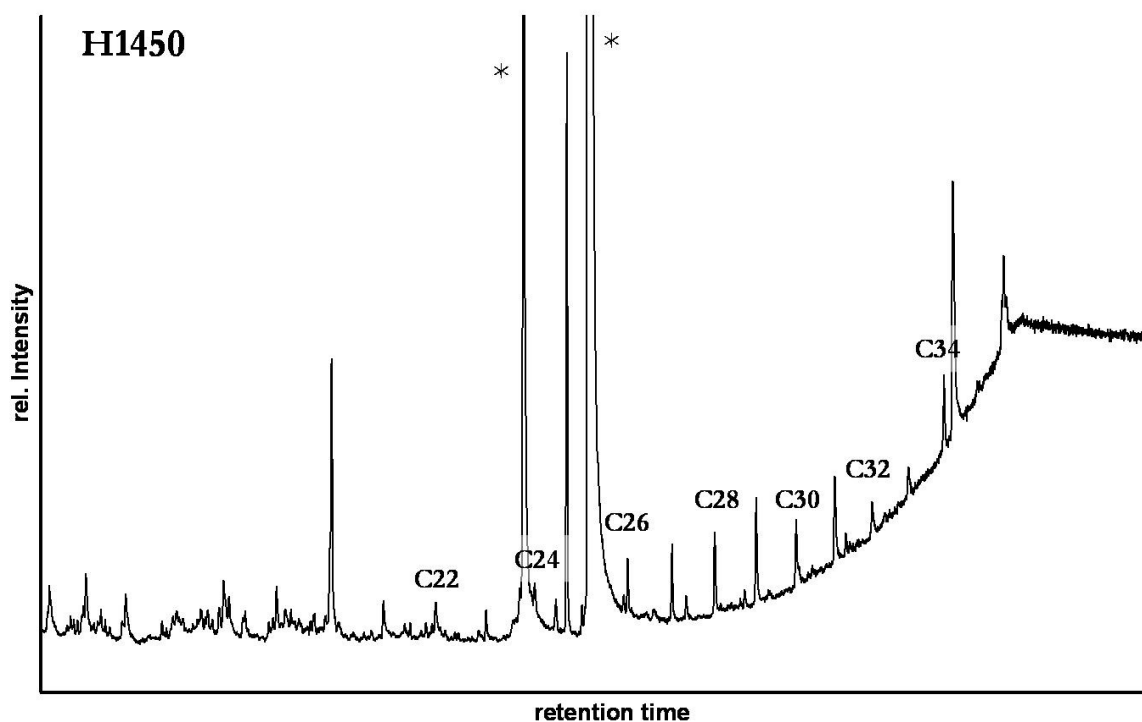


Fig. A-7: Selected ion monitoring gas chromatogram of n-alkanes ($m/z = 57$) of sample H1450 of site H. * donates contamination (phthalates) from the chemicals used. Adrostan (internal

standard) is visible in the SIM of steranes ($m/z = 217$) or in the total ion chromatogram (both not displayed).

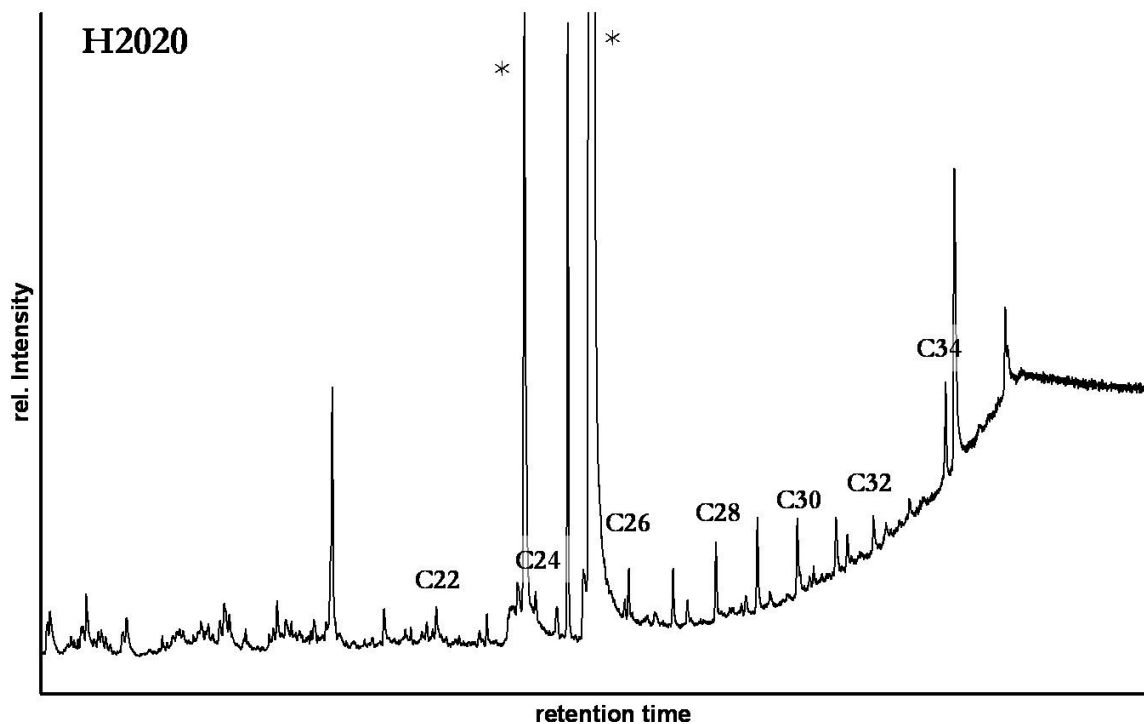


Fig. A-8: Selected ion monitoring gas chromatogram of n-alkanes ($m/z = 57$) of sample H2020 of site H. * denotes contamination (phthalates) from the chemicals used. Adrostan (internal standard) is visible in the SIM of steranes ($m/z = 217$) or in the total ion chromatogram (both not displayed).

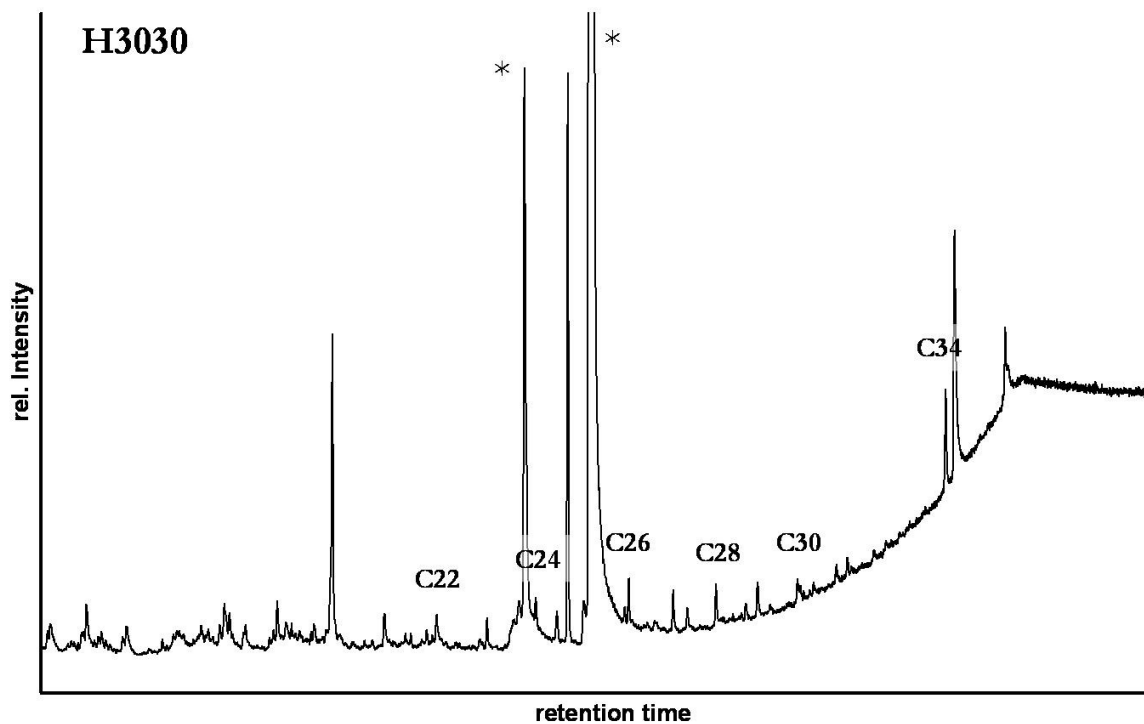


Fig. A-9: Selected ion monitoring gas chromatogram of n-alkanes ($m/z = 57$) of sample H3030 of site H. * denotes contamination (phthalates) from the chemicals used. Adrostan (internal standard) is visible in the SIM of steranes ($m/z = 217$) or in the total ion chromatogram (both not displayed).

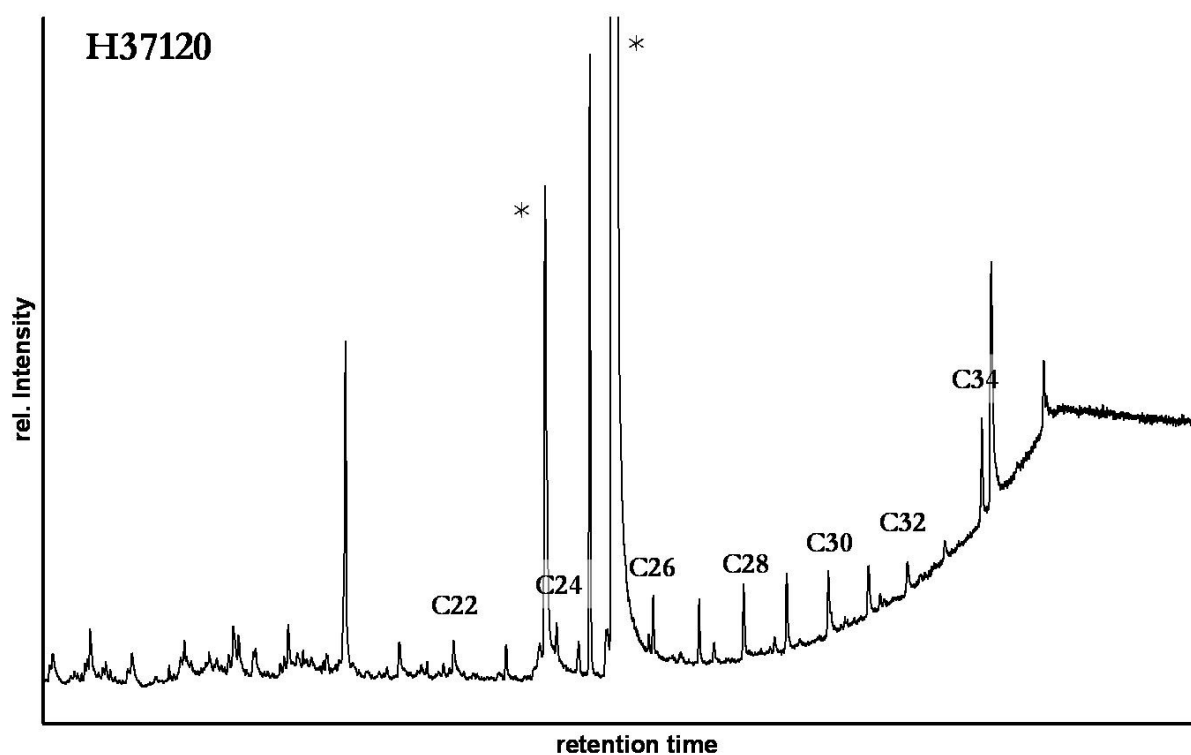


Fig. A-10: Selected ion monitoring gas chromatogram of n-alkanes ($m/z = 57$) of sample H1450 of site H* denotes contamination (phthalates) from the chemicals used. Adrostan (in-

ternal standard) is visible in the SIM of steranes ($m/z = 217$) or in the total ion chromatogram (both not displayed).

**In der Reihe "Karlsruher Geochemische Hefte" (ISSN 0943-8599)
sind erschienen:**

Band 1: U. Kramar (1993)

Methoden zur Interpretation von Daten der geochemischen
Bachsedimentprospektion am Beispiel der Sierra de San Carlos/ Tamaulipas Mexiko

Band 2: Z. Berner (1993)

S-Isotopengeochemie in der KTB - Vorbohrung und Beziehungen zu den Spuren-
elementmustern der Pyrite

Band 3: J.-D. Eckhardt (1993)

Geochemische Untersuchungen an jungen Sedimenten von der Galapagos-
Mikroplatte:
Hydrothermale und stratigraphisch signifikante Signale

Band 4: B. Bergfeldt (1994)

Lösungs- und Austauschprozesse in der ungesättigten Bodenwasserzone und
Auswirkungen auf das Grundwasser

Band 5: M. Hodel (1994)

Untersuchungen zur Festlegung und Mobilisierung der Elemente As, Cd, Ni und Pb
an ausgewählten Festphasen unter besonderer Berücksichtigung des Einflusses von
Huminstoffen.

Band 6: T. Bergfeldt (1995)

Untersuchungen der Arsen- und Schwermetallmobilität in Bergbauhalden und
kontaminierten Böden im Gebiet des Mittleren Schwarzwaldes.

Band 7: M. Manz (1995)

Umweltbelastungen durch Arsen und Schwermetalle in Böden, Halden, Pflanzen und
Schlacken ehemaliger Bergbaugebiete des Mittleren und Südlichen Schwarzwaldes.

Band 8: J. Ritter (1995)

Genese der Mineralisation Herrmanngang im Albtalgranit (SE-Schwarzwald) und
Wechselwirkungen mit dem Nebengestein.

Band 9: J. Castro (1995)

Umweltauswirkungen des Bergbaus im semiariden Gebiet von Santa Maria de la
Paz, Mexiko.

Band 10: T. Rüde (1996)

Beiträge zur Geochemie des Arsens.

Band 11: J. Schäfer (1998)

Einträge und Kontaminationspfade Kfz-emittierter Platin-Gruppen-Elemente (PGE) in
verschiedenen Umweltkompartimenten.

Band 12: M. A. Leosson (1999)

A Contribution to the Sulphur Isotope Geochemistry of the Upper Continental Crust:
The KTB Main Hole - A Case Study

Band 13: B. A. Kappes (2000)

Mobilisierbarkeit von Schwermetallen und Arsen durch saure Grubenabwässer in
Bergbaualtlasten der Ag-Pb-Zn-Lagerstätte in Wiesloch

Band 14: H. Philipp (2000)

The behaviour of platinum-group elements in petrogenetic processes:
A case study from the seaward-dipping reflector sequence (SDRS), Southeast
Greenland volcanic rifted margin

Band 15: E. Walpersdorf (2000)

Nähr- und Spurenelementdynamik im Sediment/Wasser-Kontaktbereich nach einer
Seekreideaufspülung - Pilotstudie Arendsee -

Band 16: R. H. Kölbl (2000)

Models of hydrothermal plumes by submarine diffuse venting in a coastal area: A
case study for Milos, South Aegean Volcanic Arc, Greece

Band 17: U. Heiser (2000)

Calcium-rich Rhodochrosite layers in Sediments of the Gotland Deep, Baltic Sea, as
Indicators for Seawater Inflow

In der Fortsetzungsreihe "Karlsruher Mineralogische und Geochemische Hefte"
(ISSN 1618-2677) sind bisher erschienen:

Band 18: S. Norra (2001)

Umweltgeochemische Signale urbaner Systeme am Beispiel von Böden, Pflanzen,
und Stäuben in Karlsruhe

Band 19: M. von Wagner, Alexander Salichow, Doris Stüben (2001)

Geochemische Reinigung kleiner Fließgewässer mit Mangankiesen, einem
Abfallsprodukt aus Wasserwerken (GReiFMan)

Band 20: U. Berg (2002)

Die Kalzitapplikation als Restaurierungsmaßnahme für eutrophe Seen – ihre
Optimierung und Bewertung

Band 21: Ch. Menzel (2002)

Bestimmung und Verteilung aquatischer PGE-Spezies in urbanen Systemen

Band 22: P. Graf (2002)

Meta-Kaolinit als latent-hydraulische Komponente in Kalkmörtel

Band 23: D. Buqezi-Ahmeti (2003)

Die Fluidgehalte der Mantel-Xenolithe des Alkaligesteins-Komplexes der Persani-Berge, Ostkarpaten, Rumänien: Untersuchungen an Fluid-Einschlüssen

Band 24: B. Scheibner (2003)

Das geochemische Verhalten der Platingruppenelemente bei der Entstehung und Differenzierung der Magmen der Kerguelen-Flutbasaltprovinz (Indischer Ozean)

Ab Band 25 erscheinen die Karlsruher Mineralogischen und Geochemischen Hefte im Karlsruher Universitätsverlag online unter der Internetadresse

<http://www.uvka.de/univerlag/institut.php?fakultaet=1>

Auf Wunsch sind beim Karlsruher Universitätsverlag gedruckte Exemplare erhältlich („print on demand“).

Band 25: A. Stögbauer (2005)

Schwefelisotopenfraktionierung in abwasserbelasteten Sedimenten - Biogeochemische Umsetzungen und deren Auswirkung auf den Schwermetallhaushalt

Band 26: X. Xie (2005)

Assessment of an ultramicroelectrode array (UMEA) sensor for the determination of trace concentrations of heavy metals in water

Band 27: F. Friedrich (2005)

Spectroscopic investigations of delaminated and intercalated phyllosilicates

Band 28: L. Niemann (2005)

Die Reaktionskinetik des Gipsabbindens: Makroskopische Reaktionsraten und Mechanismen in molekularem Maßstab

Band 29: F. Wagner (2005)

Prozessverständnis einer Naturkatastrophe: eine geo- und hydrochemische Untersuchung der regionalen Arsen-Anreicherung im Grundwasser West-Bengalens (Indien)

Band 30: F. Pujol (2005)

Chemostratigraphy of some key European Frasnian-Famennian boundary sections (Germany, Poland, France)

Band 31: Y. Dikikh (2006)

Adsorption und Mobilisierung wasserlöslicher Kfz-emittierter Platingruppenelemente (Pt, Pd, Rh) an verschiedenen bodentypischen Mineralen

Band 32: F. I. Müller (2007)

Influence of cellulose ethers on the kinetics of early Portland cement hydration

Band 33: H. Haile Tolera (2007)

Suitability of local materials to purify Akaki Sub-Basin water

Band 34: M. Memon (2008)

Role of Fe-oxides for predicting phosphorus sorption in calcareous soils

Band 35: S. Bleeck-Schmidt (2008)

Geochemisch-mineralogische Hochwassersignale in Auensedimenten und deren Relevanz für die Rekonstruktion von Hochwasserereignissen

Band 36: A. Steudel (2009)

Selection strategy and modification of layer silicates for technical applications

In this work the spatial variability of dissolved arsenic concentrations in aquifers was studied in a small village in the vicinity of Ha Noi, Vietnam. The main goal was to identify major geochemical, sedimentological and hydrochemical differences between high and low arsenic regions. Furthermore, the behaviour of arsenic and other elements during sequential extractions on a micrometer scale was characterized with micro synchrotron XRF analysis. Based on the results a conceptual model was developed which could explain the current situation in the village. Moreover, it could help to identify high arsenic areas throughout the world and, therefore, prevent the installation of drinking water wells in arsenic burdened regions.

